THE UNIVERSITY OF HULL

Development of Lab-on-a chip technology for the analysis of ions in natural waters

being a Thesis submitted for the Degree of Doctor of Philosophy

in the University of Hull

by

Ahmed M. Fallatah

MSc Loughborough University

Acknowledgements

I would like to express my gratitude to my supervisor, Professor Gillian Greenway, whose expertise, understanding, and patience while reviewing my manuscript added considerably to my graduate experience. I would also like to thank Dr. Ian Bell for his support, guidance, and expertise in engineering science. I would also like to thank Professor Steve Haswell for his support and encouragement during my study, and Professor Nicole Pamma for the academic writing course.

I would also like to thank all of the members of the Analytical Research Group at the University of Hull, especially the Saudi nationals and Dr. Etienne Joly for their tremendous support, and special thanks to the technicians Bob Knight, Tony Sinclair, Dr. Steve Clark, Dean and Sean Moore, Gary Kipling and Gary Robinson.

I would like to express my special appreciation of and thanks to Taif University for their unlimited financial and academic support. I also offer my profound thanks to the Saudi Arabian Culture Bureau.

I would like to thank all of my family for their love and support and my wife Sarah and my sister Ayshah for being my closest friends. Finally, I cannot express enough my appreciation and gratitude for the only people whose love and support is unlimited: my mother and father.

Abstract

There is a demand for portable *in-situ* measurement systems for measuring ions in environmental water samples. Commercially available flow injection analysis systems are not easy to install, have high power requirements, and use large volumes of reagents. Miniaturising the measurements is promising, and quite successful microfluidic automated systems have been developed. These systems, however, tend to only measure one species at a time, and what is really required is a portable system that simultaneously measures several anions and cations. The aim of this thesis was, therefore, to develop a novel analytical device that has the ability to measure several nutrient levels in water samples *in-situ*, at high-frequency measurements, by miniaturising the sample preparation and measurement. The system involved: ion extraction, ion separation, and detection with a C4D contactless conductivity detector. This analytical system to be developed needs to be able to replace the current, typical system being used in the field.

To avoid the effects of the sample matrix on the separation process, the extraction of ions from the sample before separation, was investigated. Different ion extraction approaches were explored, including ion extraction through a potassium silicate monolith and electrodialysis. The potassium silicate monolith was used to extract ions from water samples; this worked as a barrier to prevent unwanted materials present in the river water from entering the measurement system. The presence of these materials would influence the separation process.

Extraction techniques using the potassium silicate monolith were investigated, using both glass chips and glass capillaries. To prevent the electroosmotic flow (EOF) caused by the negative charge on the surface of the glass and the monolith, the

surface was silanised. Three different silanisation methods were investigated: trichloro perfluorooctyl silane (FDTS), a commercial coating, and an end-capping procedure. The extraction of the ions was achieved with all three of the silanisation methods but greater reproducibility was needed.

Electrodialysis (ED) was examined to see if it could provide a more reproducible sample introduction method. The advantage of this method was that it could be effectively combined with electrophoresis (CE) for rapid pre-concentration and the subsequent determination of inorganic ions in the river water. Different ED techniques were investigated for extracting the inorganic ions. This involved exploring different membranes including polytetrafluoroethylene (PTFE), Parafilm, cellulose acetate, and ion-exchange membranes. Different ED systems were evaluated, including a commercial flow design and microfluidic chips manufactured from cyclic olefin copolymers (COC), with both single and multiple membranes.

The cellulose acetate membrane provided good results for cation extraction from a real river water sample. Sodium, calcium, potassium and magnesium were extracted at 85%, 45%, 23%, and 10%, respectively. The anion-exchange (AEX) membrane in the ED system was successful and demonstrated good results. Cation extraction with a single cation-exchange (CEX) membrane also provided good results.

Several ED microfluidic chips were designed to improve the extraction, using the ion-exchange membranes. In this system, a gold electrode was used and positive results were obtained for both anions and cations, and the anion extraction was demonstrated using a real river water sample. Five anions were extracted: respectively comprised sulphate 65%, phosphate with 31%, 82% for chloride, nitrite with 10% and nitrate with 6%.

Initial work on the separation of the inorganic ions concentrated on a monolithic column, as reported in the literature. For the separation of anions, two different anion exchangers were investigated, lysine and DDAB. The monoliths were prepared in-house and were then coated with the anion exchanger. A commercial C18 monolith was used to compare the results obtained from the homemade monolithic column. Problems were encountered with the coated monoliths, especially in terms of high back pressures, and it was decided that capillary electrophoresis (CE) would provide a better separation solution and would more easily integrate with the ED ion extraction.

A proposed design of an integrated system was presented including the pumps that are required, the reagents, and the energy use. The proposed integrated system only required one buffer for all processes in the system, which reduces the environmental impact of the chemical reagents. The suitability of the buffer (MES/His) was extensively investigated, and the amount needed for a month was also calculated to be less than 3 L, which is ideal for the system portability. It was also calculated that the required power could be provided by a battery, although the inclusion of solar panels would be advantageous.

The proposed integrated system meets most of the requirements of the project, and promising results were obtained. Further optimisation of the design will focus on increasing the robustness of field applications.

Contents

List of figures

List of tables

Table of abbreviations

AAS	Atomic absorption spectrometry
AC	Alternating current
ACN	Acetonitrile
AES	Atomic emission spectroscopy
BET	Brunauer-Emmett-Teller
C4D	Capacitively Coupled Contactless Conductivity Detection
CE	Capillary electrophoresis
COC	Cyclic Olefin Copolymer
DC	Direct current
DDAB	Didodecyldimethylammonium bromide
ED	Electrodialysis
EOF	Electro-osmotic Flow
EPSRC	Engineering and Physical Sciences Research Council
FDTS	trichloro perfluorooctyl silane
FIA	Flow injection analysis
HV	High Voltage
IC	Ion Chromatography
ICP	Inductively coupled plasma
IEC	Ion exchange chromatography
IPC	Ion pairing chromatography
ISE	Ion selective electrode
ITP	Isotachophoresis
LIMPIDS	Linking Improved Modelling of Pollution to Innovative Development of Sensors
LOC	Lab-on-a-chip
LOD	Limit of detection
MEC	microchip-based capillary electrophoresis
MS	Mass spectrometry
PCB	Printed circuit boards
PMMA	Polymethylmethacrylate
PTFE	Polytetrafluoroethylene
RP	Revered phase
SEM	Scanning electron microscopy
SRP	Soluble reactive phosphorus
TDP	Total dissolved phosphorous
TEOS	Tetraethylorthosilicate
TP	Total phosphorus
TRP	Total reactive phosphorus
μep	Electrophoretic mobility

Posters and publications

Posters

"Overcoming sample introduction issues for Lab-on-Chip environmental analysis" poster presented at the Lab-on-Chip European congress held in Edinburgh, 28-29 March 2012.

"Overcoming sample introduction issues for Lab-on-Chip environmental analysis" poster presented at the Analytical Research Forum 2012 held at Durham University, 2-4 July 2012.

"Development of Lab-on-Chip technology for the analysis of ions in natural waters" poster presented at Lab on a Chip Europe held in Barcelona, 5-6 March 2013.

"Development of Lab-on-Chip technology for the analysis of ions in natural waters" poster presented at Waste Water Emissions Monitoring Conference held in Telford, 5-6 November 2014.

"Development of Lab-on-Chip technology for the analysis of inorganic ions in natural waters" poster presented at The 8th Saudi Student Conference in UK, held in London, 31 January-1 February 2015.

Conference talks

"Development of Lab-on-Chip technology for the analysis of inorganic ions in natural waters" at The 6th PhD Experience Conference 2015, held at the University of Hull, 7-8 April 2015. Awarded best oral presentation.

Publications

Joly, E. Bell, I. M., Fallatah, A., Greenway, G. M., Haswell, S. J., Wade, A. J. and Skeffington, R. A. Design and Test Issues for Lab-on-Chip Ion Separation for *In-situ* Water Quality Monitoring. *In Mixed-Signals, Sensors and Systems Test Workshop (IMS3TW), 2012 18th International*, 2012.

Wade, A. J., PalmerFelgate, E. J., Halliday, S. J., Skeffington, R. A., Loewenthal, M.,Jarvie, H. P., Bowes, M. J., Greenway, G. M., Haswell, S. J., Bell, I. M., Joly, E., Fallatah, A., Neal, C., Williams, R. J., Gozzard, E. and Newman, J. R. From existing *in-situ*, high-resolution measurement technologies to lab-on-a-chip – the future of water quality monitoring? *Hydrology and Earth System Sciences Discussions*, 2012, **9**, 6457-6506.

1 Introduction

The increase in demand for water and the problem of water pollution, both the quantity and quality of surface water and groundwater, are of major concern worldwide, especially in terms of the presence of nutrients and heavy metals in water, which pose a serious threat to human health.[1] The primary step for the effective management of surface and groundwater is the regular and continuous monitoring of water quality in terms of the distribution, source and identification of contaminants.[2]

Water is a very important natural resource upon which relies the sustainability of human civilisation. Unfortunately, it has been subjected to pollution due to human activities; pollutants such as nutrients, pesticides and heavy metals are transported from many different sources, through surface and groundwater pathways.[3] In addition, runoff from farms and cities is a main source of nutrients (mostly phosphorus and nitrogen) entering surface waters such as lakes, rivers and coastal waters; industries and vehicle emissions are also a major source of pollution.[3-4] Furthermore, with the high use of heavy metal salts, an alarming increase has been occurring in the concentrations of these ions in the biosphere.[5] In addition, some pollutants do not degrade in the environment and they can persist for hundreds of years because they are only transformed from one oxidation state to another, or from one organic complex to another.[4] However, contamination sources lead to damaging effects on plants and animals, and eventually, on human health, either directly or through the food chain.[6] Water pollution, therefore, poses a great potential threat to the environment and human health.

1.1 The aim of the project

The aim of this project is to develop a novel, analytical device that is capable of measuring and detecting the nutrient level of water samples *in-situ* at high-frequency

measurements, by utilising the advantages of miniaturisation for sample preparation and measurement. The system involves:

1. Ion injection
2. Ion separation
3. Detection.

The analytical system to be developed needs to be able to replace the existing system that the Environmental Agency (EA) and the Centre for Ecology and Hydrology (CEH) are already using in the field. Ideally, the system would be able to fulfil the following specifications:

- Measure Na^+, K^+, Ca^{2+}, Mg^{2+} and NH_4^+, NO_3^-, NO_2^-, SO_4^{2-}, Cl^- down to 0.01mg/L
- Measure PO_4^{3-} down to 0.001 mg/L and preferably the same for Br^+ and I^-
- The possibility to measure trace elements such as B, Li, Al, Fe and Mn down to 0.001mg/L
- Operating temperature of 0 to +35°C
- Housed in a secure unit
- Self-calibrating with the option of weekly/monthly field visits
- The running cost should be less than £2k/year and preferably less than £1k/year
- The option for automatic cleaning
- The possibility to be used without mains power, i.e., batteries
- The possibility to monitor rainfall
- The monitoring frequency should preferably be down to 15 minutes without loss of accuracy.

1.1.1 EU Water Framework Directive (WFD)

The WFD is a European Union directive that commits European Union members to accomplishing a good qualitative and quantitative status of all water bodies by 2015. It is a framework that provides steps to achieving a common target rather than adopting a more traditional approach.[7] The WFD has established a comprehensive river basin management-planning scheme to help protect and improve the ecological health of water surfaces such as rivers, lakes, and coastal and ground waters. This is achieved by the use of environmental standards to assess the quality of the water environment and identify the scale of improvements that would be required to enhance the water quality to a better condition.[8]

The WFD requires the control of nutrient inputs into water bodies, which might reach the water surfaces from farming activities and agriculture; therefore, nutrient concentrations from fertilisation has gained considerable attention.[9] The WFD states that the concentration of nutrients should be maintained; for instance, the concentration of nitrates must not exceed 50 mgL^{-1} for rivers[10] [11], and the concentration of orthophosphate and total phosphorus hould be between 0.1-0.2 mg L^{-1}, depending on the river type.[12]

1.1.2 The need for miniaturisation for environmental measurements

River water is one of the most important water sources, and yet its quality is affected by human activities such as domestic, industrial and agricultural activities.[13] Furthermore, changes in climate also affect river water and the water supply in general.[13] The changes in the stream water chemistry of rivers are difficult to predict due to the geographical, chemical and biological factors; each factor has its own impact on river water.[14] However, linking these changes by monitoring the surface water on a sub-

daily basis is highly significant because it helps in understanding the hydrochemical and biological activities of the surface water.[15]

Currently, water-monitoring procedures normally require the collection of samples from remote locations; these have to then be stabilised and transported to a laboratory. The samples are then analysed using laboratory-based systems. The procedure is slow and costly, and samples can degrade. Therefore, one of the best preventive measures is to determine the contaminants as quickly as possible *in-situ*, which is an important task in environmental monitoring.[2] This will enhance the speed of the response to adverse changes in water quality, which then leads to the effective sub-daily monitoring of water quality.

In a recent EPSRC-funded project, LIMPIDS, in which the University of Hull was a partner, portable laboratory-based technologies were deployed in the field in three monitoring sites in the catchment area of the River Thames (Figure 1-1). From these sites, high-frequency water quality data were obtained for the River Enborne, The Cut and The Kennet. Each of the three study sites was instrumented with a YSI multi-parameter 6600 sonde and a high-frequency nutrient monitor (Figure 1-2 and Figure 1-3). These instruments were programmed to send data remotely and they were connected to the Environment Agency/Meteor Communications sensor web network.

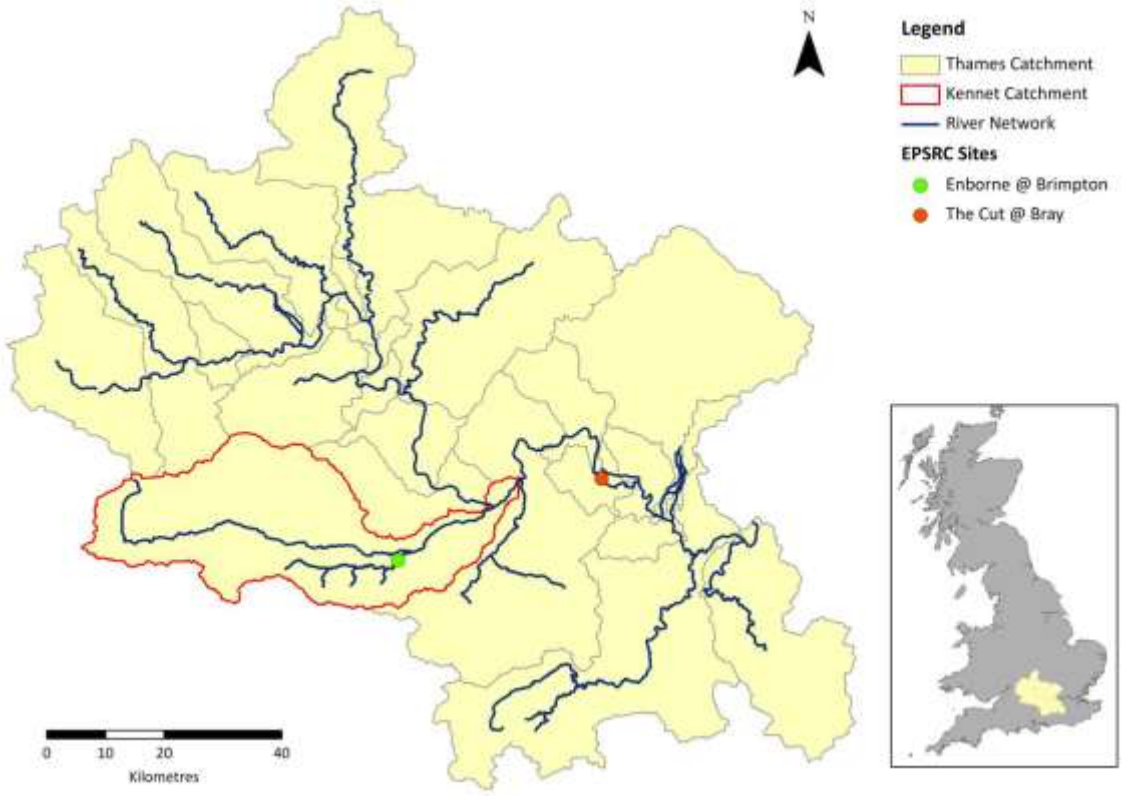

Figure 1-1: The LIMPIDS project study site map

The measurements were transmitted and accessed in real-time. The YSI 6600 sonde measured dissolved oxygen, pH, water temperature, conductivity, turbidity, and chlorophyll concentration. Two further instruments based on flow injection analysis (FIA) were used. The first instrument was a Micromac C, which was used to measure total reactive phosphorus TRP, NO_2 and NH_4. The second one was a Hach Lange Sigmatax and Phosphax Sigma to measure total phosphorus TP, total dissolved phosphorous TDP, and soluble reactive phosphorus SRP. The Hach Nitratax Plus probe was also used to measure NO_3 using a reagent-free, ultra-violet (UV) absorption technique. Such a mobile, *in-situ* laboratory made it possible to investigate dynamics at high-frequency over a range of positions.[15] More details of the operation of these instruments are provided in section 2.2.3.

Figure 1-2: The instruments used on site for water quality monitoring. (1) Hach Lange Phosphax, (2) Hach Lange Sigmatax, (3) YSI Multi-parameter Sonde, and (4) the flow cell to which water is pumped from the river.

Figure 1-3: Photos of the river monitoring station at The Cut at Barry.

Unfortunately, these monitoring stations needed lots of resources; suitable sites and locations had to be found and then they need to be installed. Factors that had to be considered included designing the appropriate structures to install the instrumentation, site suitability, security, mains power, safety and accessibility. These factors limited the choice of the best locations for continuous monitoring. In addition, these *in-situ* monitoring stations required continuous maintenance, which was time consuming and costly.

The lack of mains electricity led to the use of the propane-fuelled generator to power the instrumentation, which was expensive and resulted in measurements being taken every two hours instead of every hour. Also, winter temperatures caused problems, with too much power required for heating problems. Furthermore, the river water sample required filtration to maintain the instrumentation and avoid any interference that would affect the measurements. However, the filtration of the river water sample for the measurement on site was very difficult; even with the air-purge system within the filtration module, the filters still became clogged. This restricted the extraction of the sample and the continuous determination of filtered phosphorous fractions, which is very important for environmental monitoring (See section 1.2).

The results obtained from the instruments in the stations show that: the use of field-based laboratory instrumentation is very useful but, from the experiences of deploying and maintaining the equipment in this project, it is not ideal for river water monitoring, because it requires mains electricity. This is very significant limitation of the portability of the monitoring system, as it affects the choice of location and sampling. In addition, a field-based laboratory is very expensive, consumes large amounts of reagents and waste water, needs more infrastructure to make it portable, and is not sufficiently secure. It

also requires lots of workers and employees for maintenance, as well as the time spent on housing the equipment at the location.

New technology is needed to overcome the practical problems associated with the field-based laboratory system currently used in this project. The development of a rapid, accurate and robust *in-situ* microscale analytical technique that can solve these problems would be highly desirable. With these kinds of devices, the *in-situ* measurement of target pollutants at a specific location would explain many complex reactions of the biodegradation of toxic organics that occur in soil, biofilm and sediment.[2, 16] They might also be capable of providing continuous, *in-situ* monitoring of contaminants flowing in surface water and groundwater. The need for accurate, robust *in-situ* microscale monitoring is not just for hazardous material in river water, but is more universal. For example in the remediation of hazardous waste sites, especially for those using bioremediation techniques, there is a significant need for monitoring. Fast information feedback during waste site remediation is vital for the sustainable management of soils[17]. Other possible environmental applications include the monitoring of stream or lake sediments, water and wastewater treatment reactors, and water distribution schemes.[2]

Lab-on-a-chip devices for field or *in-situ* monitoring of river water could provide advantages over the existing *in-situ* continuous monitoring technology, since they require low power and much smaller amounts of reagents and waste.[18] Most importantly, their portability means that the measurement can be carried out in many locations within a sensor network.[15]

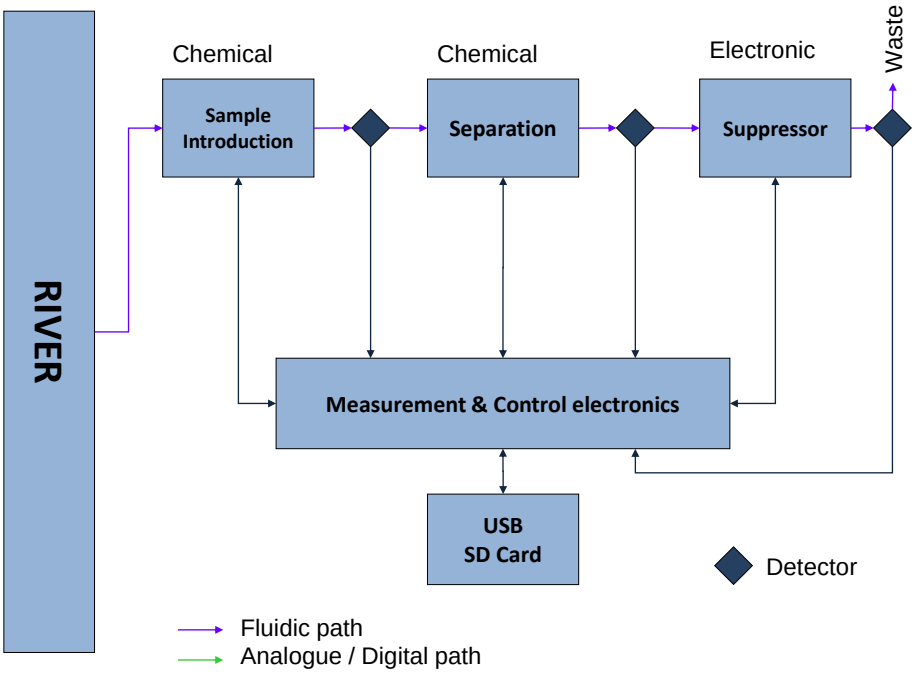

Figure 1-4: Block diagram of the analytical system

The block diagram in Figure 1-4 demonstrates an overview of the planned system. It is divided into four parts. The sample introduction would extract the target ions from the water pumped out of the river. After that, the separation system would separate the ions before they enter the detection cell. The detector, which would be combined with a baseline suppression system, measures the current conductivity of the cell and provides the results that could be stored for later use or connected to a sensor network.[19]

In this interdisciplinary project, the engineers were focused upon developing the control systems and the detector, whereas the analytical science aspect of the project focused on combining sample introduction and separation.

This project concentrates on the development of novel methodology based on microfluidics, which exploits the advantages of miniaturisation for the sample introduction and separation of a selected range of inorganic ions that can be used for *in-situ* water monitoring.

1.2 Ions in water and its implications

Inorganic ions can cause water pollution, having their own ways of entering the environment and their own specific dangers.[20] Inorganic materials are already present in the environment and river water in particular has ions from rocks and minerals, as well as from metals such as gold, silver, copper, lead, zinc, and chromium.[21] Nutrients are natural elements in the environment, which are necessary for living organisms. Calcium, magnesium, and sulphur are secondary elements, needed in smaller amounts than the primary nutrients for plants.[22] Calcium and magnesium ions come from rocks and minerals, and these two elements are responsible for creating hard water.[23] Plants in particular require relatively large amounts of the primary nutrients, nitrogen, phosphorus and potassium. These three nutrients are the ones most frequently supplied to plants during fertilisation, such as ammonium nitrate,[24] calcium phosphate[25] and potassium chloride (known as potash fertiliser).[26]

Nitrogen is an essential element for all known forms of life on Earth. It is an ingredient in all amino acids, as it is integrated into proteins, and is present in the bases that form nucleic acids such as DNA.[27] In plants, a large amount of the nitrogen is used in chlorophyll molecules, which are significant for photosynthesis and further growth[28]. Nitrogen gas (N_2) is the largest component of the Earth's atmosphere,[29] and chemical and natural processes convert gaseous nitrogen into compounds such as nitrate or ammonia, which can be used by plants. This is known as the nitrogen cycle, as shown in Figure 1-5, and it is a significant aspect of the ecosystem.[30]

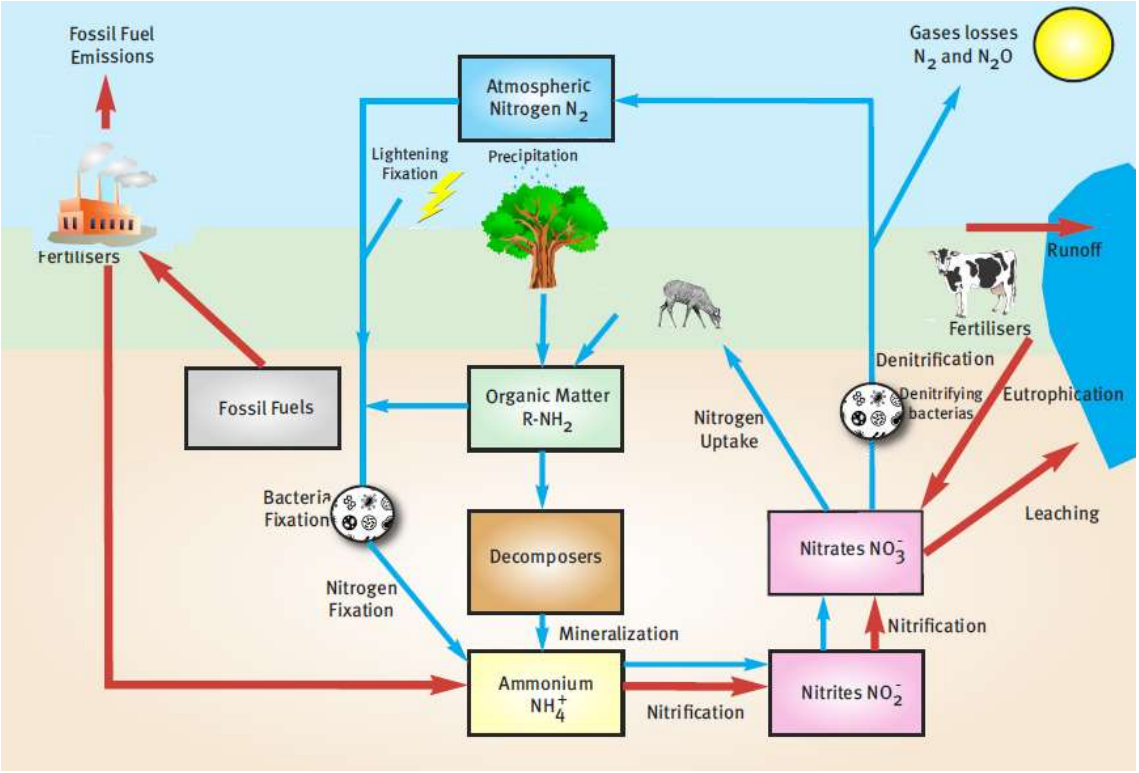

Figure 1-5: The nitrogen cycle [31]

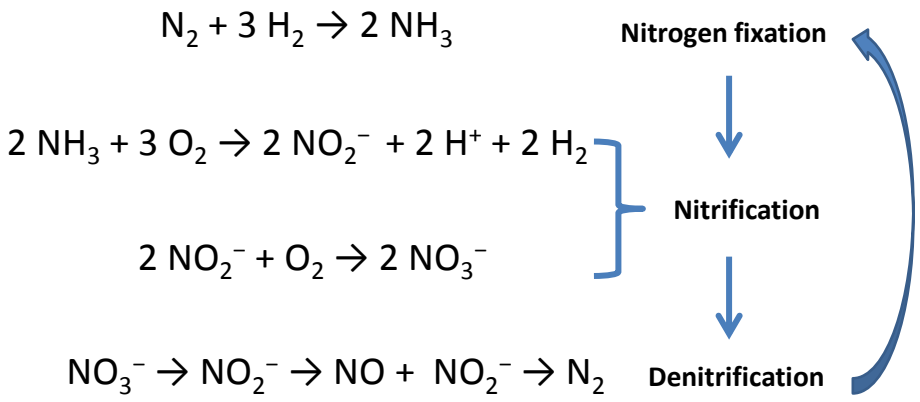

Figure 1-6: Simple diagram of the chemical reaction in the nitrogen cycle[32]

Nitrogen is present in the environment in a wide variety of chemical forms such as ammonium (NH_4^+), nitrite (NO_2^-), nitrate (NO_3^-), nitrous oxide (N_2O) and nitric oxide (NO). The processes of the nitrogen cycle convert nitrogen from one form into

another (Figure 1-5). Microbes are responsible for many of these processes. Atmospheric nitrogen is fixed in order to be used by plants. A proportion of this fixation occurs in lightning strikes, but the majority of fixation is carried out by diazotrophs (symbiotic bacteria); these bacteria have the nitrogenase enzyme that combines gaseous nitrogen from the atmosphere with hydrogen, to make up ammonia.[33] Another process that produces ammonia is ammonification, which occurs after the death of plants or animals, whereby bacteria converts nitrogen back into ammonium salts and ammonia.[34]

A nitrification step occurs in which ammonia is converted to nitrites (NO_2^-) and nitrates (NO_3^-) after ammonification. This process happens naturally and is carried out by bacteria that live in the soil,[35] such as Nitrosomonas.[36] Denitrification then occurs, whereby the reduction of nitrates (NO_3^-) back to nitrogen gas (N_2) completes the nitrogen cycle. This process is also carried out by bacteria such as Pseudomonas and Clostridium in anaerobic conditions.[37]

Phosphorus also has a cycle (Figure 1-7) but it does not enter the atmosphere; phosphorus mainly remains on land and in rock and soil minerals. Phosphorus occurs in the environment as a phosphate ion $(PO_4)^{3-}$. On land, the majority of phosphorus is found in rocks and minerals. Initially, phosphorus-rich sediment is formed in the ocean and then over time, geological processes bring ocean sediments to land. The weathering of rocks and minerals releases phosphorus to rivers in a soluble form, which is then returned back to the ocean. It could also be absorbed by plants, where it is converted to organic compounds.[38] When animals consume plants, phosphorus is either incorporated into their tissues or excreted. When animals or plants decompose following death, phosphorus is returned back to the soil where a large amount of the

phosphorus is converted into insoluble components.[39] Parts of these components are carried out by runoff and returned back to the ocean (Figure 1-7).

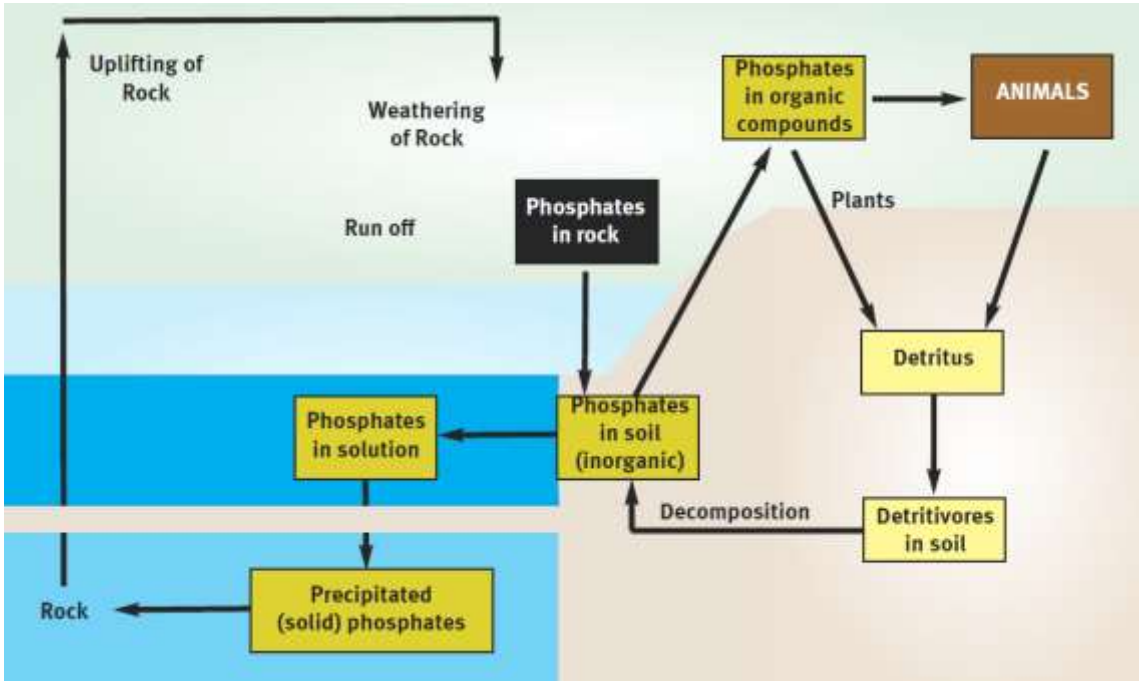

Figure 1-7: Phosphorous cycle [40]

Potassium is found in the environment in different compounds such as potassium chloride (KCl), which is usually used as a fertilizer,[41] potassium hydroxide (KOH), and potassium carbonate (K_2CO_3). Potassium can be found in vegetables, fruit,[42] meat, milk and nuts, and it plays a significant role in human physiology. It is also necessary for almost all forms of life, including plants. Most potassium occurs in the Earth's crust[43] as minerals[44] such as clays, and is then released and cycled in the environment through weathering, which is why it presents in large quantities in the sea.[45] Most soils have a large amount of potassium, although it is soluble in water, but in some areas it is not soluble in water; therefore, it cannot be absorbed by plants, hence its common use as fertilizer.[46]

1.2.1 Nutrients as a cause of pollution

Exceeding the normal, natural amount of nutrients in water will cause environmental problems by causing an unbalanced ecosystem. For instance, nitrogen and phosphorous increase the growth of algae blooms in water surfaces when healthy levels of nitrogen and phosphorus are exceeded (eutrophication).[47] The uncontrolled growth of algae causes several problems for underwater organisms; these algae block sunlight and prevent oxygen from reaching deep underwater species, which leads to serious environmental problems.[48] Moreover, some algal blooms have a negative effect on humans because they produce toxins (such as cyanobacteria[49]) and encourage bacterial growth that can cause diseases, which makes it a serious threat as it is directly toxic to humans and animals.[50] In addition, drinking water and groundwater are of specific concern, as nitrates in drinking water lead to serious human health problems such as methemoglobinemia (infantile cyanosis), cancer, neural tube effects, or spontaneous abortions.[2] In addition, the presence of ammonia in water when it is treated with chlorine, forms chloramines, which have been found to be carcinogenic.[51]

2 Critical review of the determination of ions in water techniques

There are currently several methods for detecting ions in water, which could be portable or laboratory-based systems. The latter method is the most popular as laboratory-based systems usually provide all the necessary tools for high quality measurements, with good accuracy, sensitivity and selectivity. Most of the portable systems have limitations and can only measure one ion at a time.

2.1 Laboratory-based instrumentation for ion analysis

There are two gold-standard techniques used for measuring ions in water: inductively coupled plasma (ICPAES) and ion chromatography (IC).[52] Ion chromatography (IC) is the most widely used analytical technique for the determination of ions in solutions.[53] It is the most convenient technique for the determination of inorganic cations and anions in water.[53-54] Since 1980, IC has been used for the analysis of the most popular inorganic anions in environmental waters[55] as it is fast, very efficient, and has good capacity and sensitivity.[56]

ICP is used for the determination of trace elements in water. It is a powerful technique as it has the advantages of being able to determine many elements simultaneously in a single run with low limits of detection, high accuracy, and precision.[57] There are, however, other analytical techniques used in water analysis such as ion-selective electrodes and titration; these techniques have limitations, which will be discussed later.

2.1.1 Atomic spectrometry

Atomic spectrometry is an analytical technique that determines the concentrations of elements in a sample. In this technique, substances are decomposed into atoms in a flame, furnace or plasma,[58] and the emission or absorption of ultraviolet UV or visible radiation is then measured, with each element having its own unique spectra; the concentration of the element is proportional to the measured radiation.

The most widely used analytical techniques based on atomic spectrometry are atomic absorption spectrometry (AAS) and inductively coupled plasma atomic emission spectroscopy (ICP-AES). Both techniques have been used for the analysis of elements in water samples for a long time, and both are commercially available. ICP-AES has advantages over AAS, as ICP-AES can measure multi-elements in one run, while AAS measures one element per run.[59] Furthermore, the sensitivity of ICP-AES is better than AAS. ICP-AES has excellent features, such as low detection limits, a wide linear dynamic range, and high precision.[60] This technique is very sensitive, being able to measure down to parts per billion (ng/g). It is widely used for the analysis of environmental, pharmaceutical, industrial, and geochemical samples.[61]

2.1.1.1 Inductively coupled plasma atomic emission spectroscopy ICP-AES

In order to create plasma in ICP-AES, argon gas is supplied to the torch, and a high frequency electric current is then applied to the copper coil wrapped around the outside torch,[62] allowing the plasma to form. Liquid or gas samples are then injected into the central channel of plasma via nebulisation, in which the sample solution is converted to an aerosol. Solid samples have to be acid-digested to ensure that the analytes of interest are present in the solution.

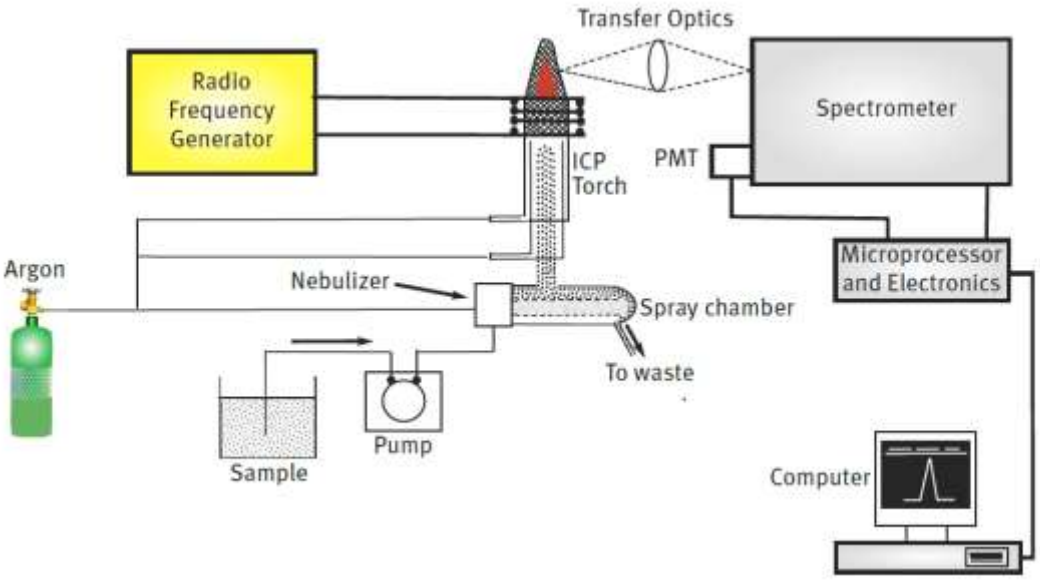

Figure 2-1: ICP-AES schematic diagram [61]

At its core, the ICP has a high temperature of between 6,000-10,000 K,[63] which rapidly vaporises the aerosol. Analyte elements become free atoms in the gaseous state. More collision within the plasma will provide more energy to the atoms, which will promote them to excited states.[64] This high energy usually converts the atoms to ions and then promotes the ions to excited states. The excited atomic and ionic species then relax to the ground state through the emission of photons; these photons have energies that are specific to each atom and ion. Therefore, the wavelength of the photons can be used to identify the elements. The amount of photons emitted is proportional to the initial concentration of element in the sample.[65]

2.1.1.2 Inductively coupled plasma mass spectrometry (ICP-MS)

Inductively coupled plasma mass spectrometry (ICP-MS) is one of the most important analytical techniques for the measurement of elements in a sample. It counts the number of ions at a certain mass of the element. The majority of samples analysed by ICP-MS

are liquid, but gas samples can also be measured directly. As with ICP-AES, solid samples can also be analysed after digestion. In ICP-MS, the plasma is used as an ion source; a proportion of the ions are extracted via an interface into a mass spectrometer, which separates into their mass and determines their concentration.[63]

As an instrument, the ICP-MS usually has the ability to measure most of the elements in the periodic table. It can measure with detection limits down to parts per trillion (ppt) due to the very high sensitivity of the electron multiplier detector, and it also has the ability to obtain isotopic information. It is routinely used in many areas of analysis, such as environmental and forensic sciences, and industries.[66] In comparison to ICP-AES, however, ICP-MS is more sensitive but has less tolerance of high solid-liquid samples, as salt can block the nickel cones used to sample the ions in the interface between the plasma and the mass spectrometer.[67]

Despite all the fantastic advantages of both ICP-AES and ICP-MS instruments, especially for water analysis, and the measurement of elements and cations in particular, they contain some major limitations, meaning that they are not ideal for *in-situ* monitoring of water. The main disadvantages are, firstly, the high cost of purchase. They also have high operational costs and require well-trained personnel for operation. Secondly, the size of the instrument is very big and requires extra room for the argon gas. Furthermore, it needs to be housed in a room that has good temperature regulation. Thirdly and most importantly is the portability of the system: the ICP is usually big in size and requires a vast amount of argon for operation, which limits the portability and movement of the system from one place to another. As previously discussed, for *in-situ* water monitoring, portability is a very important factor as it greatly helps in monitoring the changes to water surface.

2.1.2 Ion chromatography (IC)

IC has the ability to measure concentrations of most anions, such as fluoride, chloride, nitrate, nitrite, phosphate and sulphate, as well as most cations such as sodium, potassium, calcium and magnesium, with limits of detection (LOD) down to parts per billion (ppb).[68] An IC system consists of the column and the detection system, which is usually conductivity (suppressed or non-suppressed), spectrophotometry, or electrochemistry (amperometry or potentiometry).[69] There are two separation mechanisms that can be used for inorganic anions in IC: ion-exchange chromatography (IEC) and ion-pairing chromatography (IPC).

IPC depends on the addition of an ion-pairing reagent to the eluent, which is a counter ion that allows the formation of neutral ion-pairs with the charged analytes.[70] The ion-pairing agent often has an alkyl chain, which adds hydrophobicity so that the ion-pair can be retained on a reversed-phase HPLC RP column. When used with typical hydrophobic HPLC phases in the RP mode, they can be used to increase the selectivity of retention of charged analytes.[71] Negatively charged reagents that have a charge opposite to the analyte of interest, such as decane sulphonic acids, can be used to retain positively charged ionic bases.[71-72] On the other hand, a positively charged reagent, such as tetrabutyl ammonium phosphate,[73] can be used to retain negatively charged ionic acids.

IEC is the most widely used technique for the separation of inorganic ions; it utilises ion-exchange resins to separate inorganic ions based on their interaction with the resin. Its main use is for the analysis of anion, as it is a fast analytical method for such analysis,[74] but it is also used for cationic species.[75] In IEC, the analyte's molecules are retained on the stationary phase, based on ionic interactions. Separation can be selectively achieved through adsorption and the release of samples from the stationary

phase, as discussed below. Ion exchange is established with the equilibration of the exchanger, using the pH and ionic strength of the mobile phase. In the equilibrium, exchangeable groups are associated with counter ions. When equilibrium is reached and the sample added, ions undergo additional adsorption replacing the counter ions on the column and reversibly bind to the stationary phase. The unbound substances will pass through the column with the void volume. Finally, substances are removed from the column by increasing the ionic strength of the eluent.[76]

The most commonly used detection system for IC is conductivity, despite the fact that there is a high background conductivity signal from the eluent. To overcome this high background, chemically suppressed conductivity detection is widely used, as initially established by Baumann *et al*. in 1975[77] and commercialised by the Dionex Corporation.

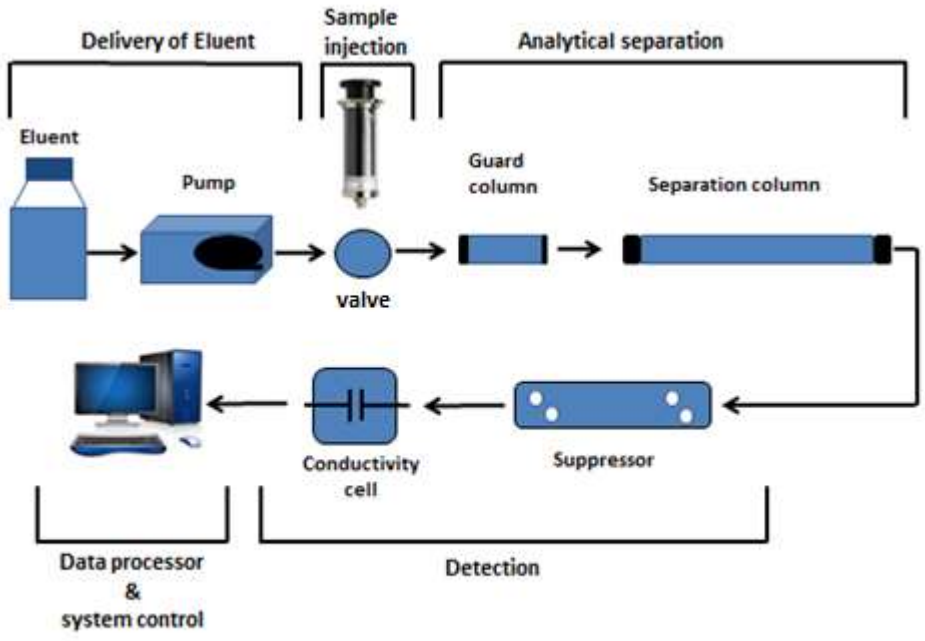

Figure 2-2: Ion chromatograph operation principle[78]

Figure 2-2 shows the operation principle of an IC system, based on ion-exchange separation with chemical suppression. The pump flushes eluent through the IC system, which is required to provide a consistent and reproducible flow rate of the eluent through the separation column. The eluent used with chemical suppression is usually potassium hydroxide.[79] Ion capacity in IC plays a great role in measuring the concentration of competing ions in the eluent. A high capacity column usually requires more concentrated eluent, as the eluent composition gives the best flexibility for optimising the retention time.[78] Different eluents can be used but NaOH or sodium hydrogen carbonate buffers are commonly used[80] because they have low conductivity, which increases the sensitivity and the limit of detection (LOD). The hydroxyl (OH^-) is the weakest ion-exchange competing anion and the high pH allows anions of weak acid to be ionised and then retained.[78] The concentration of the eluent should be high enough to elute anions with a high affinity.[81]

The sample including the analytes of interest is introduced to the top of the column by a loop injector valve, and carried through the column by the pumped eluent. The ion-exchange stationary phase in the column consists of uniform small diameters that may be inorganic or polymeric particles consisting of fixed ions and exchangeable counter-ions ($\boldsymbol{R-E^-}$), which are displaced by the eluent ions and sample ions as they move through the column.[82] In anion analysis, an anion-exchanger column is used with quaternary amine $\mathbf{-N(CH_3)_3^+OH^-}$, and in cation analysis, cation exchangers are used, such as sulphonic acid $\mathbf{-SO_3^-H^+}$.[83] Modern ion exchangers phase are porous, layered beads with an impervious centre covered in a thin (2 μm) porous outer layer with the ion-exchange layer.[84] This results in faster rates of mass transfer and higher efficiencies.

For example, in the separation of chloride Cl^- and fluoride F^- using an anion-exchange column where both are at the same concentration and the eluent is sodium hydroxide, the column must be washed by the eluent prior to injection of the sample in order to totally change the ion-exchange surface to $-\boldsymbol{OH}^-$. When chloride and fluoride are injected into the column, an equilibrium step occurs.

$$\boldsymbol{R-OH^- + Cl^- \leftrightarrow R-Cl^- + OH^-} \qquad \textbf{Equation 2-1}$$

$$\boldsymbol{R-OH^- + F^- \leftrightarrow R-F^- + OH^-} \qquad \textbf{Equation 2-2}$$

Separation in IC is measured by the retention factor (K). The analyte is distributed between the mobile and stationary phases. This was originally called the distribution constant but is now called the retention factor.[85]

$$\mathbf{K = \frac{amount\ of\ analyte\ in\ column\ stastionary\ phase}{amount\ of\ analyte\ in\ column\ mobile\ phase}} \qquad \textbf{Equation 2-3}$$

In ion chromatographic separation, each ion has a different distribution constant between the stationary and mobile phases. This constant represents a competition between these ions for exchange sites on the ion exchanger, on the column surface. For example, for chloride separation in Equation **2-1**, the equilibrium constant *k* is:

$$\boldsymbol{k = \frac{[R-Cl^-][OH^-]}{[Cl^-][R-OH^-]}} \qquad \textbf{Equation 2-4}$$

The retention factor can be written as below[86]:

$$\mathbf{K = \frac{[R-Cl^-]}{[Cl^-]}} \qquad \textbf{Equation 2-5}$$

Alternatively, the retention factor can be calculated using the retention time (t_R) of the sample ion and the dead time (t_0); this can be defined as the time taken for unretained components to pass through the column and detector.[87]

$$K = (\boldsymbol{t_R - t_0})/\boldsymbol{t_0} \qquad \textbf{Equation 2-6}$$

The importance of the retention factor is that it does not change, even when the column length or the flow rate changes.[86]

During the separation process, the stationary phase contains $\boldsymbol{R{-}Cl^-}$, $\boldsymbol{R-F^-}$ and $\boldsymbol{R-OH^-}$, and the eluent is a mixture of Cl^-, F^-, OH^- and H^+. Chloride and fluoride move down to the end of the column but because chloride has a stronger affinity to the positive charge on the column, chloride moves more slowly and elutes later than fluoride (Figure 2-3).[88]

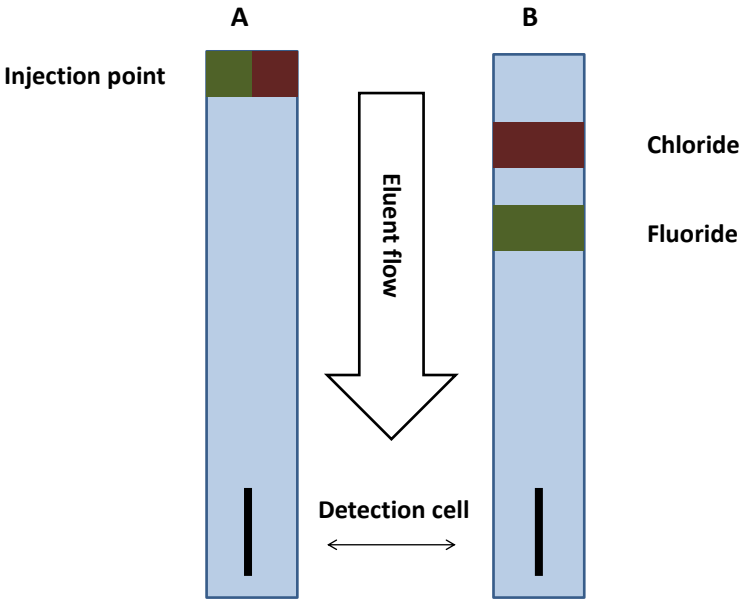

Figure 2-3: Anion-exchange column, A: at the injection point, B: following elution of KOH

Depending on the ion-exchange groups attached to the column particles, the sample analytes pass through the column at different rates, ions in the sample are slowed down

depending on their attraction to ion-exchange groups on the column surface, the ions reach the suppressor separately, and then the eluent and analyte ions are transferred to the detector cell at different times.[89]

To obtain optimal separations in chromatography, band broadening must be minimised; therefore, the efficiency of the column should be measured. This can be calculated from the number of theoretical plates of the column (N). This theoretical model supposes that the chromatographic column consists of a large number of separate layers, and it can be calculated from Equation 2-8. The analyte moves down the column through the transfer of equilibrated eluent from one plate to the next, and the higher the value of N, the better the separation. Also, the efficiency of the separation can be obtained from the plate height and the height equivalent to a theoretical plate (H); the higher the value of **H** the better the separation. This can be calculated from Equation 2-7.[90]

$$N = 5.55 \left(\frac{t}{w_{0.5}}\right)^2 \qquad \textbf{Equation 2-7}$$

$$H = \frac{L}{N} \qquad \textbf{Equation 2-8}$$

Where HETP is the height equivalent to a theoretical plate, L is the column length, $W_{0.5}$ is the width at half the peak height, and t is the retention time.

Another measure of the efficiency of the separation is the resolution (R). The resolution of two species, A and B, can be calculated from Equation 2-9.

$$R = \frac{2[(t_r)_B - (t_r)_A]}{W_A + W_B} \qquad \textbf{Equation 2-9}$$

Where R is resolution, $(t_r)_B$ is the retention of the second peak, $(t_r)_A$ is the retention of the first peak, W_A is the width of the first peak and W_B is the width of the second peak. The best resolution can be achieved when the R=1.5, which is the baseline resolution.[90]

The main function of the suppressor is to reduce the background conductivity of the eluent, which will increase the detector sensitivity for the analyte ions.[91] The detector measures the conductivity of the eluent as it passes through the detector cell. However, the conductivity of an eluent with a high level of ions such as OH^- or CO_3^{2-} could be higher than the conductivity of ions in the sample analyte, and so the eluent conductivity needs to be supressed before reaching the detector.[81] The suppressor consists of an ion-exchange membrane that converts the electrolyte eluent into water.[92]

For example, in anion exchange, the suppressor membrane is a cation exchanger, so consider if Cl^- was the analyte ion and the eluent consisted of NaOH. The eluent reacts in the suppressor column to exchange the Na^+ ions onto the column, leaving $\mathbf{RSO_3H}$ and producing $\mathbf{RSO_3Na}$ (Equation 2-10). At the same time, cations from the sample such as Na^+ are removed by the membrane suppressor and replaced by H^+ ions, further reducing the conductivity and the eluent react, as in Equation 2-11[22, 78]:

$$\mathbf{NaOH + RSO_3H \leftrightarrow H_2O + RSO_3Na} \qquad \textbf{Equation 2-10}$$

$$\mathbf{NaCl^- + RSO_3H \leftrightarrow HCl + RSO_3Na} \qquad \textbf{Equation 2-11}$$

The results of this process are that the conductivity of the eluent is greatly reduced, whereas the analyse conductivity increases because sodium ion is replaced by hydrogen ion, which eventually improves the sensitivity of the analyse.

Similarly, in cation exchange, the suppressor is an anion-exchanger column where more OH^- ions are present. The eluent is changed to water, whereas the conductivity of the sample is increased because the Cl^- ion is replaced by OH^- (Equation 2-12 and Equation 2-13).[78]

$$\mathbf{R-OH^- + H^+ + Cl^- \leftrightarrow R-Cl^- + H_2O} \qquad \textbf{Equation 2-12}$$

$$\mathbf{R-OH^- + Na^+ + Cl^- \leftrightarrow R-Cl^- + Na^+ + OH^-}$$ **Equation 2-13**

Another type of chemical suppression used for anion analysis has been developed by Metrohm; the suppressor consists of three units that work at the same time through a rotation cycle. One unit is in line with the eluent and the conductivity detector, another works in line with regeneration reagent, and the third is washed with pure water. The suppressor can be taken through one more step to remove the carbon dioxide (generated from the reaction in the suppressor Equation 2-14) and carbonate from the sample; this means that the sodium hydrogen carbonate eluent is converted to water[93] [93b].

$$\boldsymbol{R-SO_3^-H^+ + NaHCO_3 \rightarrow R-SO_3^-Na^+ + H_2O + CO_2}$$ **Equation 2-14**

As mentioned previously, conductivity detectors are by far the most widely used detector in IC, as they provide a universal detection system responding to all ions. The detector consists of flow cells containing two electrodes over a range of 1-5 mm,[94] [94b] usually made of a noble metal, e.g., platinum. In the conductivity cell are two electrodes to which an electric potential is applied. The ions passing through the detector flow cell move in response to the electrical field with anions moving towards the anode and cations moving to the cathode. The ion movement creates a current and the current is measured and amplified to produce a signal that is proportional to the concentration of the ions passing through the cell in the detector. The main disadvantage of this detection system is that it responds to the eluent composition, which has an impact on the sensitivity; this leads to the use of suppression in the IC detection system.[95]

Other detection techniques can be used for inorganic separation, such as amperometric detection, mass spectrometric detection, and direct ultraviolet UV and post-column reaction spectrophotometric detection.[96] In general, UV detection is the most commonly used detection system for chromatographic separation; however, most

inorganic ions are not suitable chromophores for UV detectors, as they do not absorb UV light. This problem can, however, be overcome by employing an indirect UV detection system, which has been demonstrated to provide good results.[97] In the indirect technique, the wavelength of detection is chosen such that the absorbance of the eluent ion is high, while it is zero for the analyte ions. Therefore, when an analyse ion passes through the detector flow cell, it displaces a specific amount of eluent co-ions, and the absorbance of the eluent reduces; this results in negative peaks, following which ions can then be detected.[98]

2.1.2.1 Spectrophotometric detection

Spectrophotometry is used to measure the amount of light that an analyte sample absorbs. It operates by passing a beam of light through a sample and measuring the intensity of light that reaches the detector (Figure 1-1).

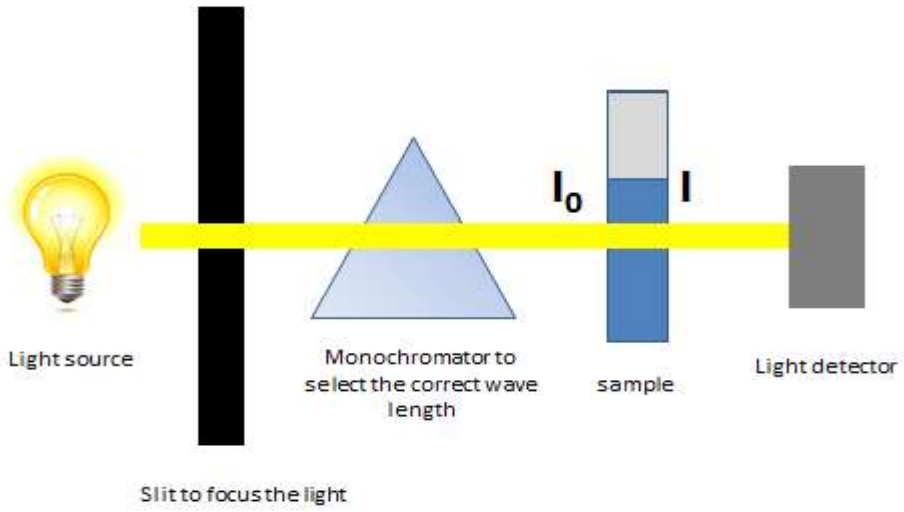

Figure 2-4: The operation principle of a spectrophotometer

The spectrophotometric detector is based upon the Beer-Lambert law:

$$A = \varepsilon bc$$ **Equation 2-15**

Where A: is Absorbance, b is path length cm, c is molar concentration M and ε: is molar absorptivity M^{-1} cm^{-1}.[99]

UV and fluorescence are the most common spectrophotometric techniques used in ion analysis. However, since many solutes absorb UV light across a wavelength range of 180 nm up to about 600 nm, this detection system is also very popular within chromatographic analysis. In this detection technique, an emission from the mercury (254 nm), zinc (214 nm) or deuterium lamp with convenient intensity passes through the flow cell,[40] and the UV light can be optimised for different analytes.

For compounds that do not absorb UV light, such as most inorganic ions, indirect UV detection can be used. In the background eluent, a UV-absorbing co-ion is dissolved, known as the UV-probe.[100] The non-absorbing analyte ion-band replaces the absorbing UV-probe. Thus, there will be less absorption at the position of the non-absorbing analyte and the signal will illustrate a negative peak. The amount of replacement depends on the charge of the UV-probe and the analyte ions, and on the ion's mobilities. The amount of replacement is known as transfer ratio,[101] and the best transfer ratio is obtained when the mobility of the UV-probe matches the mobility of the analyte ion; comparing the mobilities of the analyte ion with the UV-probe will determine the peak shape. However, indirect fluorescence[102] has been employed almost as indirect UV, with less popularity than UV because it requires further reagents to increase the sensitivity. However, the disadvantages of indirect detection are the addition of more reagents for derivatisation and the relatively low sensitivity.[103]

2.2 Low-cost instrumentation for water analysis

There are several other analytical instruments that can be used for water monitoring, such as ion-selective electrodes, titration, and electrochemical techniques. These techniques have a much lower cost than ICP-AES or IC, and they remain popular in water monitoring, especially for the determination of inorganic ions.

2.2.1 Ion-selective electrode (ISE)

These are based on potentiometry, which measures the difference in electrode potentials. Determination of pH using a pH electrode is an example of a potentiometric technique.[104] The movement of ions from a high concentration to a low concentration through selective binding with some sites within the membrane, generates a potential difference.[105] ISE can be found in different types, namely, glass membranes, solid-state electrodes, liquid-based electrodes and gas-sensing electrodes.[106] ISE is a common analytical technique for the determination of inorganic ions in water,[107] such as fluoride,[108] nitrate[109] and ammonia.[110]

ISE analysis has some advantages, such as requiring a very small amount of chemical reagent; usually, there is no waste and it responds quickly, within seconds or a minute. However, it disadvantages are: electrodes can be fouled by organic solutes,[110] and interference from other ions in the same sample solution can influence the analysis.

2.2.2 Further electrochemical techniques

Further electrochemical techniques include coulometry, where nearly 100% electrolysis occurs with the application of a voltage and the electrochemical cell's current is measured over time. Voltammetry is similar but occurs in microelectrode with only a small percentage of electrolysis occurring.[111]

Voltammetry is a technique that measures the current of an electrode as a function of the voltage that is applied to the electrode. Amperometry is similar to voltammetry but the current is measured at a fixed voltage.[112]

The voltammetry technique requires a potentiostat to control the voltage and measure the current along with an electrochemical cell. The simplest form of electrochemical cell is the one that uses two electrodes. The potential of one electrode is sensitive to the analyte's concentration (working electrode), whilst the second electrode completes the electrical circuit and provides a reference potential against which we measure the working electrode's potential.[113]

Such electrochemical techniques are inexpensive and can be employed *in-situ,* providing direct readings from the water surface in difficult positions.[114] When reactions occur at the electrode surface, the electrode is fouled. Electrodes can be fouled by organic solutes or salts and this may cause interference from other ionic species in the same sample solution, which would have an impact on the analysis.[115]

2.2.3 Flow injection analysis (FIA)

Flow injection analysis (FIA) can be defined as the injection of a sample into a moving stream of liquid, to which several reagents can be added. After a certain amount of time, the sample reacts with the reagents and reaches a detector; this detector is normally a spectrophotometric cell[116] (Figure 2-5). FIA is a powerful technique within analytical chemistry, and it is widely used for a variety of applications in areas such as industries, medicine, pharmaceutical analysis, marine analysis[117] and water analysis.[63]

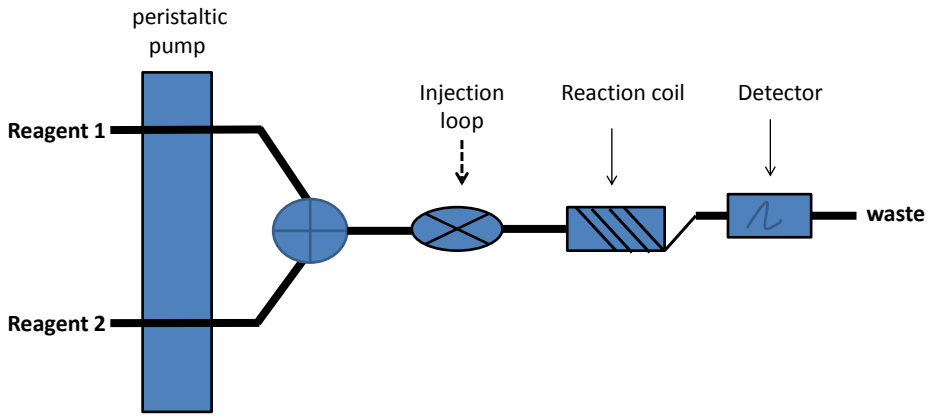

Figure 2-5: schematic drawing of FIA

FIA has been applied to the analysis of water, especially for the measurement of inorganic ions in water such as nitrite, nitrate and phosphate,[116] using spectrophotometric detectors.[118]

2.2.3.1 Nitrite and nitrate

The determination of nitrite and nitrate is usually by a colorimetric technique following the reaction of nitrite with sulphanilamide and N-(1-Naphthyl)ethylenediamine dihydrochloride (NED);[119] the diazonium-coupling reaction occurs in the presence of nitrite to give a strongly red-coloured azo compound, which is detected spectrophotometrically at 520–540 nm.[120] Nitrate is also measured spectrophotometrically, whereby nitrate is converted to nitrite by a reduction agent to create a nitrite complex that can be measured spectrophotometrically.[47]

This common FIA system for measuring nitrite concentrations is usually large in size, which limits its deployment capabilities, consumes large amounts of power, and most importantly, large amounts of reagents (mL per sample).[121] It is not technically ideal for an *in-situ* monitoring system. Therefore, Beaton *et al.* developed a miniaturised

automated nitrite sensor that was compact and required less power and minimal reagent usage.[122] This new system overcame some of the limitations associated with the typical FIA for nitrite and nitrate.

2.2.3.2 Phosphates

The majority of the phosphorus in surface water is present in the form of phosphates, and can be divided to four main parts[123]:

1. Total orthophosphate, also known as total reactive phosphorus (TRP), is an inorganic form of phosphorus, such as PO_4^{3-}. This form of phosphorus is directly absorbed by algae[124]; therefore, it is important to keep its level as low as possible to prevent the unnecessary growth of algae. The sample is measured using a colorimetric method (see below) and is not filtered; therefore, it measures both:

- Dissolved orthophosphate; and
- Suspended orthophosphate.

2. Total phosphorus is the sum of all forms of phosphorus, namely:

- Orthophosphate
- Condensed phosphates (also called polyphosphates) such as $P_3O_{10}^{5-}$, which was commonly used in detergents[125]
- Organic phosphates, which are organically bound phosphates found in human and animal waste or in decaying living species.[126]

  As most phosphorus is bound up organically and inorganically,[127] testing TRP alone (as mentioned above) is not an indication of the actual amount of phosphorus that exists in an aquatic system, it only indicates the soluble and available to plants at that point in time. Thus, in order to measure total phosphorus, the sample must

be vigorously digested (treated by strong acid and high heat) to break the strong chemical bonds. This sample can then be analysed using the colorimetric method used to measure TRP.

3. Dissolved phosphorus is the measurement of the fraction of the total phosphorus, which is in a solution in the water. This requires filtration and is then measured by the same colorimetric method used to measure TRP.
4. Insoluble phosphorus is calculated by deducting the dissolved phosphorus result from the total phosphorus result.

Spectrophotometric methods, based on colorimetric detection, have also been widely used to detect phosphate in water.[128] In this method, the sample is treated with an acidic molybdate solution to produce a phosphomolybdate complex, which is further reduced by ascorbic acid to produce an intensely coloured component. This routine analysis of phosphate is not ideal for various reasons, but the most important reason is the large amount of reagent consumed on a regular basis as the analysis is being undertaken.[129]

Quintana *et al.*[90] report an amperometric detection of orthophosphate in seawater using the batch injection analysis (BIA) technique. The phosphomolybdate complex, formed in the presence of nitric acid, ammonium molybdate and phosphate, was reduced. The system is simple, limits the consumption of reagents, and has a low detection limit (0.3 μmol l^{-1}). However, despite the fact that this system requires fewer reagents than the typical FIA, it still requires the further addition of reagents and it only measures phosphates.

FIA instruments are commercially available for the determination of nutrients, and LIMPIDS project described earlier uses *in-situ* FIA portable systems for the determination of phosphate, nitrite and ammonium.[15] The systems were shown to be

reasonably robust, reliable, and easy to calibrate.[130] Furthermore, the data obtained from the systems were significantly beneficial for the hydrochemical aspect of the project.[15] However, as previously described, they had high power requirements, needed regular maintenance, and produced large volumes of waste water (about 100 L every two weeks). Furthermore, FIA techniques are usually designed to detect one species at a time, when the measurement of several species is actually required, such as nitrite, nitrate and phosphate. Moreover, according to the Beer-Lambert law, the spectrophotometric techniques depend on the path length (b), which might be affected in a miniaturised system, as the manipulation of the size is significant in miniaturised devices[131] such as CE.

2.2.4 Lab-on-a-chip (LOC)

Lab-on-a-chip (LOC), also known as micro total analysis (μTAS), is a form of technology that can integrate miniaturised laboratory functions such as separation, extraction and detection, for the analysis of chemical compound mixtures, on one chip, by using very small fluid volumes between a range of 10^{-9} and 10^{-18} L[132] (microfluidic). LOC technology has very good advantages over the normal analytical laboratory-based instruments. It has the ability to deal with very small amounts of samples and reagents, with a high resolution of separations, good sensitivity and selectivity, low cost, and rapid analysis.[133]

The concept of miniaturising measurements started in the 1960s with the development of microelectronics, but the first reported integrated LOC device was in 1979, and it was the total "Gas Chromatographic Air Analyser Fabricated on a Silicon Wafer" developed by Terry *et al.*[134] Publications on LOC and its related subjects have increased significantly in the 1980s and 1990s, to around 3,500.[135] The trend going forward is towards more complex, integrated systems that have the capability for more

comprehensive analyses, using advanced electronics and microfabrication, mostly for biochemical analysis such as DNA.

However, the environmental analysis of inorganic ions using LOC was introduced by Greenway *et al.* in 1999,[136] and in 2001, work on inorganic ions, nitrate in particular, was carried out by Petsul *et al.*[137] In 2005, Marle *et al.* demonstrated a total system for environmental analysis[16] and in 2008, Cleary *et al*. developed an environmental *in-situ* LOC system for the analysis of phosphate.[138] In 2012, Beaton *et al.* reported an "LOC Measurement of Nitrate and Nitrite for *In-situ* Analysis of Natural Waters." This system (Figure 2-6) was based on a miniaturised FIA system: the chip incorporates a fluidic manifold that allows the selection of one of four standards (nitrate or nitrite), the sample, and a blank. The fifteen valves are used to control the fluids, which are mounted directly to the chip. A customised syringe pump is used in the system; it has been designed especially for this work. The pump is used to drive fluid through three titanium syringes for sample/standard, buffer solution, and Griess reagent (the chemical reaction used for nitrite analysis). The chip contains three absorption cells: a reference cell and two measurement cells. The system employs a spectrophotometric technique for the determination of nitrate and nitrite. This integrated system requires several mixing steps, which is very challenging.[129]

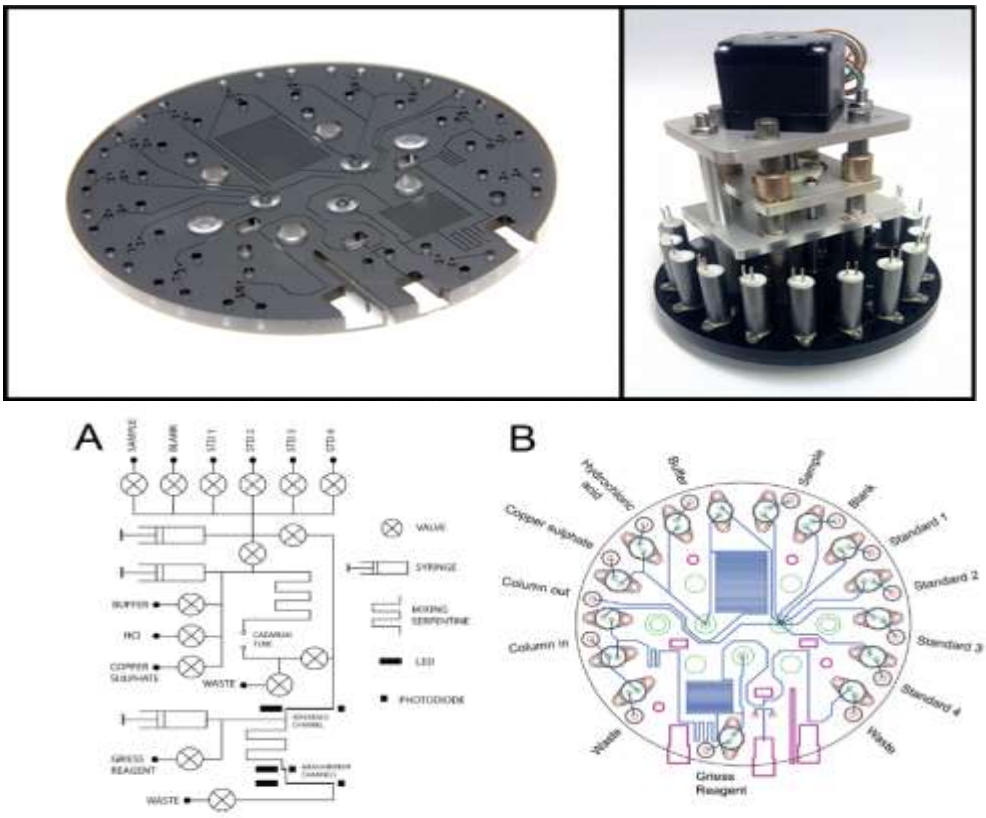

Figure 2-6: Beaton *et al.* microfluidic system for *in-situ* determination of nitrate [139]

Despite the significant progress of LOC technologies, especially the work of Cleary *et al.* and Beaton *et al.*, the systems measure one species per run, measuring nitrite or nitrate at separate runs by passing in the system. For measuring nitrite, fluid is directed through a reference cell, and is then mixed with a Griess reagent in the mixing channel. Absorption is then determined in two subsequent measurement cells. For nitrate measurement, fluid is added to an imidazole buffer, passed through a serpentine mixer, then through an off-chip cadmium tube prior to passing through the reference cell and mixing with the Griess reagent. Furthermore, LOC systems still lack the capability to measure several inorganic ions in a single run. Although these systems work automatically, they are very complex, with lots of tubing and pumping required, meaning that it is still not an ideal system.

A miniaturised system that has the ability to measure inorganic ions in one run, is highly desirable. IC systems are the golden standard for the measurement of several ions in one run, and so a miniaturised version of such a system is desirable. The aim of this work is to develop a novel analytical LOC device that is capable of measuring and detecting several inorganic ions in water samples *in-situ*, at high-frequency measurements, by utilising microfluidic advantages that include sample introduction, ion injection, ion separation and detection, all in a single run on an LOC device.

2.3 Miniaturisation of the separation of ions

Miniaturised separation has been demonstrated in different forms,[140] using monolithic columns[141] and capillary electrophoresis.[142] The application has mainly been used for large biochemical molecules but some results have been obtained for small species such as ions.[143]

The achievement of high efficiency separations with traditional ion chromatography requires columns packed with micron-sized particles, which causes high back-pressure when pumping the eluent through the column. The invention of monoliths has led to a completely new type of separation media. Monoliths are continuous and, therefore, do not contain interparticle voids, which are typical of packed columns. They are bimodal and consist of a network of large, interconnected flow-through pores that reduce back-pressure, but also small pores that contribute to a high surface area, which offer the desired interactive separation modes. Other major advantages of monoliths include the simplicity of preparation and their high permeability.[144]

2.3.1 Monolith column and IC

Recently, there has been an increased interest in monolithic stationary-phase media for high-performance separations of organic and inorganic ions. Initially, work concentrated on the separation of organic compounds, and subsequently focused on the separation of inorganic ions, and an efficiency was demonstrated that equals or even surpasses the classic packed column, even with short monolithic columns.[145]

Monolithic separation media can be divided into two categories: silica (inorganic) monoliths and polymer (organic) monoliths. Both types have been used successfully for ion-exchange chromatography. However, the most widely used monolithic stationary-phase is silica, as it provides favourable mechanical stability and flow characteristics (low pressure), and a range of chemical modification are available that allow for ion separation. Polymer-based monoliths have shown better separation of larger molecules, such as proteins and nucleic acids, whereas silica monolithic columns enable fast separations of smaller molecules.[92] Polymeric stationary phases do have an advantage over silica-based supports for anion-exchange chromatography, since they exhibit superior stability at high pH, as they are compatible with analysis using hydroxide gradients. However, a silica-based monolith has more mechanical stability than polymers, especially for the separation of inorganic ions.[146]

Monolithic columns can be used as a part of an LOC device for the separation of inorganic ions, as they can be adjusted to be within cm range[147] and have low back-pressure,[148] meaning that they do not require a high pressure pump. They can be modified with ion-exchange stationary phases to provide good selectivity, efficiency, and limit of detection LOD,[77] which is a great contribution to the miniaturisation of IC.[149]

The disadvantage of using the monolithic column in the detection of inorganic ions for river water monitoring is that it can easily be affected by contamination, because it has lots of very small pores that are easily blocked by any matrices. This could increase the back-pressure and interfere with the measurement.

2.3.1.1 Preparation of silica monolithic columns

As previously mentioned, silica monolith provide the best basis for the separation of small molecules, despite the fact that they cannot cope with a high pH eluent; otherwise, they demonstrate good chromatography performance, low back-pressure, mechanical strength, and simplicity of preparation.[150]

2.3.1.1.1 Theoretical consideration in preparing a monolith

Silica monoliths with macropores and mesopores were first introduced by Nakanishi *et al.* in 1992.[151] Since then, they have gained much attention in the field of separation. The bimodal-pore silica monolith is normally fabricated using a two-step method involving hydrolysis and the condensation of an alkoxysilane (such as tetraethoxysilane TEOS)[152] in the presence of polyethylene glycol, to create a silica skeleton with macropores.

2.3.1.1.2 Gelation

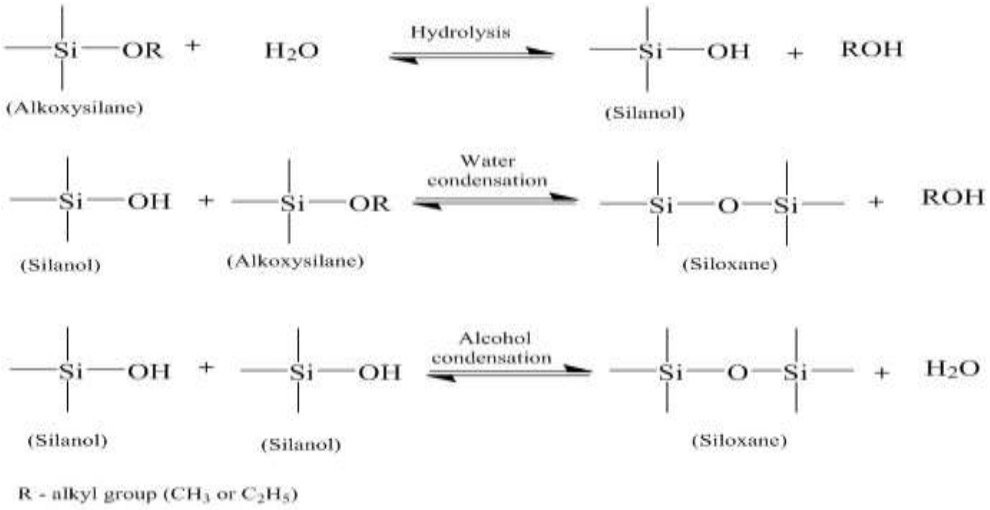

Figure 2-7: The reaction mechanism of hydrolysis and condensation steps for creating a silica monolith

Figure 2-7 shows the mechanism of hydrolysis and condensation reactions. In the hydrolysis reaction, the alkoxide groups (OR) in alkoxysilane (TEOS) are replaced with hydroxyl groups (OH). Then, condensation reactions take place where the silanol groups produce siloxane bonds (Si–O–Si) and alcohol (ROH) or water. This step can be called the gelation step. During gelation, the number of siloxane bonds increases; therefore, the number of silanol (Si-OH) and alkoxide groups decreases,[153] and the condensation reaction carries on to form a three-dimensional network resulting from polycondensation behaviour[154] [155] (Equation 2-16).

$$TEOS + H_2O \rightarrow Si(OH)(OR)_3 + ROH \quad \textbf{Equation 2-16}$$

$$Si\text{-}OH + Si\text{-}OH \rightarrow Si\text{-}O\text{-}Si + H_2O \quad \textbf{Equation 2-17}$$

$$Si\text{-}OH + Si\text{-}OR \rightarrow Si\text{-}O\text{-}Si + ROH \quad \textbf{Equation 2-18}$$

The sol–gel morphology can be managed by controlling the hydrolysis and condensation reaction in the gelation step. This can be achieved by changing the amount

of water and the catalyst; the kinetics of reactions (Equation 2-16, Equation 2-17 and Equation 2-18) depends on the catalyst. Essentially, acid catalysts are used to promote the reaction, but when the water/alkoxide mixture has a lower ratio than acid, this would result in forming gels with a lower crosslinking density. This is suitable for modification with C18 or an ion exchanger, since a large amount of unreacted alkoxy groups tend to remain in the gel network. A higher ratio of water will form a gel with a higher crosslinking density and hydroxyl groups will dominate in the inner surface of the gel network, and the pore size will be less than a few nanometres in diameter.[154]

2.3.1.1.3 Casting

Once the starting materials (such as TEOS, water and acid) have been mixed, they are cast by pouring the mixed solution into a mould before it becomes very viscous and it is then difficult to form the desired shape. The casting step is important because it determines the shape of the final monolith (column).[156] The mould has to be comprised of materials that do not chemically react with the starting materials of the monolith, and do not contain any physical materials that affect the final shape of the monolith.

2.3.1.1.4 Shrinkage

Shrinkage of the monolith occurs mainly in the final two steps of the preparation; the first step can be called aging and the second can be called drying. In the aging step, the liquid of the interior phase of the skeleton is released, causing the stiffness and strength of the skeleton structure to increase and the porosity of the monolith to decrease.[157] However, this can be modified by using factors that can change the structure of the gel during the aging process such as pH, solvent, temperature and the time of aging.[158]

The drying step is very important as the majority of liquid in the wet gel is removed, which leads to further shrinkage in the structure. This shrinkage is governed by

capillary pressure, which might damage the structure and eventually lead to the cracking of the final shape of the monolith.

2.3.1.1.5 Calcination

Finally, the calcination step follows the drying step of the silica monolith, in which a very high temperature is applied to the monolith to decompose any organic residues without damaging the monolithic structure.[157]

2.3.2 Isotachophoresis (ITP)

Isotachophoresis (ITP) is a powerful technique in the area of analytical separations and detection. ITP provides a simultaneous separation and concentration, and it can be miniaturised[102] and affectively applied to lab-on-a-chip (LOC) systems,[103] as it is highly sensitive and has decent separation resolution, even with small channel lengths and reasonable applied voltages.[159]

The principle of ITP is that it has two different electrolytes: a leading electrolyte and a terminating electrolyte. A sample mixture is injected at the zone between leading and terminating electrolyte solutions. The leading electrolyte is normally a buffer containing leading ions (L) with high electrophoretic mobility, such as chloride and potassium.[99] The terminating electrolyte contains an ion with the same charge, but with a slower mobility than that of the slowest moving sample ion. Under an applied voltage, co-ionic species focus and simultaneously separate into zones, based on their electrophoretic mobilities. Common detection can be applied within ITP such as conductivity,[100] UV, and fluorescence detection.[101]

Despite the ability of ITP and the usefulness of separating inorganic ions, the use of two different electrolyte solutions in ITP is limited with regards to our work, because of the

possible interference between the electrolyte solutions and ions of interest. Also, minimising the consumption of reagents is highly preferable.

2.3.3 Capillary electrophoresis (CE)

An alternative to chromatographic separation is electrokinetic separation. Electrophoresis is an analytical technique whereby ions in solution migrate under the influence of an applied voltage potential, as shown in Figure 2-8. The mobility of an ion can be described as the velocity in unit field strength; ions with different charge-to-size ratios have different electrophoretic mobilities and migrate at different velocities in channels under applied voltage.[160] Electrophoretic mobility μ_{ep} is directly proportional to the charge of the ion and inversely proportional to the friction coefficient. This can be described as Equation 2-19:

$$\mathbf{u_{ep}} = \frac{\mathbf{q}}{\mathbf{f}}\,\mathbf{E} \qquad \textbf{Equation 2-19}$$

Where $\boldsymbol{q}$ (coulombs) is positioned in an electric field, **E** (*V/m*) is the force on the ion *qE* (Newton). In the solution, the velocity of an ion is $\boldsymbol{u_{ep}}$, retarding frictional force is $\boldsymbol{fu_{ep}}$, and **f** is the frictional coefficient. The term (*ep*) refers to (electrophoresis).

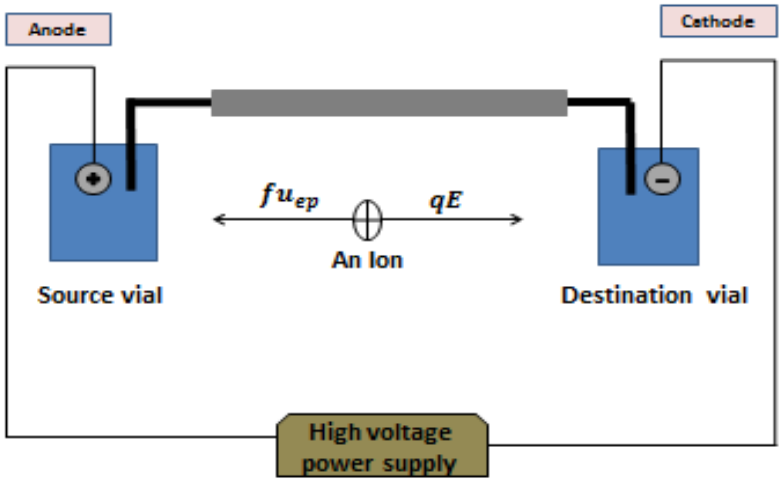

Figure 2-8: The movement of an ion through an electric field

The electrokinetic movement of ions can be affected by electroosmotic flow (EOF), which is the bulk movement of liquid induced by an applied electric field in a capillary tube or microchannel with a charge surface, such as one constructed from silica. An electric double layer occurs at the wall of the channel or the capillary, when the voltage is applied (Figure 2-9).

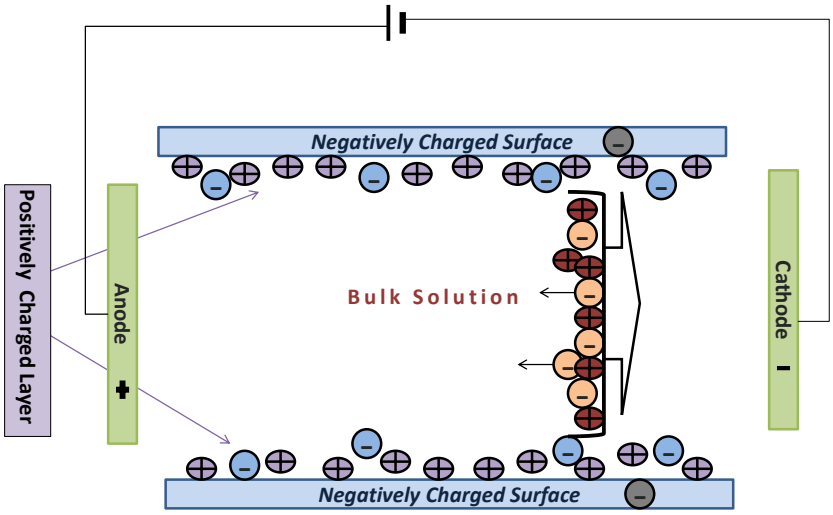

Figure 2-9: Electroosmotic flow affect in ion movement

In a glass channel, the surface is covered with silanol groups $Si\text{-}O^-$, and any cations in a solution in the channel migrate to the wall and generate a double layer. If an electric voltage is applied across the channel, the cations of the double layer will migrate towards the cathode, pulling the associated liquid with them, including the anions; this leads to a flow of liquid through the channel.[114]

The proportional constant between electroosmotic velocity (V_{eo}) and the applied voltage is known as electroosmotic mobility (μ_{eo}); this is proportional to the surface charge density on the surface of the wall and is expressed in Equation 2-20:

$$\boldsymbol{V_{eo} = \mu_{eo} . E} \ (\mathbf{m\ s^{-1}}) \qquad \textbf{Equation 2-20}$$

The electroosmotic mobility (μ_{eo}) is described as the speed of the neutral species ($\mu_{neutral}$) divided by the electric field, as shown in Equation 2-21:

$$\mu_{eo} = \frac{\mu_{neutral}}{E} = \frac{L_d/t_{neutral}}{V/L_t} \ (\mathbf{m^2\ v^{-1} s^{-1}}) \qquad \textbf{Equation 2-21}$$

Where E is the electric field, $\mu_{neutral}$ is the speed of the neutral species, L_d is the distance to the detector, and $t_{neutral}$ is the migration time to the detector, V is the applied voltage and L_t is the total length (of the channel or the column) from end to end.[114]

Another factor that might occur when applying a high voltage in this situation is Joule heating. This is because of the high surface-to-volume ratio in the microchannel and high thermal conductivity values of silicon and glass.[161] The problem of Joule heating can be solved through the use of polymeric materials instead of glass.

According to Ohm's law, Joule heating can be calculated using the following equation:

$$q = \frac{I^2}{\lambda} \ (\mathbf{w\ m^{-3}}) \qquad \textbf{Equation 2-22}$$

Where q is the Joule heating generated, I is the current and λ is the electrical conductivity of the electrolyte solution.[162]

The separations obtained through the capillary electrophoresis technique are highly efficient and rapid, and can be applied to both charged and neutral species. Capillary electrophoresis can be applied to a wide range of applications, including pharmaceuticals, food and beverages, and environmental and clinical analyses.[163] It has many advantages for miniaturisation because it is a simple technique where the separation is achieved by the relatively straightforward application of voltages. It does not require pumps, consumes a low amount of reagents, and a variety of detectors can be used in CE.[164]

Capillary electrophoresis and ion chromatography are very powerful techniques for environmental analysis and microfluidics.[165] However, in capillary electrophoresis, the number of theoretical plates is at least 10 times better than for ion chromatography (IC)[166] because there is much less band broadening in CE than in IC. Separation by CE is fast, and it is relatively easy to find experimental conditions for an adequate separation of sample ions. One of the greatest advantages of CE is its tolerance of variations in the sample matrix. However, CE also has some disadvantages that include an often poor reproducibility, especially for small molecules and ions that move very quickly in the electrical field.[166] When comparing IC to CE, a point should be addressed, which is that IC is a better-understood technique than CE, while CE is an area of research still being investigated. In the past decade, there have been many new developments in ion analysis through capillary electrophoresis.

In terms of microfluidics, capillary electrophoresis (CE) has been performed in the capillary format with dimension of tens to hundreds micrometres,[132] and microchip-based capillary electrophoresis (MCE) was one of the original formats of microfluidics. This was introduced in 1992 by Harrison *et al.*[167] and consisted of a sample injection system and a separation channel integrated on a planar glass chip. MCE devices have certain advantages over typical CE systems, especially in terms of sample introduction, but because the channel dimensions are comparable, the resolution is also comparable. As device dimensions are reduced, system throughputs increase, but automation schemes will become more complex.[168]

Capillary electrophoresis (CE) separation is achieved by the relatively direct application of voltages. Pressure pumps and eluents are not needed, which results in a very low consumption of reagents. An important further simplification for CE of small ions was the demonstration of contactless conductivity detection (C4D) based on a pair of short

tubular electrodes, as described in detail in section 3.4.1. The method is entirely electronic and relies less on construction, and has a low level of power consumption compared to other detection methods.[164] Prototype examples of miniaturised portable CE instruments combined with C4D are being reported,[19] and CE has the additional potential for extended *in-situ* measurement applications, such as environmental monitoring.[164]

The use of capillary electrophoresis (CE) for water control is challenging, due to the complex matrix embedding trace concentrations of the analyse. Selective ion isolation from a water sample can be achieved by electrodialysis (ED) techniques. ED can be combined with CE for the preconcentration of inorganic ions from a water sample; this combination can greatly enhance the analytical performance of river water in order to eliminate unwanted matrices in the analyse sample.

In ion separation, the detector must measure ions in the presence of background eluent ions. The detector should respond only to the ion of interest, excluding the ions in the eluent. Different techniques have been employed to overcome this matter but the main two categories of these techniques are spectrophotometric techniques and conductivity detection systems.

2.3.4 Electrodialysis

Electrodialysis (ED) is a well-known process for ion extraction and it has been utilised for over 50 years in the industrial field, for the production of potable water from brackish water sources. Nowadays, electrodialysis is applied in many industrial applications, such as food and drug industries. In addition, it is applied widely in waste water treatment and the production of high quality industrial water and water desalination.[169]

In ED, ions are migrated through a semi-permeable membrane, under the influence of an applied electric potential (as shown in Figure 2-10).

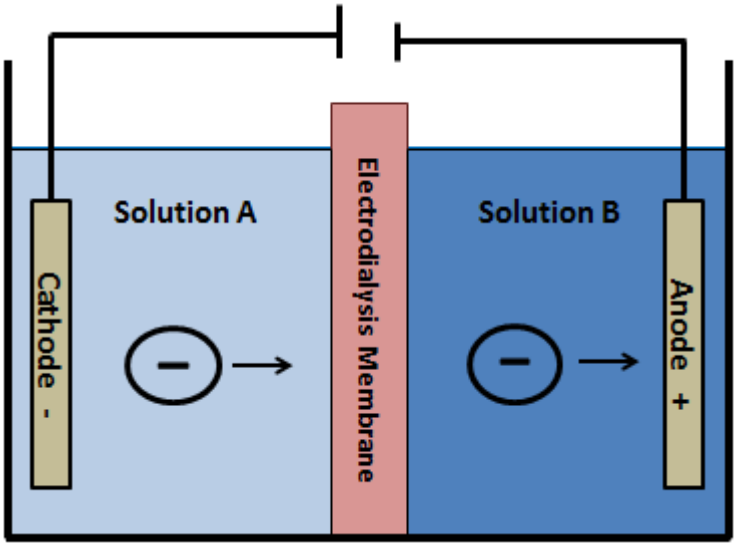

Figure 2-10: Electrodialysis process

2.3.4.1 Electrodialysis membrane

There are two different types of membranes that can be used in electrodialysis: a semi-permeable polymeric membrane or an ion-exchange membrane. Cellulose acetate was one of the first polymer membranes used for separation in aqueous solutions.[127] As it is a hydrophilic material, cellulose acetate provides good fouling resistance.[170] [171] It also does not require any chemical additives and can perform for a relatively long time.[172] The advantages of a cellulose acetate membrane make it very popular in water filtration and ED processes.

Ion-exchange membranes normally consist of ion-exchange resins. They might also contain other polymers to enhance mechanical strength and flexibility. The resin component of a membrane could be a cation or anion-exchange membrane.

2.4 Chapter Conclusion

It is clear from reading the literature that there is a demand for portable *in-situ* measuring systems for measuring ions in environmental water samples. Although commercial flow injection analysis systems are available, they are not easy to install and maintain, having high power requirements and using large volumes of reagents. Miniaturising the measurements has proved to be promising, and quite successful microfluidic automated systems have been developed based on spectrophotometric and voltammetric measurements. These systems tend to only measure one species at a time; however, what is really required is a portable system that can simultaneously measure several anions and cations. The aim of this project was, therefore, to develop a portable system for measuring a range of ions in a solution. Several approaches were taken to identify the best solution. One concern when continually operating a system is the effect of the sample matrix on the system, so it was decided that a good approach would be to extract the ions from the sample prior to separation.

The detection system selected for the application was the C4D system, which is a universal detector and does not have the electrodes in contact with the solutions, thus providing a robust detection solution, and it can be used for each of the followings:

1. To investigate methods to extract ions from water samples in microfluidic devices.

2. To investigate monolith columns for the separation of ions in microfluidic devices.

3. To investigate the electrophoresis separation of ions to include in a microfluidic device.

4. To investigate the simplest solution to designing a microfluidic device with ion extraction and separation.

3 General experimental chapter

3.1 Reagents

Table 3-1: Table of reagents

Chemical	Supplier
4-Morpholineethanesulfonic acid (MES)	Sigma-Aldrich Company Ltd, UK
L-Histidine	
Magnesium sulphate 99.5%	
Calcium phosphate dibasic	
Magnesium sulphate	
Poly (ethylene oxide) (PEO) with average relative molar masses of 100 kDa	
Tetraethoxysilane (TEOS)	
Ammonium hydroxide (5 M)	
Nitric acid aqueous solutions (1 M)	
Chloro(dimethyl)octadecylsilane (ODS) 95%	
2,6-lutidine 99%	
Multi-element ion chromatography standard solutions I, II and III	
Didodecyldimethylammonium bromide (DDAB)	
Trimethylchlorosilane	
Sodium phosphate monobasic 99% for HPLC	
Chloride IC standard	
Nitrite IC standard	
Humic acid	
Multi Anion Standard 2 & 3 for IC	
Sodium nitrite analytical grade reagent	Fisher Scientific, UK
Sodium nitrate 99%	
Potassium phosphate 97%	
Toluene	
Sodium chloride	
Sodium sulphate anhydrous	
HPLC grade acetonitrile (ACN)	
Potassium silicate	VWR international, UK
Formamide 99%	Avocado Research Chemicals Ltd, UK

1000 ppm Ca, Mg, K and Na elemental solutions	Romil Ltd, Cambridge UK
Trace metal nitric acid	Romil SpA grade, UK
18 MΩ.cm conductivity water	Elga UHQ PS or an Elga Purelab Flex2 system

3.2 Instruments

3.2.1 Ion chromatography

IC is considered to provide a gold standard for the separation and identification of inorganic anions. This can be used to monitor the extraction of anions after their extraction from the sample introduction system.

The samples were of variable amounts, usually 100 µl to 2ml, of solutions from the sample introduction system. It is important to have approximately 500 µl of sample as a minimum volume for analysis by a Dionex system, as it is practically difficult to deal with amounts less than 500 µl. The samples were directly injected without further modification to the loop with a 1 ml plastic syringe. Sometimes, certain samples require dilution with water prior to injection because some of the anion samples contain a very high amount of anions that would remain in the sample loop or column after the run, which would affect the following runs; therefore, to maintain the system, some samples required dilution.

To quantitatively calculate the concentration of anion in each sample, a set of standard concentrations of each anion were plotted against their peak areas using Microsoft Excel, and the graph was then used to calculate the concentration of each anion in the sample in millimoles (mM) using its peak area, if the sample had been diluted; the dilution factor is considered in the calculation. For the calculation of the percentage of

migration, the concentration of the initial anion sample was calculated before and after each experiment. When possible, the target results were also calculated before and after experiments.

The system used was the Dionex ICS-2000 Ion Chromatography System (ICS-2000), using suppressed conductivity detection. The conditions were: approximate pressure 1830 psi; flow rate 0.39 and 0.38 $mLmin^{-1}$; column heater 30°C; cell heater 35°C; and an injector loop of 20 µl. The manufacturer's standard anion method was followed; the eluent was comprised of 15 mM sodium hydroxide, with a running time of 10 minutes for the chromatogram. The system was purchased from Dionex (UK) Ltd in July 2007.

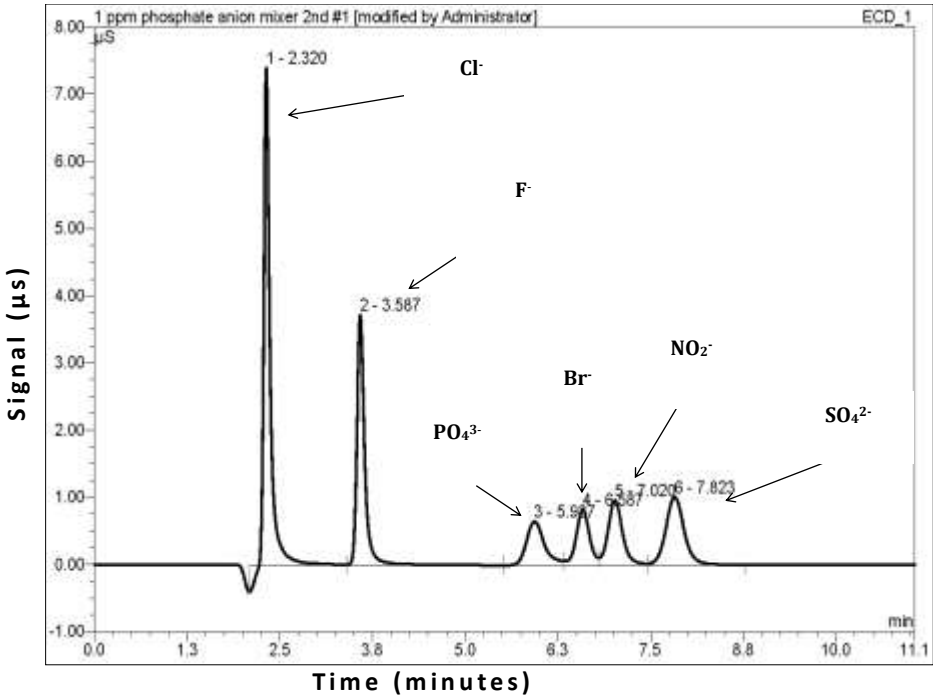

Figure 3-1: A chromatogram of anion standards

Figure 3-1 shows the chromatogram of anion standards under the previously mentioned conditions. All standards used as there sodium salts in water, the concentrations were 1 g/L (Sigma Aldrich Ltd UK).

3.2.2 Inductively coupled plasma optical emission spectrometry (ICP-OES)

The samples were variable amounts of water, usually 0.5 to 2 ml, from the sample introduction system. It is important to have approximately 5 ml of sample as a minimum volume for analysis through ICP-OES. To quantitatively prepare a 5 ml sample from these variable amounts, the sample was transferred into a tared 15 ml sample tube with a screw cap (Sarstedt Ltd, Leicester, UK), the sample weight was recorded, and it was then diluted to the 5 ml mark and weighed again. Samples were then vortexed prior to analysis, to ensure complete mixing. The ratio of the final weight to the sample weight was then a dilution factor, which was applied to the measurements of the elements of interest in the 5 ml sample in order to provide the concentrations of the elements of interest in the original sample volume.

Where possible, elements were measured at 3 or 4 wavelengths to check whether any spectral interference was affecting the measurements. Sodium and potassium only have a single wavelength available. The response was calibrated for Ca, Mg, K and Na at 0, 10, and 20 ppm using mixed standards diluted from certified single element 1000ppm solutions into 2% nitric acid, prepared from trace metal nitric acid and 18 MΩ conductivity water.

The concentrations of the elements were measured on the Perkin Elmer Optima 5300DV emission ICP instrument. K and Na were measured in the axial view, and Ca and Mg in the radial view, which is less sensitive. This analysis technique is very sensitive to Ca and Mg; therefore, the conditions were altered in this way to enable measurements to take place in one run. Measurements were made in triplicate to enable the mean, standard deviation and %RSD to be calculated for every wavelength, and for

every solution. Blank 2% HNO_3 solution was analysed several times, and the mean of the standard deviations for these blanks were calculated when the results dataset was exported into Microsoft Excel. The value of 3 times the mean SD of the blanks then provides the detection limit for all of the wavelengths. Excel was used to calculate the concentrations of the elements of interest in the original sample amount, using the dilution factors, and the detection limits (LOD) were used to evaluate whether the measurements were significant or too close to the LOD to be present in the sample.

The Optima ICP-OES sample introduction has a high solids PEEK nebuliser with liquid streams and gas streams that remain separate until the ends of the capillaries, and a vortexing spray chamber of borosilicate glass. Typical gas flows were plasma gas 15L/min, auxiliary gas 0.2L/min, and nebuliser gas 0.80L/min. RF power was 1300W, and liquid flow was 1.50 $mLmin^{-1}$. The Perkin Elmer Optima 5300DV instrument was using Winlab 32 software; this was updated in summer 2014 to the Windows 7 version 5.5.0.0714.

3.2.3 Infrared (IR) spectrophotometry

Infrared (IR) spectrophotometry is a very reliable and well-known fingerprinting technique that allows for a wide range of substances to be characterised and analysed. IR spectrophotometry has the ability to obtain spectra from many types of solids, liquids and gases. In many cases, however, some form of sample preparation is required in order to obtain a good quality spectrum.

Attenuated Total Reflectance (ATR) is an IR technique that allows for the qualitative and/or quantitative analysis of samples with sample preparation, which greatly speeds up sample analysis. The benefits of ATR sampling are its very thin sampling pathlength and the deep penetration of the IR beam into the sample of interest.

ATR was used to analyse the differences between different conditions of anion-exchange membrane, and the Nicolet™ iS5 FT-IR Spectrometer and MIRacle™ Single Reflection ATR were both purchased from Fisher Scientific UK.

3.2.4 Capillary electrophoresis

A Beckman Coulter P/ACE MDQ capillary electrophoresis (AB SCIEX Ltd, UK), was used to examine the performance of the ED system. The CE instrument separates sample components within a fused-silica capillary; the sample is injected into the capillary using vacuum, pressure, or voltage. The detection used was UV: when the separated components pass a window in the capillary, a single wavelength UV detector measures absorbance and transmits a signal to the computer, which then displays it as an electropherogram.

3.3 Chip manufacture

Microfluidic devices are normally made of silicon, glass or a polymeric material such as polydimethylsiloxane (PDMS), cyclic olefin copolymer (COC), or polymethyl methacrylate (PMMA).[173] As these are chemically compatible for different applications, they are disposable and readily manufactured at a relatively a low cost.[174]

The microfluidic chips used in this work were fabricated at the University of Hull using photolithography and wet-etching processes. The machine used is a Datron M7; this is an accurate machine for micro-drilling, engraving and the 3D machining of face plates, housing, fixtures and dyes in any material. It can operate at speeds of 5,000-50,000 revolutions per minute (RPM). The x, y and z movements can move at a maximum speed of 16 m/min. The machine is pre-installed with an automated tool-length measure, which has a resolution of 1 mm. A coolant system that uses ethanol is installed

in the machine and sprays the coolant, as well as air, around the spindle of the machine during use.

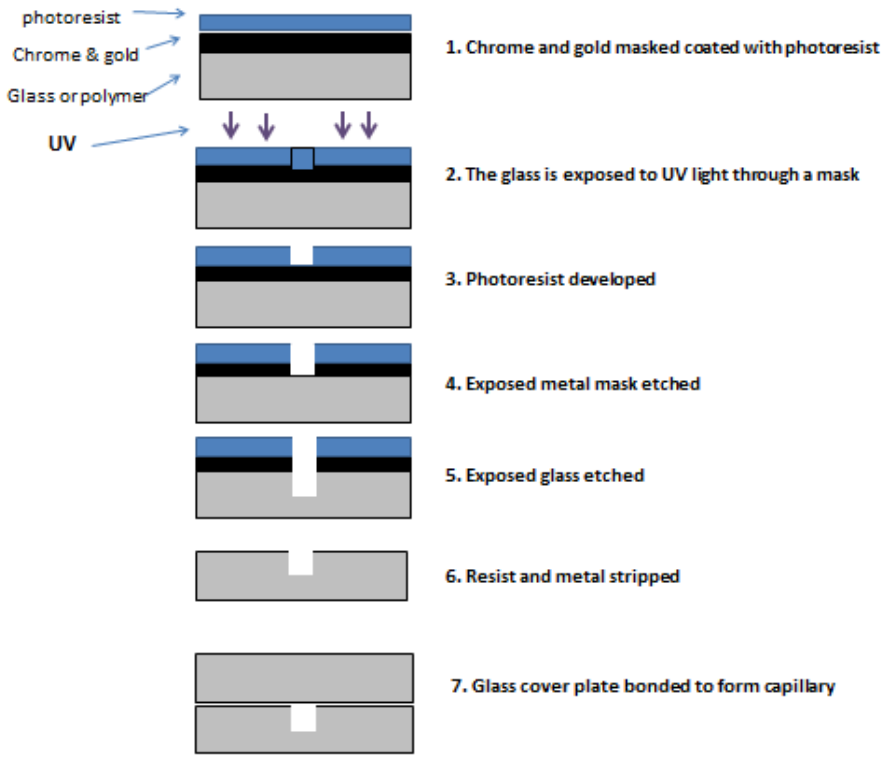

Figure 3-2: Schematic drawing of the fabrication process of the microchip[175]

Glass microdevices were fabricated by a wet-etching technique similar to McCreedy's method.[175] [176] Briefly, the design was drawn using *autoCAD* software and transferred through a commercial process (J. D. Phototools, Oldham, U.K.) to a film photomask. 1mm thick Crown white glass (B270) panels coated with chrome and photoresist (Telic Co., Valencia, California, USA) were contacted with the appropriate design on the photomask and exposed to UV radiation. The panels were then treated consecutively with Microposit© *Developer* (50% dilution in water) and *Chrome Etch 18 Solution* (Rohm-Haas materials supplied by Chestech, Ltd). The panels, now with an exposed glass channel pattern, were etched in 1% hydrofluoric acid / 5% ammonium fluoride solution at 65°C to the required channel depth (the etch rate is approximately 5 µm min-

[1]). The remaining photoresist and chrome layers were removed using Microposit© *Remover 1165* and *Chrome Etch 18 Solution*[4] (Rohm-Haas materials supplied by Chestech, Ltd), respectively.

Access holes were drilled, using diamond drill bits, into either the etched base plate or a B270 glass cover plate. After a thorough cleaning process employing solvents and aqueous detergent solution, the etched plates were thermally bonded (585°C for 2 hrs) to cover plates.

For the polymer chip, the same procedures were followed, but with no etching with the 1% hydrofluoric acid / 5% ammonium fluoride solution.

3.4 HPLC for the assessment of the monolithic column

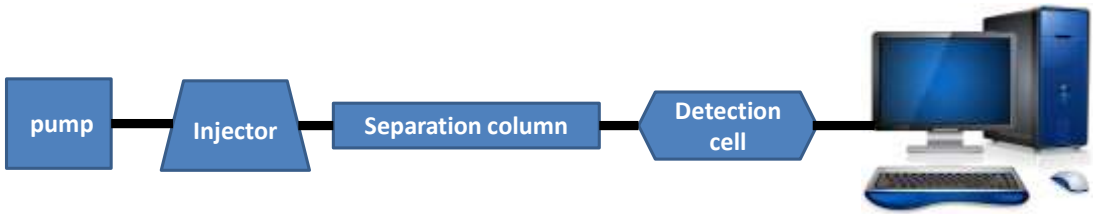

Figure 3-3: Experimental set up of the separation experiment on the monolith

Figure 3-3 shows the experimental set up of the separation of inorganic anion, performed on a silica monolith. An in-house C4D detector was developed. The eluents was degassed before the experiment using the eluent solution in a sonicator bath (Ultrawave Sonicator U 300HD, Cardiff, UK) for approximately 30 minutes. The set-up began with a syringe pump (Figure 3-4: Fusion 100 Classic Syringe Pump (chemyx US) to ensure the constant pressure of the eluent through the separation monolith that was 0.2 $mLmin^{-1}$; the eluent was placed in a 10 ml plastic syringe. PTFE tubing (1.6 mm OD

x 0.5mm ID purchased from Kinesis Ltd UK) was used to carry the eluent from the syringe to the loop injector, the separation monolith, the detection system, and eventually, to the waste container. The loop injector was used for introducing the analyte sample to the eluent (Figure 3-5), with the injector made of polymeric materials to avoid any interference with the measured ions from the normally metallic injector. The eluent carried the analyte from the injector to the monolith (6 cm×4 mm), where separation of the injected components occurred.

Figure 3-4: Fusion 100 Classic Syringe Pump (chemyx US)

Figure 3-5: A picture of the top and side of the loop injector used in the HPLC set-up for the separation on the monolith

Figure 3-5 shows the injector used in the HPLC system set-up for the separation of inorganic ions on a silica-based column. The injection is done through a designed 6-port rotary injection valve. The analyte sample is introduced at atmospheric pressure by a syringe into a constant volume loop; the loop volume is 25 µl. The injector has two fixed positions: load and inject. In the load position, the loop is not in the path of the eluent. When rotating to the inject position, the sample in the loop is moved by the eluent stream into the column. To ensure there are no air bubbles in the loop, it was important to allow some of the sample to flow into waste from the loop before rotating to the inject position.

3.4.1 Capacitively coupled contactless conductivity detection (C^4D)

Conductivity detection can be accomplished in either the contact or contactless modes. In contact conductivity detection, the electrodes are in direct electrical contact with the

solution, which leads to the possibility of corrosion or fouling of the electrode, and possibility of the electrode material interfering with the system chemistry. As a result, C^4D has gained considerable attention[177]. In 1998, Zemann *et al.*[178] and Fracassi da Silva and do Lago [179] reported what is considered to be the first approach of modern C^4D. This was based on two tubular electrodes for capacitive coupling that were both positioned on the outside of a capillary. Since then, work has continued on developing C^4D.

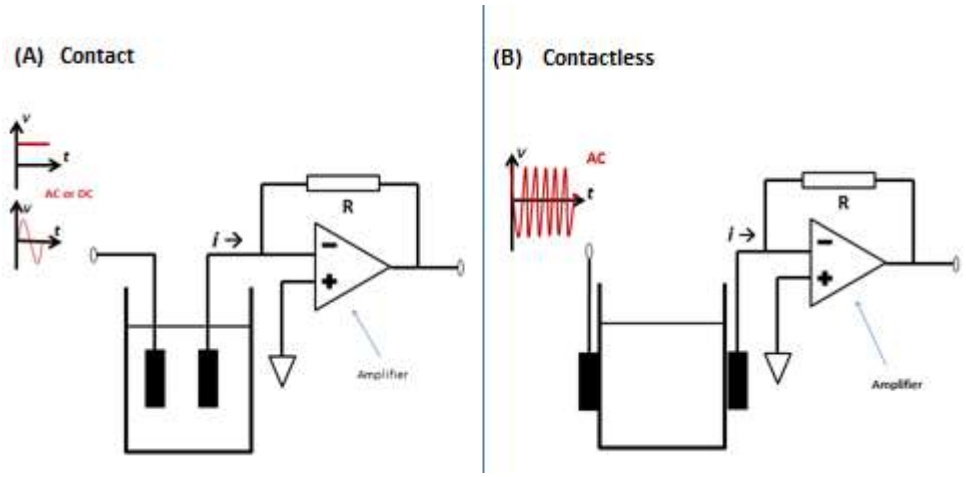

Figure 3-6: Comparison between a) contact and b) contactless conductivity detection systems[180] R = resistance, i = current.

Figure 3-6 shows a comparison between direct and C^4D detection. In direct contact conductivity detection, a small amount of alternating current (AC) or direct voltage (DC) is applied to two inert electrodes, as shown in

Figure 3-6 (a). The electrodes are in direct contact with the solution.[180] In C^4D systems, the set-up is similar except the two electrodes are placed outside the sample reservoir and only AC signal can be used (

Figure 3-6 [b]).

In both cases, the second electrode is connected to a transimpedance amplifier comprised of an operational amplifier and feedback resistor *R*. The transmittance amplifier implements an ammeter function, allowing cell current to be measured. The amplifier output voltage is given by the following equation:

$$\boldsymbol{V_{out} = Ri}$$ **Equation 3-1**

Where R is resistance and $\boldsymbol{i}$ is the current.[181]

Figure 3-7 is a redrawing of Figure 3-6 (a) that shows the system as an electrical equivalent circuit. From the figure, it can be seen that the voltage can be driven across the cell by either an AC (Alternating Current) or DC (Direct Current) source. The solution behaves as a resistor whose resistance depends on the solution's conductivity.

Figure 3-8 is a redrawing of Figure 3-6 (b), to show the system as an electrical equivalent circuit. A high-frequency signal is applied in the first electrode; this signal passes through the sample solution inside the reservoir and then goes to the second electrode, where the signal is read by an electronic circuit. The current flowing through the detection cell is proportional to the conductivity of the solution inside the sample reservoir.[22] In C^4D systems, there is no direct current (DC) because the electrodes are insulated from the solution and they are capacitively coupled to the electrolyte solution. The electrodes, the insulator (such as the capillary wall in CE) and the solution behave like three parallel plate capacitors[149] and a resistor connected in a series.

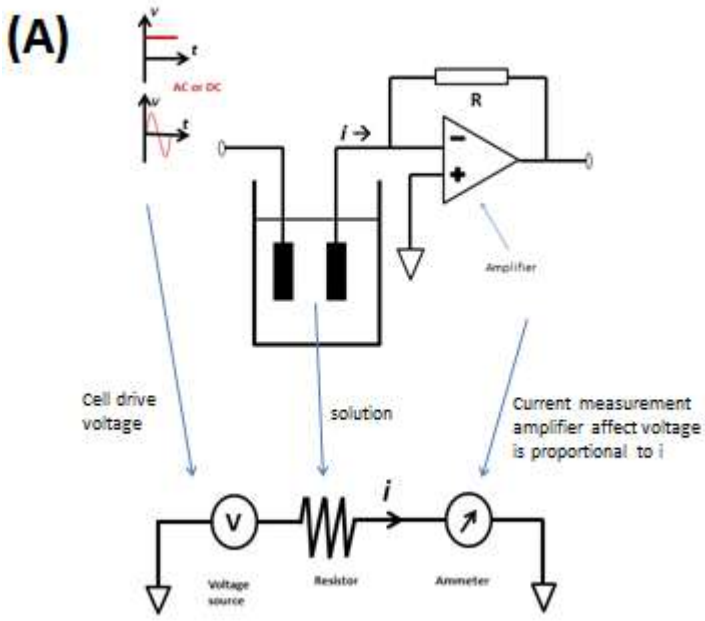

Figure 3-7: Redrawing of Figure 3-6 (a) to demonstrate an electrode equivalent circuit

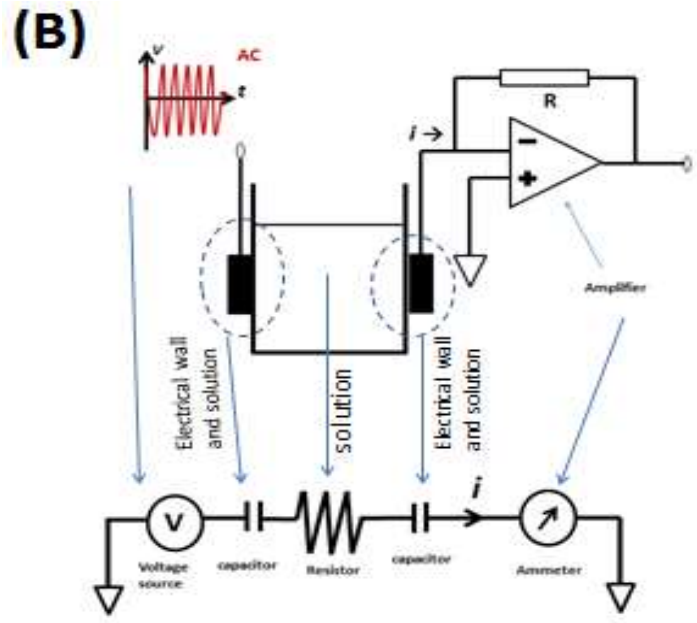

Figure 3-8: Redrawing of Figure 3-6 (b) to demonstrate an electrode equivalent circuit

Figure 3-9 is a redrawing of the circuit in Figure 3-8, demonstrating the key voltage and current in the circuit.

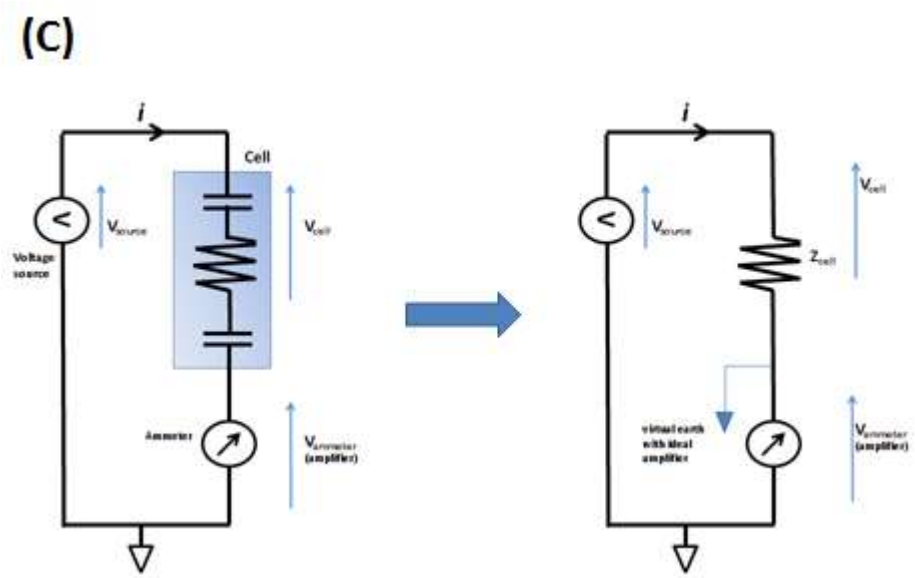

Figure 3-9: Redrawing of Figure 3-8 to demonstrate key voltages

Using Kirchhoff's voltage law[66]:

$$\boldsymbol{V_{source} = V_{cell} + V_{ammeter}} \qquad \textbf{Equation 3-2}$$

Ideally, the voltage across the cell should be equal to the known (and constant) source voltage. This requires that $V_{ammeter} = 0$. The amplifier is a feedback control circuit that attempts to achieve this condition. If a high-gain operational amplifier with a very low input current is used, conditions close to the ideal can be achieved and the amplifier input is referred to as virtual earth or virtual ground (it behaves as if it was connected to the ground).

When these conditions apply, we have $\boldsymbol{V_{source} = V_{cell}}$, then, using Ohm's law:

$$\boldsymbol{i = \frac{V_{source}}{Z_{cell}}} \qquad \textbf{Equation 3-3}$$

Where Z_{cell} is the cell impedance and i and V_{source} are RMS (root mean square) values of the AC current and voltage.[68] The output of the amplifier, again in RMS, will be:

$$V_{out} = \frac{R\,V_{source}}{Z_{cell}}$$ **Equation 3-4**

Given that V_{source} and R are constant, changes in V_{out} will only depend on changes in Z_{cell}.

Z_{cell} comprises both coupling capacitance and solution resistance. If a suitable frequency is used, Z_{cell} will be dominated by the solution resistance and V_{out} will be sensitive to changes in conductivity.

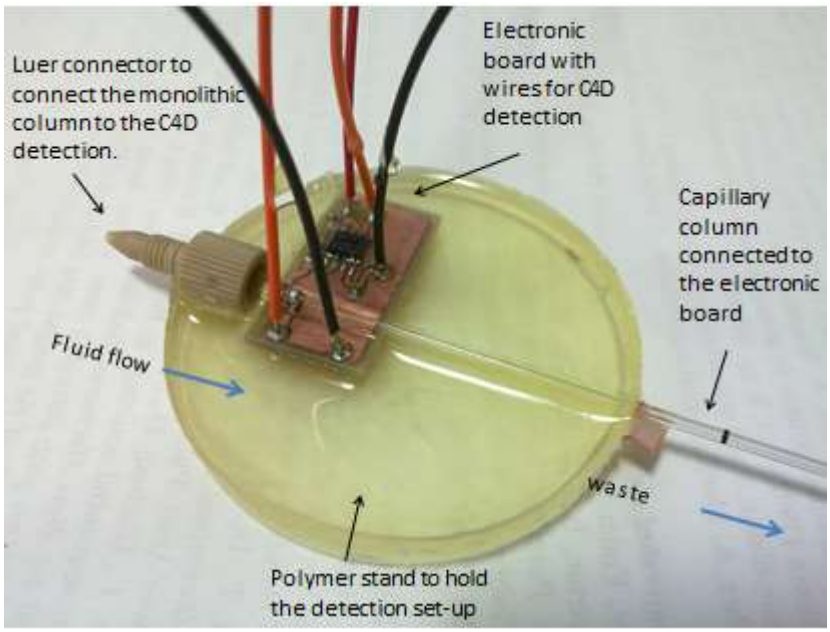

Figure 3-10: C^{4}D detection set-up

Figure 3-10 shows a C^{4}D detector developed in the Department of Engineering at the University of Hull. The initial aim was to design a detector with an electronic board and baseline suppression.

3.5 Ion extraction

3.5.1 Power supply and conductivity

The D100 power supply (Farnell UK Limited) was used to apply voltage to the reservoirs in ion extraction experiments, using Pt electrodes. Furthermore, the conductivity in the system was measured using a voltmeter (Fluke 8010A digital multimeter, Fluke, the Netherlands).

3.5.2 Ion extraction through a potassium silicate monolith in a glass capillary

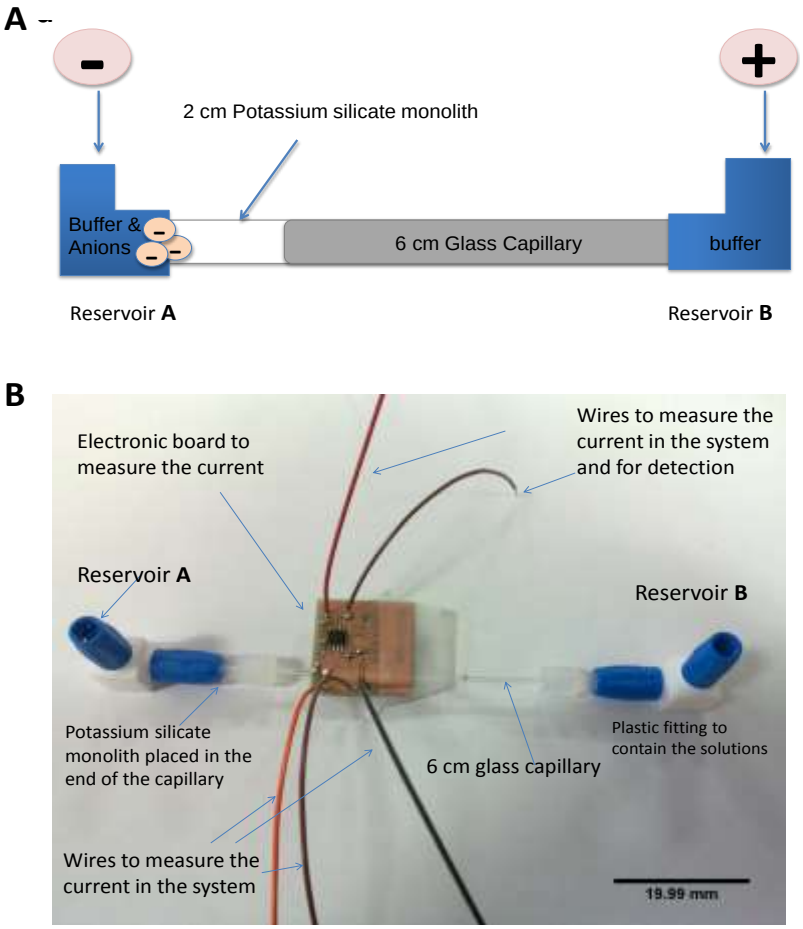

Figure 3-11: The set-up of the ion extraction through a potassium silicate monolith using a glass capillary

Figure 3-11 shows the set-up of the extraction system. There are two reservoirs: reservoir A contains a buffer and anion mixture, and reservoir B contains a buffer. Both reservoirs were linked to each other by a glass capillary (0.6 ± 0.05 mm ID) (Brand GmbH, Germany). The capillary contains a 2 cm thermally-activated silica-based monolith; the monolith was attached to reservoir A.

3.5.3 Ion extraction through Polytetrafluoroethylene (PTFE) film and Parafilm

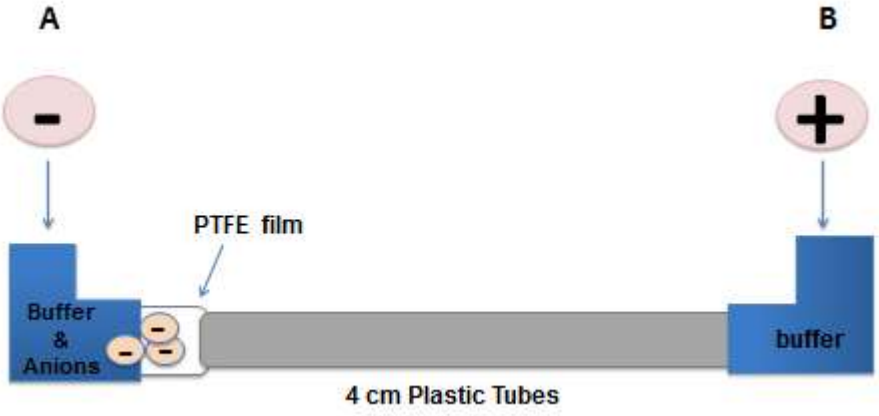

Figure 3-12: The set-up of the ion extraction through a PTFE film using a plastic tube

Figure 3-12 shows the experimental set up for ion extraction through PTFE film. This system consists of two reservoirs. The sample reservoir, which will be referred to as reservoir A, contains an anion mixture and MES/His buffer. The second reservoir is the destination reservoir, which will be referred to as reservoir B; this reservoir contains MES/His buffer. Both reservoirs are linked to each other by a plastic tube, which is covered with PTFE film (Acro Ltd, Hull, UK) or Parafilm (Sigma Aldrich Ltd, UK). The film was stretched and sealed over the end of the plastic tube. The plastic tube was placed between the two reservoirs, and the PTFE film or Parafilm was stretched and sealed around one end of the tube and then attached directly to reservoir A, as shown in Figure 3-12.

The anions should migrate from reservoir A to reservoir B through the PTFE film or Parafilm, by the attraction of the applied voltage. The conditions were: 10 mM MES/His Buffer; an applied voltage of 10-200; and times of 10, 5 and 2.5 minutes.

3.5.4 Electrodialysis for sample introduction with a commercial cell

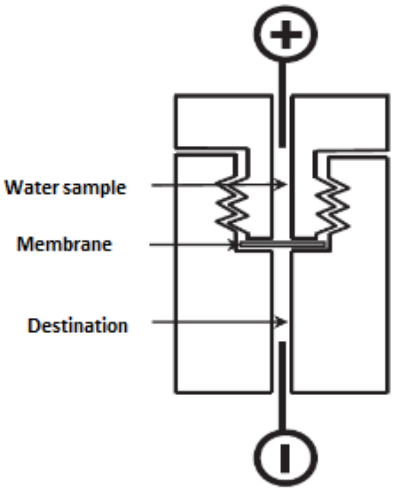

Figure 3-13: Schematic drawing of an electrodialysis system[182] consisting of two polytetrafluoroethylene link chambers separated by a cellulose acetate electrodialysis membrane

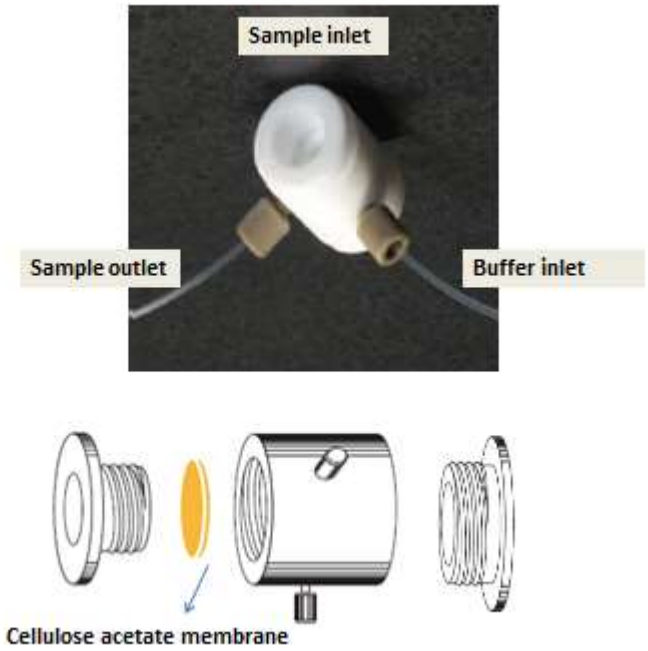

Figure 3-14: An image of the experimental set-up for ion extraction with the cellulose acetate membrane and the commercial cell (Harvard Apparatus, UK)

The system in Figure 3-13 and Figure 3-14 consists of a chamber and a cellulose acetate dialysis membrane that was placed in the chamber. Two Pt electrodes were directly inserted into the destination and sample reservoir, the sample reservoir was filled with about 500 µl analyte, and the chamber (500 µl) was filled with 5 mM MES/His buffer. The electrodialysis ED system was operated using a power supply. The ion should migrate through a cellulose acetate electrodialysis membrane with a molecular weight cut-off value of 100 Da (Harvard Apparatus, UK). The samples were then collected from the destination reservoir and analysed using ICP-AES.

3.5.5 Electrodialysis for sample introduction with a glass chip

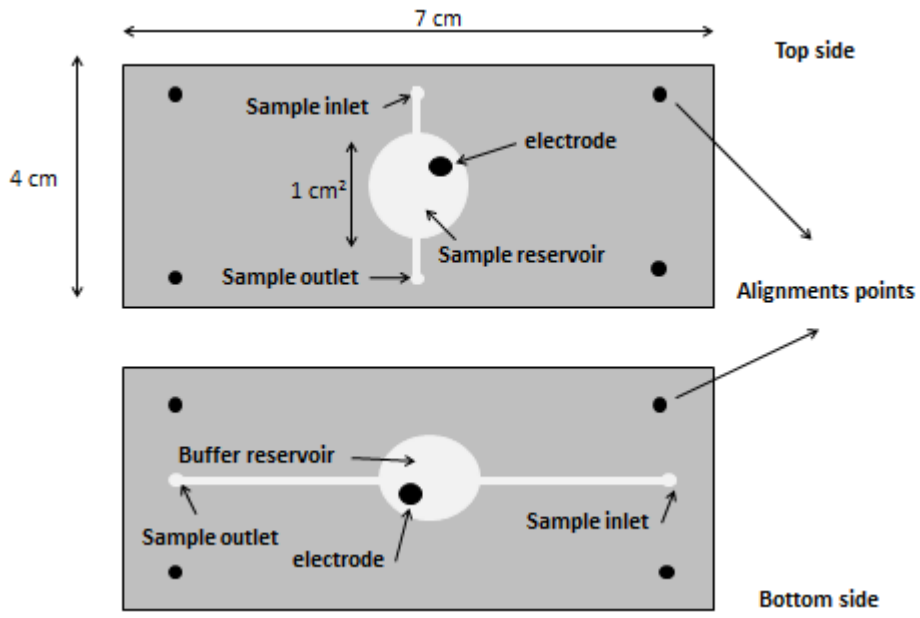

Figure 3-15: Glass microchip for an electrodialysis system for sample introduction

Figure 3-15 shows a glass chip that was used for extracting ions through a cellulose acetate membrane. The chip consists of two parts, the top and the bottom. The top part has a circle reservoir that is 1 cm^2 wide, with a depth of 3 mm. In the reservoir, there is a hole in the centre for the electrode, and the width of the hole is 0.5 mm. The reservoir

has two channels that are each 1 cm long and 100 µm in depth. The bottom part of the chip also has a 1 cm^2 reservoir that is 3 mm deep, and it also contains a hole in the centre for the electrode. There are two channels on the sides of the reservoir that are each 3 cm long and 100 µm depth. The two parts are connected to each other by double-sided tape without the reservoirs part, on both reservoirs a 1.5 cm^2 cellulose acetate membrane. Thus, the final design of the chip is two reservoirs with a cellulose acetate membrane in between them, with each reservoir containing a fluid channel where the sample and buffer can enter and exit. Each reservoir has a Pt electrode that is connected to a power supply.

3.5.6 Electrodialysis on a COC chip with a flat carbon electrode

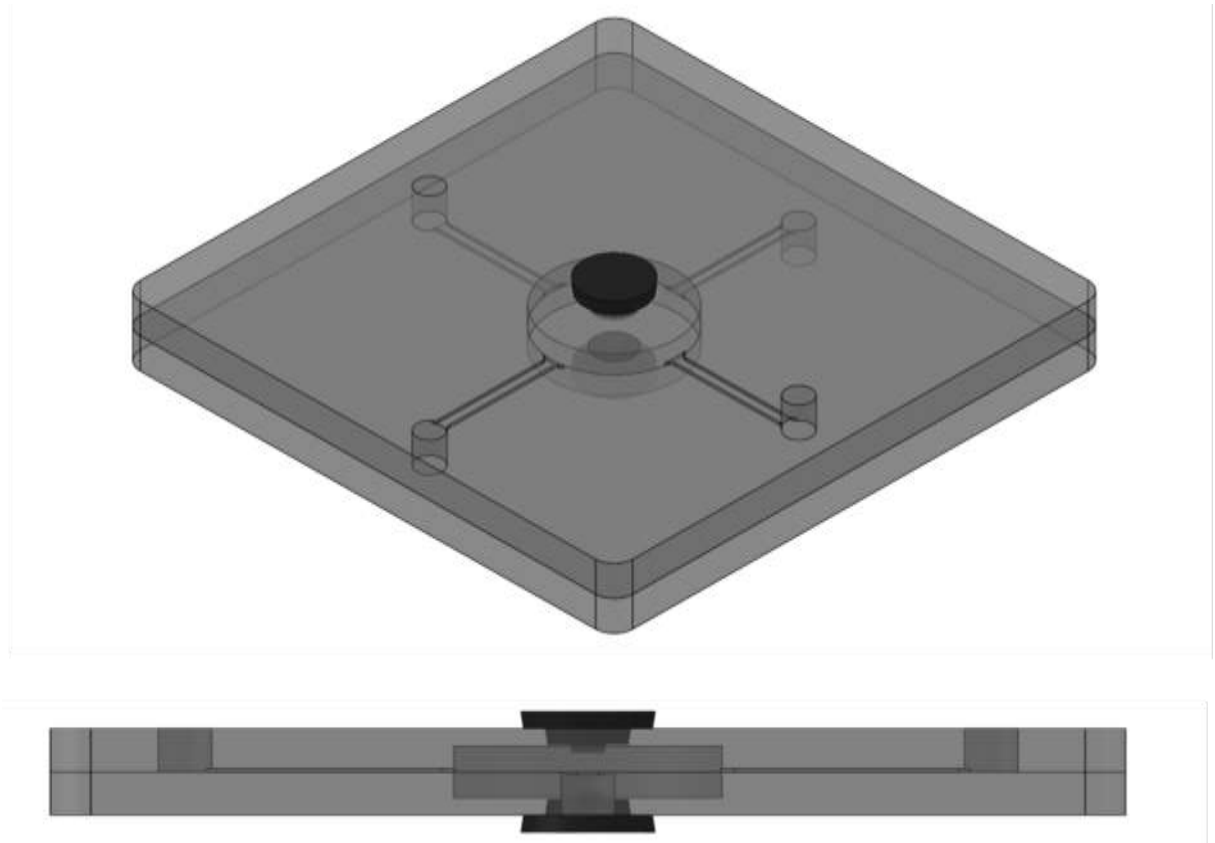

Figure 3-16: COC chip for ED, for ion extraction

Figure 3-16 shows a chip that was used for extracting ions through a cellulose acetate membrane. The chip consists of two parts: the top and the bottom. Both parts have a circle reservoir that is 1 cm^2 wide, with depth of 2 mm. In the reservoir, there is a 3 mm wide hole in the centre for a flat carbon electrode. The reservoir has two channels that are each 1 cm long and 200 μm in depth. The two parts are connected to each other with double-sided tape without the reservoirs part, on both reservoirs a 1.5 cm^2 cellulose acetate membrane. Thus, the final design of the chip is two reservoirs with a cellulose acetate membrane in between them; each reservoir has a fluid channel where the sample and buffer can enter and exit. Each reservoir has a carbon electrode that is connected to a power supply by a circuit board (see Figure 3-17), with a copper electrode that is placed on the board; and the board is connected to a power supply.

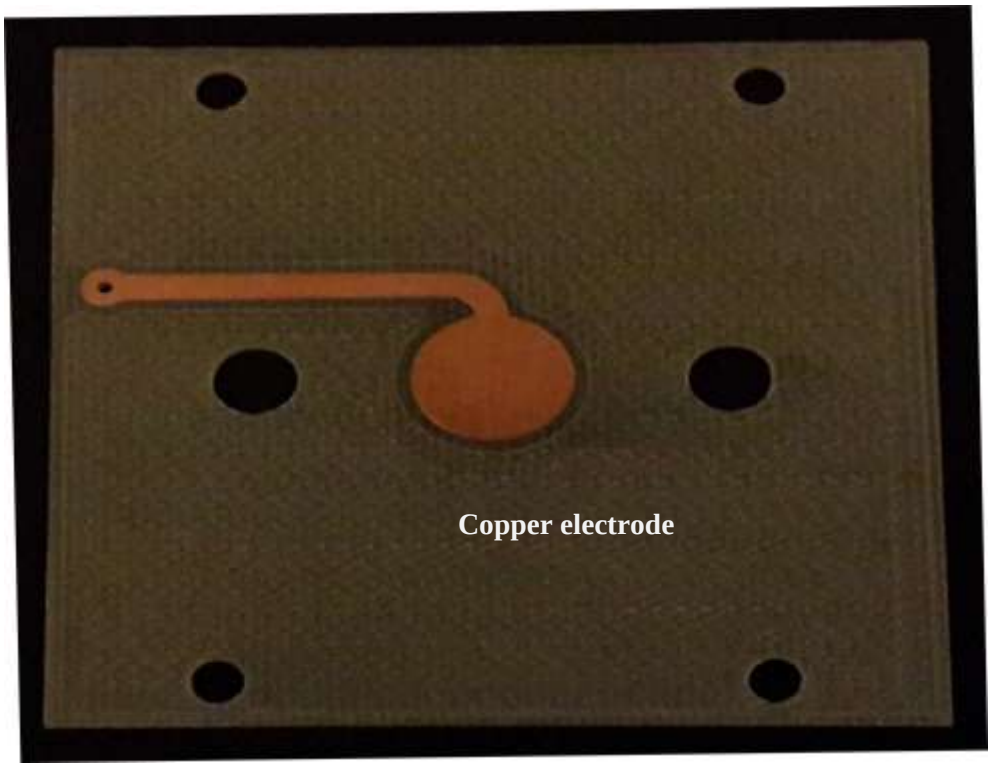

Figure 3-17: Printed circuit board with a copper electrode used to connect the carbon electrode to the power supply

3.5.7 Electrodialysis on a COC chip with a multi-membrane

In this system, two types of ion exchange membrane were used: an anion-exchange membrane for the extraction of anion and a cation-exchange membrane for the extraction of cation. The chip in this system is made from COC (using the process mentioned earlier in section 3.3).

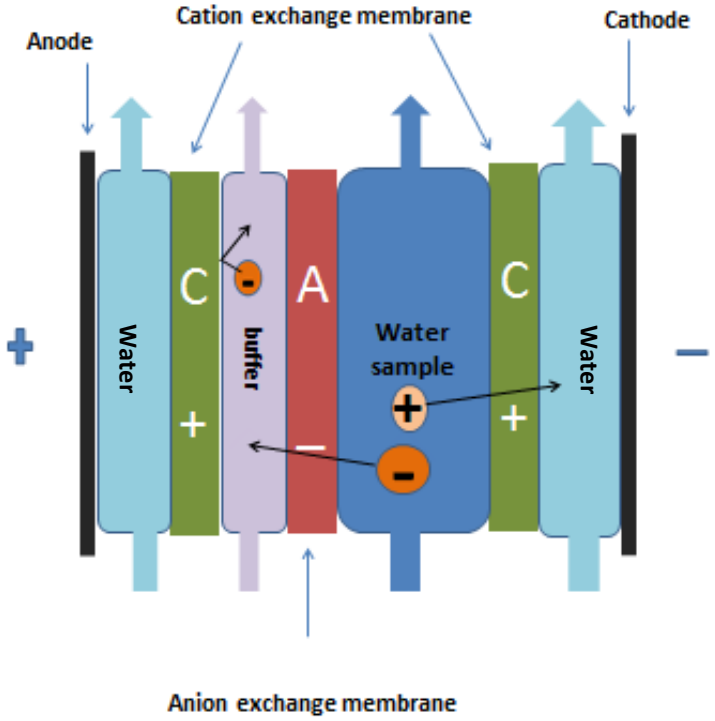

Figure 3-18: Schematic diagram of the COC chip with two membranes for ion extraction

Figure 3-18 shows a schematic of the chip, which consists of four layers. The first layer has a reservoir of deionised water (or any convenient solution), which is situated directly after the electrode (cathode); this is in order to generate enough current to complete the electric circuit and to condition the cation exchange membrane, which is situated in the other side of the water reservoir. Following this is the second layer, which contains the analyte sample; this layer is between two membranes, the anion-

exchange and cation-exchange. Following the analyte sample reservoir anion-exchange membrane, this membrane only allows the anion to pass through the membrane to the anode. The anion-exchange membrane passes anions only towards the anode on the other side of the chip. The third layer after the anion-exchange membrane has a buffer reservoir (most of the time the buffer was 5 mM MES/His); the buffer has to be compatible with the separation step. The buffer should carry the extracted anions from the water sample to the separation chip, and in order to pre-concentrate the anion in this stage, the cation-exchange membrane is placed in the other part of the reservoir to keep the anions between the two membranes. The last layer after the second cation-exchange membrane has a reservoir of water (or any convenient solution) to condition the membrane and generate current to complete the electric circuit. On the other side of the reservoir is the other electrode (anode).

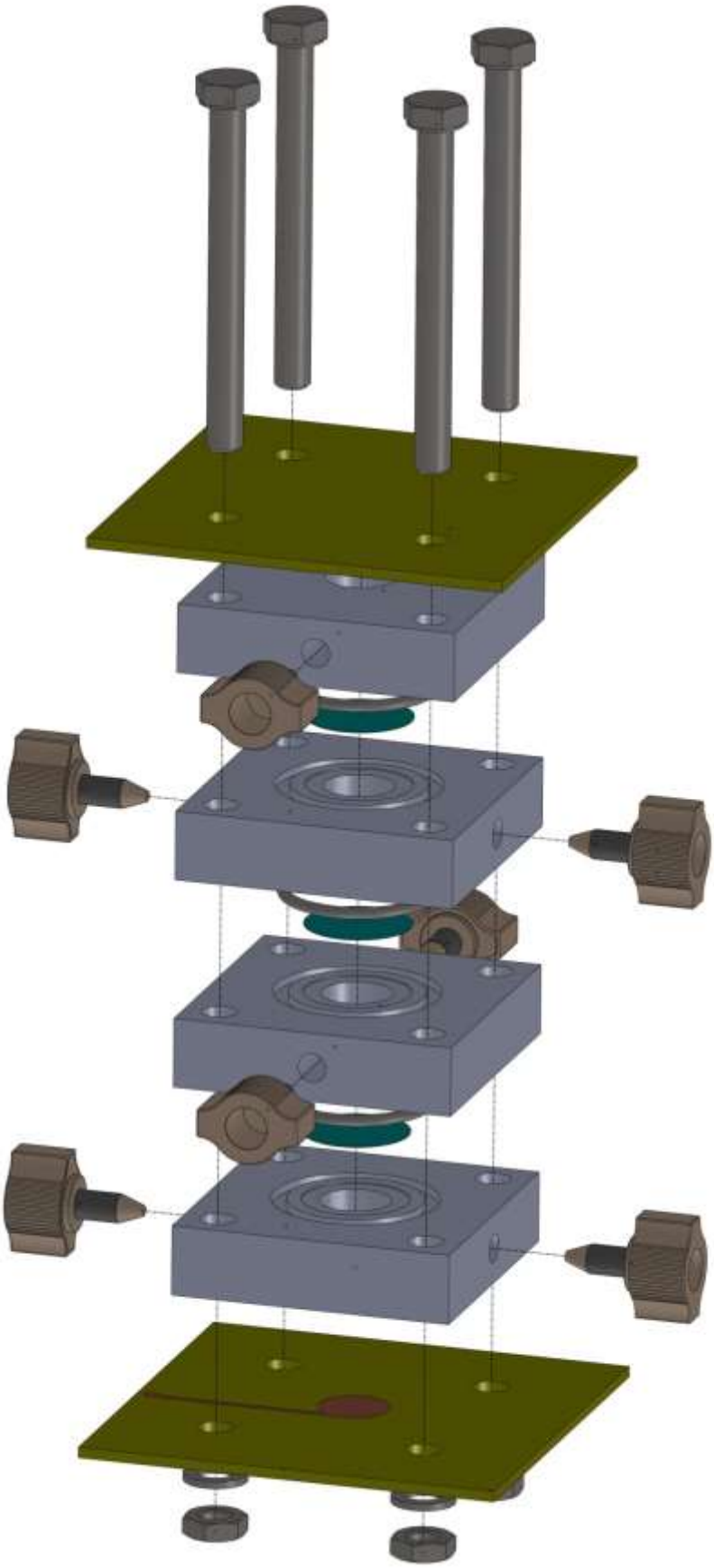

Figure 3-19: Topside view of a COC multi-membrane system for ion extraction

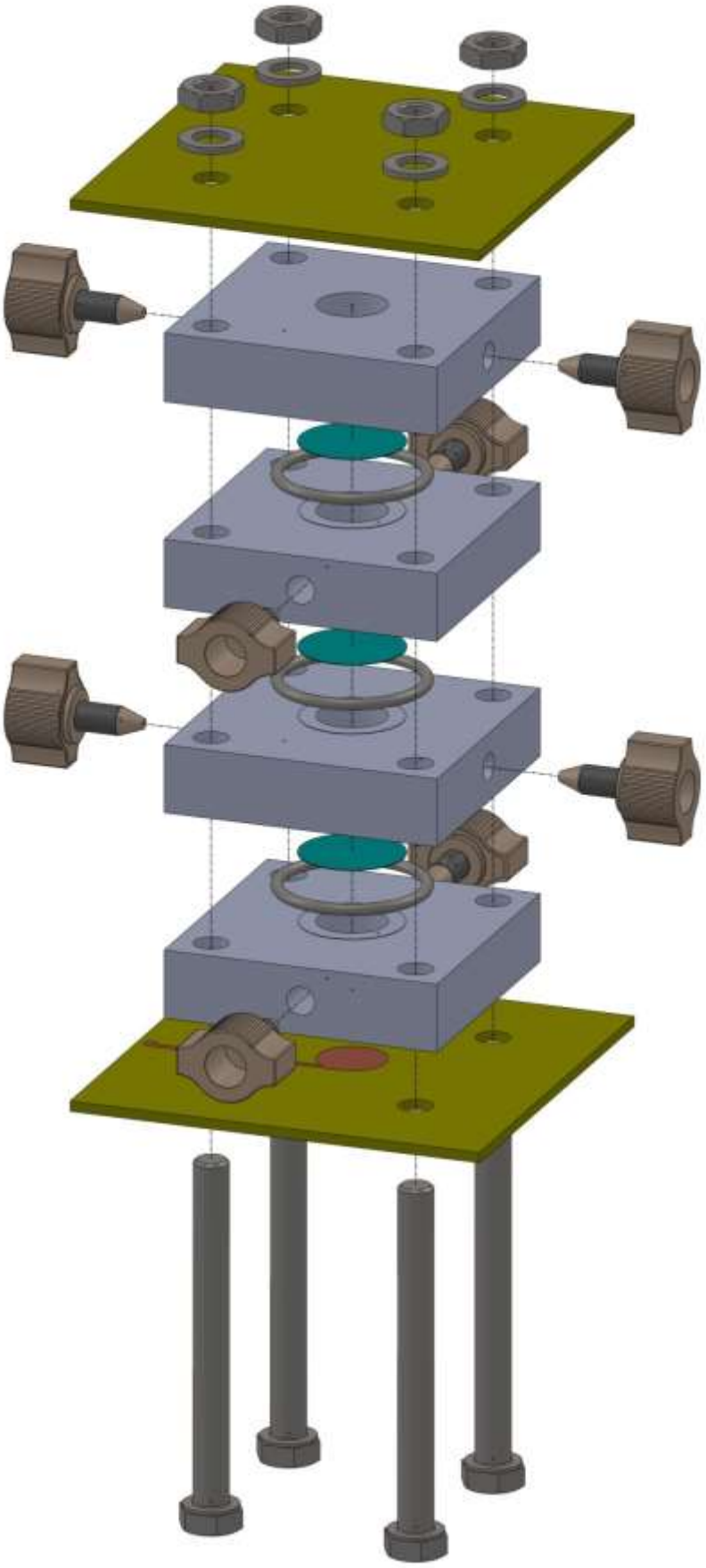

Figure 3-20: Bottom-side view of a COC multi-membrane system for ion extraction

Figure 3-19 and Figure 3-20 demonstrate the design of the multi-membrane system for ion extraction. The system has three reservoirs, mentioned earlier in Figure 3-18. The device has been assembled using double-sided tape, uses standard connection tubes and fittings (Kinesis Ltd, UK), and has side access holes leading to the reservoirs, thus allowing for interaction with the membrane. Each layer is sealed using an O-ring and a clamping arrangement. The advantages of this concept over a channel-based device include the potential reduction in leaks, easy assembly and alignment of all layers and PCBs, reusability of the components, and better incorporation of the membrane (through appropriately designed positioning). The PCBs were sealed to the cell device using double-sided tape.

3.5.8 Electrodialysis on a COC chip with one membrane

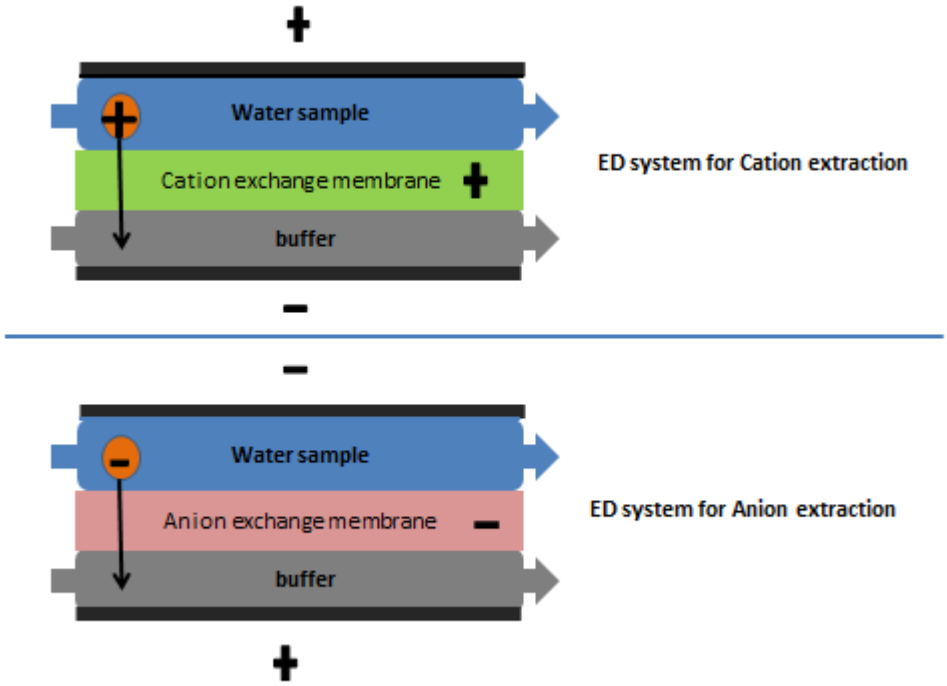

Figure 3-21: Schematic drawing of an ED chip with one membrane for the extraction of ions

Figure 3-21 shows a diagram of the ED chip design. The chip has a top inlet from the side to introduce the sample to the reservoir, and an outlet that allow the sample to exit; the bottom side also has the same, for the buffer reservoir. The fluid has been introduced to the chip and the exit by tubes connected to the chip through lure connectors (Kinesis Ltd, UK). The fluid has been pumped to the chip by a syringe pump (see Figure 3-4).

Both reservoirs are separated by a membrane, where the ED processes take place. The top and bottom reservoirs are attached to a PCB that has an electrode (for more details about the PCB and the electrode, see section 3.6.3). The PCBs are connected to a power supply. More details of the ED system are provided in the following image.

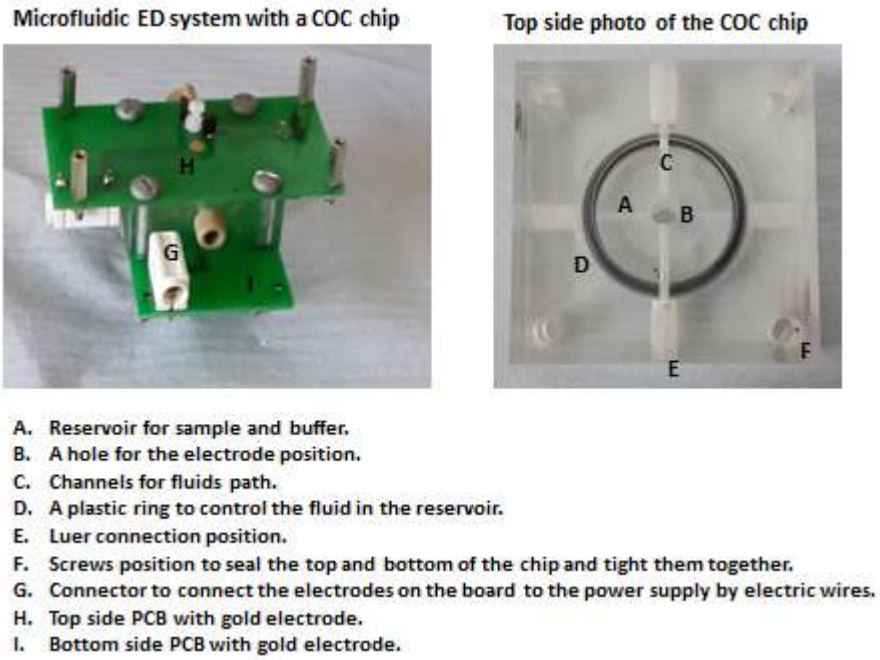

Figure 3-22: A photo of the ED system used for the extraction of ions

3.6 Printed circuit boards

A printed circuit board (PCB) is a non-conductive board that physically supports and electrically connects electronic components, using conductive tracks that are typically etched from copper sheets laminated onto a non-conductive substrate, such as polymer[183] (see Figure 3-17). The copper on the board works as an electrode to establish a conductive environment in the solutions used in electrodialysis systems. Sometimes, there are disadvantages to using copper as an electrode: it becomes easily oxidised and suffers from impurity,[184] which influences the analysis of inorganic ions. Therefore, different coating techniques have been used to overcome these issues.

3.6.1 Gold-coating of the copper electrodes on the PCB

Sputter coating is a process for applying an ultra-thin coating or layer of electrically conductive material.[41] Typically, metals such as silver, chromium, platinum and gold/palladium alloy are used for coatings. This technique is commonly used in the preparation of non-conductive samples for scanning electron microscopy. In SEM examination, the coating promotes the emission of secondary electrons from the sample surface, and prevents sample charging.[42]

For this exercise, gold has been used as the coating material. In the sputtering process, a gold target (cathode) is bombarded with a heavy gas (argon), in a vacuum chamber. If a high voltage is then applied, a discharge is created resulting in the acceleration of argon ions to the target surface. These ions eject material from the gold target, resulting in a coating on a sample that is sat below the target.[44] Modern, low-voltage sputter coaters enable coatings to be deposited at rates of up to 1nm/s.[43]

Figure 3-23: Edwards S150B gold-sputter coating instrument

The sputter coater used was an Edwards S150B (Figure 3-23). The board to be coated was "masked" with plastic film to prevent coating of the board, apart from the area comprising the electrodes (Figure 3-17). The board was placed in the vacuum chamber of the coater, approximately 50 mm from the gold target (60 mm diameter), and the rotary pump of the coater was switched on, until a suitable vacuum for coating was reached (typically 0.1 to 0.5 mbar). A voltage of approximately 1 kV was then applied to produce a discharge/plasma. A timed sputtering run of 3 minutes was applied to the board, in order to achieve a conductive gold layer of 6 to 10 nm.

3.6.2 Carbon coating of the copper electrodes on the PCB

Figure 3-24: Edwards High Vacuum Evaporator, model E12, for the carbon coating for the copper electrodes

A mask of tape and a thick plastic covered all of the board except the electrode part on the centre of the board (see Figure 3-17). The board was then placed on the baseplate of an Edwards High Vacuum Evaporator, model E12 (Figure 3-24). The carbon source was approximately 25 cm above the board. The source consisted of two spec-pure carbon rods; one sharpened to a point and the other to a slightly flattened point. The rods opposed each other under the spring pressure. The 30 cm diameter glass bell jar and its polycarbonate implosion guard were then replaced off on the machine, which was then evacuated to a pressure of <10-5 Pa. The carbon was evaporated by applying approximately 30 Volts at 30 Amps to the carbon rods (the carbon rods [300 mm x 6.15 mm] were supplied by Agar Scientific). The board was then covered with a layer of conductive carbon that was about 10 nm.

3.6.3 Commercial PCB

A more advanced technique for coating surfaces is used to overcome the problems associated with copper: electroless nickel immersion gold (ENIG).[185] ENIG is a surface-plating technique used for printed circuit boards. It is literally two layers of metallic coating of 2-8 microinches of gold over 120-240 microinches of nickel.[186] The nickel works as a barrier to the copper and is the surface to which the electrical components are soldered. The gold layer is there to protect the nickel from oxidation (Figure 3-25). ENIG has some advantages over typical surface plating techniques, such as good oxidation resistance. (The PCB was fabricated by Faraday Printed Circuits Ltd, UK.) see Figure 3-26.

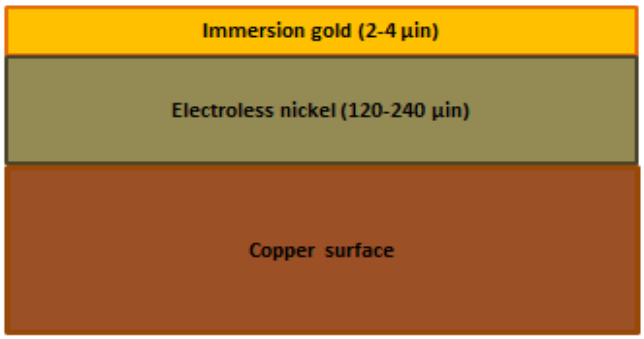

Figure 3-25: A schematic drawing of the metallic layers of electroless nickel immersion gold (ENIG).

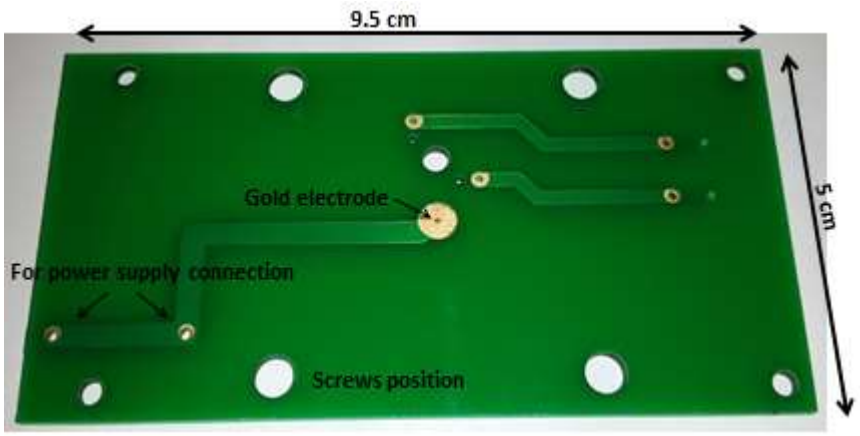

Figure 3-26: The customised commercial PCB with the gold electrode

4 Silica monoliths for the separation of ions

4.1 Introduction

For IC to be useful for *in-situ* monitoring, it is necessary to reduce the time taken to perform separations of ions of interest. Therefore, a monolithic column was used for the fast separation of inorganic ions, which can be achieved in minutes.[187] Recent investigations into the separation of inorganic molecules on monolithic columns have provided some very promising results, and have shown that a short, silica-based monolithic column can demonstrate peak efficiencies that are equivalent to, or better than, those previously obtained using the more traditionally sized particle-packed columns.[145] Furthermore, as mentioned in section 2.3.1, inorganic silica-based monolithic columns can provide good mechanical stability, and the possibility of chemical modification for IC. In addition, the separation is simple and the final shape of the monolith can be adjusted. Therefore, silica monolith was used in this research for the separation of inorganic ions.

Silica monolith was used as a stationary phase for the separation of inorganic ions, as it can be miniaturised and can perform very good separation. However, the separation of ions requires a high, specific surface area, which was achieved through the porosity of the monolith media's nm-sized pores. It is also highly permeable, which is achieved through micron-sized pores to allow for rapid mass transfer to the detector. Furthermore, it has to be mechanically strong in order to stand the pressures applied to move fluid through them. Therefore, effective monoliths must achieve a convenient compromise between these requirements, which can be obtained through the fabrication process that ensures that monoliths have both micron- and nano-scale pores. These processes are explained in the experimental section 4.2.1.1.

To separate ions on a silica monolith, the surface of the monolith has to be modified with an ion exchanger. Two promising approaches have been investigated for the separation of ions: lysine and DDAB.

4.2 Experimental

4.2.1 Preparation of analytical separation column

Silica-based monolithic columns can be prepared through hydrolysis and the polycondensation of alkoxysilanes catalysed by an acid in the presence of a porogenic agent such as Tetraethylorthosilicate (TEOS). After drying and heating treatments, the sol–gel network is derivatised by an on-column silylation reaction for chromatographic separation. The functional groups should be introduced onto the silica monolith; there are more details on the preparation of the monolithic column in the following section.

4.2.1.1 Synthesis of silica monoliths

The silica monolith was prepared using a procedure similar to that described by Nakanishi.[154] The desired amount of polymer, 0.282 g of polyethylene oxide, was added to aqueous solution of acid (0.291 ml of distilled water + 2.537 ml 1M HNO_3). The mixture was cooled in an ice bath and stirred for 20 minutes, or until a homogeneous solution was formed. The required amount of silicon alkoxide (2.256 ml) of TEOS was then added and the mixture was stirred strongly in the ice bath for about 30 minutes, to form a transparent solution. The solution was then poured into a plastic tube (diameter 4.8 mm; length 10 cm). Both ends were closed with PTFE tape and the tube was placed in a 40 °C oven for 3 days, during which a wet semi-solid gel monolith was formed. About 20% shrinkage occurred during this gel formation, which allowed for the easy removal of the wet gel monoliths from the plastic tube. The wet gel monoliths were washed with copious amounts of water to remove any possible residues

and then moved to a 1 M NH_4OH aqueous (1:4 NH_4OH: water) solution in a conical flask (100 ml), which was placed in an oil bath to ensure the uniform distribution of the heat. This system was located on a hot plate to maintain 90˚C overnight. The monolith was again washed with lots of water before drying in an oven at 40°C for 24 hours. Finally, the monolith was calcined at 550–650 °C for six hours under an air flow, to remove any remaining organic material.[188] After preparation, the silica rod was cut to the desired length of 6 cm. The silica rod was placed in a (tetrafluoroethylene) (PTFE) shrinkable tube (Adtech Polymer Engineering Ltd, UK) and then placed in the oven at 330ºC for two hours to seal the heat-shrinkable tube around the monolithic rod. Following this, the silica monolith was synthesised, with the monolith rod shown in Figure 4-1.

Figure 4-1: 6 cm long silica-based monolithic column for separation

4.2.1.2 Derivatisation of the silica monoliths with lysine

The coating procedure was based on the method of Huang *et al*.[189] Figure 4-2 shows the reaction mechanism for the generation of the desired epoxy, diol and lysine stationary phases on a silica monolith. To generate an epoxy monolith, a solution of 2-mL GPTMS (3-Glycidyloxypropyltrimethoxysilane), 100 µL of 2,6-lutidine (catalyser) and 40 mL of anhydrous toluene was used. This mixture was placed in a 10 ml glass syringe and flushed through the monolith by a syringe pump at 0.1 $mLmin^{-1}$, for about 1 hour, and the column was then reacted at 110ºC for 1 hour. This step was repeated three

times and the final reaction was carried out overnight. The monolith was then flushed with toluene by using a syringe pump at 0.5 $mLmin^{-1}$ for 1 hour, and then with methanol at 0.5 $mLmin^{-1}$; the epoxy monolith was then ready for the next treatment, to generate the lysine stationary phase.

The next step was to produce the diol. This is performed by flushing the prepared epoxy monolith with 0.1 M HCL for five hours and placing it in an oven at 60ºC for two hours, to open the epoxy ring groups and generate the diol groups. The monolith was then flushed with water and methanol, leaving the resulting diol stationary phase on the monolith surface ready to use.

The next step involved the preparation of the lysine stationary phase: 4.38 g of lysine was dissolved in 30 mL NaH_2PO_4 (50 mM) at pH 8.0, adjusted by 1 M NaOH. The prepared epoxy monolith was perfused with this solution for 1 hour and reacted at 75ºC for 1 hour. This step was repeated twice before the final reaction was carried out overnight, for 16 hours. The monolith was then rinsed with water and methanol prior to use.

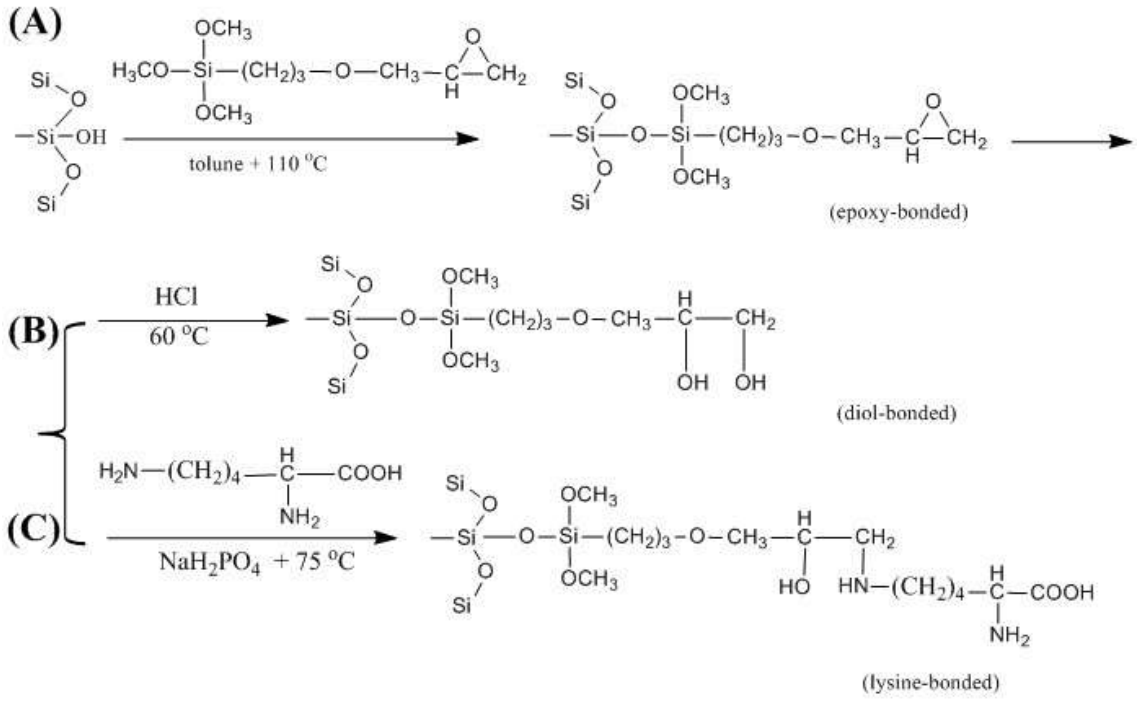

Figure 4-2: Derivatisation of the silica monolith with lysine. A) epoxy monolith, B) diol monolith and C) the lysine modification

4.2.2 Derivatisation of the silica monolith with DDAB

The derivatisation of the silica monolith column with DDAB requires a C18 coating prior to coating the column with DDAB. As bare silica monoliths do not possess anion-exchange sites, they may demonstrate a low retention for anion separation.[190] Furthermore, DDAB as a reverse phase has shown a good separation of anions and it has performed fast separations of anions of less than a minute.[191]

4.2.2.1 Derivatisation of the silica-based monolith with C18

The monolith was modified by C18 using a procedure similar to that described by Xie.[192] Briefly, the derivatisation reagent was 1 g chloro(dimethyl)octadecylsilane (ODS) as the silanisation reagent in 10 ml toluene and few drops 2,6-lutidine. The derivatisation was coated on the monolith by a continuous flow from a syringe pump at

a flow rate of 30 ml/mins for six hours at 80 °C in a water bath. After the derivatisation, the monolith was flushed with toluene and then with methanol, using a syringe pump for one hour; finally, the derivatised silica column was placed in an oven for 24 hours at 70°C prior to use.[193]

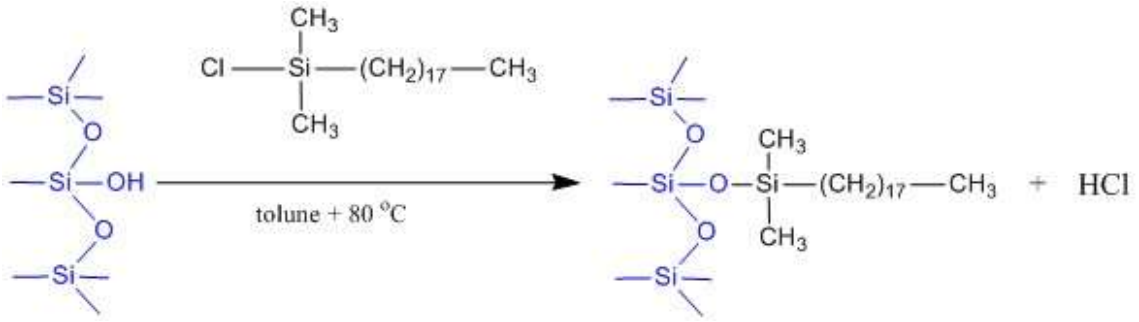

Figure 4-3: Derivatisation of the silica monolith with C18

After preparation, the silica rod was cut to the desired length of about 6 cm. The silica rod was placed in a (tetrafluoroethylene) (PTFE) shrinkable tube and then placed in the oven at 330ºC for two hours to seal the heat shrinkable tube around the monolithic rod. Following this, the silica monolith is ready for modification, with the monolith rod demonstrated in Figure 4-1.

4.2.2.2 Coating the C18 silica monolith with ion exchange; didodecyldimethylammonium bromide (DDAB)

The monolith was coated using the procedure of Hatsis and Lucy.[150b] Briefly, the monolith was conditioned with 33% ACN in water, and then flushed with 1mM DDAB (didodecyldimethylammonium bromide) in 33% ACN in water at a 0.2 $mLmin^{-1}$flow rate, until DDAB breakthrough was observed. The monolith was flushed with water for about one hour at a 0.2 $mLmin^{-1}$flow rate to wash out any unbound DDAB. The detector was reattached and the coated monolith was then conditioned with the eluent (65%

ACN in water) at 0.5 $mLmin^{-1}$ flow rate, until the conductivity stabilised. The ion-exchange capacity of the coated monolith was estimated from the DDAB Breakthrough time, using the following equation:

$$Q = C\,F\,(t_b - t_0) \qquad \textbf{Equation 4-1}$$

Where C is DDAB concentration in the coating solution (μmol/ml), F is the flow-rate ($mLmin^{-1}$), t_b is the breakthrough time of DDAB (min) and t_0 is the hold-up time of the monolith (min). The ion-exchange capacity of the monolith can be varied by adjusting the ACN content of the coating solution.[150b]

4.2.2.3 Coating the commercial C18 monolith with DDAB

A commercial C18 monolithic column (100 x 4.6 mm size Onyx Monolithic C18, Phenomenex Inc., UK) was first tested on a HPLC system, and was then conditioned with 100% ACN. Following this, the column was conditioned with 65% ACN: 35% water solution and then flushed with 1mM DDAB in 65% ACN: 35% water at 2 $mLmin^{-1}$, until a stable baseline was observed on the detection. The column was flushed with water for 30 min at 1 $mLmin^{-1}$ to wash out the unbound DDAB. This was repeated at least two times to ensure the best possible coating of DDAB.

4.2.3 Evaluation of the structure of monoliths

4.2.3.1 Scanning electron microscopy (SEM)

The morphology of the monolith was characterised by scanning electron microscopy (SEM), using a Cambridge S360 scanning electron microscope (Cambridge Instruments, Cambridge, UK). The monolith was cut to an appropriate size and then images of a cross-section were obtained, using an accelerating voltage of 20 kV and a probe current of 100 pA in high vacuum mode. The monoliths were coated with a thin layer of 2 nm thick gold-platinum using a SEMPREP 2 Sputter Coater (Nanotechnology Ltd, Sandy, UK).

4.2.3.2 Brunauer-Emmett-Teller (BET) model

The physical properties of the monolith such as surface area, average pore diameter and pore volume, were studied through the Brunauer-Emmett-Teller (BET) model using a surface area and porosity analyser (Micromeritics Ltd, Dunstable, UK). The porous monolith was fabricated inside a 1 mL disposable plastic syringe. The monolithic rod was then removed from the syringe and dried using N_2 gas. The porous properties of the monoliths were determined using the BET isotherms of nitrogen adsorption and desorption at 77 K. The isotherms were analysed to obtain the surface area according to the BET model. The BJH (Barrett-Joyner-Halenda) model was used to measure the pore volume, and the pore size distributions of pores within the monoliths were measured from the nitrogen adsorption isotherm.

4.2.3.3 Ion-separation experiment

The HPLC experimental set-up described in section 3.4 was used to perform the separation of an anion mixture. Characterisation started with a 1mM nitrite solution (was used as sodium salts). The set-up began with a syringe pump to ensure constant pressure of the eluent through the separation monolith that was 0.02 $mLmin^{-1}$, with the eluent 50 mM phosphate buffer placed in a 10 ml plastic syringe. A plastic tub with 0.5 mm diameter was used for carrying the eluent from the syringe to the loop injector, the separation monolith and then the detection system, and eventually to the waste container.

4.2.4 Results and discussion

4.2.4.1 Evaluation of the lysine monolith structure

The aim of the lysine approach was to produce high-performance ion exchangers on the silica monolith, for the separation of inorganic ions. The silica monolith has been

modified with lysine to produce a high-performance monolithic zwitterionic ion-exchanger. This has been investigated elsewhere, showing promising results.[194]

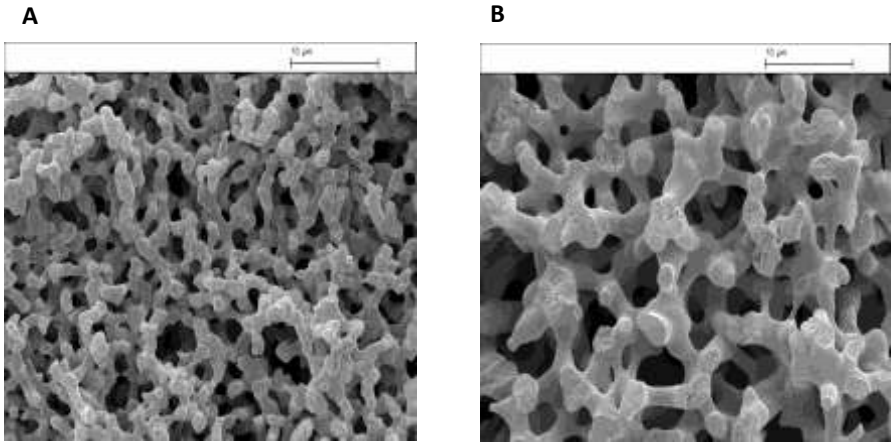

Figure 4-4: SEM images of the cross-section of a final monolith (A) before lysine modification and (B) after lysine modification

Figure 4-4 demonstrates that the structure of the monolith surface is highly porous, containing a rigid silica backbone; the physical geometry is random, without any apparent regular lattice "sponge-like" structures that are continuous. The continuous monolithic structure of silica skeletons shows a range of macropores sizes between 1 and 10 µm; these macropores allow for convective flow through the continuous column bed. Further treatment of the monolith with an alkaline aqueous solution, such as ammonium hydroxide, generates mesoporous silica structures with a pore-size ranging between 5 and 30 nm. These mesopores allow the analyte to diffuse through, which makes them responsible for the selective separation by adsorption or desorption. This structure simultaneously enables a high efficiency of separation and low back pressure.[151, 154, 195] [196]

The chemically-modified silica monolith surface with lysine was characterised by SEM and BET to identify the differences between the modified and non-modified silica-based

monoliths. Figure 4-4 shows the SEM image of the surface of the silica monolith before (A) and after (B) modification with lysine, and they are characterised by a bimodal pore structure with continuous macropores and mesopores. The SEM image demonstrated no noticeable differences in the structural morphology of the two monoliths. The BET analysis of the surface area of the lysine-modified silica monolith, however, demonstrated a decrease from 356 m^2g^{-1} before lysine modification to 150 m^2g^{-1} after modification with lysine. The pore sizes have also decreased from 130 Å (non-modified silica-based monolith) to 111 Å for the modified monolith.

4.2.4.2 Evaluation of the structure of the DDAB monolith

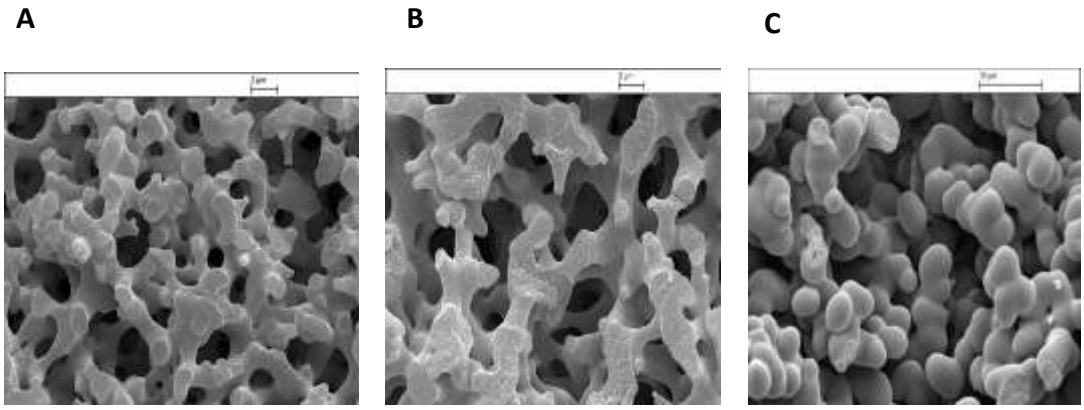

Figure 4-5: SEM images of a cross-section of a final monolith (A) after formation; (B) after the treatment of ammonium hydroxide which creates extra surface area; and (C) after calcination and coating with cationic surface DDAB to create an anion-exchange surface

Figure 4-5 shows that the structure of the monolith surface is highly porous, containing a rigid silica backbone; the physical geometry is random, without any apparent regular lattice "sponge-like" structures that are continuous. The continuous monolithic structure of silica skeletons shows a range of macropore sizes between 1 and 10 µm; these macropores allow for convective flow through the continuous column bed. Further treatment of the monolith with an alkaline aqueous solution, such as ammonium

hydroxide, generates mesoporous silica structures with a pore-size range between 5 and 30 nm. These mesopores allow the analyte to diffuse through, which makes them responsible for the selective separation by adsorption or desorption. This structure simultaneously enables a high efficiency of separation and low back pressure.[151, 154, 195] [196]

4.2.4.3 Chromatography of a lysine monolith

In sections 4.2.3.3, the procedure of the modification of the silica monolith and the experimental work were demonstrated. In order to investigate the optimum conditions for the separation of an anion using this experimental set-up, 1 mM sodium nitrite was injected into the system.

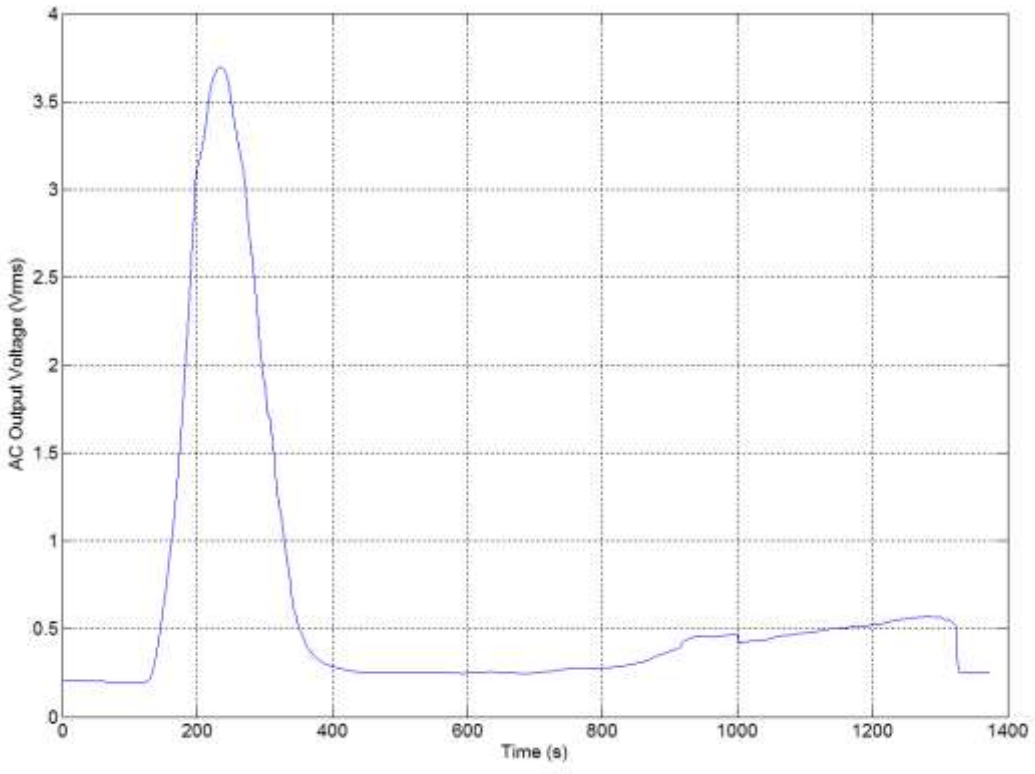

Figure 4-6: Chromatogram of a 1 mM sodium nitrite solution, eluent of 50 mM phosphate buffer, flow rate of 0.025 mLmin^{-1}

Figure 4-6 shows the chromatogram of 1 mM sodium nitrite on a monolithic column coated with lysine, using a conductivity detection system. The chromatogram demonstrates a peak retained at 250 s. Using Equation 2-7, the value for N was 27, which is low.

The results obtained from the silica monolith coated with a lysine ion exchanger for the purpose of optimising the conditions, are very promising but require further optimisation. The low value for N might be due to the HPLC system. The syringe pump could not pump consistently against the resistance in the monolith.[197]

It has been proved that a shorter monolith has demonstrated the successful separation of inorganic ions,[77] and longer columns have also demonstrated the successful separation of inorganic ions[194]; further optimisation of the length of the monolith will probably enhance the separation.

Another issue with the lysine coating is that, practically, it was hard to coat the column with lysine because of the lengthy preparation procedure. During the coating process, there was a considerable blockage of the monolith due to the nature of the monolith surface (further discussion below), which required halting the coating process a few times and restarting the procedure with a new monolith. This was indicated at times with changes in the colour, especially after the reaction when removing the monolith from the oven during the heating step. The long procedure steps and the addition of chemical reagents is not ideal for continuous *in-situ* monitoring, because it will eventually affect the separation process and the reproducibility[197] of the chromatogram, which were examined a few times and showed considerable changes in the chromatogram. Further examination of the effect of the lysine coating is to follow.

The decrease in the surface area of the monolith following the modification could be the reason for the blockage of the monolith during the modification process, as it was creating high back pressure that was difficult to deal with, making the preparation of the monolithic column slightly difficult. This problem could be overcome by modifying the monolith's surface area, but this requires a longer period of investigation.

4.2.4.4 Chromatography of a DDAB monolith

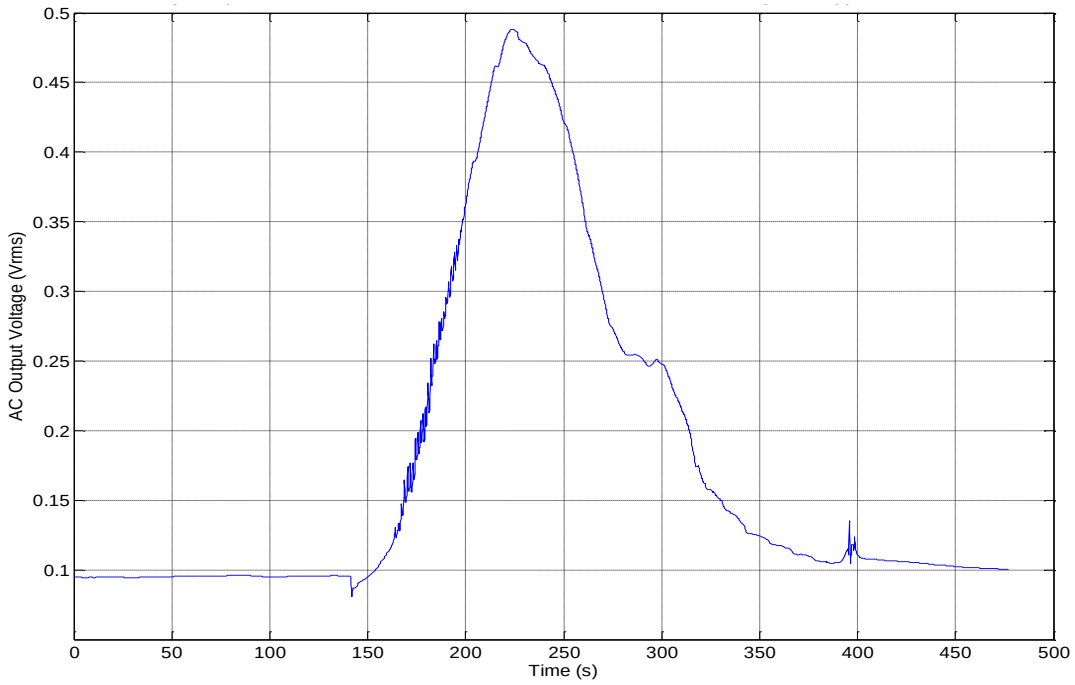

Figure 4-7: Chromatogram of the separation of 1 mM sodium nitrite and 1 mM sodium sulphate on a DDAB monolith, flow rate 0.2 mLmin^{-1}. The buffer 65% ACN, and the detector was homemade conductivity detection system.

Figure 4-7 shows the chromatogram of the separation of a 1 mM nitrite and 1 mM sulphate mixture on a monolithic column coated with DDAB, using a conductivity detection system. The choice of these two anions was due to the fact that they normally have a relatively large retention time gap in a typical chromatography separation. However, the chromatogram demonstrates two overlapping peaks: the first one retained

at 225 s, which could be a nitrite peak, and the second retained at 300 s, which could be sulphate peak. In order to distinguish between these two peaks, typical chromatogram of nitrite can be seen in Figure 4-8.

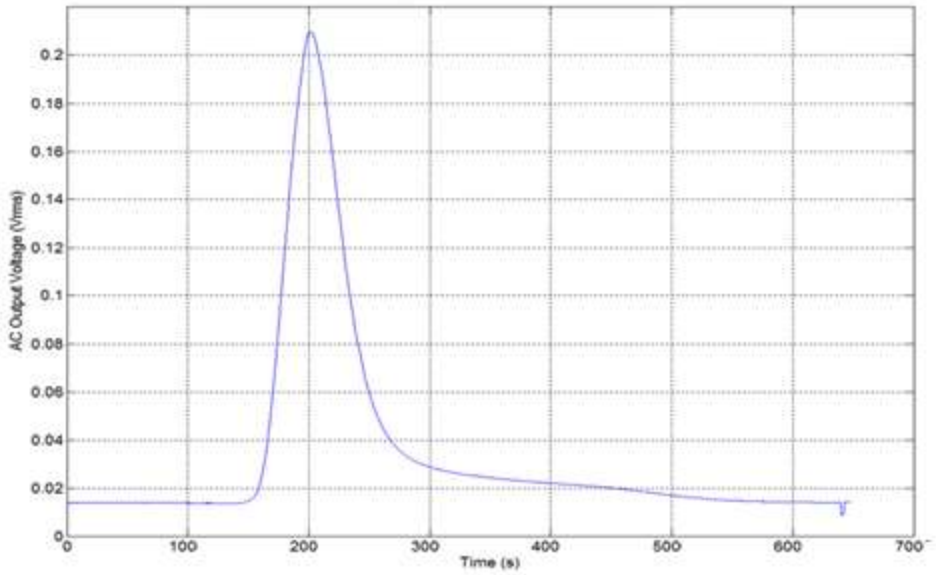

Figure 4-8: Chromatogram of the separation of 1 mM sodium nitrite on a DDAB monolith, flow rate 0.2 mLmin^{-1}. The buffer 65% ACN, and the detector was homemade conductivity detection system.

Figure 4-8 shows a chromatogram of a single peak retained just after 200 s. The peak is relatively wide and has a long tail, and it has a low intensity, as the peak height is about 0.2 Vms. Using Equation 2-7, *N* for nitrite in the chromatogram was 79.

Using Equation 2-8, *h* for nitrite chromatogram (Figure 4-7) was 1.45 ×10^{-3}, and *h* for nitrite chromatogram (Figure 4-8) was 0.075. Using Equation 2-9, the resolution of the nitrite peak and the sulphate peak in Figure 4-7 was 6.8.

Figure 4-8 shows an unexpected peak as it demonstrated a lower intensity than Figure 4-7; the peak height is 0.2 V ms while it is 0.5 V ms in Figure 4-7. Also, there was a slight shift in the retention times of both peaks. Both chromatograms should show

identical nitrite peaks, or at least peaks that are similar to each other. Both chromatograms have demonstrated an improved number of theoretical plates. The first chromatogram for the separation of nitrite and sulphate (Figure 4-7) has poor resolution and considerable loss of efficiency; this is probably due to the extra column length from connector and the glass rods at the end of each monolith, as they are relatively big in size when compared to the monolith (see Figure 4-1). The extra-column band broadening has to be minimised as much as possible to improve the efficiency.[191]

However, the estimated capacity of the monolith has to be calculated to compare the results with the literature.

$$\boldsymbol{Q = C\,F\,(t_b - t_0)}$$

Equation 4-2

Where *C* is the DDAB concentration in the coating solution (µmol/ml), ***F*** is the flow-rate ($mLmin^{-1}$), t_b is the breakthrough time of DDAB (min) and t_0 is the hold-up time of the monolith (min). The concentration of DDAB in a I mM solution was 115.66 mg, the flow rate was 0.2 $mLmin^{-1}$, the breakthrough time was about 50 s (0.83 min), and the void time was around 5 s (0.083 min); therefore, the capacity was 17.279 µeq/column. The capacity here is lower than the theoretical one in the literature, which was 44 µeq/column.

In general, the estimated calculation of the capacity, *N* and R, demonstrate unexpected results. However, this was from one attempt, as it is extremely difficult to optimise the separation conditions as there was a continuous leakage from the monolith, even when a commercial column was used for comparison. Also, the syringe pump used was creating bubbles because it was not pumping continuously. Moreover, the monolith was first derivatised with a C18 layer before the layer was coated with DDAB; this double layer

might have had a negative effect on the diffusion of the analyte through the monolith, leading to poor resolution.

4.2.4.5 Chromatography of DDAB on a commercial monolith

A commercial Monolithic HPLC Column was used to compare the chromatographic behaviour of the homemade monolithic columns with DDAB, and to compare the results obtained with DDAB derivatisation to the literature.

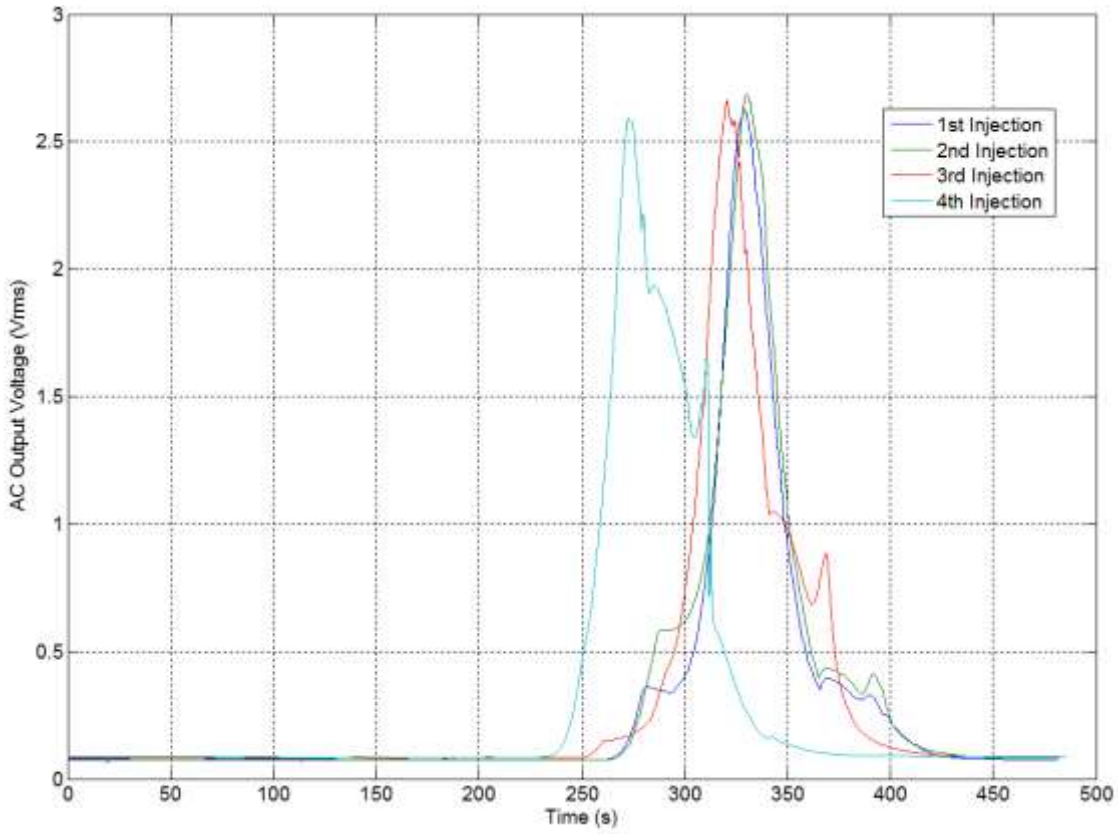

Figure 4-9: Chromatograms of 1 mM sodium nitrite in four injection attempts. The column was an onyx C18 column coated with DDAB, the buffer was 65% CAN, the flow rate was 02 mlmin^{-1}

Figure 4-9 shows the chromatograms of 1 mM sodium nitrite in a commercial C18 column coated with DDAB. The chromatograms demonstrate nitrite peaks in four different injections. At the first injection, the peak retained at 270 S; the peak is not a great shape and has a second minor peak on its side. The second, third and fourth peaks

were retained between 300 and 350 S; the peaks have different shapes, especially at the bottom, which indicates different peak areas.

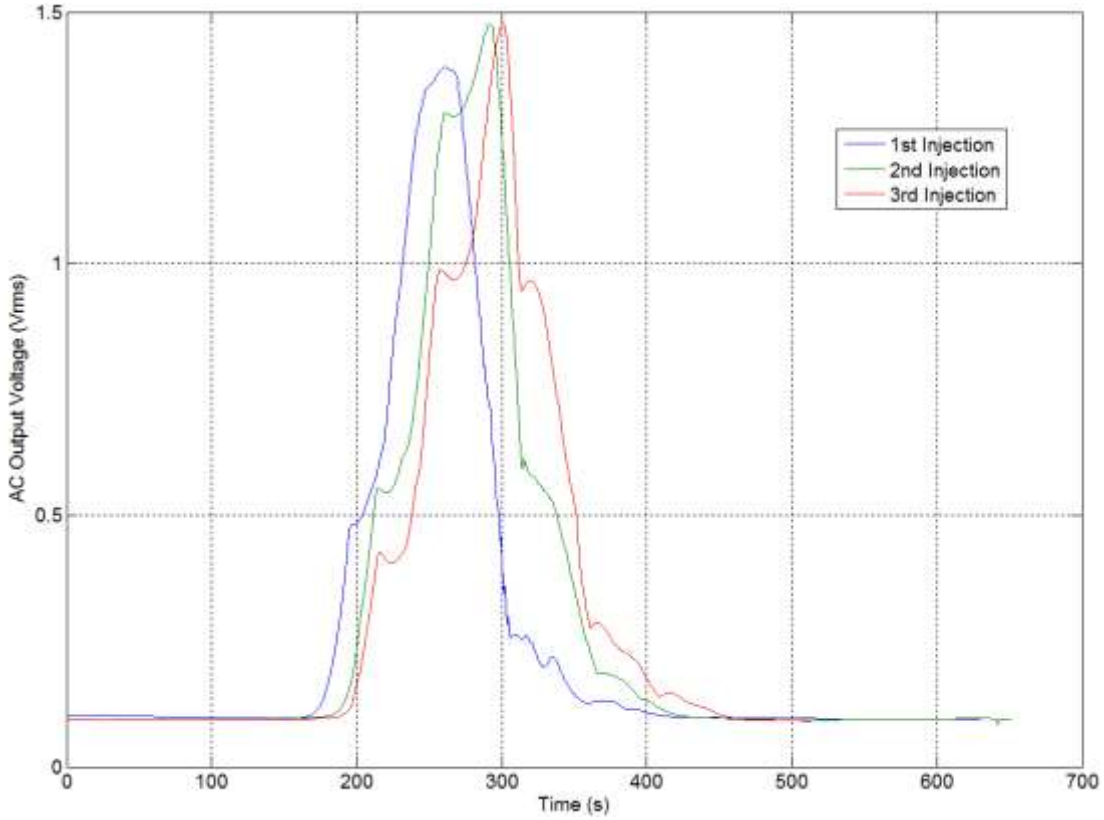

Figure 4-10: Chromatograms of 1 mM sodium sulphate in four injection attempts. The column was an onyx C18 column coated with DDAB, the buffer was 65% CAN, the flow rate was 02 mlmin-1

Figure 4-10 shows the chromatograms of 1 mM sodium sulphate in a commercial C18 column coated with DDAB. The chromatograms demonstrate the sulphate peaks for three different injections. The peaks were not a good shape: they have second minor peaks on their sides. The peaks were retained between 250 and 300 S, and have different shapes, especially at the bottom, which indicates different peak areas.

The main purpose of using the commercial C18 column was to compare its behaviour with the behaviour of the prepared in-house monolithic column. Both figures (Figure 4-9 and Figure 4-10) demonstrate a lack of reproducibility in the chromatogram

using the commercial C18 column with DDAB. They also have very close retention times of nitrite and sulphate; these two anions usually have a good gap in retention times due to their differences in charge density. Furthermore, the peak shapes are totally different when comparing the chromatograms of nitrite that used the prepared in-house monolith to those using the commercial monolith.

4.3 Chapter conclusion

The monolithic column was used as a possible stationary phase for the separation of inorganic ions, as it demonstrated very good results in the literature. For the separation of anions, two different anion exchangers were investigated, lysine and DDAB. The monolith was prepared in-house and then coated with the anion exchanger. A commercial C18 monolith was used to compare the results obtained from the homemade monolithic column.

Two anions were used to perform the chromatography on the monolithic columns, nitrite and sulphate. On the lysine monolith, the nitrite chromatogram showed a good peak but coating the column was time-consuming and back pressure occurred. With the DDAB homemade monolith, the separation of nitrite and sulphate showed poor resolution, and a low number of theoretical plates was observed. When nitrite was evaluated on its own on the same monolith, a shift was seen in the retention time, and the peak intensity decreased. The commercial C18 monolith was also coated with DDAB and showed poor reproducibility for nitrite and sulphate.

Good chromatographic performance was not observed on the monolith. This could have been due to two factors. One is the problem of high back pressures which was obtained by pumping liquid through the monolith. The second problem is the operation of the detector, which needs further development. In relation to these problems, it was decided

that IC would not be suitable for the portable device, and electrophoresis would be a better approach.

5 The application of a potassium silicate monolith in sample introduction

5.1 Introduction

A potassium silicate monolith was used to extract ions from a water sample, as a possible media for extracting ions from a river water sample. A potassium silicate monolith works as a barrier against unwanted materials that are already present in the river water. The presence of these materials would influence the separation process. As a pre-concentration and pre-treatment step before separation, a potassium silicate monolith is permeable enough to allow only ions to pass through and blocks anything else, under the influence of applied voltage.

The bulk body of the monolith contains micropores (< 2 nm), mesopores (2-50 nm), or macropores (> 50 nm),[198] and the extraction of small molecules requires monoliths with pore sizes ranging from 8 to 10 nm (mesopores).[199] In 1996, Fields[200] prepared a silica xerogel monolith from a potassium silicate solution. This potassium silicate monolith can be formed into the desired shape, the surface can be chemically modified, the pore size can be modified, and it can be made physically strong. Therefore, extraction of inorganic ions can be performed in a silica monolith, for pre-concentration and pre-treatment prior to separation.

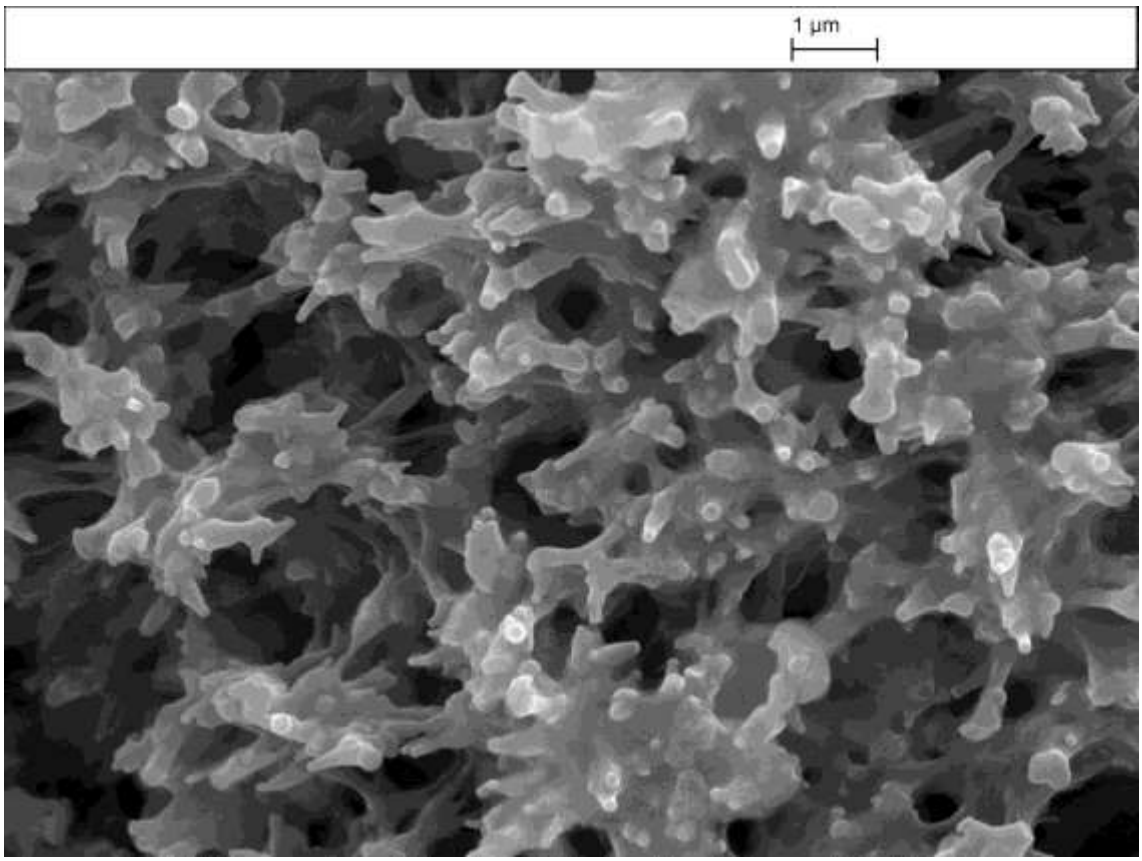

Figure 5-1: SEM image of a potassium silicate monolith

Figure 5-1 shows the structure of a potassium silicate monolith, by SEM. The structure is highly porous, containing a rigid silica backbone; the physical geometry is random, without any apparent regular lattice structure. This shows a good media for the extraction of ions through the monolith.[198]

5.2 Ion extraction on a chip

5.2.1 Experimental

5.2.1.1 Preparation of a potassium silicate monolith

Microporous silica frits were prepared from 1:10 formamide and potassium silicate solutions, at room temperature (25 °C).[201] The reagents were manually mixed for about 10 minutes and then injected into the chip's middle reservoir (Figure 5-2). In order to

control the position of the monolith in the microchip, glycerol was mixed with a food dye (the dye was to allow for visual control of the glycerol, as it is colourless), forming a highly viscous material that provides resistance to the mixture. The glycerol gel was pressure-injected with a syringe into the chip; the mixture was injected against the glycerol and held in position. The microchip was then placed in an oven at 90 °C for about 20 hours, before being removed and allowed to cool. The coloured glycerol gel was then removed with water and the device placed back in the oven, overnight.

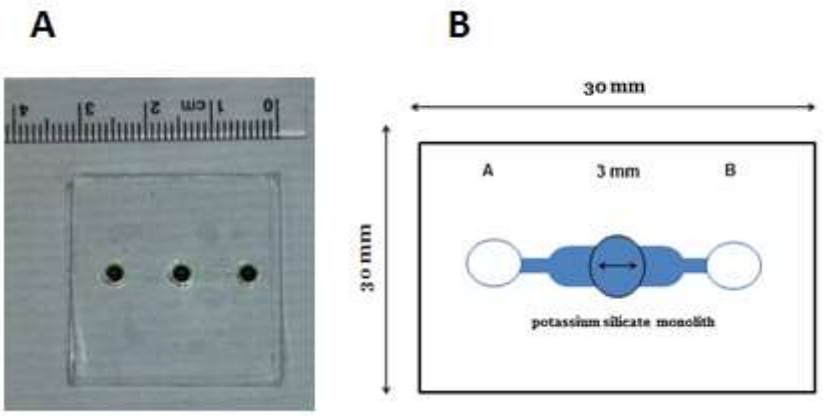

Figure 5-2: A) an image of the chip used for ion extraction, the channel contains glycerol and dye. B) is a diagram of the chip describing the channel design.

In order to place the solution in the chip, two Eppendorf tips were cut and their size adjusted to fit on both reservoirs (Figure 5-3). A Pt electrode (of about 1.5 cm long and 0.5 mm wide) was dipped in each reservoir; the electrodes were connected to a power supply.

On the chip used (see Figure 5-2), there were two reservoirs: the sample reservoir, referred to as reservoir (A) and the destination reservoir, referred to as reservoir (B).

Figure 5-3: Eppendorf tips placed on the glass chip to hold solutions in place

5.2.1.2 The ion extraction procedure

Initially, a phosphate buffer was used for separation following Huang *et al.*[189] (see section 4.2.3.3); furthermore it was used due to the convenient pH range (between 5-8), and its long-term stability under different temperatures for separation. Therefore, it was used for ion extraction, as the latter is the starting point of the analysis in this project, and so maintaining the same buffer for both steps (ion extraction and separation) is desirable.

A few experiments were run earlier to find the suitable voltage and timing. The experiment was performed by applying a voltage of 700 V to both reservoirs in the chip, for two hours. Reservoir A contained a 0.2 ml phosphate buffer (1mM) and 0.1 ml NaCl (1mM), and reservoir (B) only contained 0.3 ml phosphate buffer (1mM) . If the experiment were successful, the amount of anions in reservoir A should have decreased after the application of voltage, and increased in reservoir B. Solutions were then measured by ion chromatography (see section 3.2.1).

5.2.2 Results and discussion

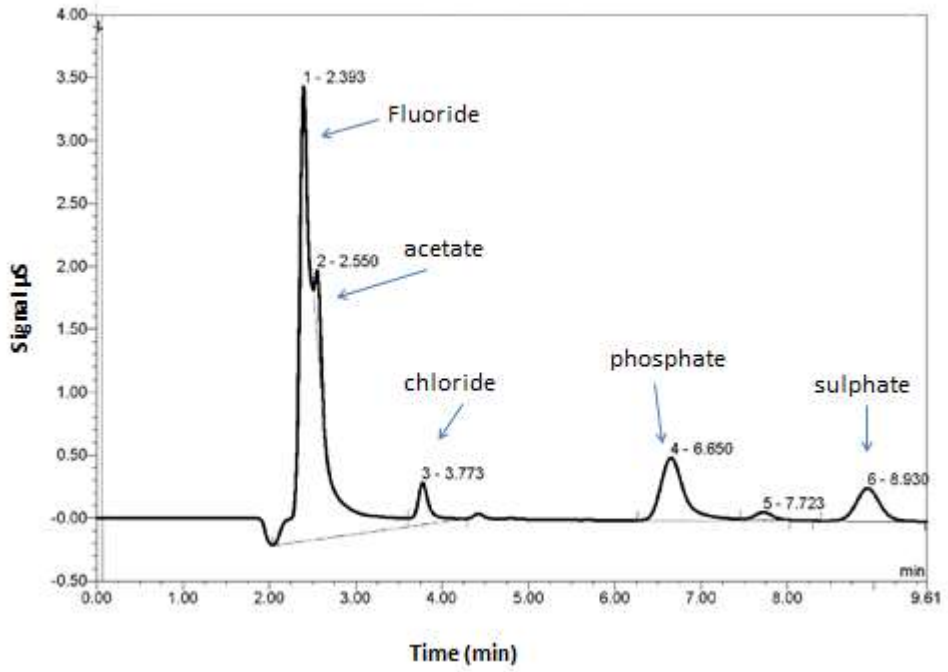

Figure 5-4: Chromatogram of 1 mM phosphate buffer that used for the extraction experiment.

Figure 5-4 shows the blank chromatogram for 1 mM phosphate buffer. An individual chromatogram of each anion was obtained in order to identify the peaks in Figure 5-4. The first overlapping peak was the fluoride ion, retained at 2.39 minutes, with the acetate ion retained at 2.55 minutes. The third peak retained at 3.77 minutes was for chloride ions. The fourth peak retained at 6.65 minutes was for phosphate ions from the buffer. The last peak retained at 8.93 minutes was for sulphate ions. However, the most important peak was the chloride peak, which is the ion of interest in this part (the chloride peak height is 0.33 µs and the peak area 0.06 µs.min). The presence of fluoride in the buffer was higher than normal, due to a contamination of fluoride already in the column.

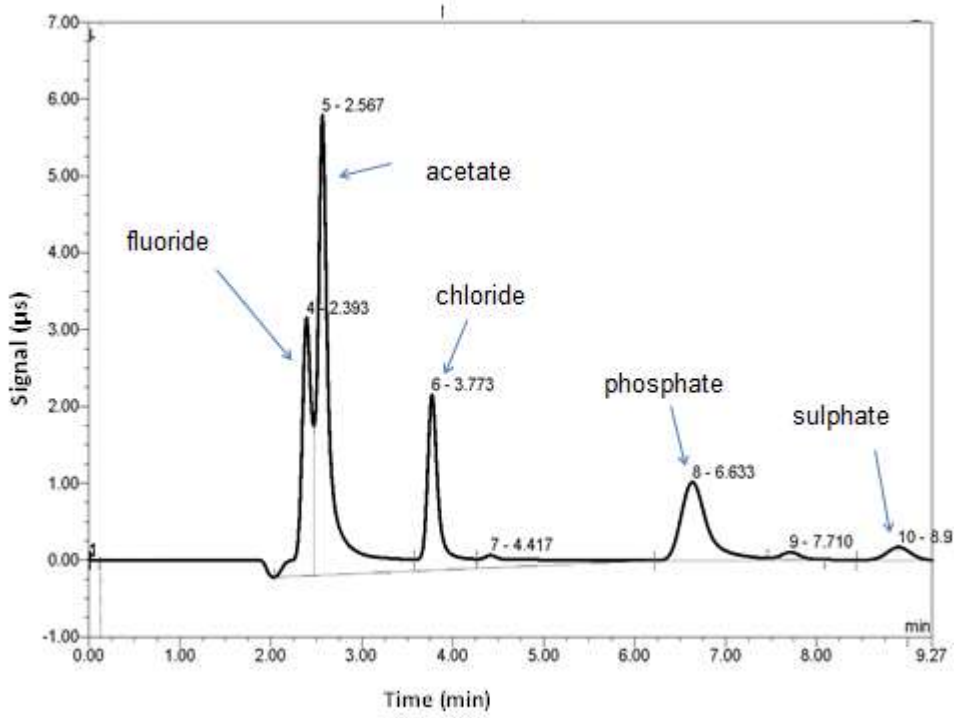

Figure 5-5: Chromatogram of the solution in reservoir B after ion extraction

Figure 5-5 shows the chromatogram of solution in reservoir B in the extraction chip, after the application of the voltage. This chromatogram was the best of three chromatograms obtained for the solutions in reservoir B. On the chromatogram, four peaks of fluoride, chloride, phosphate and sulphate, and fluoride and sulphate are already present in the blank sample, with the phosphate peak representing the buffer. However, the most important peak from the chromatogram is the chloride peak (the chloride ion peak which retained at 3.72 minutes), which is the point of investigation in this experiment, as it represents the extracted amount of chloride from reservoir A to reservoir B.

The concentration of chloride in reservoir B of the chip, after applying the voltage of 700 V for two hours, shows that the chloride ion successfully migrated from reservoir A in the chip to reservoir B. The amount of migrated chloride was 4.52 µg from 5.8 µg; about 78% of the chloride moved to reservoir B. The mass balance was calculated by

setting a set of standards in different concentrations for each anion, and a graph was then plotted for each anion, using the peak areas of the standards against their concentrations. The equation then was used to calculate the concentration of anions in every chromatogram, by using the peak area of the anion of interest.

In order to ensure the reproducibility of the results, the experiment was repeated three times on the same chip and two times on a different chip, under the same conditions. A further experiment was carried out under the same conditions but with no voltage applied. The results show that there was no migration without the application of voltage.

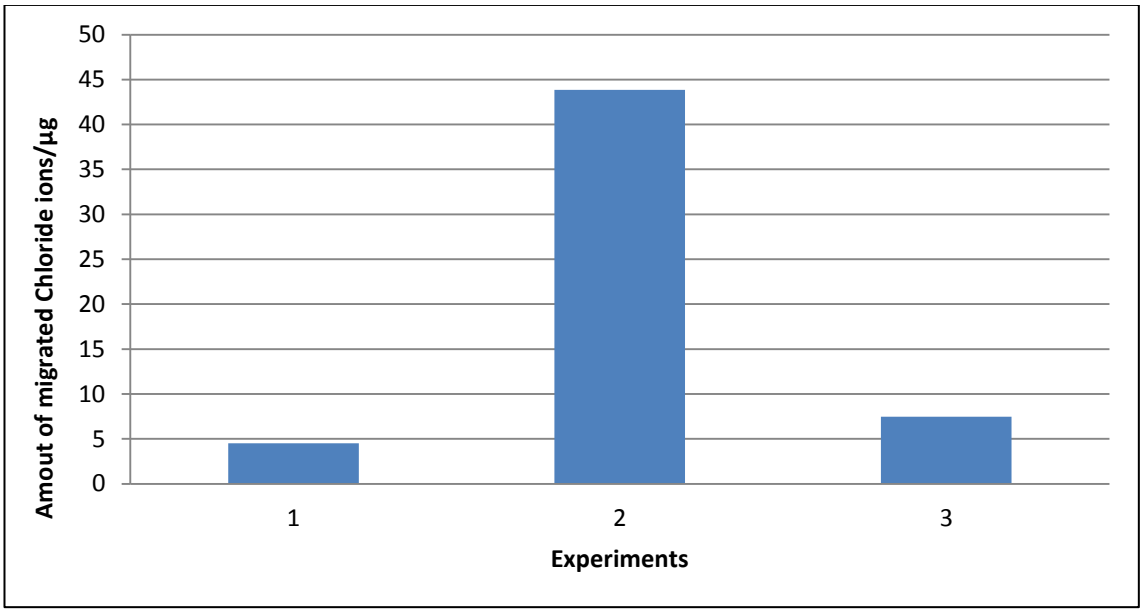

Figure 5-6: The amount of extracted chloride in the glass chip after an applied voltage of 700V for two hours

Figure 5-6 shows the repeated measurements of chloride extraction, which jumped from about 5 µg in the first experiment to about 45 µg in the second experiment and then dropped dramatically to about 8 µg. Migration occurred but the amount of chloride moved, fluctuated every time. The fluctuation of the chloride level might be due to Joule heating or electrolysis (see section 2.3.3), which causes a bubble formation that

plays a great role in the migration of the ions. Also, when the current was measured during the extraction of chloride, it was found to be very low (between 0.1-10 μA) , which means that there was a high resistance from the monolith. This might be due to the length of the potassium silicate monolith in the chip.

5.2.3 Nitrite (NO_2^-) extraction on a glass chip

The aim of this part was to investigate the migration of anions by measuring nitrite instead of chloride, because chloride was found to be present in the chromatograms of the phosphate buffer. The extraction of nitrite was compared to chloride extraction.

5.2.3.1 Experimental

The same experimental conditions used for chloride extraction were used for the extraction of nitrite (see section 5.2.1). Two variations were investigated in the experiment: time (30, 45 and 60 minutes) and voltage (700 and 1000).

5.2.3.2 Results and discussion

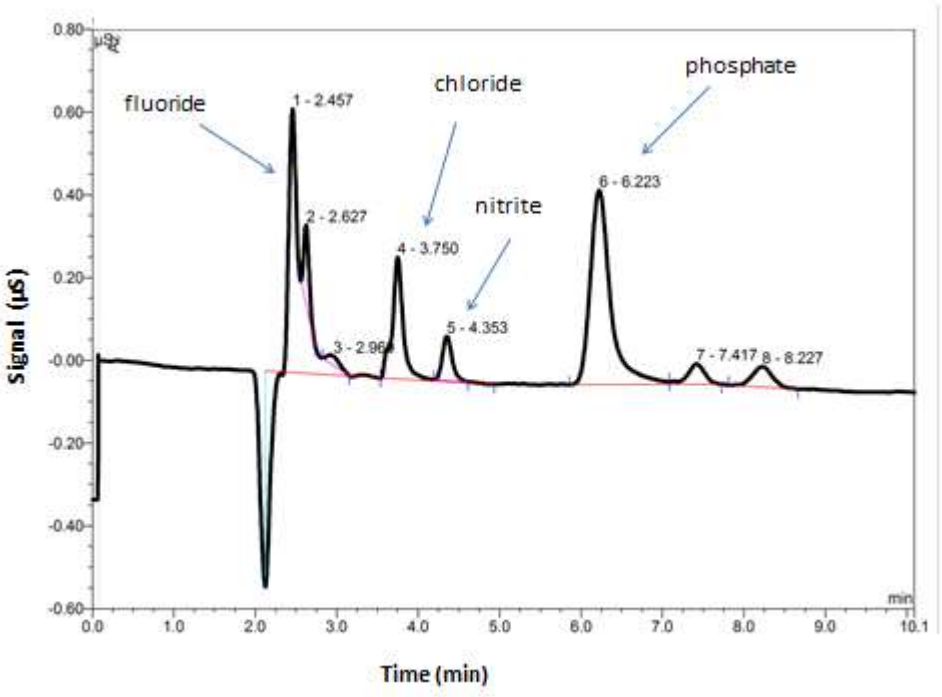

Figure 5-7: Chromatogram of 6.9 µg nitrite with 27.5 µg phosphate buffer, reservoir A, before applying the voltage of 700 V for two hours

Figure 5-7 shows the chromatogram for the solution in reservoir A, which was a nitrite and phosphate buffer. The first peak, which retained at 2.45 minutes, was the fluoride peak; the second peak, which retained at 3.75 minutes, was the chloride peak; the third peak at 4.35 minutes was the nitrite ions peak; and the peak at 6.22 minutes was the phosphate buffer. The nitrite peak area is 0.01 µs.min, which equals 6.89 µg.

The amount of nitrite in this chromatogram should decrease after applying a voltage, as nitrite should move to reservoir B, bearing in mind that reservoir B has no nitrite.

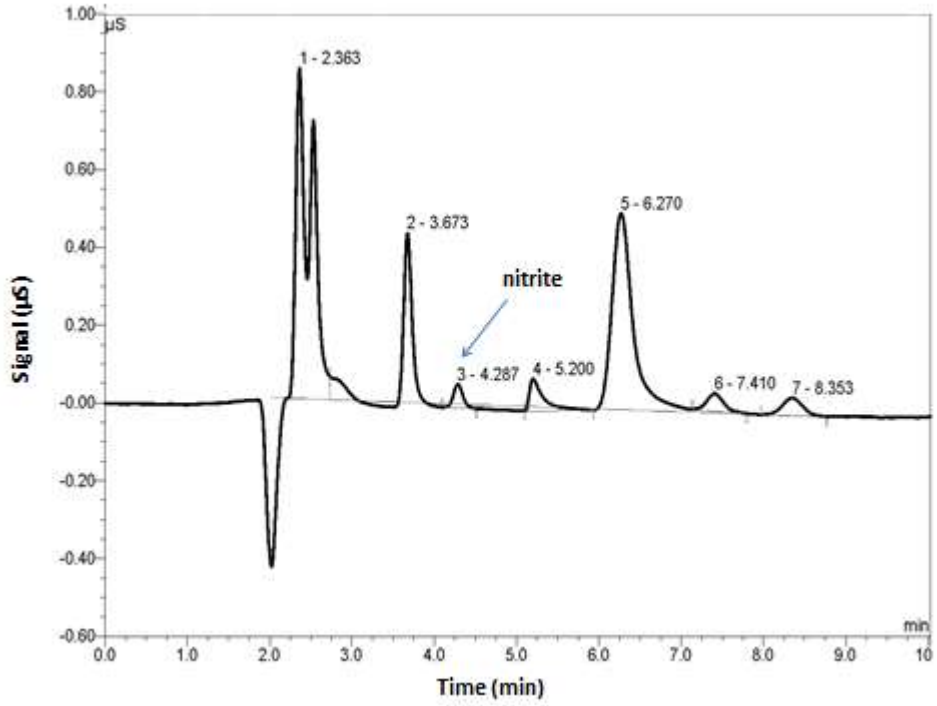

Figure 5-8: Chromatogram of nitrite with phosphate buffer in reservoir A, after applying the voltage of 700 V for two hours.

Figure 5-8 shows a chromatogram of the solution in reservoir A of the chip, after applying a voltage. The most important peak is the nitrite peak, which represents the amount of nitrite, and this retained at 4.287 minutes. The peak area was 0.008 µs.min, and the calculated amount of the moved nitrite ions was 3.68 µg.

This shows that the amount of nitrite in reservoir A decreased from 6.89 µg to 3.68 µg (about 53%), after applying a voltage of 700 V for two hours.

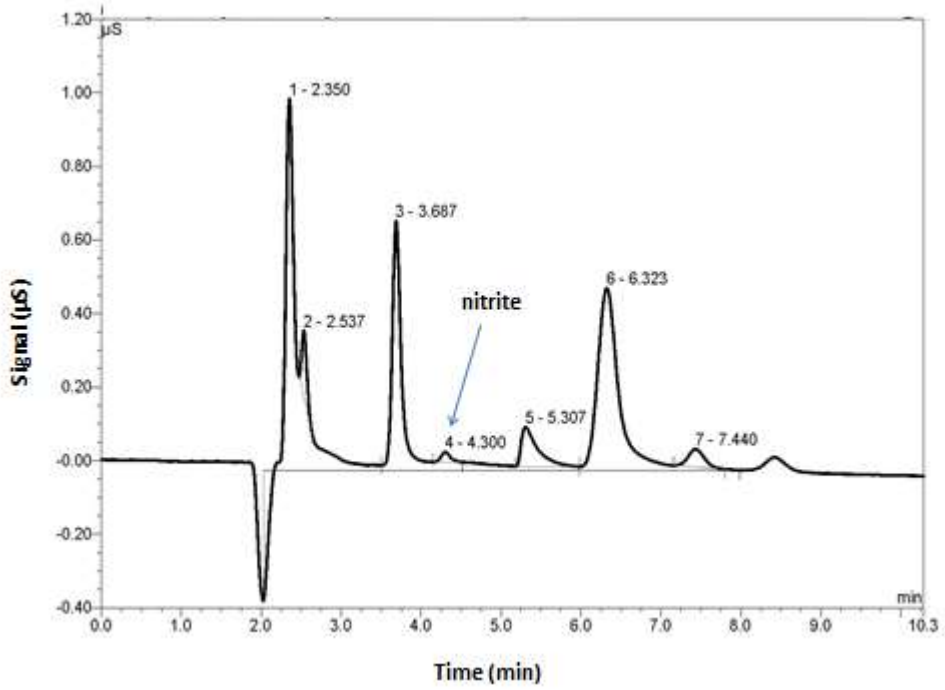

Figure 5-9: Chromatogram of the reservoir B solution after applying a voltage of 700 V for two hours

Figure 5-9 shows a chromatogram of solution in reservoir B after applying a voltage of 700 V for two hours. The nitrite peak was at 4.30 minutes, the peak area was 0.004 µs.min, and the calculated amount of nitrite was 1.83 µg. This means that the amount of nitrite moved to reservoir B from reservoir A after applying the voltage.

The amount of nitrite in reservoir A decreased after applying the voltage, as indicated in Figure 5-8, as the amount of nitrite ions was 3.68 µg, which means that the amount of nitrite decreased by 53%. Subsequently, reservoir B, the destination reservoir, demonstrated an increase in the amount of nitrite by 1.83 µg (see Figure 5-9); this is a 26% extraction of nitrite.

Despite the extraction of nitrite through the potassium silicate monolith using the glass chip, there was a loss of 21% of the nitrite amount; this might be trapped in the monolith body due to the large surface area of the monolith, or lost during the transfer

of the sample for analysis by IC. Also, the total amount of nitrite is very low and this small amount might be affected, especially during the lengthy experiment time. Furthermore, the voltage applied might be very high for such an application, but this requires further investigation.

The amount of nitrite was increased in reservoir A by about 1,000 times (0.1 M nitrite) to enhance the extraction, but less than 2 µg of the nitrite migrated to reservoir B. To optimise the process, the voltage and time of extraction were investigated. The applied voltage was increased from 700 V to 1,000 V, and the extraction time was changed three different times: 60, 45 and 30 minutes. Despite changing theses parameters, the small amount of nitrite migrated to reservoir B can be described as irreproducible.

However, the results showed that the applied voltage had an effect on the concentration of nitrite in reservoir A, but the migration to reservoir B was still unclear and requires further investigation. This is clearly a difficult problem to investigate.

5.3 Ion extraction on a potassium silicate monolith in a glass capillary

A potassium silicate monolith was used as a barrier to stop unwanted materials from entering the separation system, as they are very likely to change the separation of ions. The work on the glass chip has some difficult issues. Therefore, a new set-up was used to enhance the extraction system.

To investigate the behaviour of chloride and nitrite, a glass capillary was filled with the potassium silicate monolith used, instead of using the glass chip. The reasons for this are that a shorter potassium silicate monolith (between 0.5 - 3 cm long) can be fabricated, as well as narrower channel (25 µm) for the faster migration of ions, and

there is less resistance from the monolith. The monolith aims to work as a barrier to allow only ions to pass through it; therefore, it should be as small as possible to ensure easier migration and integration with separation in the following step. Furthermore, it is easier to prepare, allowing for the possibility to measure the current in the capillary, which helps to optimise conditions.

5.3.1 Experimental

The system shown in Figure 3-11 (section 3.5.2) illustrates reservoir A, which contains buffer and an anion mixture and reservoir B, which contain buffer. The anion should migrate from reservoir A (sample reservoir) to reservoir B (destination reservoir) through a potassium silicate monolith.

A solution of 1 mM sodium nitrite was prepared in 10 mM of phosphate buffer, as the buffer should keep the monolith wet enough to allow for a conductive environment on the side of reservoir A (and at this stage, the proposed design of the total integrated system of sample introduction and separation should use one buffer for both parts). 300 µl of this solution was placed in reservoir A and 300 µl phosphate buffer in the destination reservoir (B). 10 V was applied directly to both reservoirs, with the running times of 10, 20 and 30 minutes.

The reason for decreasing the voltage and time significantly is that the potassium silicate monolith in this set-up is smaller than the one used earlier in the glass chip. Timing was also decreased for these reasons, and because the target is to measure ions in the shortest possible time, meaning that the extraction time should be short. Nevertheless, the voltage and timing were investigated and optimised in this section of the research.

5.3.2 Results and discussion

Poor migration of the anions was observed in this work. The amount of solution in reservoir A increased dramatically during the experiments; this was observed by marking the volume level in the reservoirs. This was noticeable during the experiment for two reasons: the EOF (see section 2.3.3), which was causing the bulk solution to move towards the cathode in reservoir A; and the bubble formation in the system, which was also visual as it stopped the conductivity of the system, even after decreasing the applied voltage. Both issues will affect the extraction process and will definitely affect the reproducibility of the analysis, which would eventually lead to incorrect results.

The surface of the monolith and the glass has a negative charge due to the silanol group at the surface of the silica (Si-OH), which might also exist as a $Si\text{-}O^-$ group.[131] This is because both the surface of the monolith and the glass capillary might interfere with the same charge of anions, and create an EOF in the system. This might have a significant impact on the migration of anions from reservoir A to reservoir B.

5.4 Silanisation of glass capillary for ion extraction

Because of effect of EOF on the capillary, which affects the migration of anions, a silanised glass capillary is used to enhance the migration. The silanisation suppresses electroosmotic flow (EOF), which was present in the glass capillary because of the negative charge on the hydroxyl group (OH-) of the glass surface.

Three approaches were investigated as a possible silanisation technique to suppress the EOF. The first approach was a silanised glass capillary with trichloro perfluorooctyl silane (FDTS). The second approach was a silanised glass capillary with a commercial

coating, and the third approach was a silanised glass capillary with an end-cap procedure.

5.4.1 Experimental

5.4.1.1 Silanisation procedure

5.4.1.1.1 Silanisation procedure with trichloro perfluorooctyl silane (FDTS)

The capillary (containing a potassium silicate monolith) was dried in the oven and then flushed for 5 minutes at a flow rate of 5 µl/min with a silanisation reagent (1ml iso-octane + 145 µl trichloro perfluorooctyl silane [FDTS]).[202] It was then washed with iso-octane, acetone and water, respectively, before being dried at 60ºC overnight.

5.4.1.1.2 Silanisation procedure with a commercial coating

For silanisation, the capillary (which contained a potassium silicate monolith) was flushed for 5 minutes at a flow rate of 5 µl/min with a silanisation reagent (SafetyCoat Nontoxic Coating, Ultrapure Bioreagent, J.T. Baker, US) to block the charge on the silanol group on the surface. The capillary was then dried in an oven for 24 hours at 90^{o}C, prior to use.

5.4.1.1.3 Silanisation with an end-cap procedure

The end-cap procedure used was 1 g of trimethylchlorosilane in 10 ml toluene. This mixture was flushed through the capillary for two hours in order to block unreacted silanol on the capillary wall and the monolith surface. It was then flushed with toluene, and then with methanol using a syringe pump for 30 minutes. Finally, the capillary was placed in an oven for 16 hours at 90˚C, prior to use.[193]

5.4.2 Experimental set-up and conditions

To examine the EOF suppression of each silanisation method, the capillary was placed in the same set-up described in section 3.5.2. Reservoir A contained a buffer and 0.58 µg chloride, and reservoir B contained only a phosphate buffer. The level of liquid was marked; therefore, if the level were to increase in reservoir A then this would be due to EOF. A voltage of 100 V was applied for one hour.

5.4.2.1 Experimental set-up and conditions for silanisation with FDTS and silanisation with an end-cap procedure

The same set-up described in section 3.5.2 on Ion extraction through a potassium silicate monolith in a glass capillary, was used. Reservoir A contained a 300 µl solution of 20.7 µg sodium nitrite (or an anion mixture in end-cap silanisation), and reservoir B contained a 300 µl phosphate buffer. The voltage applied was 10-100 V and the running time was 10-30 minutes.

5.4.2.2 Experimental set-up and conditions for silanisation with a commercial coating

The buffer used in this step was changed from a phosphate buffer to a MES/His buffer, as this is more suitable for the separation of ions. The MES/His buffer (pH 6) is a well known buffer in the separation of ions in CE with C4D, as it has good stability under different conditions.[203] [149]

In addition, the previously used phosphate buffer would interfere with other anions, and phosphate itself is one of the anions of interest in this work, which would make the use of a phosphate buffer undesirable.

Two different conditions were examined for ion extraction on a silanised glass capillary:

- Reservoir A contained 25 µl anion mixture + 150 µl buffer (10 mM, MES/His), and reservoir B contained 200 µl buffer. The running time was 30 minutes and the voltage applied was 500 V.
- Reservoir A contained 50 µl anion mixture + 150 µl buffer (10 mM, MES/His), and reservoir B contained 200 µl buffer. The running time was 10 minutes and the voltage applied was 1000 V.

5.5 Results and discussion

5.5.1.1 Silanisation with FDTS

The extraction of nitrite through a potassium silicate monolith with a silanised capillary with FDTS, was investigated.

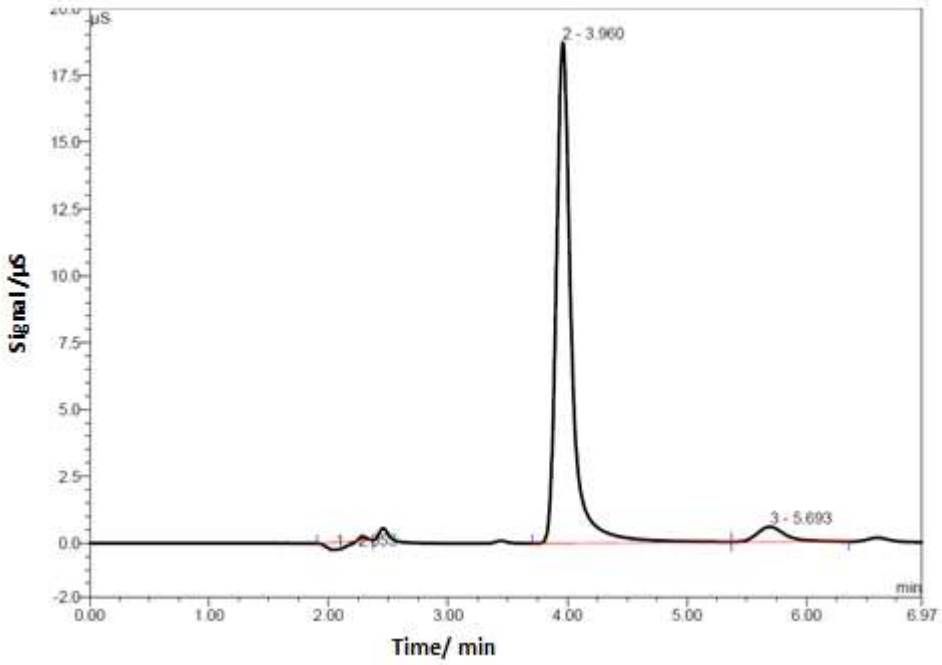

Figure 5-10: Chromatogram of solution in reservoir A, containing 1 mM phosphate buffer and 1 mM sodium nitrite, before the experiment

Figure 5-10 shows a chromatogram consisting of two main peaks. The first peak retained at 3.960 minutes; this peak is the nitrite peak, representing the amount of nitrite in reservoir A. The second peak retained at 5.693 minutes; this is the phosphate peak, representing the amount of phosphate in the buffer.

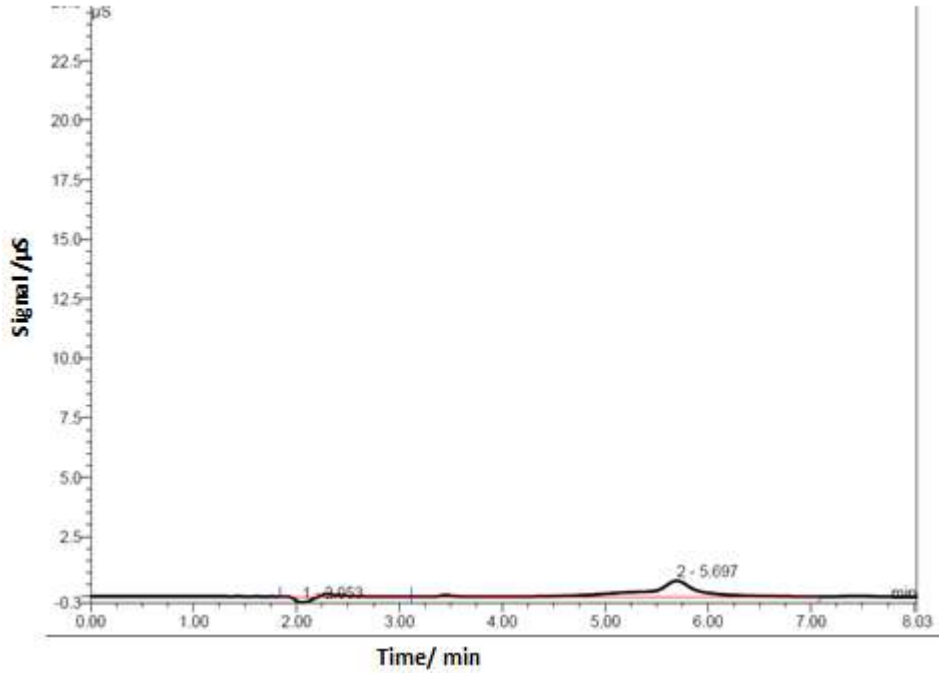

Figure 5-11: Chromatogram of solution in reservoir B, which originally contained 1 mM phosphate buffer. The voltage applied was 10 V, and the run time was 10 minutes

Figure 5-11 shows a chromatogram of reservoir B after applying a voltage. The chromatogram demonstrates a peak that retained at 5.690 minutes, which is phosphate from the buffer.

From the chromatogram in Figure 5-10, it can be noticed that nitrite was present in reservoir A; nitrite should migrate from reservoir A to reservoir B. Figure 5-11 shows that there was no presence of nitrite, which means that it did not migrate under these conditions (10 V, 10 minutes); therefore the conditions were changed in order to

enhance the extraction of nitrite. Different voltages were applied between 10 and 100 V, and different running times were also tested; unfortunately no progress was observed.

However, the results obtained using this method were not surprising, because during the examination of the capillary for EOF suppression (see experimental section 5.4.1), the level of liquid in both reservoirs changed significantly, especially when the voltage was increased. Furthermore, the amount of bubbles generated in the capillary was very obvious. The liquid in the capillary looked like a layer of oil due to the very high hydrophobicity of the capillary, owing to the silanisation method used in this part. The reason for continuing to work on the experiment despite these obvious problems was that the capillary might needed further conditioning with plenty of water after the silanisation process was complete and prior to running the extraction experiment. The conductivity of the system was measured before and after the capillary was washed with water, and it increased significantly after washing the capillary with water.

This method of silanisation was not ideal, as its main purpose was to supress the EOF in the capillary, but EOF still has an impact on the extraction process. Furthermore, bubbles in the capillary were accumulated during the experiment, which might have stopped the conductivity and eventually stopped the migration of nitrite from reservoir A to reservoir B. In addition, adding more water to condition the capillary would form small particles as a result of the silanisation reagents containing water.[202] This might have already happened but was not visual enough to notice, and it could be the reason behind the formation of bubbles in the system.

5.5.1.2 Silanisation with a commercial coating

In order to supress the EOF in the capillary, another silanisation method was used to avoid the problems associated with the previous silanisation method (see

section 5.5.1.1). This method uses a commercial silanisation reagent. The process was easier than the previous method and it should not react with water. Also, the hydrophobicity of the silanisation should not be very high.

The number of anions in the reservoir A sample were increased to more anions, in order to investigate their movement before the separation step.

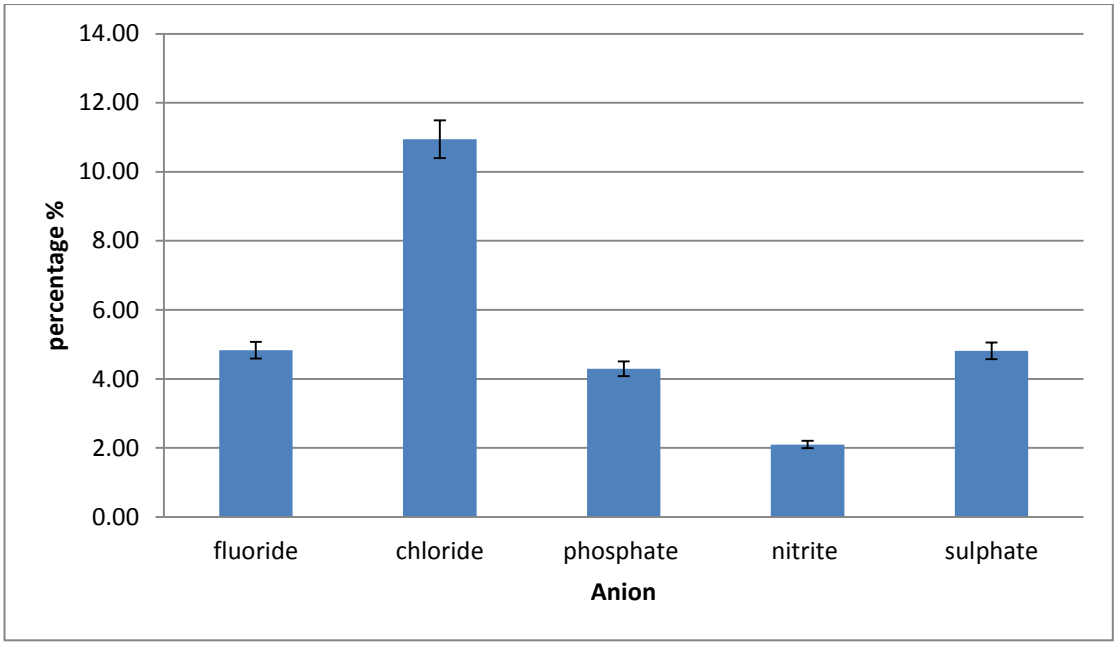

Figure 5-12: Percentage of migrated anions through a silanised glass capillary. 25 µg of each anion in reservoir A was spiked with 10 mM of MES/His buffer. The voltage was 500 V and the running time was 30 minutes. The number of experiment was three.

Figure 5-12 shows the percentage of migrated anions through a silanised glass capillary. From the graph, it can be noticed that about 5% fluoride, 10% chloride, 4% phosphate, 2% nitrite and 5% sulphate out of 25 µg was migrated from reservoir A to reservoir B. Chloride has the highest percentage (10%) and nitrite has the lowest (2.1%). These results demonstrate a successful extraction of the anions, with a variation in the values of migration from reservoir A to reservoir B. The calculation used the percentage of

migration, as it demonstrates the mass balance more clearly than showing the original and extracted amounts of ions.

However, considering the initial amount in reservoir A, the result is very small and barely enough for the purpose. These results might suffer from reproducibility because of the bubble generation in the capillary that was noticeable after 10 minutes of each run, as the current in the capillary dropped dramatically and suddenly stopped just after 10 minutes. Therefore, less experimental time to 10 min and a higher voltage, might improve the results. Also, the amount of anions in reservoir A should be increased in order to investigate the concentration effect. Therefore, the next experiment was modified, with the time reduced to 10 minutes, the voltage increased to 1000 V, and the concentration in reservoir A increased to 50 µg of each anion.

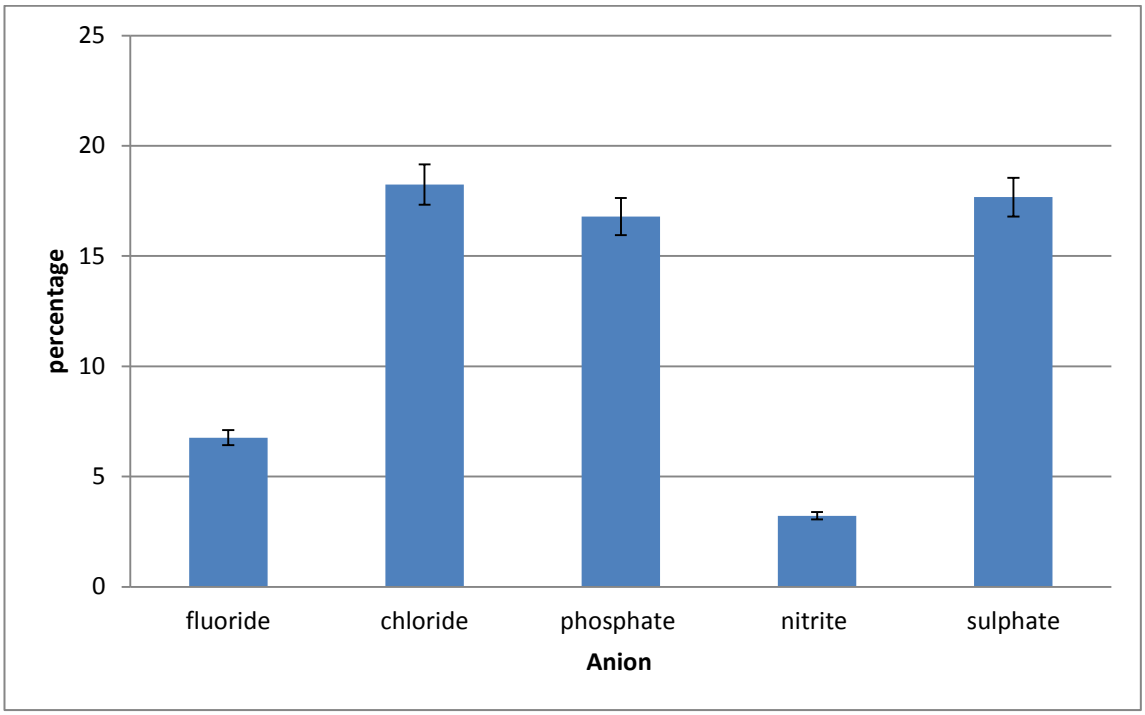

Figure 5-13: Percentage of migrated anions through a silanised glass capillary. 50 µg of each anion in reservoir A was spiked with 10 mM of MES/His buffer. The voltage was 1000 V and the running time was 10 minutes. There were three experiments.

Figure 5-13 shows the percentage of migrated anions through a silanised glass capillary. From the graph, it can be observed that about 7% fluoride, 18% chloride, 17% phosphate, 3% nitrite and 17% sulphate, out of 50 µg, was migrated from reservoir A to reservoir B. Chloride has the highest percentage (85.48%) and nitrite has the lowest (3.22%). These results demonstrate a successful extraction of anions, with a variation in the values of migration from reservoir A to reservoir B.

The results in Figure 5-13 demonstrate good progress and better results than the results in Figure 5-12, with a similar variation in the values of migration. This improvement was due to the changes in conditions by increasing the voltage and the concentration, as well as the running time. This was expected, but needed further investigation, especially with regards to the generation of bubbles in the capillary. This problem might be overcome by manipulating the conditions, especially the length of the capillary and the timing. Therefore, the same experiment was run with a 5 cm long capillary that contained a 5 mm monolith, and was silanised as described earlier in the experimental section (5.4.1.1.2). The running time was shortened to 3 minutes, the voltage remained at 1000 V, and reservoir A contained three different concentrations: 10, 20 and 30 µg.

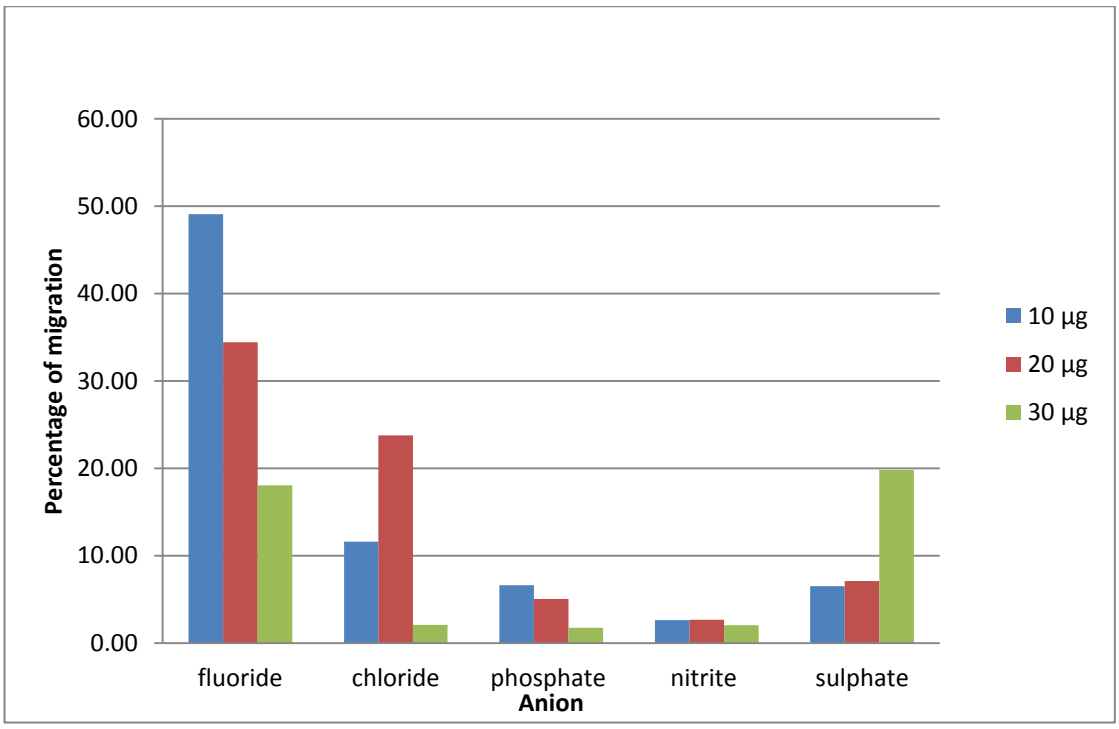

Figure 5-14: Percentage of migrated anions through a 5 cm long silanised glass capillary. 10, 20 and 30 µg of each anion in reservoir A was spiked with a 10 mM MES/His buffer, with a running time of three minutes

Figure 5-14 shows the percentage of migrated anions through a silanised glass capillary, with three different concentrations of anion in reservoir A. From the graph, it can be observed that fluoride has the highest percentage of migration from reservoir A to reservoir B, with 10 µg (48%), before decreasing to 20 µg (around 35%) and continuing to decrease to less than 20%, with 30 µg. Chloride maintains the second highest percentage (just above 10%), with 10 µg, before it jumps to 24% with 20 µg and decreases to less than 5%. Phosphate decreased following a trend similar to fluoride but with a much lower percentage than 10%. Nitrite had the lowest percentage, with slightly similar numbers for the three conditions. Finally, sulphate behaved differently to fluoride and phosphate, increasing to about 6%, 7% and 20% for 10, 20 and 30 µg, respectively. The details of the data used in Figure 5-14 are presented in Table 5-1.

Table 5-1: Percentage of migrated anions through a 5 cm long silanised glass capillary

Anion concentration in reservoir A	% anion extracted				
	Fluoride	Chloride	Phosphate	Nitrite	Sulphate
10 µg	49.10	11.58	6.60	2.61	6.52
20 µg	34.42	23.75	5.03	2.66	7.09
30 µg	18.05	2.08	1.76	2.05	19.82

Figure 5-14 and Table 5-1 show the percentage of migrated anions through the silanised potassium silicate monolith in a glass capillary, using the commercial silanisation. The suppression was successful, extraction of the anion through the monolith was good, and the amount of migrated anions noticeably increased. However, the migration percentages are random and demonstrate the unsystematic behaviour of anions, which is slightly surprising. For example, the fluoride percentage is the highest at the smallest concentration in reservoir A, and the chloride percentage is the highest at 20 µg (23.75%) and lowest at 30 µg (2%). Unfortunately this makes the extraction uncontrollable, which is most likely due to the bubble formation in the capillary. Furthermore, the high hydrophobicity of the capillary surface makes the extraction more uncontrollable, because the hydrophobicity of the glass causes the accumulation of bubbles in the capillary that delays and eventually stops the anion movement.

Despite the hydrophobic surface, anions were moving towards reservoir B. This indicates very promising extraction but needs to be easily controlled, in order to ensure reproducible results. Thus, to overcome this problem, a less hydrophobic surface is required, meaning that another silanisation method is necessary.

5.5.1.3 Silanised glass capillary with an end-cap procedure

In order to enhance the migration of anions through a potassium silicate monolith, end capping was used. End capping is a secondary bonding step used to cover silanol on the silica surface. It is a well-known technique in high-performance liquid chromatography HPLC columns, in which end-capped packing materials eliminate unpredictable, secondary interactions on the column surface.

Table 5-2: Table of migrated anions in an end-capped glass capillary and the monolith

Anion	Fluoride	Chloride	Phosphate	Nitrite	Sulphate
	0.000838	0.000896	0.622933	0	0.00082
% of migration (µg)	0.0025	0.00221	0	0.001	0.00222
	0.001	0.00025	0	0	0.000532
Mean	0.001446	0.001119	0.207644	0.000333	0.001191

Table 5-2 shows the percentage of migrated anions. The experiment was repeated three times to ensure the reproducibility of results. The table shows the triplicate in percentages and then the average of the percentage of each anion.

However, it can be seen that the percentage of migrated anions is very small, under 0.5 in all triplicates; even phosphate, which has the highest number (0.6%), is perhaps too small to consider as a migration. The reason for this low value could once again be the EOF that is still affecting the migration of anions.

5.6 Chapter conclusion

In conclusion, anion extraction through a potassium silicate monolith in a glass capillary was performed, because it has good characteristics for the extraction of ions: a potassium silicate monolith can be easily formed into a desired shape; the surface can be

chemically modified; the pore size can be modified; and it can be made physically strong. Therefore, extraction of inorganic ions can be performed in a silica monolith, for pre-concentration and pre-treatment prior to separation. However, experiments on the bare silica capillary showed poor results due to the interference of the negative charge on the surface of the glass and the monolith causing EOF. Therefore, the surface needed to be silanised. Three different silanisation methods were investigated: ion extraction on a silanised glass capillary with trichloro perfluorooctyl silane (FDTS); ion extraction with a silanised glass capillary with a commercial coating; and ion extraction with a silanised glass capillary with an end-cap procedure. Different factors in the extraction were investigated, including applied voltage and the time of extraction.

The results of the extraction with FDTS were less successful than the other methods, as there was noticeable EOF during the extraction process. A commercial silanisation reagent was used to overcome the EOF problem. This shows very promising results but they were irreproducible and difficult to control. This might have been caused by the high hydrophobicity of the capillary surface, which makes the extraction more uncontrollable as the hydrophobicity of the glass causes the accumulation of the bubbles in the capillary that delays and eventually stops the anion movement. The end-capping procedure as a silanisation method was also investigated, and it showed much less results than the extraction with the commercial reagent method. The percentages of anion extraction were very small, under 0.5% in all triplicates. The reason for these low values could once again be due to the EOF affecting the migration of anions.

In general, the extraction with a potassium silicate monolith could be enhanced by using a polymer capillary rather than a glass capillary. This was already attempted but it was practically hard to keep the monolith in place. Further investigation of a different design is required; such a design would be in a suitable polymer chip, for example, to avoid the

EOF. The system might include the potassium silicate monolith as the main extraction part, as it has already shown promising results.

6 Electrodialysis (ED) for sample introduction

A combination of electrodialysis ED and electrophoresis CE was investigated, for the rapid pre-treatment and subsequent determination of inorganic cations in river water samples. A combination of ED with CE will improve the analytical performance of ion separation by keeping only ions in the separation channel (see section 2.3.4.1 for more details).

6.1 Ion extraction through Polytetrafluoroethylene (PTFE) film and Parafilm

To increase the extraction performance, a plastic tube was used instead of a glass capillary in order to avoid the associated problems such as the silanisation process and the EOF. The surface of plastic does not have any charges that would interfere with ions during the extraction process. Also, PTFE was used as a membrane rather than using a potassium silicate monolith, to gain better mass transfer. PTFE is highly hydrophobic and has a high melting point (about 327˚C), which makes it highly stable in harsh environments and hard to dissolve. PTFE membrane techniques have been widely used to isolate gas and liquid in solutions.[204]

Parafilm is a polymer film used for a variety of applications such as sealing or protecting vessels (such as flasks or cuvettes). It is flexible, waterproof, partly transparent and has the ability to be deformed and stretched without losing toughness.[205] Parafilm has been used in scientific research and laboratories for years.[206] Since Parafilm is a moisture-resistant polymer,[207] it was investigated as a possible membrane that would only allow ions to pass through under the influence of voltage.

6.1.1 Experimental

For anion extraction, a 10 mM MES/His buffer was used and the conditions examined were: reservoir A contained 25 µl anion mixer + 150 µl buffer; and reservoir B contained a 200 µl buffer. The running times were 5 and 2.5 minutes and the voltage applied was 200 V. The set-up has been explained in section 3.5.3.

For cation extraction, the buffer was 5 mM MES/His (the concentration of the buffer was decreased from 10 mM in anion extraction to 5 mM in cation extraction, as the conductivity in the system was improved in cation extraction), and the cation standard solution was used as a sample (cation standard 1 for IC, purchased from Sigma Aldrich, UK). The solution consisted of 200 mg/L each of sodium, potassium and 1,000 mg/L calcium.

The system set-up was described in Figure 3-13 and in section 3.5.4, whereby the PTFE was wrapped around the top screw part of the fitting to seal the bottom of it and then screwed back to form the sample reservoir. The sample reservoir contained 30 µl of the cation standard and 500 µl of buffer, and the destination reservoir contained only buffer. The voltage applied was 100 V for 5 minutes.

6.1.2 Results and discussion

In anion extraction, the conductivity in the system was measured prior to any experiment in this section ((section 3.5.3) extraction of anion by PTFE and Parafilm). Most of the time, the conductivity in the system was very low and at times the system was not conductive. Therefore, it was practically hard to establish a conductive environment in the sample reservoir that allowed anions to form electrolytes in the solution.

This might be why this method was not successful; there was no migration of anions from reservoir A to reservoir B. This could result from the resistance of the PTFE film or the Parafilm, due to the high hydrophobicity of the films. It also could be a result of the set-up, as it was difficult to ensure that the solution reached the bottom end of reservoir A (see Figure 3-12), which led to no conductivity in the system.

Initially, the ED system was used to investigate the extraction of anions but the IC was not operated for a period of time; this had to be carried on with cations. Thus, in order to investigate the movement of ions through the PTFE membrane, an ED system was used. One of the problems of the previous system was that it was hard to establish a conductive environment within the system; therefore, the set-up was changed to a better system (see section 3.5.4) with a larger reservoir whereby it was practically easier to ensure the wettability of the membrane, and the conductivity could be investigated further.

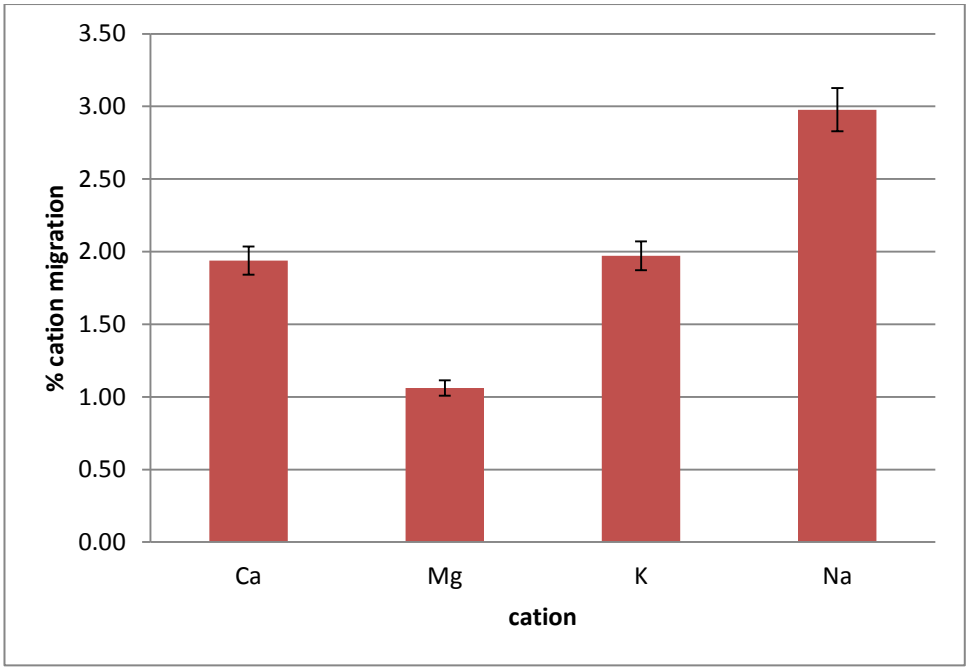

Figure 6-1: Percentage of cations migrated through PTFE film, with a running time of 5 minutes and an applied voltage of 100 V. The cation sample was a cation standard solution consisted of 200 mg/L each of sodium, potassium and 1,000 mg/L calcium.

Figure 6-1 shows the migration percentages of four cations (calcium, magnesium, potassium and sodium) through a PTFE membrane in the ED system. Sodium had the highest percentage of migration with 3.6 µg out of 122 µg (about 3%), followed by potassium with 1.97% (4.2 out of 212.4 µg), and calcium with 1.94% (5 out of 256.3 µg). Magnesium had the lowest migration percentage of 1% (1.7 out of 163 µg).

The results demonstrated the extraction of cations through the PTFE membrane, and the improved set-up was successful. However, the migration percentage was low and needed enhancing; this could perhaps be achieved through decreasing the membrane thickness by stretching it further.

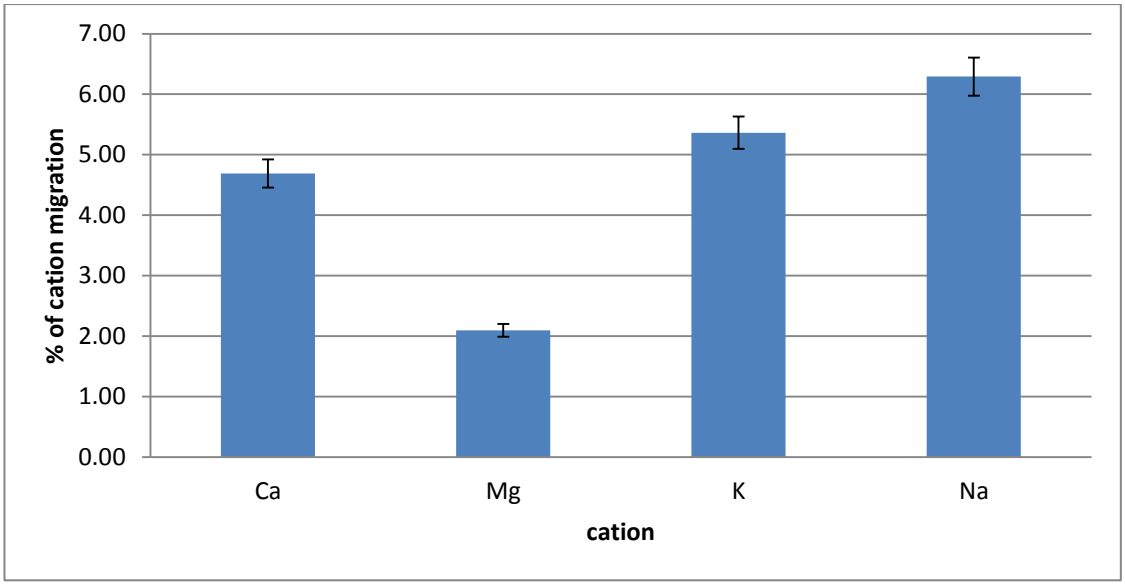

Figure 6-2: Percentage of cations migrated through stretched PTFE film, with a running time of 5 minutes and an applied voltage of 100 V. The cation sample was a cation standard solution consisted of 200 mg/L each of sodium, potassium and 1,000 mg/L calcium.

Figure 6-2 shows the migration percentages of four cations (calcium, magnesium, potassium and sodium) through a stretched PTFE membrane in an ED system. A running time of 5 minutes was the proposed maximum extraction time, and it was used here to allow for the best possible migration of ions. 100 V was the maximum voltage

that could be applied from the power supply. Sodium has the highest percentage of migration with 7.7 out of 122 µg (about 6.3%), potassium has the second highest percentage (5.4%) with 11.4 out of 212.4 µg, calcium comes third with 4.7% (12 out of 256.3 µg), and lastly, magnesium has the lowest migration percentage of 2.1% (3.4 out of 163 µg).

This experiment aimed to achieve the better extraction of cation through a PTFE membrane by making the thickness of the membrane smaller through stretching it. The results demonstrated successful and improved cation extraction.

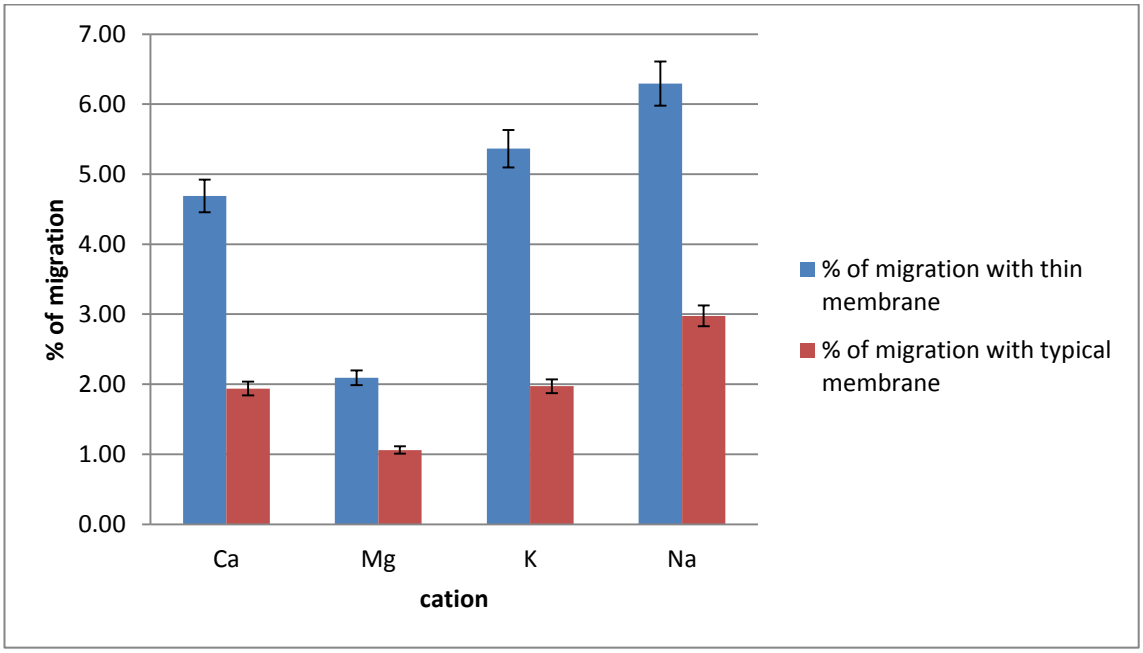

Figure 6-3: Comparison of the cation migration percentages through stretched and typical PTFE membranes

Figure 6-3 shows a comparison of the migration percentages of four cations (calcium, magnesium, potassium and sodium) through two PTFE membranes in the ED system: a typical PTFE membrane and a thin PTFE membrane. In both systems, sodium has the highest percentage of migration, potassium has the second highest percentage, calcium has the third highest, and magnesium has the lowest migration percentage.

The amounts of migrated cations were approximately doubled with the thinner membrane, but the amount of migrated potassium more than doubled. The thinner membrane provided a better result, which was expected, as there would be less resistance and less interaction between the ions and the membrane, allowing for migration through the membrane.

These results are still quite low; however, this could be improved by further optimisation, such as a higher voltage or more running time. The problem, however, was that the membrane would not tolerate a high voltage for a long time as the heat produced would damage the membrane or at least affect the results; therefore, the membrane has to be changed regularly to maintain reproducible results. Even with a different new membrane, the reproducibility might be affected, as the stretched membrane that provided the better results was stretched through a manual procedure that caused irreproducibility, which is not ideal for long-term monitoring. A stronger and more reliable membrane was needed for water monitoring, which could cope with the high voltages.

In conclusion, the PTFE membrane and Parafilm are not ideal for long-term monitoring; it might work for a period of time, for less continuous applications.

6.2 Ion extraction with a cellulose acetate (CA) electrodialysis (ED) membrane

Dialysis membranes are widely used and a cellulose acetate seems to be suitable as a membrane material because of it is: cost-effective; relatively easy to manufacture; practically easy to handle; non-toxic; a renewable resource of raw material; and has high salt-rejection properties.[208] It has been widely used in water research due to its

unique properties.[209] Cellulose acetate membrane has been used in this work for its physical strength and chemical convenience in ED applications.

6.2.1 Anion extraction with a cellulose acetate (CA) membrane in a commercial ED cell

6.2.1.1 Experimental

The experiment was carried out using a 500 µl mixed anion solution (1 g/L) in the sample reservoir, and 500 µl of 5 mM MES/His buffer was placed in the chamber, which was the destination reservoir. A voltage of 10-100 V was applied for 1, 5 and 10 minutes. The system set-up has been explained in section 3.5.4.

6.2.1.2 Results and discussion

The extraction of anions through the cellulose acetate membrane was not successful, even after changing the voltage and the extraction time. Looking at the cellulose chemical structure, the problem can be addressed (see Figure 6-4). The presence of oxygen in the chemical structure of the cellulose acetate membrane would affect the migration of anions because this oxygen is partially negative, which repels anions away from the membrane; this means that the use of a cellulose acetate membrane in the electrodialysis system is not ideal for anion extraction.

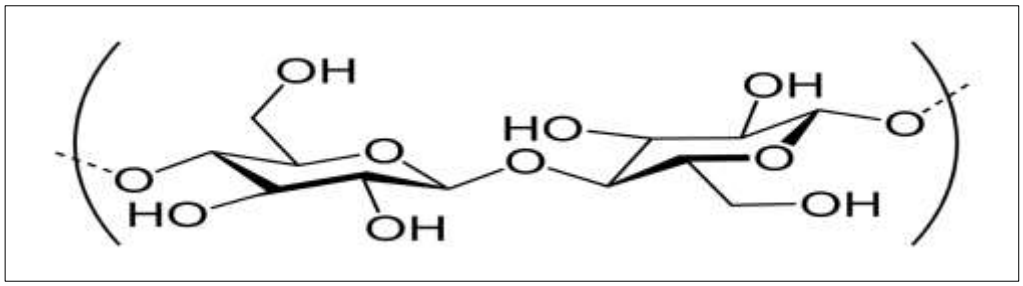

Figure 6-4: The chemical structure of a cellulose acetate

6.2.2 Cation extraction with a CA membrane in the commercial ED cell

6.2.2.1 Experimental

The cation solutions were prepared from the chloride salts of calcium and potassium, but the magnesium was prepared from magnesium sulphate (all analytical grade and purchased from Fisher Scientific, UK). The concentration was 1 mM for each salt.

Initially, the first experiment was carried out using a cation mixture, whereby a 500 µl cation mixture (Ca^{++}, Mg^{++} and K^{+}) was inserted into the sample reservoir and 500 µl of MES/His buffer was placed in the chamber that was the destination reservoir. A voltage of 100 V was applied for 10 minutes. The system set-up has been explained in section 3.5.4.

6.2.2.2 Results and discussion

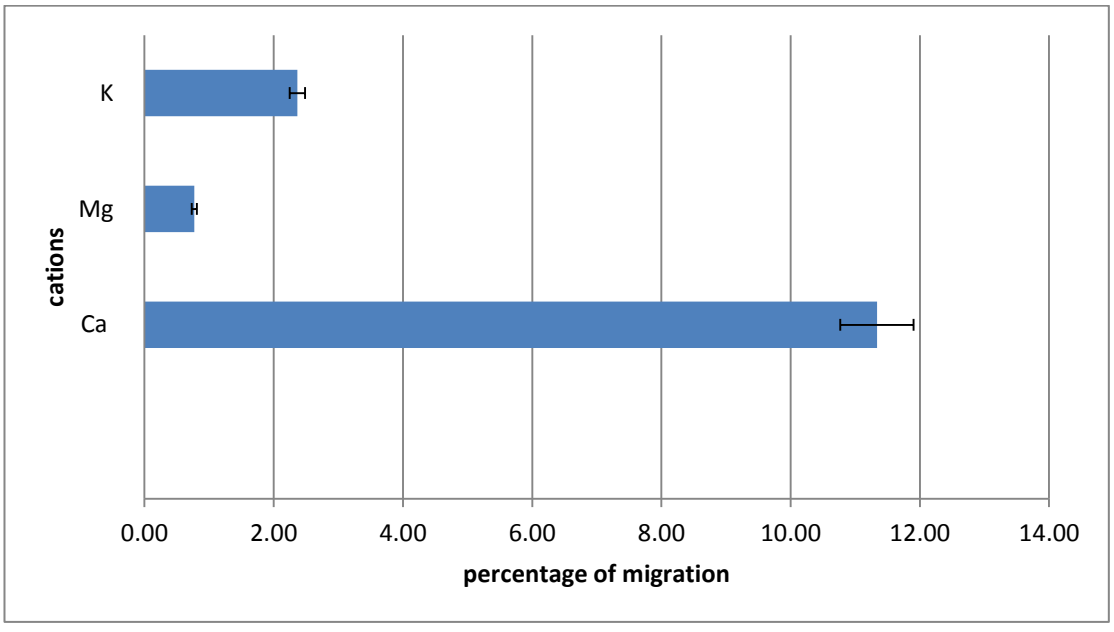

Figure 6-5: Percentage of cations migrated through a cellulose acetate membrane with 100 V applied for 10 minutes. Extractions of 124.74 µg out of 1100 µg calcium chloride, 17.66 µg out of 745.5 µg potassium chloride, and 9.24µg out of 1200 µg magnesium sulphate, were migrated from the sample reservoir to the destination reservoir

Figure 6-5 shows the migration percentages of three cations (potassium, magnesium and calcium) through the membrane. Calcium has the highest migration percentage, 11.34%, while potassium has a lower percentage of 2.37% and magnesium has the lowest migration percentage of approximately 0.77%.

This result is promising, demonstrating the successful extraction of cations through a cellulose acetate membrane. However, the amount of migrated cations is still small and requires further optimisation to enhance the extraction. For instance, the voltage was slightly high and caused the generation of bubbles in the reservoir, which was probably due to the electrode position in the reservoir (the electrodes were directly facing each other; see Figure 3-13). Also, the running time needs to be reduced, as the process of extracting ions should be within 5 minutes, in the total integrated system.

6.2.2.3 Optimisation of cation extraction through a cellulose acetate membrane

Optimising the conditions for cation extraction through a cellulose acetate membrane, would allow for better investigation of the issues that might affect the extraction. These issues include the extraction time, the voltage applied, the suitability of the buffer and the set-up materials. Initially, timing and voltage were optimised.

6.2.2.4 Results and discussion

In order to optimise the extraction, the voltage was fixed at 100 V and different timings were examined: 30 seconds and 1, 2, 3, 4, and 5 minutes. Also, to optimise the timing of the extraction, the timing was fixed at 5 minutes and different voltages were examined, from 10 V to 100 V. The same set-up mentioned in section 3.5.4 was used; the buffer

was 5 mM MES/His, and the cation standard solution contained 200 mg/L potassium and magnesium, and 1,000 mg/L calcium.

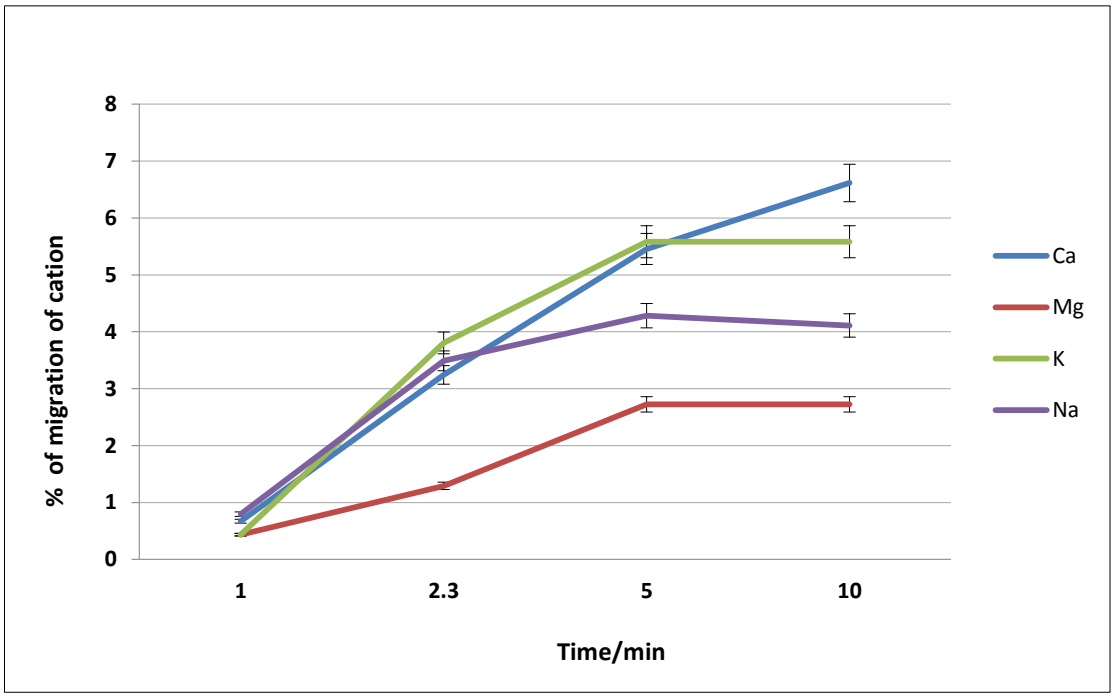

Figure 6-6: Optimisation of extraction time through a cellulose acetate membrane, with 5 mM MES/His and cation standards

Figure 6-6 shows the changes in the amount of migration during different timings, from 1 to 10 minutes. The percentage of migration started from less than 1% for all of the cations and then gradually increased until it reached 5 minutes, after which it levelled off for all cations except for sodium, which carried on increasing to more than 6% at 10 minutes. In general, sodium has the highest percentage of migration and magnesium noticeably has the lowest, which requires further investigation. However, the level of migration increased along with the increase in time from 1 to 10 minutes. The average level of migration is slightly low, less than 6%, but the aim of this optimisation step is to examine the behaviour at different timings, with further investigation to follow later in this work, to enhance the migration.

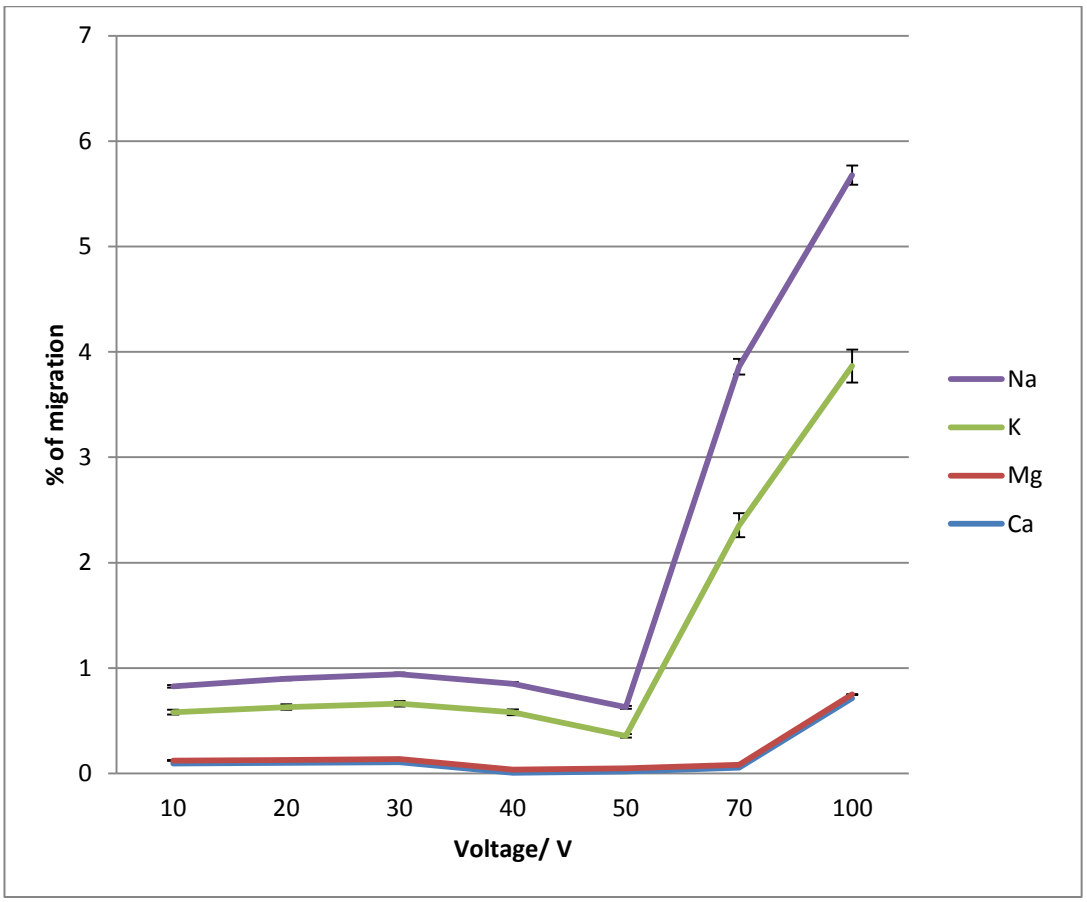

Figure 6-7: Optimisation of voltage applied to the reservoir in the extraction of cations through a cellulose acetate membrane, with 5 mM MES/His and cation standards

Figure 6-7 demonstrates the cation behaviour during extraction through a cellulose acetate membrane with different voltages. The figure showing the changes of voltages versus the percentage of migration, the migration levels of in the graph between 10 to 50 V, and it dropped at 50 V, which was surprising and could be due to the bubble formation on the reservoir at that particular point. Nevertheless, the percentage noticeably increased again after 50 V to the highest value, except for magnesium and calcium, whose percentages levelled off up to 70 V and then increased at 100 V.

The cation behaviour with different voltages should gradually respond to the increasing voltage, but this only occurred at 70 V onwards, at high voltages. The problem with a high voltage is the production of bubbles in the reservoir, which might affect the

extraction process. However, further optimisation of the set-up will improve the migration, because the electrode position in the sample reservoir requires better positioning. Most important at this stage is reproducible behaviour; the linear response would be optimised with an improved design of the set-up that includes online detection, which is better and more accurate than the offline detection currently being used. The online detection will be discussed later in this thesis.

6.2.3 Cation extraction through a cellulose acetate membrane following optimisation

From the time optimisation, it was found that the longer the timing, the better the extraction, and from the optimum conditions between 5 to 10 minutes, 7 minutes will be the fixed running time, in order to compromise between sodium and the other cations. The voltage, however, behaved differently; the extraction was quite similar at low voltages but it was stable and there was no bubble formation affecting the process. Also, low voltage is better for low energy consumption.

6.2.3.1 Results and discussion

The same ED set-up described in section 3.5.4 was used, with a 5 mM MES/His buffer and cation standard solutions. The voltage was 15 V and the time was 7 minutes.

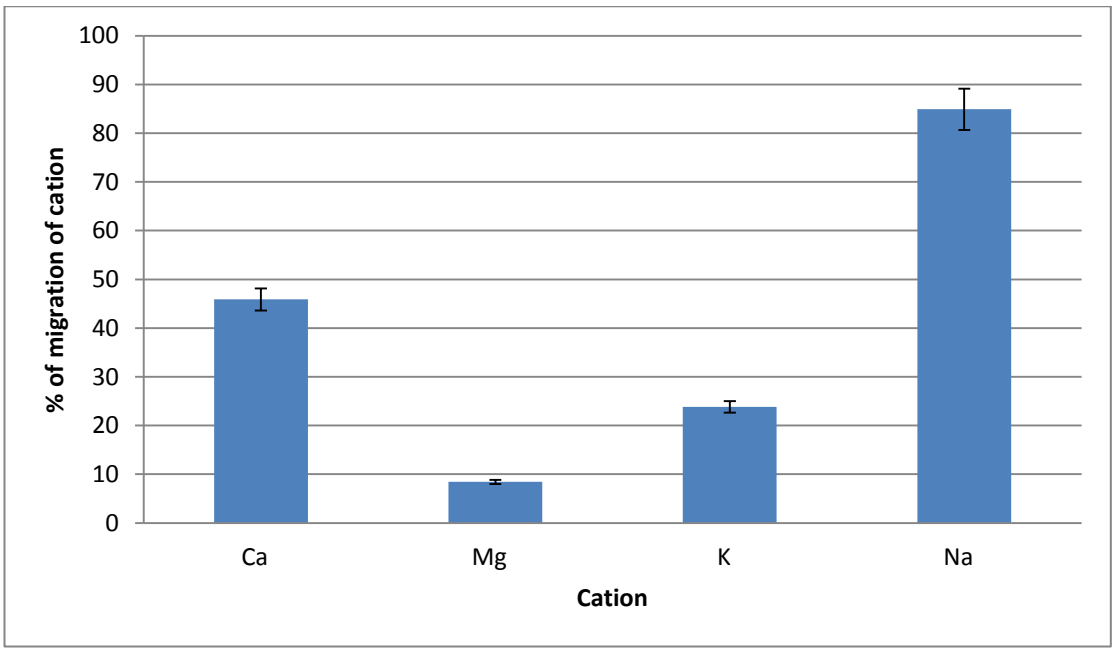

Figure 6-8: Percentage of cations migrated through a cellulose acetate membrane, with a 5 mM buffer and 15 V in 7 minutes

Figure 6-8 shows the cation migration through a cellulose acetate membrane with a 5mM buffer. It can be noticed that sodium has the highest migration rate, approximately 85%, whereas calcium comes next with 45%, followed by potassium with 23%. The lowest migration amount was for magnesium, with less than 10%. This result demonstrates the successful extraction of the cation, with a higher migration percentage than the initial results, as potassium, magnesium and calcium showed extractions of 2.3%, 0.7% and 11.3%, respectively (see section 6.2.2.2).

However, despite the improved extraction, further optimisation was required, especially for magnesium, as it seems that magnesium has a very low migration percentage, even though it has similar physical properties to the other cations. Thus, in order to investigate the behaviour of magnesium, the cellulose acetate membrane was placed in water overnight after finishing the extraction experiment, and then in 2% nitric acid.

The water was then analysed using the ICP-AES, to find out if magnesium was trapped in the membrane more so than the other cations.

Table 6-1: The concentration of cations trapped in the cellulose acetate membrane after experiments

Cation	Ca	Mg	K	Na
Concentration in the membrane/ µg	1.78	8.28	0.86	2.36

Table 6-1 shows the amount of ions trapped in the cellulose acetate membrane. Magnesium has the highest amount of cations trapped in the membrane (8.3 µg), with the second highest amount for sodium (2.3 µg), followed by calcium (1.8 µg). Finally, the lowest amount was for potassium, with less than 1 µg.

It can be noticed from the table that the amount of magnesium in the membrane is four times higher than the other cations. This is expected, and explains the low percentage of magnesium migration through the membrane.

In order to improve the extraction of cations through a cellulose acetate membrane, the amount of cations trapped in the membrane has to be quickly released during the run time. One approach investigated was the addition of acid to the buffer, as acid can chemically help in speeding up the extraction process. Nitric acid was used earlier to examine the amount trapped in the membrane, but nitric acid might have a severe effect on the polymer set-up used in this section.[210] Acetic acid is weaker than nitric acid and might be suitable for the set-up. Therefore, 5 mM of acetic acid was added to the MES/His buffer to investigate the low migration of magnesium.

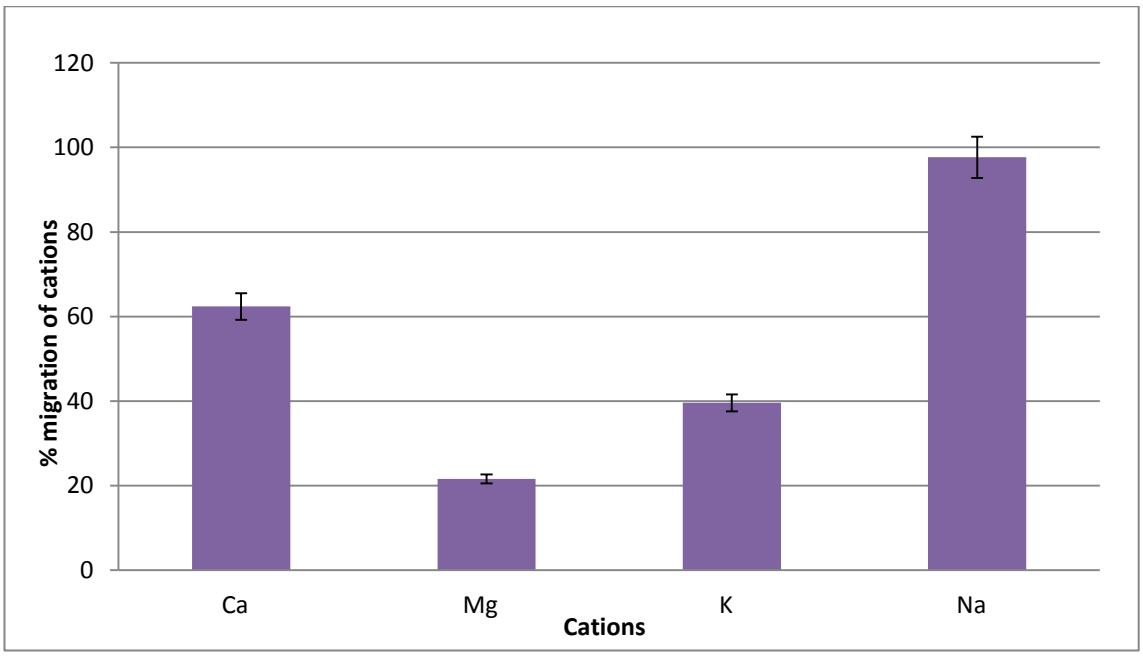

Figure 6-9: Percentage of cations migrated in 7 minutes at 15 V, with a 5 mM acetic acid buffer

Figure 6-9 shows the percentage of cation migration through a cellulose acetate membrane with an acidified buffer. From the figure, it can be seen that sodium has the largest migration, with more than 90%, calcium comes second, with more than 60%, followed by potassium with 40%. The lowest percentage is for magnesium, with slightly more than 20%. These results demonstrate progress after the addition of acid to the buffer, whereby the general rate of migration has increased and improved.

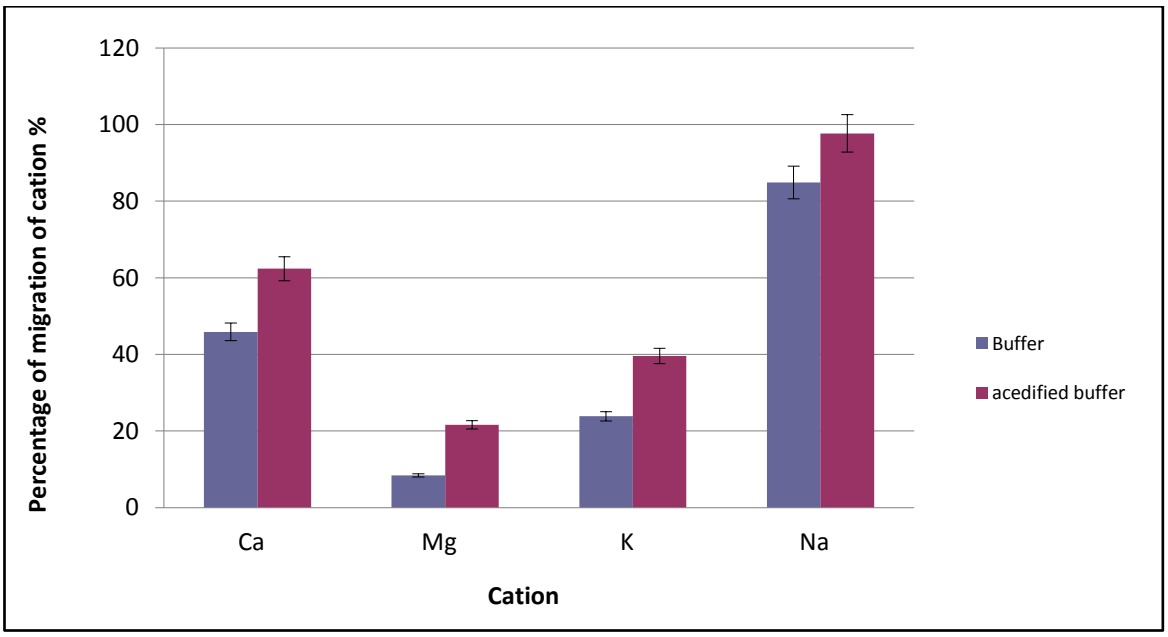

Figure 6-10: The percentage of cations migrated through a cellulose acetate membrane, with two different buffers, 5 mM MES/His and 5 mM MES/His + 5 mM acetic acid

Figure 6-10 shows the comparison of cation migration through a cellulose acetate membrane between two buffers: the MES/His buffer and the acidified MES/His buffer. The individual buffers have been discussed earlier (Figure 6-9 and Figure 6-8). Nevertheless, sodium has the highest percentage in both buffers, increasing from 84% to 97%. Calcium has also increased, from 45% to 62%, and potassium from 23% to 39%. The lowest migration is again for magnesium, from 8% to 21%. This shows the progress made with the acidified buffer, but that magnesium still has the lowest migration percentage. The acid has increased the general rate of migration but greater control over the extraction of magnesium is required. However, the separation system used in this work contains a PMMA chip, which was severely affected when the acetic acid buffer was used for the separation step; therefore, the use of this buffer will not be beneficial for future use, and the use of the MES/His buffer without acetic acid, although working, needs further optimisation.

Another issue that might affect extraction when using this system is the accumulation of unwanted white solid materials at the phase interfaces of the membrane or on the electrode surface (fouling). This issue is one of the major problems regarding electrodialysis.[180] Calcium in particular is most likely to form calcium oxide or calcium hydroxide on the surface of the electrode. The calcium composition in a solution in the operation of electrodialysis will affect the migration kinetics of the cations, as will the composition of cations in the sample.[211]

The fouling problem with regards to the electrodialysis system might be solved through the continuous movement of the fluid in the system. This could protect the electrodes and membranes from the accumulation of this solid material, and also clean the system between runs, removing the leftover material from previous runs. Therefore, another design for the ED system is preferable, in order to avoid fouling and ensure the better positioning of the electrodes.

6.3 Ion extraction with glass and cyclic olefin copolymer (COC) chips with a flat carbon electrode

Initially, work began with a glass chip (Figure 3-15), but there was a severe problem with sealing the membrane in the chip. Furthermore, there was another serious problem with the EOF, and so work had to stop on the glass chip, and was carried on with the COC chip.

In order to enhance the extraction of ions through the ED membrane to avoid the problems associated with the system in the previous section (6.2), a new ED chip was designed for the extraction. The design of the new chip should be more compatible with the final, integrated total system that includes both parts (separation and sample introduction).

The new chip material, COC polymer, was selected for the new chip design; COCs are engineering thermoplastics with good, unique properties such as transparency, low density that makes it light, withstanding relatively high temperatures, high rigidity, and good surface hardness. The most important feature is that it can chemically stand aqueous acids and bases[212]; this is very good for the pH optimisation of the ED system.

6.3.1 Results and discussion

The system mentioned earlier (sections 3.5.5 and 3.5.6) was used. The voltages applied were 10, 15, 50, and 100 V. The run times were 1, 3, 5 and 10 minutes, and the buffer was 5 mM MES/His. The samples were anion and cation standard solutions.

There were problems with this design, which caused severe leaking. This was mainly due to difficulties in sealing the electrode. There was also a problem with balancing the pressure on either side of the membrane. To overcome all of these problems and improve the system, another system was designed, which will be discussed in the following section.

6.4 Ion extraction on a COC chip with a multi-membrane

The design is shown in Figure 3-19. In order to overcome the problems associated with a cellulose acetate membrane for anion extraction, the possible formation of unwanted materials in the system (fouling), and to control leakages in the system, the design in section 3.5.7 was tested. In this new system, ion-exchange membranes were used rather than the cellulose acetate membrane. Two types of membrane were examined: an anion-exchange membrane for the extraction of anions and a cation-exchange membrane for the extraction of cations. The electrode used was copper coated with gold and the coating process has been described in section 3.6.1.

6.4.1 Results and discussion

The system in section 3.5.7 was mainly used for anion extraction, as the cellulose acetate was not satisfactory for anion extraction (see section 6.2).

The buffer was 5 mM MES/His and the anion sample included the IC standard solutions of fluoride, chloride, nitrate, phosphate and sulphate. The voltage applied was 100 V for 15 minutes, three times continuously. This involved a 5-minute run, before switching off the voltage, collecting the results and filling the destination reservoir with buffer, followed by another run of 5 minutes. This was repeated three times in order to collect enough samples to be measured by the IC system and to concentrate the extracted anion.

When the voltage is applied, hydrogen ions will appear at the cathode, and oxygen ions will appear at the anode. A reduction reaction takes place, with electrons (e^-) from the cathode being given to hydrogen cations, to form hydrogen gas (the half-reaction balanced with acid):

Reduction at cathode: $2\ H^+_{(aq)} + 2e^- \rightarrow H_{2(g)}$

At the anode, an oxidation reaction occurs, generating oxygen gas and giving electrons to the anode to complete the circuit:

Oxidation at anode: $2\ H_2O_{(l)} \rightarrow O_{2(g)} + 4\ H^+_{(aq)} + 4e^-$

The same half reactions can also be balanced with base, as listed below:

Cathode (reduction): $2\ H_2O(l) + 2e^- \rightarrow H_2(g) + 2\ OH^-_{(aq)}$

Anode (oxidation): $4\ OH^-_{(aq)} \rightarrow O_{2(g)} + 2\ H_2O_{(l)} + 4\ e^-$

Combining either half-reaction pair yields the same overall decomposition of water into oxygen and hydrogen:

Overall reaction: $2\ H_2O_{(l)} \rightarrow 2\ H_{2(g)} + O_{2(g)}$

The number of hydrogen molecules produced is therefore twice the number of oxygen molecules. Hence, the electrode used has to be compatible with hydrogen production, and gold and platinum are the best electrode materials,[213] although a gold electrode has less hydrogen production than platinum.[214]

This could be the reason behind the unsuccessful initial experiment with the copper electrode; therefore, the copper electrode was coated with gold for better conductivity, and the gold coating was mentioned earlier, in section 3.6.1.

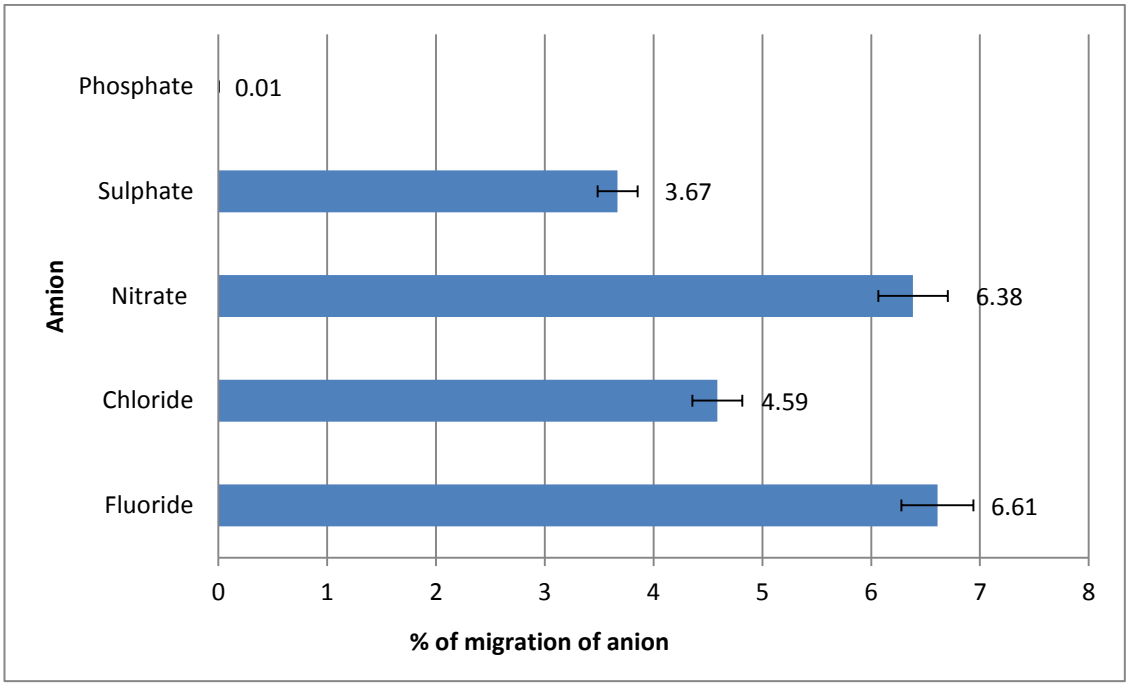

Figure 6-11: The percentage of anion extraction with gold-coated electrodes. The buffer used was 5 mM MES/His and the anion concentration was 1 g/L of each anion.

Figure 6-11 shows the percentage of anion extraction using the multi-membrane ED chip with a gold coating on the copper electrode. The highest extraction was for fluoride, with about 6.6%, followed by nitrate with 6.3%, chloride with 4.5%, and sulphate with less than 4%. The lowest extraction was for phosphate, with 0.01%. This shows that extraction was improved with the gold coating.

The extracted percentage was a relatively small amount and this might have been caused by the low conductivity, as the gold coating was a thin layer of around 10-100 nm. Also, the stability of the coating was important and was thus examined. It was found that the gold coating could be physically washed off the copper after several runs. This could be solved by thickening the layer of gold to ensure better conductivity, although it would eventually be washed off again, meaning that the coating is not ideal for such an application. In addition, the gold might become oxidised and not conductive after several runs, as it is unstable over the copper. However, in both cases, it will not be conductive enough to attract the anion to migrate through the membrane, which would eventually affect the migration process and decrease the migration amount.

To overcome this potential problem, a layer of carbon coating was placed over the gold coating (see section 3.6.2 for the coating process). This was to protect the gold from oxidisation and to keep it in place; if the carbon washed off, then the gold layer would remain there for a longer period. Also, the carbon is a conductive material that will not stop conductivity in the system during the runs, and it can increase the conductivity in the system. The same experimental procedure used previously was used here (see section 6.4.1).

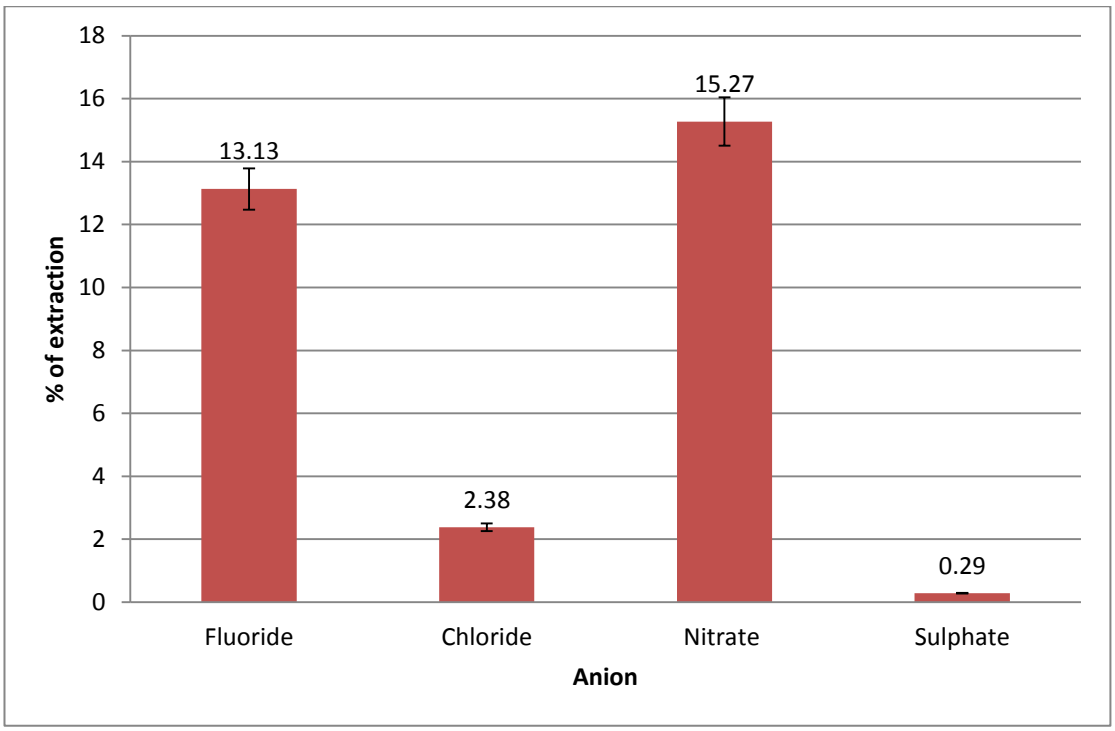

Figure 6-12: The percentage of anion extractions, with carbon coating over gold-coated electrodes. The buffer used was 5 mM MES/His and the anion concentration was 1 g/L each of anion.

Figure 6-12 shows the percentage of anion extraction using a multi-membrane system with carbon coating over gold coating, over the copper electrode. The largest extraction percentage was 15.3% for nitrate, followed by 13% for fluoride, 2.4% for chloride, and 0.3% for sulphate. Phosphate did not show any extraction. This demonstrated good extraction performance for fluoride and nitrate but phosphate and sulphate showed poor extraction. That might have been caused by the concentration of anions in the sample and the anions ability to migrate through the membrane, which requires further investigation. Nevertheless, the aim of this step was to increase conductivity in the system by coating the gold layer on the electrode with carbon. Increasing the conductivity will improve the extraction performance. The conductivity of the system following the carbon coating did not increase as expected; it fluctuated quite

considerably but overall, there was no great difference in conductivity between the two coating methods.

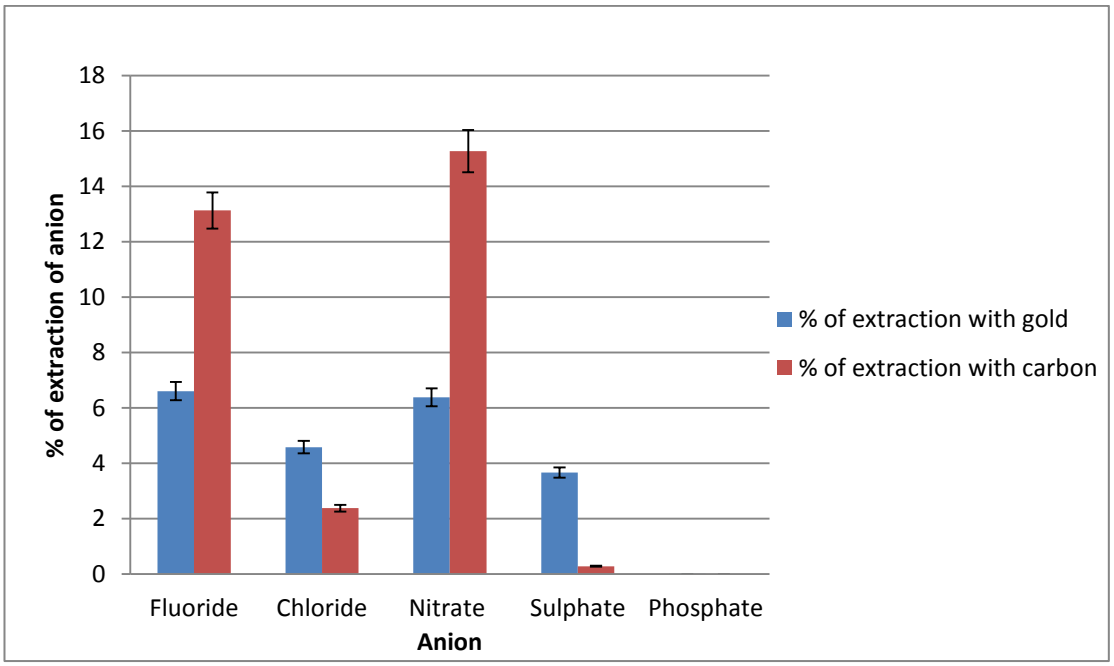

Figure 6-13: The percentage of anion extraction using a desalination cell, with two different electrode coatings, gold and carbon

Figure 6-13 shows the percentage of migration using a multi-membrane chip with two different electrodes: copper coated with gold, and copper coated with gold and carbon over the gold. The extraction of fluoride and nitrate seems to be twice as high with carbon coating than with gold alone, while it is twice as low for chloride, much lower for sulphate, and slightly better for gold than carbon.

Generally, gold seems better for overall extraction whereas carbon showed no extraction of phosphate. A fluctuation in conductivity was observed that might be due to the design of the system, as the electrode might be not in good contact with the sample, or the buffer in the channel has not been filled. This could also be a result of the gold coating over the electrode, which might physically wash off the electrode or become

oxidised. However, in both cases, the conductivity had to be increased to attract the anion to migrate through the membrane. Further optimisation was needed to enhance the extraction, including the system design, to ensure better contact with the fluid in the system and robust electrodes.

6.5 ED with an ion-exchange membrane using a commercial ED cell

6.5.1 Anion extraction with one anion-exchange (AEX) membrane using a commercial ED cell

In the multi-membrane system previously described (section 6.4), there were three layers of ion-exchange membrane. The main reason for this was to enhance the anion extraction. However, the anion-exchange membrane can be used on its own to extract anions. The membrane was used to examine its extraction behaviour in this system, which will then be adjusted for the suitable set-up of a fully integrated system.

6.5.1.1 Results and discussion

The commercial system described earlier in section 3.5.4 (Figure 3-13 and Figure 3-14) was used here because this system is practically easier to handle, and the system in this stage needed to be disassembled a few times in order to optimise the extraction. The system consisted of a chamber and an anion-exchange membrane that was placed in the chamber. Two Pt electrodes were directly inserted into the destination and sample reservoirs; the sample reservoir was filled with about 500 µl analyte (anion mixer) and the chamber (500 µl) was filled with 5 mM MES/His buffer.

The voltage applied was 100 V and the run time was 1 minute. The results were collected from the destination reservoir and then analysed using the IC Dionex system.

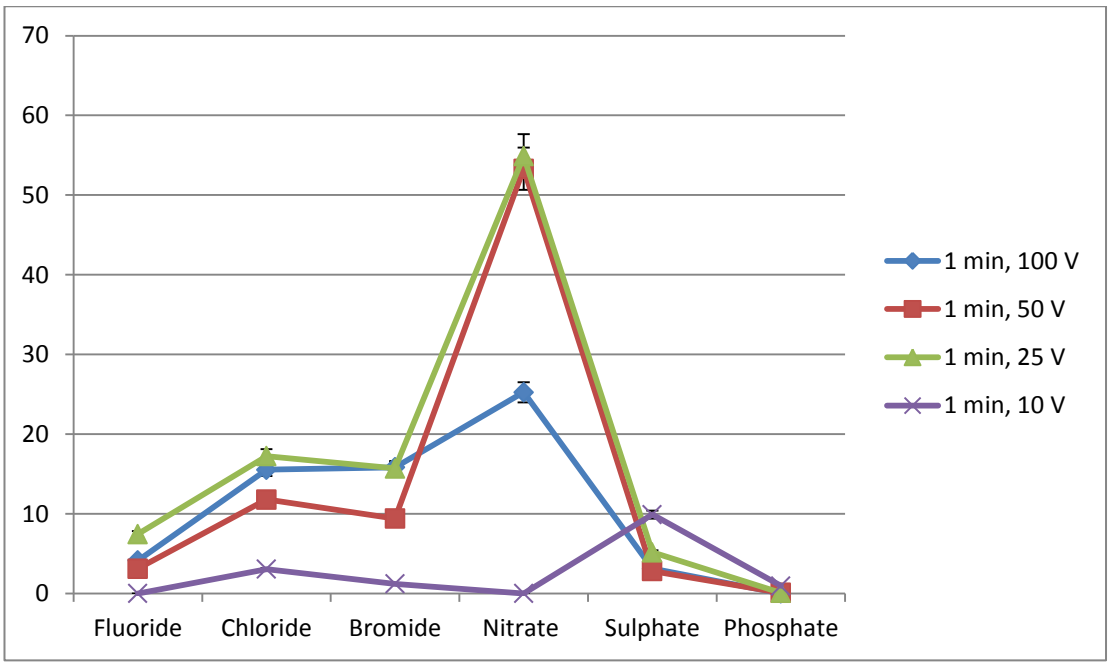

Figure 6-14: The percentage of anion extraction through an anion-exchange membrane, at different voltages. The sample uses an anion standard solution, 1 g/L of each anion, with a 5 mM MES/His buffer

Figure 6-14 shows the percentage of anion extraction from the sample reservoir to the destination reservoir, through an anion-exchange membrane at different voltages (10, 25, 50 and 100 V), with a running time of 1 minute. From the figure, it can be observed that the extraction was examined under four different voltages at a fixed time of 1 minute. At the first point, 10 V, the system has its lowest rate of migration percentage, with its largest at around 10%, for sulphate. The second point, 25 V, seems to be the largest rate of extraction for all anions except for sulphate, with a maximum higher than 50%, for nitrate. The third point, 50 V, has a similar rate to the 25 V rate but is slightly lower. Finally, the last point, 100 V, follows a similar trend to 25 and 50 V but is 50% lower for nitrate.

At 10 V, sulphate extraction was low. This might be due to the ability of sulphate to migrate faster than the other anions, or to a sulphate contamination that accumulated at that point; this requires further investigation. At 50 and 25 V, the extraction follows a

similar trend but is slightly lower for 50 V, which is surprising, as the increase in voltage should in theory increase the extraction performance. At 100 V there was a similar but lower trend, with the high voltage causing the production of bubbles in the sample reservoir. The bubble formation was noticeable and the current flowing into the system stopped suddenly after 30 seconds. It seems that 25 V was the best voltage at this point for the extraction of anions using this system; however, the results in general require more investigation for the extraction of individual anions.

6.5.1.1.1 Timing optimisation

After the optimisation of the voltage using the ED system, the same set-up from the previous work was used to optimise the timing, using 25 V as an optimum voltage. Three different extraction times were examined: 1, 2.5 and 5 minutes as in this stage in the total system the extraction time have to be less than 5 minutes if possible.

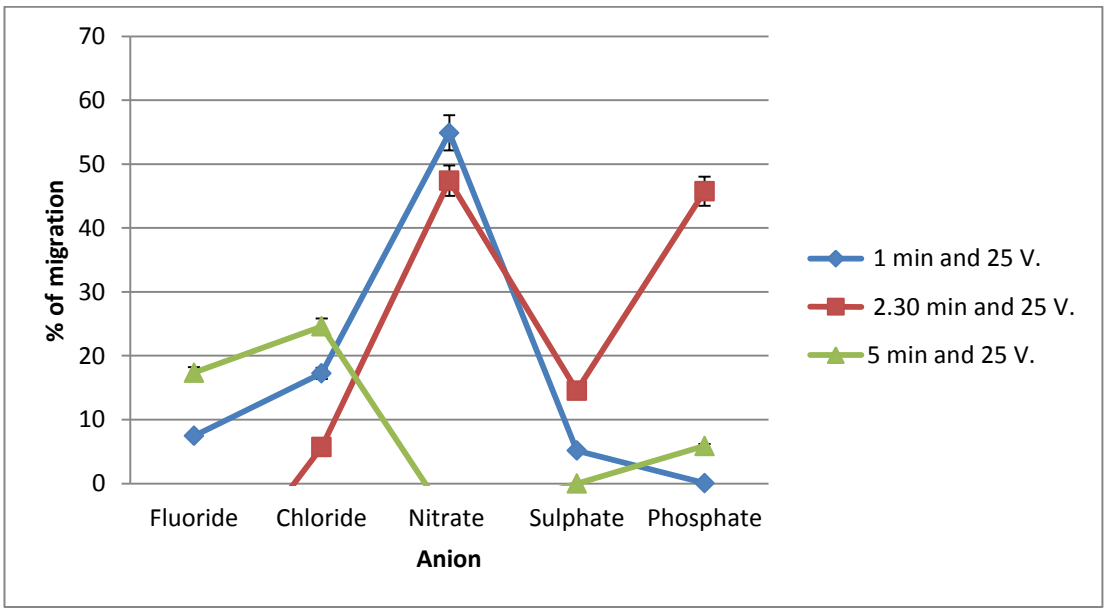

Figure 6-15: The percentage of anion extraction through an anion-exchange membrane, with different timings. The sample was an anion standard solution of 1 g/L of each anion, with a 5 mM MES/His buffer is. The experiment was run three times.

Figure 6-15 shows the migration percentages of five anions through an anion-exchange membrane at different timings (1, 2.5 and 5 minutes) and a fixed voltage of 25 V. From the figure, it can be seen that the migration percentage at 1 minute was less than 20% for fluoride and chloride but it was at the maximum of more than 50% for nitrate, and less than 10% for both sulphate and phosphate. At 2.30 minutes, it was less than 10% for chloride, jumping to around 45% for nitrate and phosphate, and it was less than 20% for sulphate. At 5 minutes, fluoride and chloride migration was between 15 and 25%, while it was very low for sulphate and phosphate, with less than 10%. It has to be mentioned that some of the points in the graph had to be excluded due to contaminations at those particular points, which will be discussed later.

However, the figure is showing that the anion-exchange membrane was extracting anions in the ED system. The results were good and further improvement of the ED system will show even better results. Yet, at higher voltage and longer timing, fluctuation and irreproducibility occur due to the bubble formation in the systems which affect the results. A positive point is that it was reproducible but this was unexpected and was probably due to the ability of the membrane to stand chemically and physically for a long period (around 60 runs). One membrane was used at least three times for each run, to ensure reproducibility under the same conditions and to keep the practical set-up fixed, so that the results would be as accurate as possible. Also, the membrane had to be conditioned with water before each run at the same position. These factors might affect the performance of the membrane during experiments.

6.5.1.2 Examination of the used AEX membrane

In order to investigate the membrane ability under different conditions, IR was used to examine the membrane that was used in the extraction experiments.

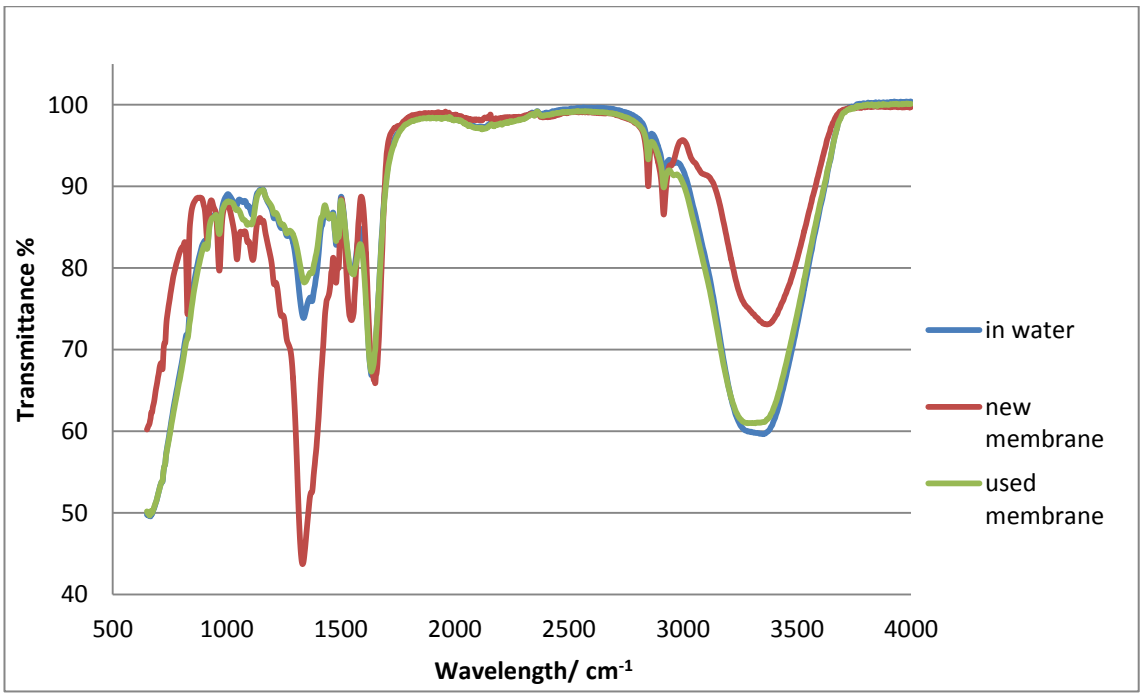

Figure 6-16: IR spectra for the AEX membrane at three different conditions: only in water overnight; a new membrane; and a used membrane

Figure 6-16 shows the IR spectrums of three different anion-exchange membranes under different conditions. The first condition was a membrane placed in water overnight and then dried at room temperature overnight. The second condition was a new dry membrane and the third condition was a membrane that had been used for ED experiments several times (about 100 runs) and then allowed to dry at room temperature overnight. Figure 6-16 shows that the membranes have similar trends but that the new membrane and the one placed in water were almost identical, with a slight difference in the region between 1,000 and 1,500 cm^{-1}. The new membrane demonstrated a different spectrum, especially in the regions between 500 and 1,500 cm^{-1}, and 3,000 and 3,500 cm^{-1}.

The peak between 3000 and 3500 cm^{-1} was the O-H peak from water [127], and it was smaller for the new membrane because it was dry, and it was similar for the other two conditions because they have more water. The two peaks between 2800 and 3000 cm^{-1}

were for C –H [129]; and they were nearly identical for all the three conditions. The peaks at 1655 and 1670 cm^{-1} were for H-C=O (amide) peaks [215], and they were very similar for the three conditions. The peak at 1340 cm^{-1} might be for CO_3^{2-} [127], it was long peak for the new membrane, and then was depleting for the membrane that kept in water, and it decreased further for the used membrane. This indicated that the membrane was a polyamide membrane and it might be modified or coated (with carbonate). The chemistry of the coating layer or the modification was hard to identify.

However, there were chemical differences and changes in the spectrums. The new membrane had a different spectrum while the other two indicated changes that occurred following the use of the membrane in the ED system. Overall the three conditions showed similar spectrums, and the changes on the original membrane occurred when the membrane was exposed to water, except the peak at 1340 cm^{-1} and this is probably the reason behind the membrane behaviour. However, more investigation is required to accurately examine the membrane ability for ED, such as how many runs it could last for and what type of conditions might affect the anion extraction.

6.5.2 Cation extraction with one cation-exchange (CEX) membrane using a commercial ED cell

In the ED system described earlier (section 6.4), there were three layers of ion-exchange membrane, two AEX membranes, and a CEX. However, the cation-exchange membrane can be used on its own to extract cations.

In this extraction, the CEX membrane was compared to the cellulose acetate membrane (CA) for the extraction of cations (see section 6.2.1.2).

6.5.2.1 Results and discussion

The system described earlier in section 3.5.4 was used here, for the previously described reasons. The sample reservoir was filled with about 500 µl analyte (cation mixer) and the chamber (500 µl) was filled with 5 mM MES/His buffer. The results were collected from the destination reservoir and then analysed using a ICP-AES system.

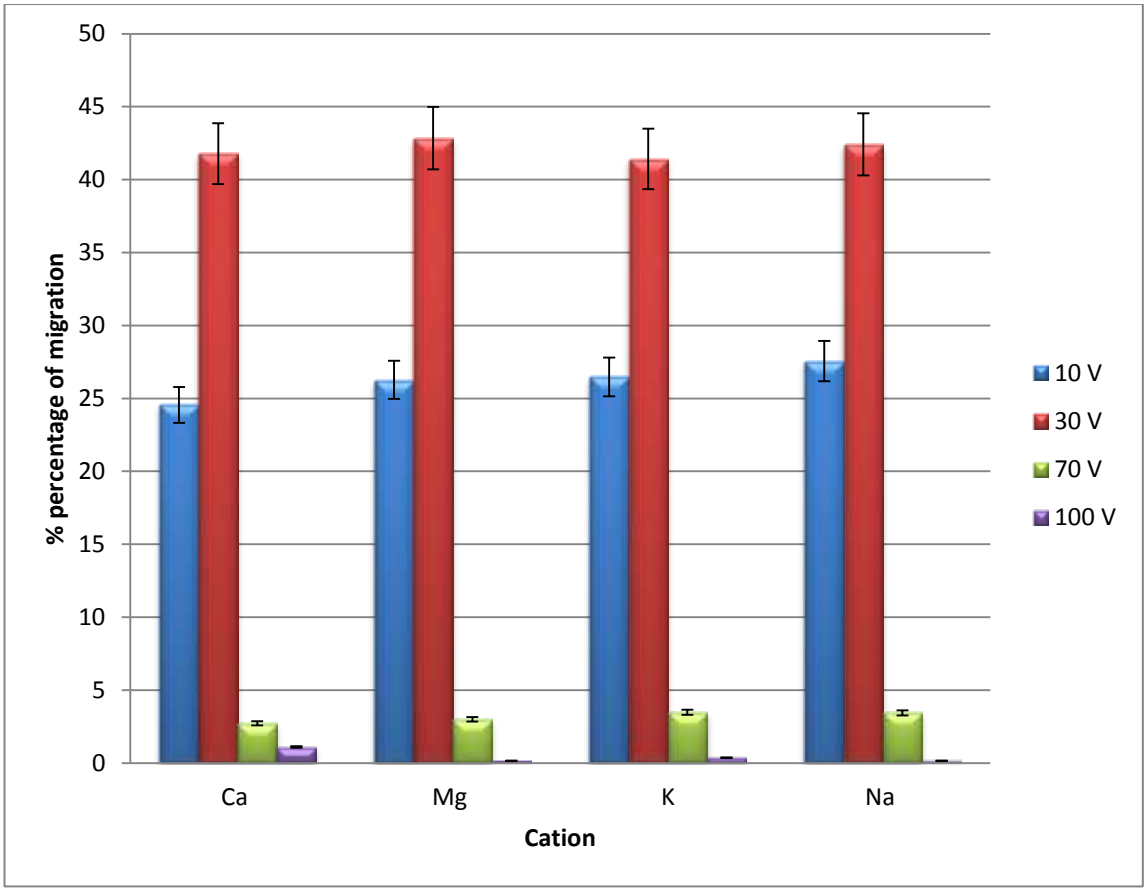

Figure 6-17: The extraction percentages of four cations through a cation-exchange membrane at a fixed time of 1 minute, with different voltages (10, 30, 70, and 100 V) and a 5 mM MES/His buffer

Figure 6-17 shows the percentage of extracted cations at a fixed time with different voltages. From the figure, it can be seen that the extraction has a similar trend for all cations, but with different behaviours. At 10 V, the extraction was between 25-30% for

all cations, whereas it was between 40-45% at 30 V, and it was less than 5% for 70 V. The lowest extraction percentage occurred at 100 V.

The best percentage was obtained at 30 V and the lowest was at 100 V. This was due to the bubble formation in the system at high voltages affecting the migration of cations from the sample reservoir to the destination reservoir in the ED system. Therefore, the optimum condition at this point was the relatively low voltage of about 30 V. However, in a further improved system, this might change to a higher voltage in order to enhance the extraction.

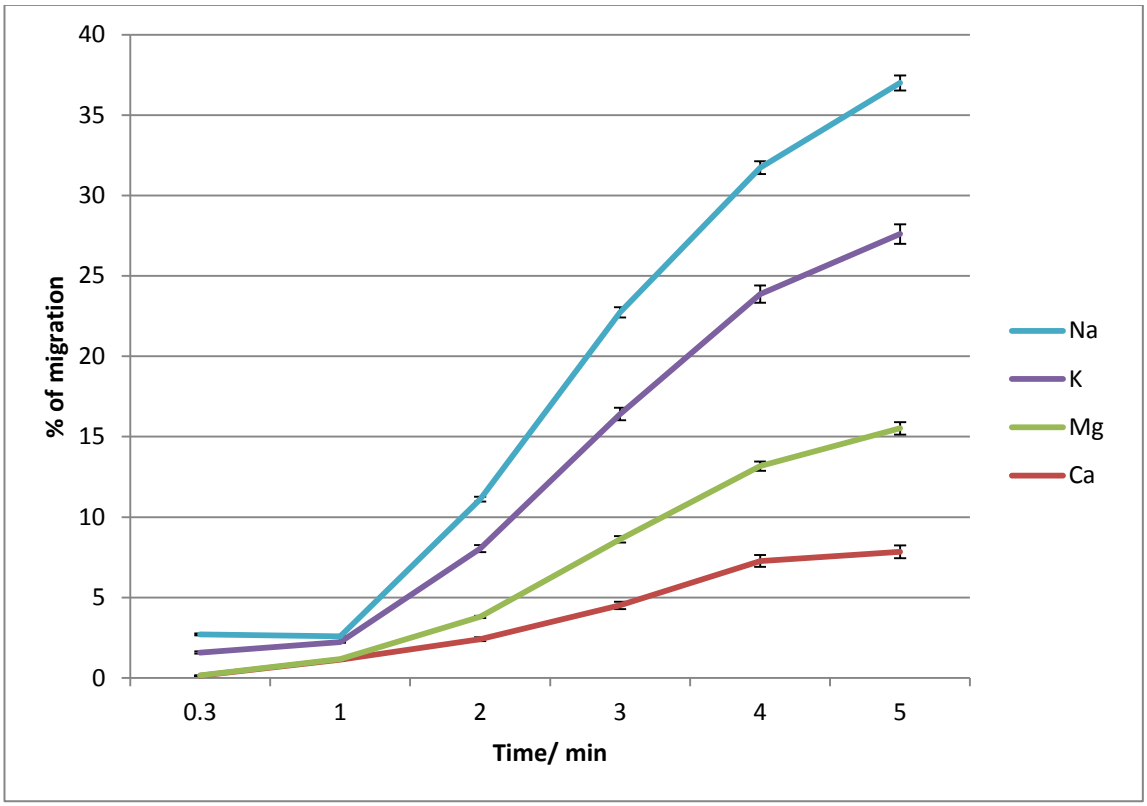

Figure 6-18: The extraction percentages of four cations through a cation-exchange membrane at a fixed voltage of 30 V and different timings (0.3, 1, 2, 3, 4, and 5 minutes), with a 5 mM MES/His buffer

Figure 6-18: shows the changes in migration for different extraction times, from 30 seconds to 5 minutes. The amount of migrated cation increased from less than 5% at 30

seconds to more than 35%. In general, sodium has the highest migration percentage and calcium has the lowest. However, the increasing trend of the migration percentage was expected, despite the fact that it levels off between 30 seconds and 1 minute, which is a short time. The most important point is that a longer time is better for extraction in these conditions.

6.6 Ion extraction in a COC chip with one membrane

Initially, both anion- and cation-exchange membranes were used in the multi-membrane (see section 3.5.7) for the extraction of anions, and they were then examined as individual membranes for the extraction of anions through an anion-exchange membrane and the extraction of cations through a cation-exchange membrane. Both have shown promising results and they could potentially be used for ion extraction with further modification of the ED chip, to enhance and improve the extraction of ions.

Using the ED system (see section 3.5.8), the system was examined for three main points:

- The physical stability of the chip under pressure. The pressure from the pump that was used to load the sample and collect the results would affect the chip, leading to leakage in the system. (This is practically critical as it requires appropriate tubing.) This point was examined by pumping buffer at different flow rates (0.1- 1 mL min^{-1}) into both reservoirs.
- The stability of the gold coating on the electrode (see section 3.6.3). This was examined by analysing gold in the flushed buffer that was used to examine the physical stability.
- The behaviour of cations in the system without the applied voltage, as they might migrate through the membrane without the attraction of electrical power.

This point was examined by leaving a cation solution in the sample reservoir for five hours before collecting and analysing the buffer in the destination reservoir.

6.6.1 Results and discussion

Table 6-2: Cation extraction with an ED system

Amount of cation	Ca	Mg	K	Na	Au
Original sample/µg	337.374	531.244	604.794	819.304	-0.042
Blank (system flush)/µg	0.456	0.190	1.233	1.198	-0.074
Destination reservoir after 5 hrs/ µg	0.233	0.083	1.183	1.591	-0.022

Table 6-2 shows the amount of cations and the amount of gold (on the electrode), which was analysed by ICP-AES for the new ED system. The first row represents the concentration of original cation standard samples that were used in this experiment. The second row is the concentration of cations present in the buffer and the ED system (this includes the chip, tubing and syringe), as the buffer was flushed at different flow rates through the system, before analysing the flushed buffer. The third row is the amount of cations and gold in the destination reservoir after leaving the original sample (displayed in the first row) for five hours.

The table shows that there are cations in the system and contamination of the buffer that probably accumulated from the tubes or during preparation; however, the levels are extremely small compared to the original cation sample, and would not affect the results obtained from the system. The destination reservoir after five hours also shows an extremely small amount of cations in the reservoir. The concentration of gold in the entire system even after five hours is zero, which means that the gold coating has not been removed.

The results obtained from the table are excellent and demonstrate that the gold electrode is stable. Also, there is no migration without voltage for five hours. Thus, the system is reliable for ion extraction.

6.6.2 Optimisation of cation extraction in a COC chip with one CEX membrane

In order to find the optimum conditions for the extraction of ions, and after the investigation of the cation-exchange membrane behaviour in an ED commercial cell (see section 6.5.2), the CEX membrane was shown to be effective for cation extraction. In this section, ED was carried out with microfluidic-based ED chip, as described in section 3.5.8.

6.6.2.1 Experimental

The buffer used was 5 mM MES/His at a flow rate of 0.5 mL min^{-1}, using a syringe pump. The buffer was introduced to the destination reservoir in the system. Samples were collected and analysed by the ICP.

The effects of changing the extraction times (1-5 minutes) at the applied voltage (1-5 V), was investigated.

6.6.2.2 Results and discussion

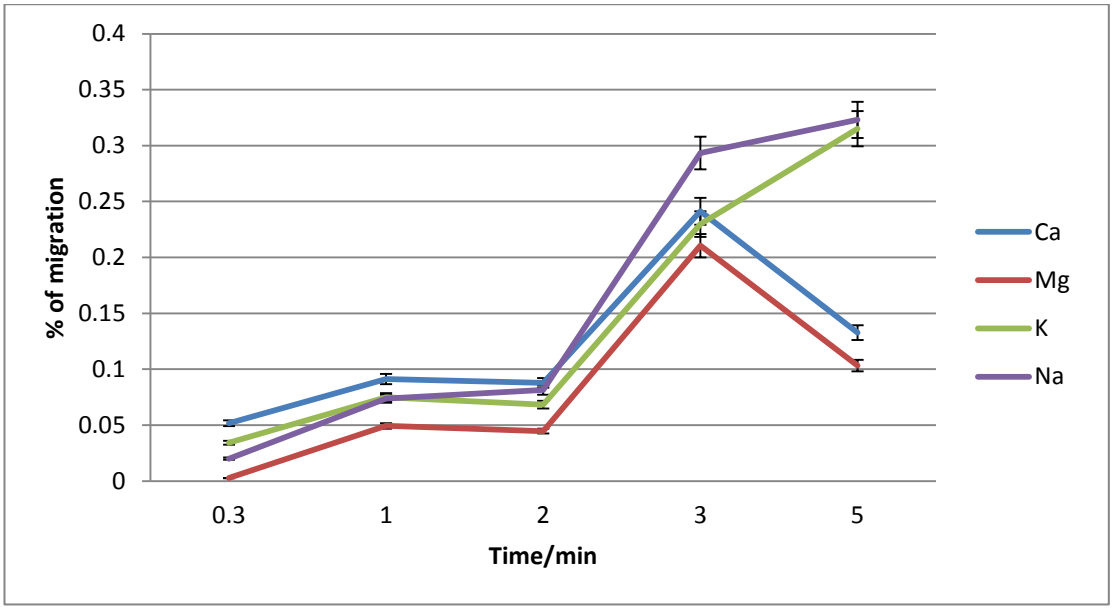

Figure 6-19: The percentage of the extraction for four cations through a CEX membrane at a fixed voltage of 100 V and different timings (0.3, 1, 2, 3, 4 and 5 minutes)

Figure 6-19 shows the extraction percentages of four cations through the CEX membrane at a fixed voltage of 100 V, at an increasing extraction time. The cation extraction can be seen to increase along with the increased extraction time. The extraction percentages increased for all cations from 0.3 to 1 minute, before levelling off between 1 and 2 minutes. After this, it increased at 3 minutes. At 5 minutes, the sodium and potassium percentages increased, while the calcium and magnesium percentages decreased.

The extraction for this system showed an increasing trend along with the increasing run time. However, the general extraction percentage was very low, as was the conductivity in the system. This was probably due to the position of the electrodes, especially the top-side electrode of the chip, as the fluid in the sample reservoir might not have good

contact with the electrode, which then leads to a low conductive environment and the low migration of cations from the sample reservoir to the destination reservoir.

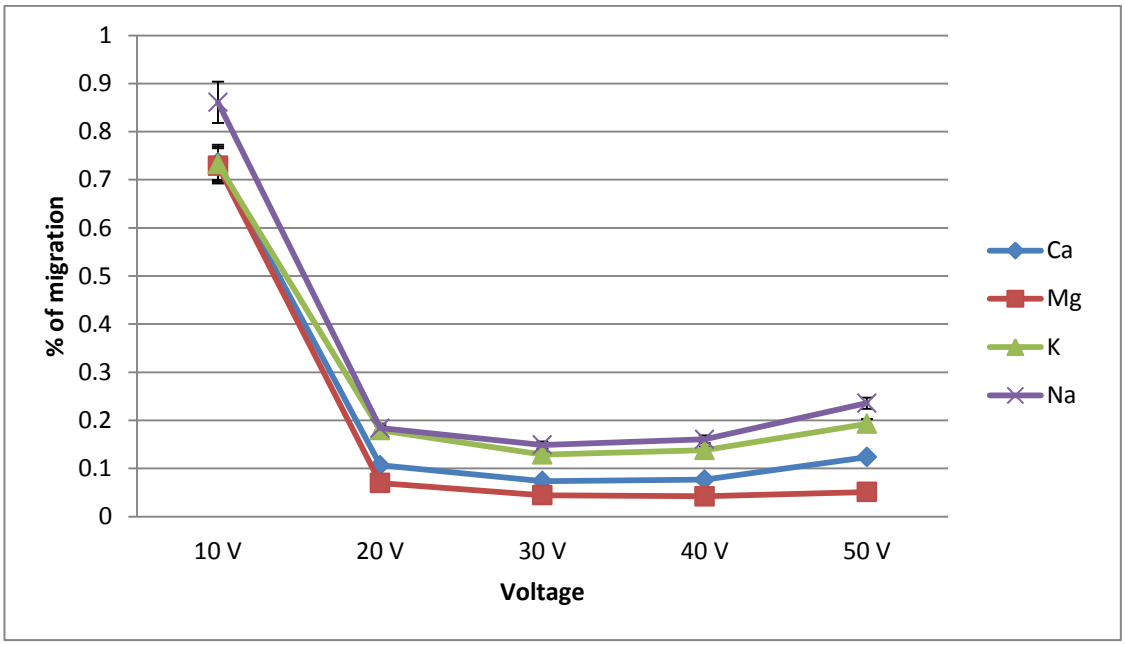

Figure 6-20: The extraction percentages of four cations through the CEX membrane at a fixed extraction time of 3 minutes and different voltages, with a 5 mM MES/His buffer

Figure 6-20 shows the extraction percentages of sodium, magnesium, calcium and potassium through a CEX membrane in an ED system with a MES/His buffer. From the figure, it can be seen that there is a similar trend for all cations. At 10 V, the trend was around 0.8%, decreasing at 20 V and then remaining the same between 20-50 V, with a slight increase at 50 V.

However, despite the successful extraction of cations, the extraction percentages were very low (under 1%) and the conductivity in the system was also very low. This was probably due to the electrode position.

In order to investigate the conductivity of the system, a platinum electrode was placed in the reservoir with the buffer, and voltage was applied. Another platinum electrode (as

rods, because it can be easily controlled) was used instead of the gold electrodes to investigate the low conductivity in the system, and this showed a very large increase in the conductivity of the system, indicating that the design of the system requires further optimisation.

To examine whether the cation was trapped in the membrane or the chip, the membrane and the chip were washed with acid and buffer and then analysed, and the extractants were also analysed.

Table 6-3: The amount of cations in the membrane and ED system after washing them with 0.1 mM acetic acid and 5 mM MES/His buffer, with analysis carried out through ICP-AES

The concentration of cations/ µg	Cations			
	Ca	Mg	K	Na
Original cation concentration	442.93	267.67	308.24	424.25
System wash before experiment	0.25	0.11	0.45	0
Buffer	0.17	0.11	0.03	0.09
Membrane	2.64	5.16	3.75	3.98
Membrane wash with acetic acid and buffer	267.95	5.84	32.62	40.26

Table 6-3 shows the amount of remaining cations in the membrane by washing the membrane and the ED system with 0.1 mM of acetic acid and buffer. The first row is the original cation concentration used in the experiments. The second row is the cation concentration present in the system before it was used; this is to find out if there was a system contamination. The third row is the cation concentration in the buffer, as it might have undergone some contamination of the cations. The fourth row is the concentration of cations in the membrane, when the membrane was placed in a buffer overnight and the buffer was then analysed by ICP-AES. The fifth and the final row is the cation concentration in the membrane after treating it with acid; the membrane was placed in acid and buffer overnight and then analysed through ICP-AES.

As found in section 6.6.1, the buffer and the system both had a very small amount of cations that would not affect the results. The concentration of cations in the membrane was only small. The membrane following the acid treatment should have a higher presence of cations, especially with calcium at 267.95 µg, which is very high; this could be a result of contamination during the analysis process but requires further investigation. Magnesium, on the other hand, was normal; it demonstrated a similar amount to the initial amount in the membrane before washing it with acid. Potassium and sodium demonstrated slightly higher concentrations of 32.6 and 40.2 µg, which is high but within an acceptable range. These values indicate that there are some cations that are trapped or delayed in the membrane; releasing this amount from the membrane, especially the calcium, is very important and would enhance the extraction.

The extraction in a COC chip with one membrane has shown extraction, but with a small amount of cation extracted. This might be due to a few factors such as the membrane strength, the offline detection of the ions, and the position of the electrode. A new design of the system would improve the extraction and enhance the system. Online detection would significantly improve the system, as the offline system has less accuracy than the online one, and the sample could be lost during the transfer process. Nevertheless, work is being undertaken to design a total integrated system that includes sample introduction, separation and conductivity detection, all with online, real-time analysis. Thus, the low results in the current system might appear better with the new, integrated system.

6.6.3 Optimisation of an anion extraction in a COC chip with one AEX membrane

Anion extraction has not been reported in the literature for CE as a simple system. This work aims to extract anions through an AEX membrane using a novel ED system in a microfluidic chip, with different techniques having been used for the extraction of anions in this work.

6.6.3.1 Experimental

The system described earlier in section 3.5.8 was used with the commercial PCB (see section 3.6.3). IC standards (chloride, nitrite, nitrate, phosphate and sulphate) were used, each with a concentration of 1 g/L (Sigma Aldrich, UK). The sample used here was diluted to the following concentrations: chloride 1 μg, nitrite 2 μg, and nitrate, phosphate and sulphate concentrations of 6 μg each. A 5 mM MES/His buffer was used. The flow rate was at its convenient between 0.1-3 $mLmin^{-1}$ from the syringe pump in order to introduce the buffer to the destination reservoir in the system, before the sample was collected and analysed by the IC Dionex. The run time was 3 minutes and the voltage applied on the system was 100 V.

In this work, we aimed to analyse a real river water sample that was collected on 21 May 2015 from the River Hull, in Kingswood.

6.6.3.2 Results and discussion

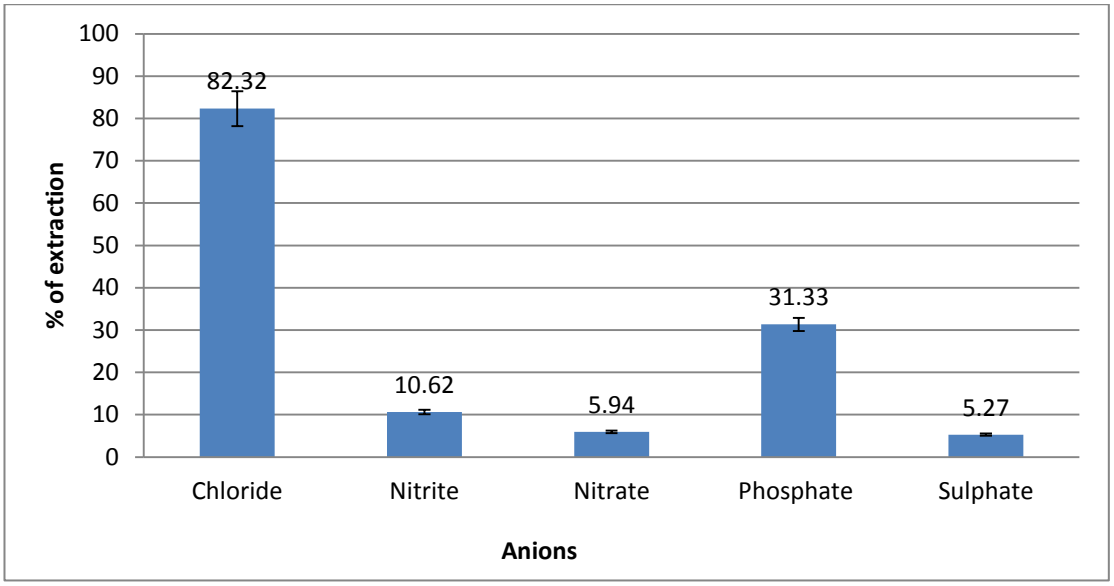

Figure 6-21: The percentage of anion extractions through an AEX membrane in an ED chip

Figure 6-21 shows the percentage of anion extractions for chloride, nitrite, nitrate, phosphate and sulphate, through an AEX membrane in the ED chip. From the graph, it can be seen that the percentage of chloride was the highest with 82%, followed by phosphate with 31%, nitrite with 10.6%, and nitrate with about 6%, followed by the lowest percentage of migration, which was sulphate with 5%.

The chloride extraction was high while the other anions showed lower extraction. This is possibly because of the charge density of each anion. Considering the low amount of anion in the original sample, these results are very good. Furthermore, these results are more likely to improve further with an online detection system, which would be more accurate as the sample would be in real-time and less analyte would be lost during transfer.

6.6.3.2.1 Real river water analysis of anions

A sample of River Hull water was collected and analysed using the same conditions mentioned earlier (see section 6.6.3.1).

As described in section 6.5.1.2, the efficiency of the membrane decreased; therefore, the River Hull sample was analysed with the same conditions, with two different membranes. The first one was a new membrane and the second one had been used for several runs.

Table 6-4: The results of anion extractions (from River Hull water sample) through AEX in the ED chip

Anion	Original River Hull water sample μgL^{-1}	Extracted concentration/$\mu g\ L^{-1}$	
		New membrane	Used membrane
Chloride	7.18	1.62	0.65
Nitrite	0.60	0.04	0.03
Nitrate	6.46	0.36	0.01
Phosphate	8.44	2.96	0.13
Sulphate	0.97	0.64	0.16

Table 6-4 shows the amount of five anions in a River Hull water sample using an ED chip. The second and third columns are the extracted amount of anions through an AEX membrane in the ED chip, using a new membrane and a used membrane.

The original sample contains a variety of anion concentrations. The highest concentration was for phosphate, with 8.44 μgmL^{-1}, followed by chloride with 7.18 μgmL^{-1}, nitrate with 6.46 μgmL^{-1}, and then nitrite and sulphate with 0.60 and 0.97 μgmL^{-1}, respectively.

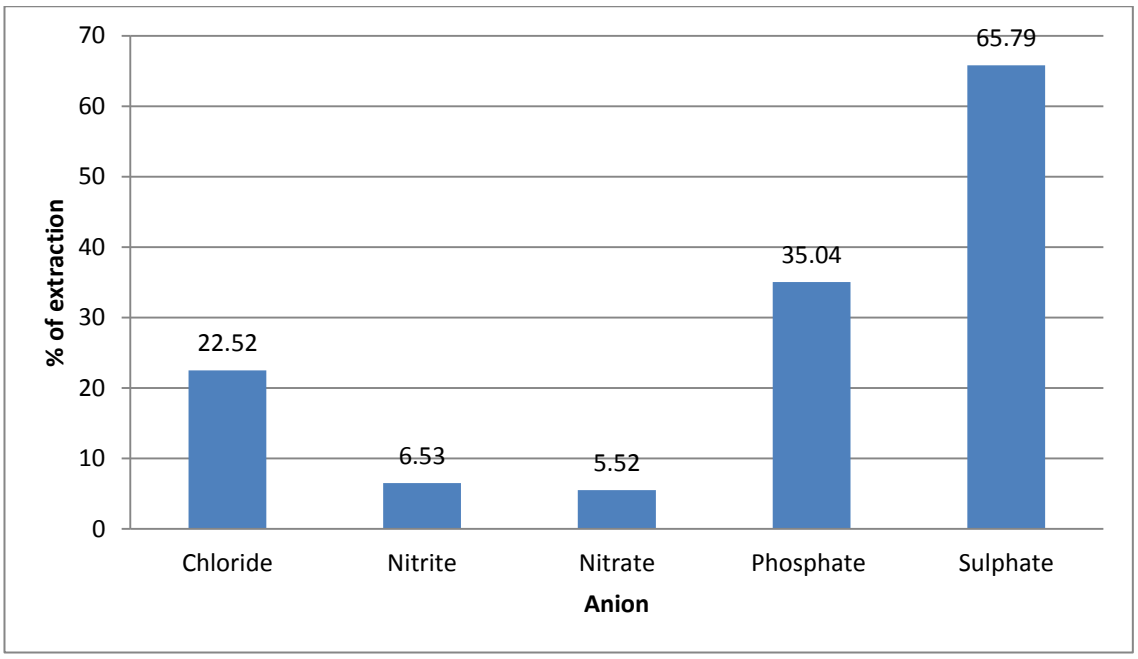

Figure 6-22: The percentages of anion extractions through a new AEX membrane in an ED chip

Figure 6-22 shows the extraction percentages of five anions through a new AEX membrane. From the figure, it can be observed that the largest extracted amount was for sulphate with 65%, followed by phosphate with 35%, chloride with 22.5%, nitrite with 6.5%, with lowest percentage of extraction for nitrate, with 5.5%.

The figure again demonstrates a great success in extracting anions using this system. All anions were extracted with a variation in the migrated amount of each anion. Sulphate seems to be the largest and this is possibly because of the small concentration of sulphate in the original River Hull sample, which migrated better than the other anions. Phosphate, on the other hand, had the largest amount in the original sample but 35% was migrated to the destination reservoir. Chloride was one of the largest concentrations in the original River Hull water sample but about 22% of this was extracted. Nitrate was also one of the anions with the highest presence in the sample and 5.5% of it was migrated through the membrane. Finally, nitrite demonstrated a 6.5% extraction.

The same conditions were used to extract anions from the membrane used for 15 runs, with a range of 1-5 minutes for each run.

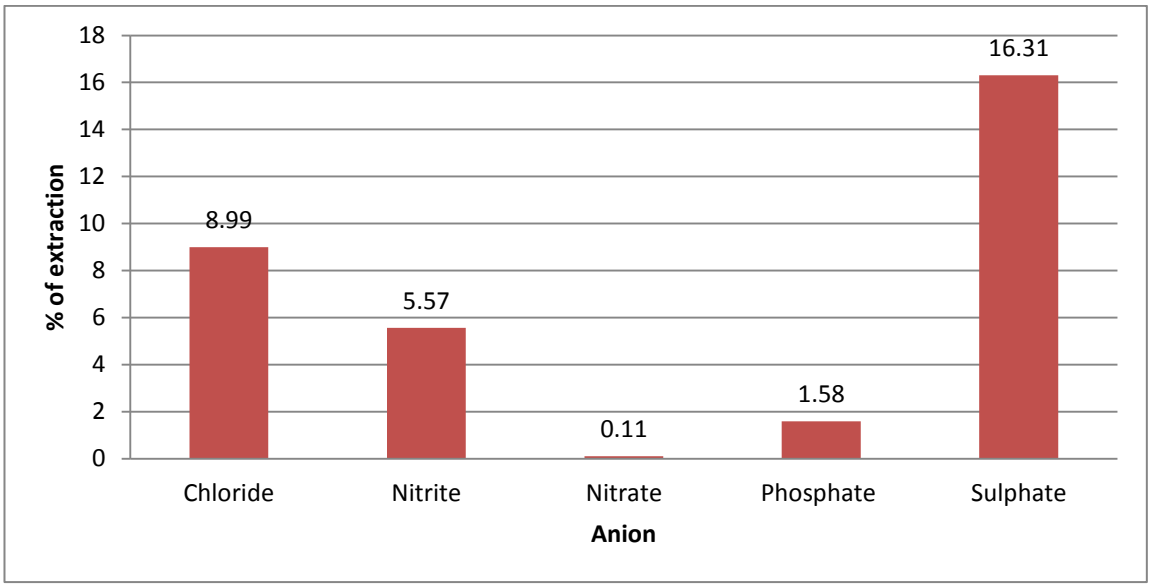

Figure 6-23: The percentage of anion extractions through a used AEX membrane in an ED chip

Figure 6-23 shows the extraction percentages of five anions through a used AEX membrane. From the figure, it can be observed that the largest extracted amount was for sulphate with 16.3%, followed by chloride with 9%, nitrite with 5.5%, and phosphate with 1.5%. The lowest percentage of extraction was for nitrate, with 0.11%.

The figure again demonstrates a great success in extracting anions using this system. All anions were extracted with a variation in the migrated amount of each anion. Sulphate seems to be the largest and this is very likely because of the small concentration of sulphate in the original River Hull sample, which migrated better than the other anions. Phosphate, on the other hand, had the largest presence in the original sample but only 1.5% was migrated to the destination reservoir. Chloride was one of the largest concentrations in the original River Hull water sample but about 9% of it was extracted. Nitrite had a 5.5% extraction followed by nitrate, which was one of the highest present

anions in the sample, of which 0.1% was migrated through the membrane; this was the lowest extraction percentage in the graph.

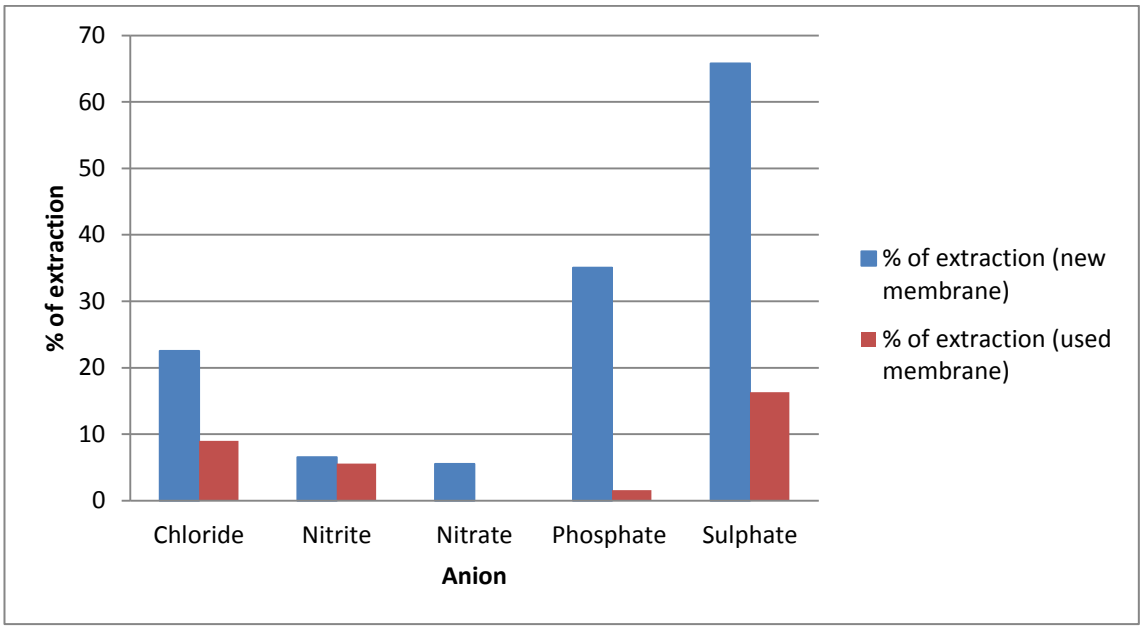

Figure 6-24: Comparison of the extraction percentages of five anions through new and used AEX membranes in an ED chip

Figure 6-24 shows the difference in extraction results between new and used membranes in an ED chip. The figure illustrates that the extraction with both membranes has variations at some points; the trend is not the same. This can be noticed more clearly with phosphate and sulphate, both of which have a large variation between the membranes. Nitrite, on the other hand, has very similar results with both membranes.

However, despite the good extraction obtained by the used membrane, the rate of extraction between the new and used membranes might be an issue, as it would affect the reproducibility and reliability of the extraction. This issue could be solved through the continuous flush of the membrane in the system with an appropriate reagent to regenerate the membrane, or by changing the membrane when it reaches a limit where

the extraction can be affected and the membrane is no longer reproducible. Both possibilities are considered in the total integrated system under development.

6.7 Chapter conclusion

Electrodialysis (ED) was examined as a possible sample introduction method because it can be combined with electrophoresis (CE) for rapid pre-treatment and the subsequent determination of inorganic ions in river water. The analytical performance of ion separation in CE can be significantly improved with pre-treatment, with ED as a sample introduction technique.[123]

Different ED techniques were investigated for extracting inorganic ions from a river water sample, including ion extraction through polytetrafluoroethylene (PTFE) film and Parafilm; ion extraction with a cellulose acetate (CA) ED membrane; ion extraction with a cyclic olefin copolymer (COC) chip; ion extraction with a COC multi-membrane; ion extraction with an ion-exchange membrane; and ion extraction through an ion-exchange membrane in an ED chip.

Ion extraction through polytetrafluoroethylene (PTFE) film and Parafilm initially began with a set-up that involved a plastic capillary; this was practically hard and subsequently showed no results. Therefore, another ED set-up was used and it was successful but it showed a low migration of ions. Thus, to improve the migration of ions, the film was stretched to reduce the thickness of the film. This provided better results and the amount of migrated ions was doubled after reducing the thickness. Despite the successful migration, PTFE and Parafilm are not ideal for a few reasons, the most important reason being that the stretching was manual and would influence the reproducibility of the results in the future, as manual stretching cannot ensure the exact same thickness every time the film is used.

A cellulose acetate (CA) ED membrane was also used for extracting ions from a sample of river water. Unfortunately, anion extraction through the cellulose acetate membrane was unsuccessful, which could be due to the cellulose acetate chemical structure. However, cation extraction through a CA membrane was successful, showing very good results. The extraction time, applied voltage and different buffers were investigated to optimise the extraction, and good progress was made after the optimisation. Further optimisation, such as the mechanical design of the system, will improve the extraction performance.

In order to enhance the extraction of ions through an ED membrane, a new ED chip was designed for the extraction (Figure 3-15 and Figure 3-16). The design of the new chip should be more compatible, physically and chemically, with the final integrated total system. Work on this COC chip was unsuccessful due to the continuous leakage, despite the effort made to control the leakage. This will cause inaccurate results as the fluid would be easily contaminated, or the sample would leak out of the chip, resulting in the incorrect reading of the extraction.

However, to overcome the problems associated with the COC chip and improve the extraction, especially for anions, a COC multi-membrane system was designed. In this system, ion-exchange membranes were used rather than the cellulose acetate membrane. Two types of membrane were examined: an anion-exchange membrane for the extraction of anions and a cation-exchange membrane for the extraction of cations. Different electrodes were used in the system to examine their suitability, including a gold-coated electrode and a carbon-coated electrode. Generally, extraction with a gold electrode was overall slightly better than extraction with carbon; the problem with the carbon electrode was that it demonstrated no phosphate extraction. Nevertheless, both methods showed good extraction despite the low conductivity in the system. This might

be due to the design of the system. This could also be a result of the gold coating over the electrode which might physically wash off the electrode, or become oxidised. Further optimisation is needed to enhance the extraction, including the system design.

To enhance the extraction of ions and simplify the multi-membrane system to a single membrane, ion extraction with an ion-exchange membrane was investigated as a possible extraction media for both anions and cations. Anion extraction with an anion-exchange (AEX) membrane in an ED system was successful and demonstrated good results, yet the AEX membrane has one disadvantage: its inability to tolerate chemical and physical stress for long periods. Cation extraction with a single cation-exchange (CEX) membrane has also shown very good results for the extraction of cations.

Initially, both anion- and cation-exchange membranes were used in the multi-membrane for the extraction of anions, and they were then examined as individual membranes for the extraction of anions by an AEX membrane and the extraction of cations by a CEX membrane in an ED system (plastic fitting). Both have shown promising results and they can be used for ion extraction with further modification of the ED system. Therefore, a new ED chip was designed to improve the extraction. In this system, a new gold electrode was used, and its physical and chemical suitability was examined for an ion extraction system in an ED chip. The extraction using this system has shown great results for both anions and cations, and an even better anion extraction was tested using a real river water sample, also demonstrating great results.

To summarise, different ED techniques and methods were used to extract ions from a river water sample. Most of these techniques were successful, with some disadvantages. Some of these disadvantages can be overcome but this requires further work. However, the most successful and suitable technique for anion extraction was anion extraction with an AEX single-membrane in an ED chip. The best cation extraction was obtained

using the ED system with a cellulose acetate (CA) membrane. Both systems have shown very good results and these results can be further improved with a greater optimisation to suit the total integrated systems.

7 Combined CE and ED for a fully integrated system

7.1 Introduction

Chip-based CE is one of the fastest and potentially convenient techniques for the separation of inorganic ions,[22] and has shown very promising results,[216] indicating that it can be used *in-situ* for the analysis of inorganic ions as part of a total integrated analytical system. The combination of CE and C4D for LOC analysis has become very attractive for *in-situ* analysis due to several factors such as the low consumption of reagents and samples, fast analysis time, and good detection sensitivity.[217] Therefore, this work has concentrated on developing an LOC system that uses the advantages of both CE and C4D.

To increase the sensitivity of the CE system, the ED system (chapter 6) has been used as a sample introduction system as well as a pre-concentration technique. In the proposed LOC total integrated system, the ED system should be placed prior to the CE chip and the C4D placed last.

7.1.1 System specifications

The analytical system should be able to measure ions in the field every 15 minutes, logging all of the collected data at any time on a network. Hence, the ideal system should be able to operate without intervention for at least three months, allowing for a minimum of three-monthly measurements.

This means that the quantity of reagents should be enough for three months. Ideally, the system should have as few reagents as possible, including washing reagents and those for conditioning the membrane. Therefore, the buffer is the only chemical reagent in the system and that will be discussed in detail later on in this chapter. The use of one

chemical reagent is good because it reduces the environmental impact of chemical waste produced by the system. The volume of buffer used in the system for three months should be as small as possible to make the system portable enough; the proposed maximum buffer volume should be no more than 2 L and this will be discussed later on in this chapter.

The system has to be portable enough to be carried to remote, difficult locations, with the preferable approach being to place as many systems as possible in different locations. In addition, in case of the failure of one system, its portability means that it could be quickly replaced with an alternative system.

The energy requirements and power budget for the system has to be as small as possible, and this will be discussed later in the chapter. Finally, one of the most important specifications of the system is that it must have a low environmental impact in case of failure.

7.2 Proposed design for a total integrated LOC system

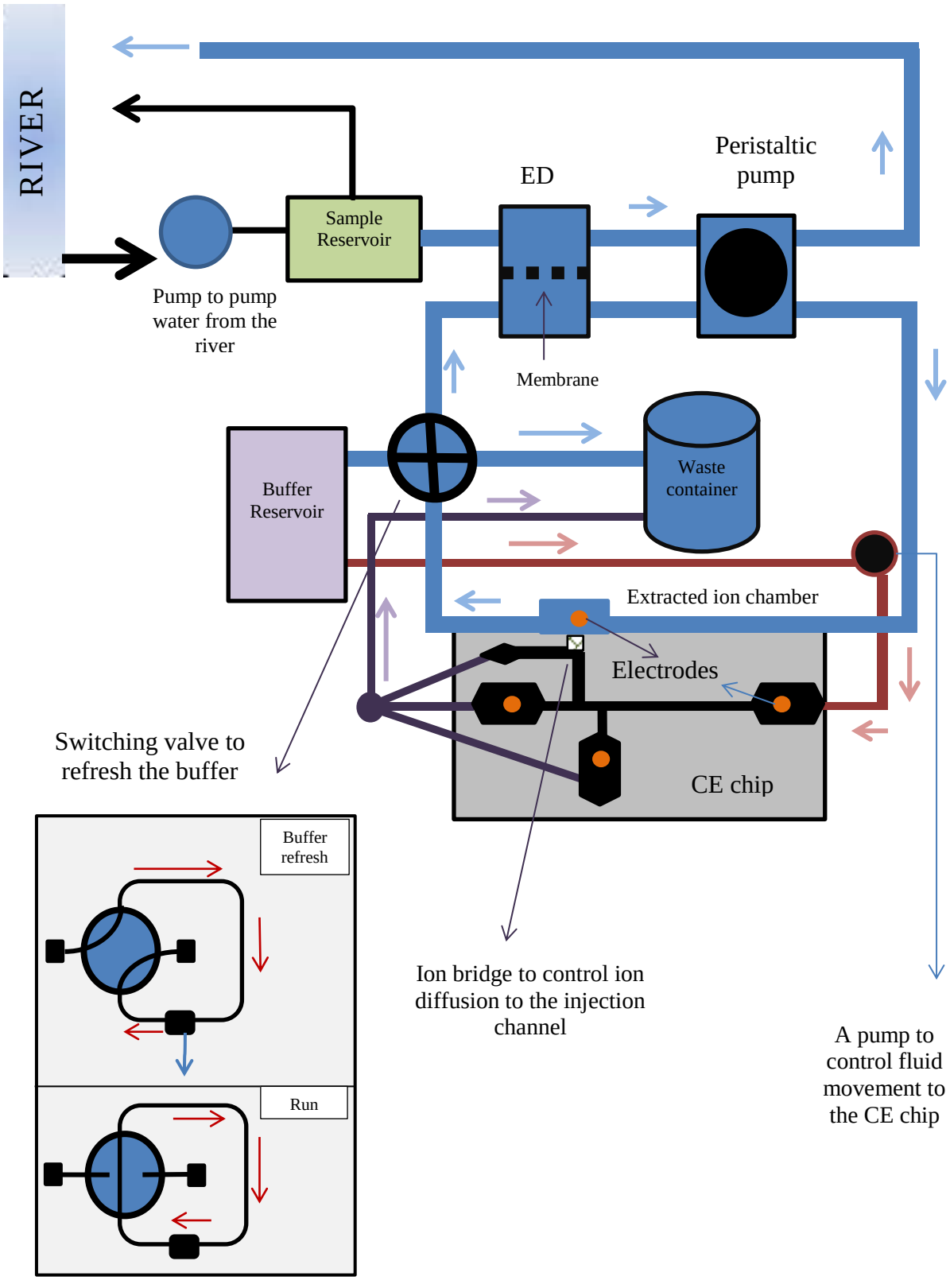

Figure 7-1: Proposed design of an ED and CE integration system in a total LOC system.

Figure 7-1 shows the potential design of the LOC system. The design begins with a sample reservoir. This reservoir contains the river water sample collected from the river by a standard water pump. The fluid is then placed in a sample reservoir and the extra amount of the water sample goes back into the river. The fluid is introduced to the ED chip from the sample reservoir by a peristaltic pump. The sample side of the ED chip is connected to a tube that exits the fluid back to the river, and the fluid is controlled by the peristaltic pump. This pump should keep pumping long enough to extract sufficient ions from the river water, by continuously extracting ions from a large amount of water. The other side of the chip, which is the side with the extracted ions, is also connected to a tube; this tube works as a loop that circulates the buffer and the ions. The buffer is introduced to the loop by the peristaltic pump, and the fluid of the buffer is controlled by an injection valve placed after the buffer reservoir. When the valve is switched on, the buffer moves to the loop to fill in the system, including the other side of the ED system. During the analytical run, the valve should be closed in order to continue circulating the buffer in the loop. Following the analytical run, the valve should open to clean the system of any possible residues and to refresh the buffer.

After the extraction of ions, the ions and the buffer are moved by the peristaltic pump to the extracted ion chamber. In this chamber, the ions are introduced to the CE chip in order to be separated, and the introduction of the ions from the chamber to the sample reservoir in the CE chip is electrokinetically controlled. An ion bridge can be placed at the interface between the extracted ion chamber and the sample injection channel in the CE chip; this bridge aims to stop the fluid from entering the injection channel and only allows ions to pass through.[98] The purpose of this step is to avoid any interference caused by the conflict between the two different flows of fluid in the sample loop and

on the CE chip. This conflict is due to the different dimensions of the loop and the CE chip (or directions of fluid). The ions are injected into the separation channel by applying a voltage to force the ions to move to the separation channel. More details are provided later in the chapter.

The buffer is introduced to the system by a valve that allows the buffer to enter the loop and wash it after each run, and then refresh the loop with a new buffer. After each run, the used buffer goes to a waste container in order to be disposed of appropriately. Ideally, the amount of buffer should be less than 2 L to ensure that the system is portable. By using the following equation,[46] the amount of buffer in the system can be calculated:

$$\boldsymbol{V = \pi \left(\frac{id}{2}\right)^2 h} \qquad \textbf{Equation 7-1}$$

Where **V** is the volume of buffer, $\boldsymbol{id}$ is the internal diameter of the tubes or the channel, and *h* is the length of the tubes or the channel that carries the buffer.

The total amount of buffer in the system is the subtotal of volumes in the tubes and channels in the system, which can be calculated by using the following equation:

$$\boldsymbol{V_{total} = V_{ED} + V_{sep} + V_{flush} + V_{tubing} + V_{E.I.C}} \qquad \textbf{Equation 7-2}$$

V_{total} is the total volume of buffer needed in the system, V_{ED} is the volume of buffer in the side of the ED chip with the extracted ions, V_{sep} is the volume of buffer in the CE chip, V_{flush} is the volume needed to flush the system after each run to clean the system, V_{tubing} is the volume of buffer in the tubing, and $V_{E.I.C}$ is the volume in the extracted ions chamber (EIC).

From the previous equations (Equation 7-1 and Equation 7-2), the volume of buffer in the system is 0.53 ml per run and each run is 15 minutes; therefore, the amount of buffer needed is 52 ml a day. As the volume in the tubing is 0.015 ml (h = 500 mm and id = 200 µm), the volume in the ED system is around 0.5 ml based on the ED experiments and the volume of the CE chip is 0.369 µl including the waste path (h = 78 mm [the separation channel] + 10 mm [the injection channel] + 100 mm [the waste path], and r = 50 µm). The volume in the extracted ion chamber is 0.0125 ml (r = 400 µm and h = 100µm). This amount does not include the washing step; to include the washing step, this volume is doubled, as the system should be flushed once after every run, which means that the total volume needed is 104 ml a day.

7.2.1 CE separation chip

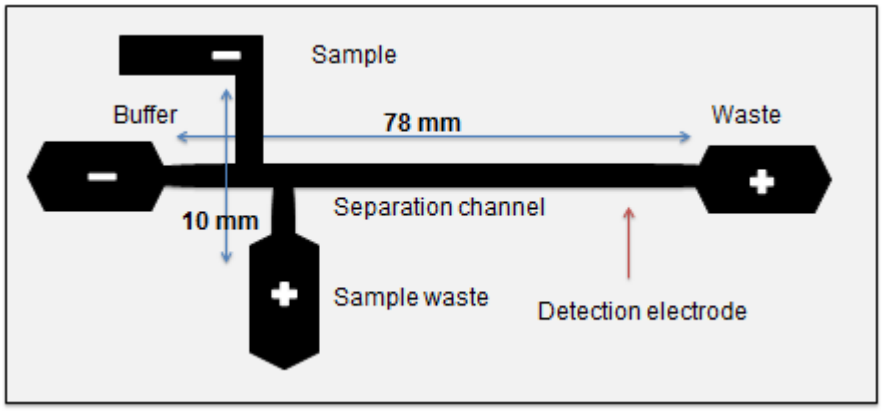

Figure 7-2: A diagram of the capillary electrophoresis used for the separation of ions

Figure 7-2 shows the CE microchip used for the separation of ions. The chip consists of two channels in a cross shape, the separation and injection channels. At the beginning and end of each channel there is an electrode. In the injection channel, the sample introduction point has an electrode with the same charge as the ions of interest, to push the ions to move to the separation channel through the ion bridge. At the end of the

sample channel, the electrode has the opposite charge to pull ions towards it. The separation channel also has two electrodes to move ions in the channel to be separated. At the end of the separation channel, just before the waste exit, there is a detection area (see section 3.4.1). The separation channel is 78 mm long and 100 µm deep; it is relatively long to allow for the good separation of ions.[104] At the beginning and end of the separation channel, and at the end of the injection channel in the CE chip, expanded chambers ensure the buffer capacity. The expanded buffer chambers for the electrodes are used to simplify electrode addressing and counteract buffering capacity depletion caused by the high electrophoretic current.[124]

The channels in the chip must be filled with a buffer, by pumping the buffer from the buffer reservoir to fill the CE chip. The buffer fills the chip via a tube; this tube is connected directly to the buffer reservoir. The buffer should remain in the chip during the run, and the buffer position in the CE is controlled by a pump.

After the analytical run, the system should be flushed with a buffer to clean the system of any possible residues. Finally, the buffer from the entire system goes to one waste container, to make the system portable.

7.2.2 Separation process

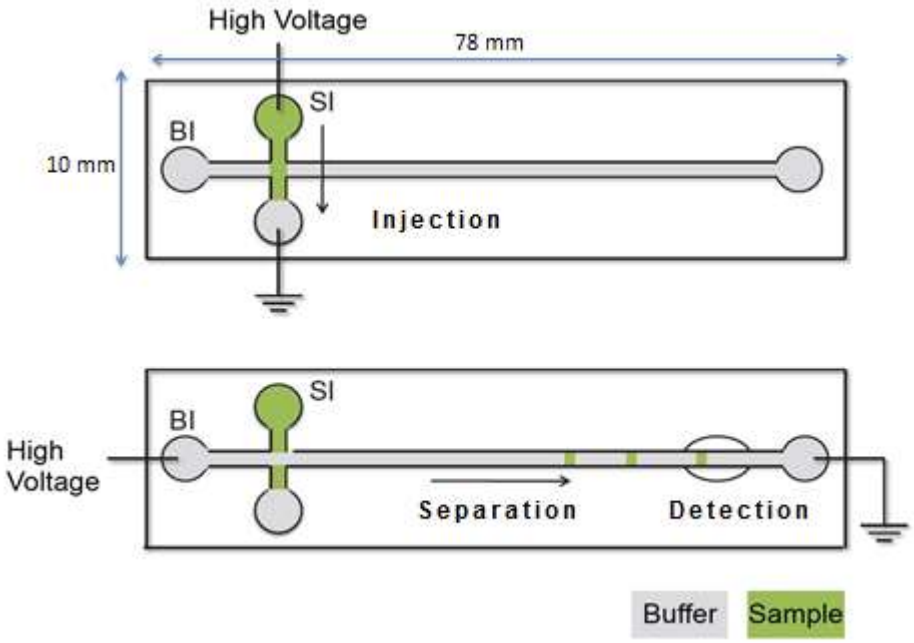

Figure 7-3: A diagram to explain the injection and separation process

After the extraction of ions through the ED chip in the previous part of the system (section 7.2), followed by the pre-concentration of ions in the other side of the membrane in the system, the process of the electrokinetic injection of ions to the separation channel in the CE chip, begins. In the case of anions, for example, in the extracted ion chamber they are injected into the separation channel by applying a voltage (200-500 V) for a few seconds (5-10 Sec)[218]; the ions should move through the attraction of a negative charge at the beginning of the sample injection channel, and a positive charge at the end of the sample injection channel. When the ions move to the junction in the chip, a high voltage is applied across the separation channel to force ions to move through the channel in order to be separated and detected. The movement also occurs through the influence of a negative charge at the beginning of the separation channel and a positive charge at the end of the separation channel. The time required for

separation is between 2-5 minutes or less,[10] depending on the separation conditions such as the chip materials, for example, Poly(methyl methacrylate) (PMMA). The voltage applied should be in the range of 2-4 KV.[69]

7.3 Buffer

The buffer must be stable at different conditions and withstand changes in the environment such as temperature. Therefore, the buffer chemistry was investigated under various conditions. The analysis was carried out using a fluorescence spectrometer instrument (LS 55 Fluorescence Spectrometers, Perkin Elmer, UK), with an excitation wavelength of 440 nm and an emission wavelength of 470-350 nm.

The buffer (10 mM MES/His) was prepared in 100 ml stock and this 100 ml buffer solution was then distributed in ten 10 ml sample glass vials. Each vial was treated differently. The first condition was the buffer vial left in a freezer for a week, the second condition was the fresh buffer, and the third condition was the buffer vial left in a 5ºC fridge for 48 hours. The rest of the buffer was then placed in a box with the temperature fixed at 40ºC, and the sample vials were then left in the box for different timings: 1, 3, 5, 10, 24 and 48 hours, and 4 months. Each sample was then measured using a fluorescence spectrometer.[219]

These conditions represent different environmental conditions that would affect the buffer in an LOC system in the field. However, leaving the buffer for 4 months is not recommended, as the buffer might be changed biologically by bacterial activities. Technically, the frozen sample of the buffer would represent the most extreme temperature in winter, which is unlikely to occur because the box contains a system that will raise the temperature inside the box due to the presence of the electronics in the system, which means that most of the time, the buffer will not be in a frozen condition.

The changes in UK temperature are usually not as warm as 40ºC for a long time, but this would be the most extreme condition. Conditions colder than 5ºC would not usually change the buffer chemistry; therefore, the buffer was mostly examined at high temperatures, as they are likely to change the conditions of chemical reagents.

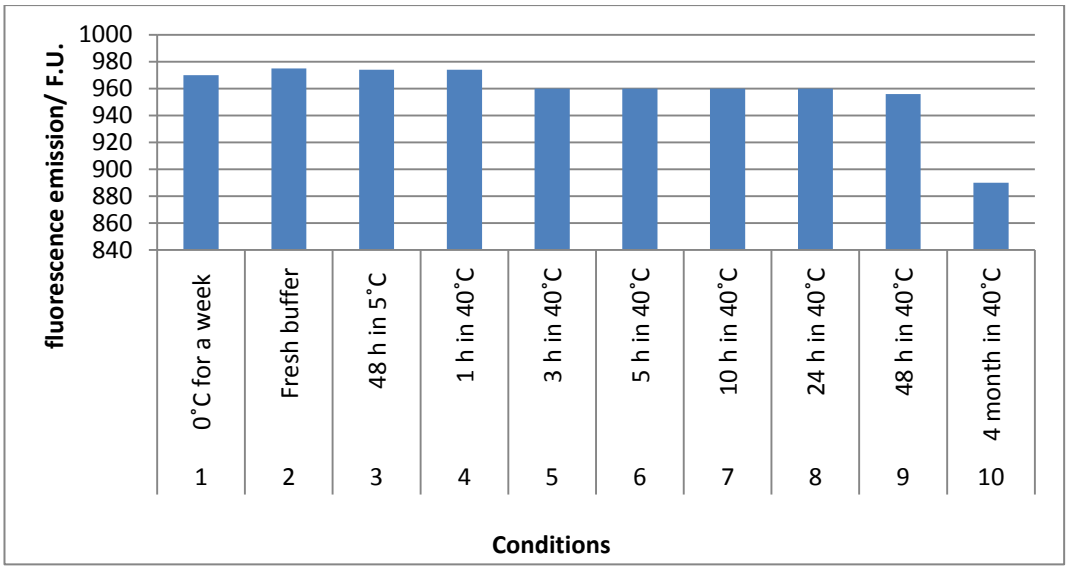

Figure 7-4: Fluorescence emission of a MES/His buffer under different conditions

Figure 7-4 shows the changes in the chemistry of the buffer under different conditions. The first condition emission was at 970 FU. The second (the fresh buffer), third and fourth conditions showed very similar emissions at about 975 FU. After this, it decreased at the fifth condition and remained the same until the ninth condition, at 960 FU. The tenth and last condition showed an emission of 860 FU.

From Figure 7-4, it can be seen that the MES/His buffer demonstrates similar emission figures, which means that the buffer is able to stand the adverse changes in the field conditions.

7.3.1 Buffer conductivity

Table 7-1: Buffer conductivity at different concentrations

Sample	Conductivity µS/cm
Deionised Water	0.46
5 mM MES/Histidine	1.34
10 mM MES/Histidine	2.60
30/10 MES/Histidine	3.59

Table 7-1 shows three different concentrations of the MES/His buffer. The deionised water used in the preparation of the buffer has a conductivity of 0.46 µS/cm. The 5 mM buffer conductivity was 1.34 µS/cm, the 10 mM buffer conductivity was 2.60 µS/cm, and the 30/10 MES/His buffer conductivity was 3.59 µS/cm.

The buffer conductivity was examined at different concentrations as the concentration of the buffer might change depending on the separation suitability, due to a conflict in the buffer concentration in the sample introduction and separation. The buffer concentration used for separation can be used for the ion extraction. Different concentrations of the buffer were also examined for the ED system, and the lowest concentration of buffer (5 mM) was used. The 5 mM concentration was the less conductive concentration, and a higher concentration of the buffer should be more conductive, allowing for better extraction of ions in the ED system.

7.3.2 Buffer safety

The buffer consisted of two chemical compounds: 2-(N-morpholino)ethanesulfonic acid (MES) and Histidine (His). According to most chemical reagent suppliers, neither of the compounds are hazardous substances.[45] However, hazards might occur from some emissions including carbon oxides, nitrogen oxides and sulphur oxides. This might

occur in the case of fire and a solid state (powder). The system only used a buffer solution and so the hazard is not relevant to this content.

To keep the environment safe from any possible buffer spillage, it is necessary to consider the possibility of spillage, which could be due to any failure. Two main causes of spillage could occur. The first cause is an internal system failure, which leads to a leakage of the buffer. In this case, the system should have an electronic leakage sensor or self-testing technique that stops the pump and minimises the leakage. The self-testing process should also be able to identify a number of issues that result in errors or faults in the measurements[11]; for example, blockages in the fluidic system or dramatic changes to the temperature of the system. In addition, the system should be in a physically strong box that is designed to keep the reagents inside the system, in case of spillage.

The second cause of spillage is physical damage that causes the total destruction of the system, due to a catastrophe such as a falling a tree or vandalism. In such an extreme incidence, the box containing the system should involve a technique to prevent the buffer from entering the environment. For example, the inner wall of the box could be covered with materials that can absorb liquid, such as sponge. However, both chemical compounds in the buffer are diluted in water with a small concentration; this will further reduce the risk associated with the buffer, in the case of a spillage that is out of control.

7.4 Pumps

In this work, two different pumping systems are required. The first pump is a standard water pump to pump the water sample from the river to a sample collection subsystem (reservoir). The second type of pump is for pumping the water sample from the reservoir to the LOC device, and to move the fluid inside the device. An example of this pump is a peristaltic pump. Figure 7-1 shows a peristaltic pump in the LOC system.

This pump aims to move the buffer and the extracted ions in the other side of the membrane.

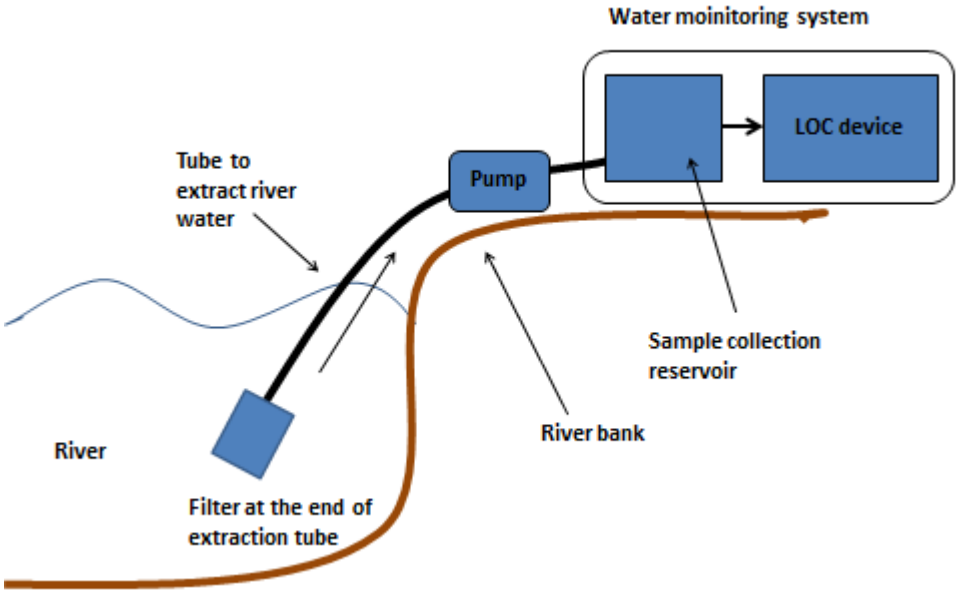

Figure 7-5: Rough sketch of a water-quality monitoring system highlighting the possible collection reservoir

Figure 7-5 shows a possible process for extracting a water sample from the river to the LOC system. The system on the riverbank should begin with a standard filter to stop any large particles from entering the system. The filter is at the end of a tube that is connected to a pump that pulls water from the river. The water sample should be collected in a reservoir, prior to passing through the system. The LOC system is then running the required amount for analysis, and the rest of the water sample in the sample collection reservoir goes back into the river.

The pumps should operate as long as the analytical system is running and it should stop when no analysis is running, such as a system failure or when changing the buffer or the waste container. Based on the ED experiments in chapter 6, the ED time should be within 5 minutes, hence, the peristaltic pump should operate continuously for 5 minutes

in every run, and then stop working until the next run. The system should be able to perform a run every 15 minutes, which comes to 2,942 runs a month, and so the pumping time is 246 hours a month. The best pump performance is a compromise between factors such as the tubing size and life, and the flow rate.[7] However, a standard peristaltic pump should be able to operate for three months based on this calculation, and some peristaltic pumps can run for more than 1,000 hours,[49] which make long-term pumping achievable.

7.4.1 Energy

Considering the fact that the analytical system should consume as little energy as possible and be portable, a portable battery is required to operate the pump. 12 V batteries should be able to operate the pumps for the time required; motorcycle or car batteries should be suitable for such a task.

Table 7-2: Estimated power consumption of the LOC system components

Subsystem	Power (W)	Usage in 15 min sample cycle (min)	Average continuous power (W)
HV Electronic	1	4	0.27
Peristaltic pumps	0.3	6	0.12
Main power	1	2	0.13
Main electronic	0.1	15	0.10
Total			0.62

Table 7-2 shows the estimated power consumption of the proposed LOC system. The table contains the system components, the power required to operate them, and the usage time of that particular component. The values were estimated from very similar commercial products for each part.[220] [221] However, the total average of the system's

power consumption is 0.62W, using the following equation to calculate the power consumption per day:

$$\boldsymbol{E = Pt} \qquad \textbf{Equation 7-3}$$

Where E is the energy, P is the power and t is the time in seconds.[222] [83] Thus, the energy is 53568 J (0.62 W per day).

From the previous calculation, the energy consumption was calculated, which then has to be fulfilled with the appropriate battery. If the system is running for 720 hours a month, the energy capacity of the system is 446.4 Wh. A typical 12 V battery weighs 6 KG, which is relatively portable and can also deliver up to 480 Wh.[80]

However, these figures can be adjusted to suit the system, but they are reliable enough to a realistic stage to prove that the LOC system energy is far less than the current standard analytical system that measures ions in the field. These typical systems require mains power supply or a higher voltage power supply (230 V).[84]

7.5 Chapter conclusion

To summarise, the proposed analytical system should fulfil the project requirements and the demand for an LOC system that can monitor water quality *in-situ.* The project requirements were a robust, portable LOC system with reduced time, reagent consumption and power. The run time was significantly reduced as this LOC system can measure all of the required species in one run, in 15 minutes, while the current standard system measures one species at a time, in a few minutes. The reagent consumption of the current standard system is 100 L every two weeks,[12] while for this LOC system it is 1.5 L every two weeks. This also significantly reduces the amount of waste from the system and makes the system portable. The portability of the system is

very convenient, as it could be carried by an ordinary person; the entire system should be the size of a briefcase. The power needed is also reduced, less than the current system, and the portability of the system might be limited by the battery size, but a possible compromise could be considered that involves using a smaller capacity battery and reducing the usage time.

8 Conclusion

There is a demand for portable *in-situ* measuring systems for measuring ions in environmental water samples. Although commercially available flow injection analysis systems are available, they are not easy to install and maintain, having high power requirements and using large volumes of reagents. Miniaturising the measurements has proved to be promising, and quite successful microfluidic automated systems have been developed, based on spectrophotometric and voltammetric measurements. These systems tend to only measure one species at a time, and what is required is a portable system that can simultaneously measure several anions and cations. The aim of this project was, therefore, to develop a novel, analytical device capable of measuring and detecting nutrient levels in water samples *in-situ,* at high-frequency measurements, by utilising the advantages of miniaturisation for sample preparation and measurement. The system involves ion injection, ion separation, and detection. This analytical system to be developed needed to be capable of replacing the existing systems being used in the field.

Work started on the separation of ions using a monolithic column, as they demonstrated good results in the literature.[92, 194] For the separation of anions, two different anion exchangers were investigated, lysine and DDAB. The monolith was prepared in-house and then coated with the anion exchanger, and a commercial C18 monolith was used to compare this to the results obtained from the homemade monolithic column.

Two anions were used to perform the chromatography on the monolithic columns, nitrite and sulphate. With the homemade lysine-coated monolith, a good peak shape was observed for nitrate but it was practically difficult to continue with lysine, due to the continuous blockage of the monolith. On the homemade DDAB-coated monolith, the

separation of nitrite and sulphate was poor. When nitrite was on its own on the same monolith has shown shift in retention time, and the peak intensity was decreased, which means that the peak was changed, making the results irreproducible. A commercial C18 monolith was coated with DDAB and this showed poor reproducibility for nitrite and sulphate.

It was clear that the monolith was not providing the required separation for small ions, and there were also problems with high back-pressure with regards to prolonged use; therefore, it was decided that another approach was necessary for a portable system.

The work on ion separation was changed from an IC to a CE, which does not require pressure pumps or complex eluents and has a very low reagent consumption. Also, no blockage or leakage occurs in the CE, whereas in the IC, these are a major problem. Furthermore, low-cost CE systems can be obtained using simple manufacturing techniques, and the separation of inorganic ion solutions has successfully been performed in LOC devices.[22]

One concern with continually operating a system is the effect of the sample matrix on the system; therefore, it was decided that a good approach would be to extract the ions from the sample prior to separation. Different ion extraction approaches were investigated, including ion extraction through a potassium silicate monolith and through electrodialysis (ED). The potassium silicate monolith was used to extract ions from river water samples. The potassium silicate monolith worked as a barrier that stopped unwanted materials already present in the river water from entering the measurement system. The presence of these materials would influence the separation process.[94a]

However, different extraction techniques using the potassium silicate monolith were investigated, using both a glass chip and a glass capillary. The bare silica capillary

showed poor results due to the interference of the negative charge on the surface of the capillary, and the monolith causing EOF; therefore, the surface was silanised. Three different silanisation methods were investigated: trichloro perfluorooctyl silane (FDTS), commercial coating, and an end-capping procedure. Different extraction factors were investigated, including the applied voltage and extraction time.

The extraction was successful for all three silanisation methods, showing promising results. The results of the extraction with FDTS were less successful than the other methods, as there was noticeable EOF during the extraction process. The end-capping procedure was better but not as good as the commercial coating. The commercial silanisation reagent showed promising results but they were irreproducible and difficult to control. The high hydrophobicity of the coated surface of the capillary caused the accumulation of bubbles in the capillary, which affected the anion movement. The glass capillary could be replaced by a polymer capillary but then the frit could not be kept in place. Further investigation of a different design was required. This design would be in a suitable polymer chip to avoid, for example, the EOF. The system could include the potassium silicate monolith as the main extraction part, as it has already shown very promising results.

Electrodialysis (ED) was examined as a possible alternative sample introduction method because it can be combined with electrophoresis (CE) for rapid pre-concentration and the subsequent determination of inorganic ions in river water. The analytical performance of ion separation in CE can be significantly improved by pre-treatment with ED as a sample introduction technique.[94b] [96]

Different ED techniques were investigated for extracting inorganic ions from a river water sample, including: ion extraction through a polytetrafluoroethylene (PTFE) film and Parafilm, ion extraction with a cellulose acetate (CA) ED membrane; ion extraction

in a cyclic olefin copolymer (COC) chip; ion extraction with a COC multi-membrane; ion extraction with ion-exchange membranes; and ion extraction through an ion-exchange membrane in an ED chip.

Ion extraction through polytetrafluoroethylene (PTFE) film and Parafilm did not produce reproducibility, as the films had to be stretched in order to reduce the thickness of the film. Despite the successful migration of ions, PTFE and Parafilm were not ideal for such an application.

A cellulose acetate (CA) ED membrane was also used for extracting ions from a river water sample. Anions could not be extracted due to the chemical structure of cellulose acetate; however, they were successfully extracted through the AEX membrane.

In order to enhance the extraction of ions through the ED membrane, a new COC ED chip was designed. The new chip had to be both physically and chemically compatible with the final integrated total system, and the initial COC-chip design was not practically ideal. Thus, to overcome the problems associated with the initial design and to improve the extraction, especially of anions, a COC multi-membrane system was designed. In this system, ion-exchange membranes were used rather than the cellulose acetate membrane. Two types of membrane were examined: an anion-exchange membrane for the extraction of anions and a cation-exchange membrane for the extraction of cations. Different electrodes were used in the system to examine their suitability, including a gold-coated electrode and a carbon-coated electrode. Generally, extraction with a gold electrode was better than extraction with carbon. Nevertheless, both methods demonstrated good extraction, despite the low conductivity in the system.

To enhance the extraction of ions and to simplify the multi-membrane system to a single membrane, ion extraction with just one ion-exchange membrane was investigated

as a possible extraction media for both anions and cations. Anion extraction with the anion-exchange (AEX) membrane in an ED system was successful and showed good results, but the AEX membrane was not very robust, with the disadvantage that it has no ability to stand chemically and physically for a long period of time. Cation extraction with a single cation-exchange (CEX) membrane has shown very good results for the extraction of cation, and it can be used for about 100 runs.

To summarise the work on ED, different ED techniques and methods were used to extract ions from a river water sample. Most of these techniques were successful, with some disadvantages that can be overcome with further work. The most successful and suitable technique for anion extraction was anion extraction with an AEX single membrane in an ED chip, whereas ED extraction using a cellulose acetate (CA) membrane was the best cation extraction. Both systems have shown very good results and these results can be further improved with a greater optimisation to suit the total integrated systems.

A design for a total LOC system is proposed, which includes the pumps, buffer and the energy required to operate the system. Two different types of pumps should work together in the system, one to extract the water from the river and peristaltic pumps to work in the system. Ideally, the system should be in operation *in-situ* for three months. The energy required for the pumps should be supplied by a portable battery that is able to function for a long period, with relatively low voltage. The suitability of the buffer (MES/His) was extensively investigated, and the amount needed for a month was also calculated. The amount of buffer needed for a month is less than 3 L, which is ideal for system portability. The power needed can also be reduced, as in the current system. The portability of the system might be limited by the battery size, but a compromise could be considered, using a smaller capacity battery and reducing the usage time.

8.1 Future work

The proposed LOC system can meet most of the requirements from a chemistry perspective, and it was linked to the electronic and mechanical design. It showed highly promising results and with further optimisation, the system could be operated and achieve the requirements. The system can measure ions and with slight modification, it could also measure elements with the required LOD. The portability of the system was intensively considered and the system should be small enough to be carried by a person and placed in different, difficult locations; it could be powered by a large battery (perhaps backed up with solar power). The analytical run can be achieved within 15 minutes, and could be reduced. The development of the system still requires further work, especially on the separation. However, the separation of ions in such a system has been investigated elsewhere, and it can be accomplished.[97]

9 References

[1] D. Ning, Y. Huang, R. Pan, F. Wang and H. Wang, *Science of The Total Environment* **2014**, *485–486*, 596-603.

[2] M. AG in *850 Professional IC Manual*, *Vol. 2015* http://www.metrohm.com/en-us/company/, **2009**.

[3] B. Flores, J. Ren, S. Krishnamurthy and W. Belzer in *Assessment of Nutrient and Heavy Metal Levels in Manadas Creek, an Urban Tributary of the Rio Grande in Laredo, Texas*, *Vol.* Eds.: D. Ramirez, J. Ren, K. D. Jones and H. Lamm), Springer Netherlands, **2014**, pp. 97-115.

[4] C. Ye, S. Li, Y. Zhang and Q. Zhang, *J Hazard. Mater.* **2011**, *191*, 366-372.

[5] G. E. Brown, A. L. Foster and J. D. Ostergren, *Proceedings of the National Academy of Sciences* **1999**, *96*, 3388-3395.

[6] M. Hendryx, J. Conley, E. Fedorko, J. Luo and M. Armistead, *International Journal of Health Geographics* **2012**, *11*, 9.

[7] h. apparatus in *Peristaltic Pump '1200' Series User's Manual*, *Vol. 2015* **2015**.

[8] I. Bharodiya and A. Parikh, **2014**.

[9] W. Theodore, *Electrical machines, drives and power systems, 6/E*, Pearson Education India, **2007**, p.

[10] J. Wang, M. Pumera, G. Collins and I. Jelínek, *Analyst* **2002**, *127*, 719-723.

[11] E. Joly, I. M. Bell, A. Fallatah, G. M. Greenway, S. J. Haswell, A. J. Wade and R. Skeffington, *Mixed-Signals, Sensors and Systems Test Workshop (IMS3TW), 2012 18th International* **2012**, pp. 28-33.

[12] A. Wade, E. Palmer-Felgate, S. Halliday, R. Skeffington, M. Loewenthal, H. Jarvie, M. Bowes, G. Greenway, S. Haswell and I. Bell, *Hydrology and Earth System Sciences* **2012**, *16*, 4323-4342.

[13] I. Haddeland, J. Heinke, H. Biemans, S. Eisner, M. Flörke, N. Hanasaki, M. Konzmann, F. Ludwig, Y. Masaki, J. Schewe, T. Stacke, Z. D. Tessler, Y. Wada and D. Wisser, *Proceedings of the National Academy of Sciences* **2014**, *111*, 3251-3256.

[14] P. Whitehead, D. Butterfield and A. Wade in *Potential impacts of climate change on river water quality Vol.* (Ed. E. agency), **2008**.

[15] A. J. Wade, E. J. Palmer-Felgate, S. J. Halliday, R. A. Skeffington, M. Loewenthal, H. Jarvie, M. J. J.Bowes, G. M. Greenway, S. J. Haswell, I. M. Bell, E. Joly, A. Fallatah, C. Neal, R. J. Williams, E. Gozzard and J. R. Newman, *Hydrology and Earth System Sciences* **2012**, *16*, 4323-4342.

[16] L. Marle and G. M. Greenway, *TrAC Trends in Analytical Chemistry* **2005**, *24*, 795-802.

[17] J. G. E. Gardeniers and A. van den Berg, *Analytical and Bioanalytical Chemistry* **2004**, *378*, 1700-1703.

[18] J. E. Prest, S. J. Baldock, P. R. Fielden, N. J. Goddard and B. J. Treves Brown, *Journal of Chromatography A* **2003**, *990*, 325-334.

[19] E. P. Joly in *Development of an autonomous lab-on-a-chip system with ion separation and conductivity detection for river water quality monitoring*, *Vol.* University of Hull, **2013**.

[20] P. E. Kenneth M. Vigil, *Clean Water An Introduction to Water Quality and Water Pollution Control*, Oregon State University Press, United States of America, **2003**, p. 176.

[21] K. C. Cheung, B. H. T. Poon, C. Y. Lan and M. H. Wong, *Chemosphere* **2003**, *52*, 1431-1440.

[22] J. S. Fritz, *Journal of Chromatography A* **2000**, *884*, 261-275.

[23] H. Thea and M. Fred, *Nutrient on the move* International institute for Environment ans Development, London, **2000**, p. 146.

[24] J. Paul, N. Dinn, T. Kannangara and L. Fisher, *Journal of Environmental Quality* **1998**, *27*, 528-534.

[25] S. V. Dorozhkin and M. Epple, *Angewandte Chemie International Edition* **2002**, *41*, 3130-3146.

[26] S. Khan, R. Mulvaney and T. Ellsworth, *Renewable Agriculture and Food Systems* **2015**, 1-4.

[27] C. Lee, *Marine Ecology Progress Series* **1993**, *98*, 135-148.1993.

[28] J. A. J. Dungait, L. M. Cardenas, M. S. A. Blackwell, L. Wu, P. J. A. Withers, D. R. Chadwick, R. Bol, P. J. Murray, A. J. Macdonald, A. P. Whitmore and K. W. T. Goulding, *Science of The Total Environment* **2012**, *434*, 39-50.

[29] J. H. Seinfeld and S. N. Pandis, *Atmospheric chemistry and physics: from air pollution to climate change*, John Wiley & Sons, **2012**, p.

[30] D. E. Canfield, A. N. Glazer and P. G. Falkowski, *science* **2010**, *330*, 192-196.

[31] K. H. v. Mogel in *Will cover crops feed the world?*, *Vol. 2015* (Ed. biofortified.org), biofortified.org, biofortified.org, **2011**.

[32] A. C. Anthonisen, R. C. Loehr, T. B. S. Prakasam and E. G. Srinath, *Journal (Water Pollution Control Federation)* **1976**, *48*, 835-852.

[33] J. P. Montoya, C. M. Holl, J. P. Zehr, A. Hansen, T. A. Villareal and D. G. Capone, *Nature* **2004**, *430*, 1027-1032.

[34] H. L. Golterman, *The chemistry of phosphate and nitrogen compounds in sediments*, Kluwer Academic Publishers, **2004**, p.

[35] F. Lipschultz, O. Zafiriou, S. Wofsy, M. McElroy, F. Valois and S. Watson, **1981**.

[36] J. Shi, S. Fujisawa, S. Nakai and M. Hosomi, *Water Research* **2004**, *38*, 2323-2330.

[37] R. Knowles, *Microbiological reviews* **1982**, *46*, 43.

[38] K. B. Föllmi, *Earth-Science Reviews* **1996**, *40*, 55-124.

[39] K. Ruttenberg, *Treatise on geochemistry* **2003**, *8*, 585-643.

[40] Pregun Csaba and J. Csaba in *Water Resources Management and Water Quality Protection*, *Vol. 2015* (Ed. http://www.tankonyvtar.hu/en), http://www.tankonyvtar.hu/en, **2011**.

[41] P. Echlin, *Scanning Electron Microsc* **1975**, *7*, 1019-1028.

[42] W. E. Graves Jr, D. Boys and F. T. Turner in *Sputter-coating system, and vaccuum valve, transport, and sputter source array arrangements therefor*, *Vol.* Google Patents, **1982**.

[43] S. Mathur, S. Barth, H. Shen, J. C. Pyun and U. Werner, *Small* **2005**, *1*, 713-717.

[44] G. C. Lane, C. A. Cartwright and K. W. Elmslie in *Sputter coating method*, *Vol.* Google Patents, **1976**.

[45] S. Aldrich in *Sigma-Aldrich MSDS*, *Vol. 2015* Sigma-Aldrich, **2015**.

[46] J. SITZIA, *European journal of cancer care* **1995**, *4*, 11-16.

[47] M. J. Moorcroft, J. Davis and R. G. Compton, *Talanta* **2001**, *54*, 785-803.

[48] U. S. E. P. Agency in *Nutrient Pollution: The Problem*, *Vol. 2015* United state of America

2012.

[49] Saint-Gobain in *Comparative Peristaltic Pumps Tubing life*, *Vol. 2015* www.tygon.com, **2015**.

[50] a) K. K. Gill, H. S. Sandhu and R. Kaur, *Pesticide Biochemistry and Physiology*; b) A. H. Wolfe and J. A. Patz, *AMBIO: A Journal of the Human Environment* **2002**, *31*, 120-125.

[51] L. N. Kolonel, J. H. Hankin, J. Lee, S. Y. Chu, A. M. Nomura and M. W. Hinds, *British Journal of Cancer* **1981**, *44*, 332-339.

[52] M. C. Bruzzoniti, S. Cavalli, A. Mangia, C. Mucchino, C. Sarzanini and E. Tarasco, *Journal of Chromatography A* **2003**, *997*, 51-63.

[53] S. Wilbur in *The Agilent 7700x ICP-MS Advantage for Drinking Water Analysi*, *Vol.* (Ed. I. Agilent Technologies, 2009), **2009**.

[54] B. Michalke, *TrAC Trends in Analytical Chemistry* **2002**, *21*, 142-153.

[55] R. Roehl, R. Slingsby, N. Avdalovic and P. E. Jackson, *Journal of Chromatography A* **2002**, *956*, 245-254.

[56] S. AB in *A practical guide to Ion chromatography an introduction and troubleshooting manual Vol.* **1998-2007**.

[57] J. W. Olesik, *Analytical Chemistry* **1991**, *63*, 12A-21A.

[58] R. D. Cowan, *The Theory of Atomic Structure and Spectra* University of California Press **1992**, p. 568.

[59] G. Tyler in *AA or ICP - Which do you choose?*, *Vol.* (Ed. V. A. P. Ltd), Australia **1991**.

[60] J. W. Olesik in *Elemental Analysis Using An Evaluation and Assessment of Remaining Problems*, *Vol.* **1991**.

[61] PerkinElmer in *Atomic Spectroscopy A Guide to Selecting the Appropriate Technique and System*, *Vol.* (Ed. PerkinElmer), **2008-2013**.

[62] D. A. Skoog, F. J. Holler and S. R. Crouch, *Principles of instrumental analysis*, Thomson Brooks/Cole, Belmont, CA, **2007**, p. 1039 p.

[63] D. C. Harris, *Quantitative Chemical Analysis*, Craig Bleyer, New York, **2007**, p. 663.

[64] R. L. Dahlquist and J. W. Knoll, *Applied Spectroscopy* **1978**, *32*, 1-30.

[65] X. Hou and B. T. Jones in *Inductively Coupled Plasma/Optical Emission Spectrometry*, *Vol.* (Ed. R. A. Meyers), John Wiley & Sons Ltd, Ch, Chichester, **2000**, pp. 9468–9485.

[66] S. Toumpis and S. Gitzenis, *INFOCOM 2009, IEEE* **2009**, pp. 1656-1664.

[67] J. L. Todolí and J. M. Mermet, *Spectrochimica Acta Part B: Atomic Spectroscopy* **2006**, *61*, 239-283.

[68] H. Zhang, X. Liu, X. Zhang and R. Weng, *Nano/Micro Engineered and Molecular Systems (NEMS), 2013 8th IEEE International Conference on* **2013**, pp. 1104-1107.

[69] X.-J. Huang, Q.-S. Pu and Z.-L. Fang, *Analyst* **2001**, *126*, 281-284.

[70] T. Cecchi, *Critical Reviews in Analytical Chemistry* **2008**, *38*, 161-213.

[71] R. M. Smith, *Anal. Proc.* **1984**, pp. 72-75.

[72] S. AbuRuz, J. Millership and J. McElnay, *Journal of Chromatography B* **2003**, *798*, 203-209.

[73] B. A. Bidlingmeyer, *Journal of Chromatographic Science* **1980**, *18*, 525-539.

[74] E. Sugrue, P. N. Nesterenko and B. Paull, *Journal of Chromatography A* **2005**, *1075*, 167-175.

[75] L. Kisley, J. Chen, A. P. Mansur, B. Shuang, K. Kourentzi, M.-V. Poongavanam, W.-H. Chen, S. Dhamane, R. C. Willson and C. F. Landes, *Proceedings of the National Academy of Sciences* **2014**, *111*, 2075-2080.

[76] A. Williams and V. Frasca in *Ion-Exchange Chromatography*, *Vol.* John Wiley & Sons, Inc., **2001**.

[77] D. Schaller, E. F. Hilder and P. R. Haddad, *Journal of Separation Science* **2006**, *29*, 1705-1719.

[78] L. Lu, X. Han, J. Li, J. Hua and M. Ouyang, *Journal of power sources* **2013**, *226*, 272-288.

[79] K. R. Elkin and J. M. Riviello, *Talanta* **2014**, *119*, 353-360.

[80] W. www.smartbattery.com in *Lithium Battery*, *Vol. 2015* **2015**.

[81] F. James and GjerdeDouglas, *Ion Chromatography*, WILEY-VCH, Weinheim, **2009**, p. 377.

[82] F. Zhang, G. Shen, S. Ji and B. Yang, *Journal of Liquid Chromatography & Related Technologies* **2015**, *38*, 349-352.

[83] J. Loehr, J. E. Loehr and T. Schwartz, *The power of full engagement: Managing energy, not time, is the key to high performance and personal renewal*, Simon and Schuster, **2005**, p.

[84] in *PHOSPHAX sc Phosphate analyser on-site, 0.05-15 mg/L, 1 channel*, *Vol. 2015* **2015**.

[85] J. S. Fritz, *Journal of Chromatography A* **2005**, *1085*, 8-17.

[86] J. S. Fritz and D. T. Gjerde, *Ion Chromatography*, Wiley, **2009**, p.

[87] J. E. MacNair, K. C. Lewis and J. W. Jorgenson, *Analytical chemistry* **1997**, *69*, 983-989.

[88] W. Joachim, *Ion Chromatography*, VCH Verlagsgesellschaft mbH, Cambridge **1995**, p. 464.

[89] M. J. Shaw and P. R. Haddad, *Environment International* **2004**, *30*, 403-431.

[90] D. C. Harris, *Exploring chemical analysis*, Macmillan, **2004**, p.

[91] S. Wouters, B. Wouters, S. Jespers, G. Desmet, H. Eghbali, C. Bruggink and S. Eeltink, *Journal of Chromatography A* **2014**, *1355*, 253-260.

[92] F. Svec and C. G. Huber, *Analytical chemistry* **2006**, *78*, 2100-2107.

[93] a) E. Joly, I. M. Bell, A. Fallatah, G. M. Greenway, S. J. Haswell, A. J. Wade, R. A. Skeffington, and *18th International Mixed-Signals, Sensors and Systems Test Workshop (IMS3TW)* **2012**; b) H. Schäfer, M. Läubli and R. Dörig, *Metrohm, Herisau* **1998**.

[94] a) P. R. Haddad, P. Doble and M. Macka, *Journal of Chromatography A* **1999**, *856*, 145-177; b) T. K. O. Doan, P. Kubáň, P. Kubáň, I. K. Kiplagat and P. Boček, *Electrophoresis* **2011**, *32*, 464-471.

[95] in *Chapter 9 Electrolytic Conductivity Detector*, *Vol. Volume 36* (Ed. M. Dressler), Elsevier, **1986**, pp. 181-207.

[96] M. Kelly, K. Altria and B. Clark, *Journal of Chromatography A* **1997**, *768*, 73-80.

[97] A. R. Timerbaev, *Electrophoresis* **2004**, *25*, 4008-4031.

[98] S. Park, T. D. Chung and H. C. Kim, *Microfluidics and nanofluidics* **2009**, *6*, 315-331.

[99] F. M. Everaerts, J. L. Beckers and T. P. Verheggen, *Isotachophoresis: theory, instrumentation and applications*, Elsevier, **2011**, p.

[100] B. Graß, A. Neyer, M. Jöhnck, D. Siepe, F. Eisenbeiß, G. Weber and R. Hergenröder, *Sensors and Actuators B: Chemical* **2001**, *72*, 249-258.

[101] B. Toussaint, P. Hubert, U. Tjaden, J. Van der Greef and J. Crommen, *Journal of Chromatography A* **2000**, *871*, 173-180.

[102] L. Chen, J. E. Prest, P. R. Fielden, N. J. Goddard, A. Manz and P. J. Day, *Lab on a Chip* **2006**, *6*, 474-487.

[103] J. E. Prest, S. J. Baldock, P. R. Fielden, N. J. Goddard and B. J. T. Brown, *Analytical and bioanalytical chemistry* **2003**, *376*, 78-84.

[104] Y. Tachibana, K. Otsuka, S. Terabe, A. Arai, K. Suzuki and S. Nakamura, *Journal of Chromatography A* **2004**, *1025*, 287-296.

[105] Y. Tani and Y. Umezawa, *Sensor Letters* **2005**, *3*, 99-107.

[106] N. Lakshminarayanaiah, *Membrane electrodes*, Elsevier, **2012**, p.

[107] R. Wetzel and G. Likens in *Inorganic Nutrients: Nitrogen, Phosphorus, and Other Nutrients*, *Vol.* Springer New York, **2000**, pp. 85-111.

[108] J. E. Harwood, *Water Research* **1969**, *3*, 273-280.

[109] E. Hansen, A. K. Ghose and J. Růžička, *Analyst* **1977**, *102*, 705-713.

[110] R. De Marco, G. Clarke and B. Pejcic, *Electroanalysis* **2007**, *19*, 1987-2001.

[111] V. S. Bagotsky, *Fundamentals of electrochemistry*, John Wiley & Sons, **2005**, p.

[112] R. O. C. DIOXIDE in *ELECTROCHEMISTRY. PRINCIPLES, METHODS AND APPLICATIONS*, *Vol.*

[113] K. Rajeshwar and J. G. Ibanez, *Environmental electrochemistry: Fundamentals and applications in pollution sensors and abatement*, Academic Press, **1997**, p.

[114] D. C. Harris, *Quantitative Chemical Analysis*, W. H. Freeman and Company, New York, **2003**, p. 645.

[115] J. Wang, M. Jiang and F. Lu, *Journal of Electroanalytical Chemistry* **1998**, *444*, 127-132.

[116] J. Ružicka, *Flow injection analysis*, John Wiley & Sons, **1988**, p. 493.

[117] K. S. Johnson, R. L. Petty and J. Thomsen in *Flow-injection analysis for seawater micronutrients*, *Vol.* DTIC Document, **1985**.

[118] A. Kazemzadeh and A. A. Ensafi, *Microchemical Journal* **2001**, *69*, 61-68.

[119] M. B. Shinn, *Industrial & Engineering Chemistry Analytical Edition* **1941**, *13*, 33-35.

[120] J. Gómez, N. Sanjuán, J. Bon, J. Arnau and G. Clemente, *Journal of Food Engineering* **2015**, *149*, 188-194.

[121] K. S. Johnson and L. J. Coletti, *Deep Sea Research Part I: Oceanographic Research Papers* **2002**, *49*, 1291-1305.

[122] A. D. Beaton, V. J. Sieben, C. F. Floquet, E. M. Waugh, S. A. K. Bey, I. R. Ogilvie, M. C. Mowlem and H. Morgan, *Sensors and actuators B: Chemical* **2011**, *156*, 1009-1014.

[123] B. Buscher, U. Tjaden and J. Van der Greef, *Journal of Chromatography A* **1997**, *788*, 165-172.

[124] B. M. Paegel, C. A. Emrich, G. J. Wedemayer, J. R. Scherer and R. A. Mathies, *Proceedings of the National Academy of Sciences* **2002**, *99*, 574-579.

[125] K. S. Ritter, Paul Sibley, Ken Hall, Patricia Keen, Gevan Mattu, Beth Linton, Len, *Journal of Toxicology and Environmental Health Part A* **2002**, *65*, 1-142.

[126] U. Förstner and G. T. Wittmann, *Metal pollution in the aquatic environment*, Springer Science & Business Media, **2012**, p.

[127] H. Al-Hosney and V. Grassian, *Physical Chemistry Chemical Physics* **2005**, *7*, 1266-1276.

[128] A. Amine and G. Palleschi, *Analytical letters* **2004**, *37*, 1-19.

[129] L. Allamandola, S. Sandford, A. Tielens and T. Herbst, *The Astrophysical Journal* **1992**, *399*, 134-146.

[130] H. A. M. FACILITY in *MICROMAC C On line analyzer for potable, surface and waste water monitoring*, *Vol. 2014* **2014**.

[131] S. H. Behrens and D. G. Grier, *The Journal of Chemical Physics* **2001**, *115*, 6716-6721.

[132] G. M. Whitesides, *Nature* **2006**, *442*, 368-373.

[133] R. Daw and J. Finkelstein, *Nature* **2006**, *442*, 367-367.

[134] S. C. Terry, J. H. Jerman and J. B. Angell, *Electron Devices, IEEE Transactions on* **1979**, *26*, 1880-1886.

[135] Z. He in *Microarrays*, *Vol.* (Ed. Z. He), Caister Academic Press, University of Oklahoma, Norman, OK, USA, **2014**, p. 258.

[136] G. M. Greenway, S. J. Haswell and P. H. Petsul, *Analytica Chimica Acta* **1999**, *387*, 1-10.

[137] P. H. Petsul, G. M. Greenway and S. J. Haswell, *Analytica Chimica Acta* **2001**, *428*, 155-161.

[138] J. Cleary, C. Slater, C. McGraw and D. Diamond, *Sensors Journal, IEEE* **2008**, *8*, 508-515.

[139] A. D. Beaton, C. L. Cardwell, R. S. Thomas, V. J. Sieben, F.-E. Legiret, E. M. Waugh, P. J. Statham, M. C. Mowlem and H. Morgan, *Environmental Science & Technology* **2012**, *46*, 9548-9556.

[140] L. Chen, J. E. Prest, P. R. Fielden, N. J. Goddard, A. Manz and P. J. R. Day, *Lab on a Chip* **2006**, *6*, 474-487.

[141] Z. Walsh, B. Paull and M. Macka, *Analytica Chimica Acta* **2012**, *750*, 28-47.

[142] R. Gupta, S. J. Baldock, P. R. Fielden and B. D. Grieve, *Journal of Chromatography A* **2011**, *1218*, 5362-5368.

[143] J. E. Prest, S. J. Baldock, P. R. Fielden and B. J. T. Brown, *Analyst* **2001**, *126*, 433-437.

[144] J. P. Hutchinson, E. F. Hilder, M. Macka, N. Avdalovic and P. R. Haddad, *Journal of Chromatography A* **2006**, *1109*, 10-18.

[145] B. Paull and P. N. Nesterenko, *TrAC Trends in Analytical Chemistry* **2005**, *24*, 295-303.

[146] P. G. Wang, *Monolithic chromatography and its modern applications*, ILM publications, **2010**, p.

[147] A. Strancar, A. Podgornik, M. Barut and R. Necina in *Short Monolithic Columns as Stationary Phases for Biochromatography*, *Vol. 76* (Ed. R. Freitag), Springer Berlin Heidelberg, **2002**, pp. 49-85.

[148] K. Cabrera, D. Lubda, H.-M. Eggenweiler, H. Minakuchi and K. Nakanishi, *Journal of High Resolution Chromatography* **2000**, *23*, 93-99.

[149] D. S. Burgi and R. L. Chien, *Analytical Chemistry* **1991**, *63*, 2042-2047.

[150] a) H. Guo, C. Chu, Y. Li, B. Yang and X. Liang, *Analyst* **2011**, *136*, 5302-5307; b) K. M. Glenn, C. A. Lucy and P. R. Haddad, *Journal of Chromatography A* **2007**, *1155*, 8-14.

[151] K. Nakanishi and N. Soga, *Journal of non-crystalline solids* **1992**, *139*, 1-13.

[152] S. Donath, H. Militz and C. Mai, *Wood Science and Technology* **2004**, *38*, 555-566.

[153] K. Sinkó, *Materials* **2010**, *3*, 704-740.

[154] K. Nakanishi, *Journal of Porous Materials* **1997**, *4*, 67-112.

[155] O. Núñez, K. Nakanishi and N. Tanaka, *Journal of Chromatography A* **2008**, *1191*, 231-252.

[156] C. Liang, S. Dai and G. Guiochon, *Chemical Communications* **2002**, 2680-2681.

[157] A. K. Khattab in *Fabrication, functionalization and characterization of silica monolith for forensic chemistry applications*, *Vol.* University of Hull, **2014**.

[158] A.-M. Siouffi, *Journal of Chromatography A* **2003**, *1000*, 801-818.

[159] G. Kaigala, M. Bercovici, M. Behnam, D. Elliott, J. Santiago and C. Backhouse, *Lab on a Chip* **2010**, *10*, 2242-2250.

[160] E. Oosterbroek and A. van den Berg, *Lab-on-a-Chip: Miniaturized Systems for (Bio)Chemical Analysis and Synthesis*, Elsevier Science, **2003**, p. 384.

[161] L. Gui and C. L. Ren, *Langmuir* **2008**, *24*, 2938-2946.

[162] G. Tang, C. Yang, J. Chai and H. Gong, *International Journal of Heat and Mass Transfer* **2004**, *47*, 215-227.

[163] N. Anastos, N. W. Barnett and S. W. Lewis, *Talanta* **2005**, *67*, 269-279.

[164] T. D. Mai, S. Schmid, B. Müller and P. C. Hauser, *Analytica chimica acta* **2010**, *665*, 1-6.

[165] D. Wu, J. Qin and B. Lin, *Journal of Chromatography A* **2008**, *1184*, 542-559.

[166] J. S. Fritz, *Journal of Chromatography A* **2000**, *884*, 261-275.

[167] D. J. Harrison, A. Manz, Z. Fan, H. Luedi and H. M. Widmer, *Analytical chemistry* **1992**, *64*, 1926-1932.

[168] B. Mohammadi, R. Bharadwadj and J. Santiago, *Electrophoresis Journal* **2002**, *23*, 2729-2744.

[169] H. Strathmann, *Desalination* **2010**, *264*, 268-288.

[170] J.-J. Qin, Y. Li, L.-S. Lee and H. Lee, *Journal of membrane science* **2003**, *218*, 173-183.

[171] S. Waheed, A. Ahmad, S. M. Khan, T. Jamil, A. Islam and T. Hussain, *Desalination* **2014**, *351*, 59-69.

[172] M. Yoshikawa and K. Tharpa in *Application of Membranes from Cellulose Acetate Nanofibers*, *Vol.* Springer, **2015**, pp. 369-394.

[173] M. Sequeira, M. Bowden, E. Minogue and D. Diamond, *Talanta* **2002**, *56*, 355-363.

[174] P. A. Greenwood and G. M. Greenway, *TRAC Trends in Analytical Chemistry* **2002**, *21*, 726-740.

[175] T. McCreedy, *TrAC Trends in Analytical Chemistry* **2000**, *19*, 396-401.

[176] T. McCreedy, *Analytica chimica acta* **2001**, *427*, 39-43.

[177] P. Kubáň and P. C. Hauser, *Analytica chimica acta* **2008**, *607*, 15-29.

[178] A. J. Zemann, E. Schnell, D. Volgger and G. K. Bonn, *Analytical Chemistry* **1998**, *70*, 563-567.

[179] J. A. Fracassi da Silva and C. L. do Lago, *Analytical Chemistry* **1998**, *70*, 4339-4343.

[180] L. Bazinet and M. Araya-Farias, *Journal of colloid and interface science* **2005**, *281*, 188-196.

[181] X. Wang, J. Song, J. Liu and Z. L. Wang, *Science* **2007**, *316*, 102-105.

[182] K. P. Doan TK, Kubáň P, Kiplagat IK, Boček P., *Electrophoresis.* **2011**, *32*, 464-471.

[183] E. C. Craig in *Printed Circuit Boards*, *Vol.* Springer, **1994**, pp. 77-82.

[184] T. Oishi, K. Koyama, S. Alam, M. Tanaka and J.-C. Lee, *Hydrometallurgy* **2007**, *89*, 82-88.

[185] G. O. Mallory and J. B. Hajdu, *Electroless plating: fundamentals and applications*, William Andrew, **1990**, p.

[186] K. Johal, H. Roberts, S. Lamprecht and C. Wunderlich, *Americas 25*, 35.

[187] P. Hatsis and C. A. Lucy, *Analyst* **2002**, *127*, 451-454.

[188] P. I. Fletcher, S. Haswell, P. He, S. Kelly and A. Mansfield, *Journal of Porous Materials* **2011**, *18*, 501-508.

[189] G. Huang, Q. Lian, W. Zeng and Z. Xie, *Electrophoresis* **2008**, *29*, 3896-3904.

[190] M. E. Ibrahim and C. A. Lucy, *Talanta* **2012**, *100*, 313-319.

[191] P. Hatsis and C. A. Lucy, *Analytical chemistry* **2003**, *75*, 995-1001.

[192] C. Xie, M. Ye, X. Jiang, W. Jin and H. Zou, *Molecular & cellular proteomics : MCP* **2006**, *5*, 454-461.

[193] E. Alzahrani and K. Welham, *Analyst* **2011**, *136*, 4321-4327.

[194] E. Sugrue, P. N. Nesterenko and B. Paull, *Journal of Chromatography A* **2005**, *1075*, 167-175.

[195] J. Guo, Y. Lu and R. Whiting, *BULLETIN OF THE KOREAN CHEMICAL SOCIETY* **2013**, *34*, 447-452.

[196] J. Guo, Y. Lu and R. Whiting, *Bull. Korean Chem. Soc* **2013**, *34*, 447.

[197] N. Tanaka, H. Kobayashi, N. Ishizuka, H. Minakuchi, K. Nakanishi, K. Hosoya and T. Ikegami, *Journal of Chromatography A* **2002**, *965*, 35-49.

[198] X. Chen, D.-F. Cui, C.-C. Liu and H. Li, *Microsystem Technologies* **2008**, *14*, 51-57.

[199] J. Kirkland, F. Truszkowski and R. Ricker, *Journal of Chromatography A* **2002**, *965*, 25-34.

[200] S. M. Fields, *Analytical chemistry* **1996**, *68*, 2709-2712.

[201] P. Christensen, S. Johnson, T. McCreedy, V. Skelton and N. Wilson, *Anal. Commun.* **1998**, *35*, 341-343.

[202] R. Arayanarakool, L. Shui, A. van den Berg and J. C. Eijkel, *Lab on a Chip* **2011**, *11*, 4260-4266.

[203] F. Tan, B. Yang and Y. Guan, *Analytical sciences* **2005**, *21*, 955-958.

[204] L.-T. Huang, P.-S. Hsu, C.-Y. Kuo, S.-C. Chen and J.-Y. Lai, *Desalination* **2008**, *233*, 64-72.

[205] B. company in *Parafilm M® Brand Products and Floral Flexible Stemwraps*, *Vol. 2015*.

[206] Y.-L. Hung, M.-J. Wang, J.-W. Huang and S.-Y. Lin, *Experimental Thermal and Fluid Science* **2013**, *48*, 102-109.

[207] Y.-L. Hung, M.-J. Wang, Y.-C. Liao and S.-Y. Lin, *Colloids and Surfaces A: Physicochemical and Engineering Aspects* **2011**, *384*, 172-179.

[208] H. Kamal, F. Abd-Elrahim and S. Lotfy, *Journal of Radiation Research and Applied Sciences* **2014**, *7*, 146-153.

[209] S. Fischer, K. Thümmler, B. Volkert, K. Hettrich, I. Schmidt and K. Fischer, *Macromolecular Symposia* **2008**, pp. 89-96.

[210] C.-P. I. Company. in *Chemical Compatibility Results*

Vol. 2015 **2015**.

[211] L. Bazinet and M. Araya-Farias, *Journal of colloid and interface science* **2005**, *286*, 639-646.

[212] R. R. Lamonte and D. McNally, *Advanced materials & processes* **2001**, *159*, 33-36.

[213] G. Wang, L. Zhang and J. Zhang, *Chemical Society Reviews* **2012**, *41*, 797-828.

[214] L. Burke and P. Nugent, *Electrochimica acta* **1997**, *42*, 399-411.

[215] C. Y. Tang, Y.-N. Kwon and J. O. Leckie, *Desalination* **2009**, *242*, 149-167.

[216] A. A. Elbashir and H. Y. Aboul-Enein, *Biomedical Chromatography* **2010**, *24*, 1038-1044.

[217] T. D. Mai and P. C. Hauser, *Journal of Chromatography A* **2012**, *1267*, 266-272.

[218] G. Chen, Y. Lin and J. Wang, *Talanta* **2006**, *68*, 497-503.

[219] J. R. Lakowicz, *Principles of fluorescence spectroscopy*, Springer Science & Business Media, **2013**, p.

[220] H. I. G. C. KG in *Heidolph Peristaltic Pumps Overview*, *Vol. 2015* www.heidolph.com

[221] http://www.ultravolt.com in *Vol. 2015* **2015**.

[222] D. C. Giancoli and J. J. Boyle, *Physics: principles with applications*, Pearson Education, **2005**, p.